



IEEE TRANSACTIONS ON

GEOSCIENCE AND REMOTE SENSING

JANUARY 1986

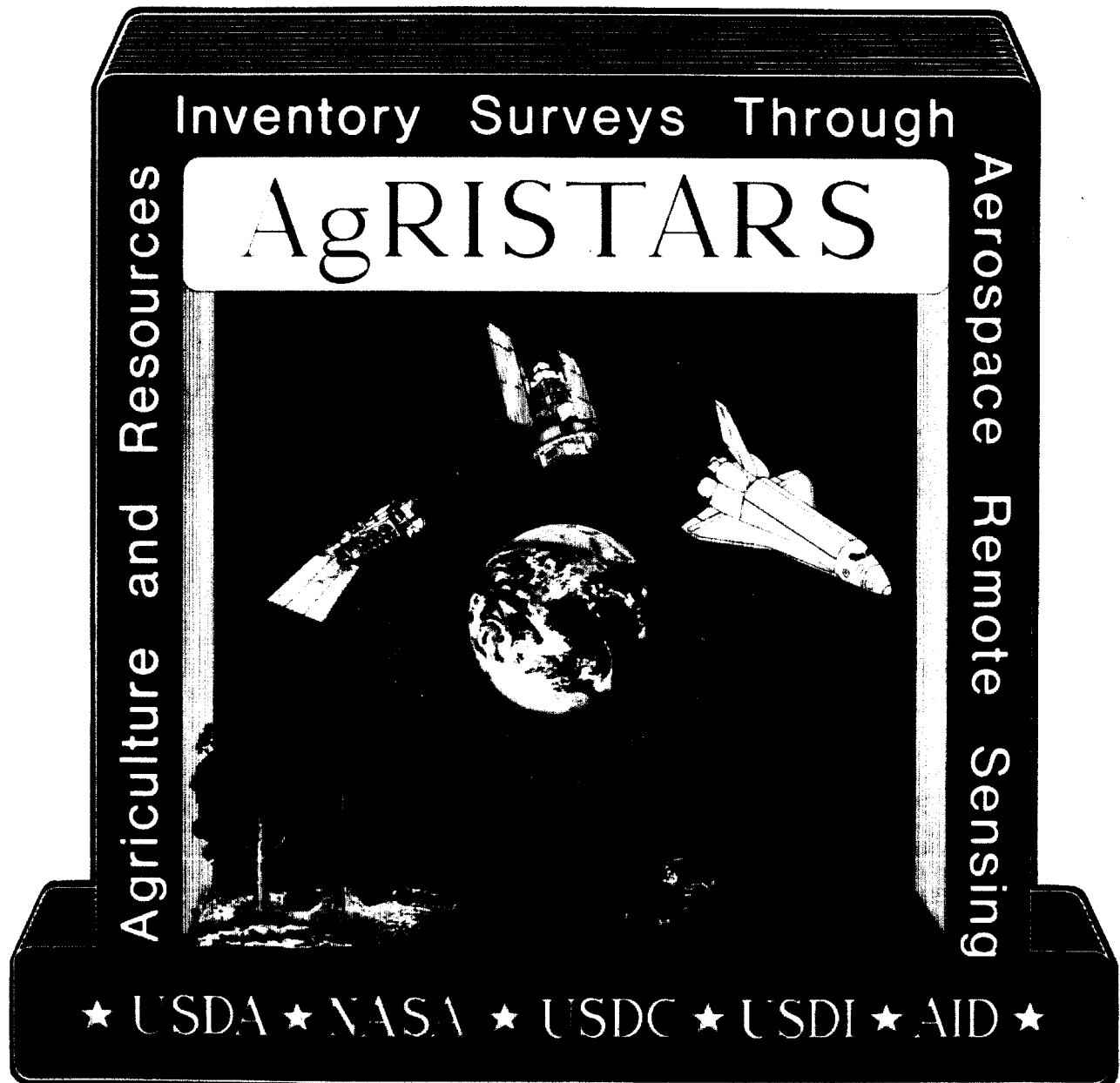
VOLUME GE-24

NUMBER 1

(ISSN 0196-2892)

A PUBLICATION OF THE IEEE GEOSCIENCE AND REMOTE SENSING SOCIETY

SPECIAL ISSUE ON AGRICULTURE AND RESOURCES INVENTORY SURVEYS THROUGH AEROSPACE
REMOTE SENSING (AgRISTARS)





IEEE GEOSCIENCE AND REMOTE SENSING SOCIETY

The Geoscience and Remote Sensing Society is an organization, within the framework of the IEEE, of members with principal professional interest in geoscience and remote sensing. All members of the IEEE are eligible for membership in the Society and will receive this TRANSACTIONS upon payment of the annual Society membership fee of \$7.00. For information on joining, write to the IEEE at the address below.

ADMINISTRATIVE COMMITTEE

D. A. LANDGREBE, *President*

R. K. RANEY, *Vice President*

J. A. REAGAN, *Secretary-Treasurer*

1986

1987

1988

K. R. CARVER
J. ECKERMAN
A. J. SIEBER

C. T. SWIFT
K. TOMIYASU

F. BECKER
P. GUDMANDSEN
W. KEYDEL

D. A. LANDGREBE
F. T. ULABY

R. BERNSTEIN
A. BLANCHARD
W. CHEW

V. KAUPP
R. K. RANEY

Standing Committee Chairmen

C. A. BALANIS
A. J. BLANCHARD
E. M. DIDWALL

J. ECKERMAN
V. H. KAUPP
D. A. LANDGREBE

R. E. MCINTOSH
K. TOMIYASU
F. T. ULABY

W. T. WALTON
E. A. WOLFF

IEEE TRANSACTIONS* ON GEOSCIENCE AND REMOTE SENSING

Editor

FAWWAZ T. ULABY
The University of Michigan Radiation Laboratory
Department of Electrical and Computer Engineering
4072 East Engineering Building
Ann Arbor, MI 48109

Associate Editors

M. T. CHAHINE, *Atmospheric Remote Sensing*
W.-C. CHEW, *Electromagnetic Subsurface Remote Sensing*
R. E. MURPHY, *Extraterrestrial Geophysics and Remote Sensing*
L. S. WALTER, *Geodynamics*
J. M. MENDEL, *Geophysical Signal Processing*

C. H. CHEN, *Information Processing*
E. NJOKU, *Microwave Remote Sensing*
R. K. RANEY
J. A. SMITH, *Visible and Infrared Remote Sensing*
P. N. SLATER

THE INSTITUTE OF ELECTRICAL AND ELECTRONICS ENGINEERS, INC.

Officers

BRUNO O. WEINSCHEL, *President*
HENRY L. BACHMAN, *President-Elect*
EMERSON W. PUGH, *Executive Vice President*
EDWARD J. DOYLE, *Treasurer*
MICHIOYUKI UENOHARA, *Secretary*

CYRIL J. TUNIS, *Vice President, Educational Activities*
CARLETON A. BAYLESS, *Vice President, Professional Activities*
CHARLES H. HOUSE, *Vice President, Publication Activities*
DENNIS BODSON, *Vice President, Regional Activities*
MERLIN G. SMITH, *Vice President, Technical Activities*

N. REX DIXON, *Director, Division IX—Signals and Applications*

Headquarters Staff

ERIC HERZ, *Executive Director and General Manager*
ELWOOD K. GANNETT, *Deputy General Manager*

THOMAS W. BARTLETT, *Controller*
DONALD CHRISTIANSEN, *Editor, IEEE Spectrum*
IRVING ENGELSON, *Staff Director, Technical Activities*
LEO FANNING, *Staff Director, Professional Activities*
SAVA SHERR, *Staff Director, Standards*

DAVID L. STAIGER, *Staff Director, Publishing Services*
CHARLES F. STEWART, JR., *Staff Director, Administration Services*
DONALD L. SUPPERS, *Staff Director, Field Services*
THOMAS C. WHITE, *Staff Director, Public Information*
JOHN F. WILHELM, *Staff Director, Educational Services*

Publications Department

Production Managers: ANN H. BURGMAYER, GAIL S. FERENC, CAROLYNE TAMNEY
Associate Editor: RICHARD C. DODENHOFF, II

IEEE TRANSACTIONS ON GEOSCIENCE AND REMOTE SENSING is published bimonthly by The Institute of Electrical and Electronics Engineers, Inc. **Headquarters:** 345 East 47 Street, New York, NY 10017. Responsibility for the contents rests upon the authors and not upon the IEEE, the Society, or its members. **IEEE Service Center** (for orders, subscriptions, address changes, Region/Section/Student Services): 445 Hoes Lane, Piscataway, NJ 08854. **Telephones:** Headquarters 212-705 + extension: Information-7900, General Manager-7910, Controller-7748, Educational Services-7860, Publishing Services-7560, Standards-7960, Technical Services-7890, IEEE Service Center 201-981-0060. Professional Services: Washington Office 202-785-0017. **NY Telecopier:** 212-752-4929. **Telex:** 236-411 (International messages only). Individual copies: IEEE members \$6.00 (first copy only), nonmembers \$12.00 per copy. Annual subscription price: IEEE members, dues plus Society fee. Price for nonmembers on request. Available in microfiche and microfilm. **Copyright and Reprint Permissions:** Abstracting is permitted with credit to the source. Libraries are permitted to photocopy beyond the limits of U.S. Copyright law for private use of patrons: (1) those post-1977 articles that carry a code at the bottom of the first page, provided the per-copy fee indicated in the code is paid through the Copyright Clearance Center, 29 Congress Street, Salem, MA 01970; (2) pre-1978 articles without fee. Instructors are permitted to photocopy isolated articles for noncommercial use without fee. For other copying, reprint or republication permission, write to Director, Publishing Services at IEEE Headquarters. All rights reserved. Copyright © 1986 by The Institute of Electrical and Electronics Engineers, Inc. Printed in U.S.A. Second-class postage paid at New York, NY and at additional mailing offices. **Postmaster:** Send address changes to IEEE TRANSACTIONS ON GEOSCIENCE AND REMOTE SENSING, 445 Hoes Lane, Piscataway, NJ 08854.



GEOSCIENCE AND REMOTE SENSING

JANUARY 1986

VOLUME GE-24

NUMBER 1

(ISSN 0196-2892)

A PUBLICATION OF THE IEEE GEOSCIENCE AND REMOTE SENSING SOCIETY

SPECIAL ISSUE ON AGRICULTURE AND RESOURCES INVENTORY SURVEYS THROUGH AEROSPACE REMOTE SENSING (AgRISTARS)

A Tribute to the Late R. Jeffrey Lytle ... F. T. Ulaby 2

Foreword ... H. C. Hogg 3

PAPERS

Hydrologic Research Before and After AgRISTARS ... E. T. Engman 5
Passive Microwave Soil Moisture Research ... T. J. Schmugge, P. E. O'Neill, and J. R. Wang 12
Active Microwave Soil Moisture Research ... M. C. Dobson and F. T. Ulaby 23
Soil Water Modeling and Remote Sensing ... T. J. Jackson 37
Progress in Snow Hydrology Remote-Sensing Research ... A. Rango 47
Early Warning and Crop Condition Assessment Research ... G. O. Boatwright and V. S. Whitehead 54
Field Spectroscopy of Agricultural Crops ... M. E. Bauer, C. S. T. Daughtry, L. L. Biehl, E. T. Kanemasu, and F. G. Hall 65
Light Interception and Leaf Area Estimates from Measurements of Grass Canopy Reflectance ... G. Asrar, E. T. Kanemasu, G. P. Miller, R. L. Weiser 76
Spectral Components Analysis: A Bridge Between Spectral Observations and Agrometeorological Crop Models ... C. L. Weigand, A. J. Richardson, and P. R. Nixon 83
Development of Agrometeorological Crop Model Inputs from Remotely Sensed Information ... C. L. Weigand, A. J. Richardson, R. D. Jackson, P. J. Pinter, Jr., J. K. Aase, D. E. Smika, L. F. Lautenschlager, and J. E. McMurtrey, III 90
Detection and Evaluation of Plant Stresses for Crop Management Decisions ... R. D. Jackson, P. J. Pinter, Jr., R. J. Reginato, and S. B. Idso 99
Vegetation Assessment Using a Combination of Visible, Near-IR, and Thermal-IR AVHRR Data ... V. S. Whitehead, W. R. Johnson, and J. A. Boatright 107
Analysis of Forest Structure Using Thematic Mapper Data ... D. L. Peterson, W. E. Westman, N. L. Stephenson, V. G. Ambrosia, J. A. Brass, and M. A. Spanner 113
A Correlation and Regression Analysis of Percent Canopy Closure versus TMS Spectral Response for Selected Forest Sites in the San Juan National Forest, Colorado ... M. K. Butera 122
Use of Remotely Sensed Data for Assessing Forest Stand Conditions in the Eastern United States ... D. L. Williams and R. F. Nelson 130
Coniferous Forest Classification and Inventory Using Landsat and Digital Terrain Data ... J. Franklin, T. L. Logan, C. E. Woodcock, and A. H. Strahler 139
On the Design of Classifiers for Crop Inventories ... R. P. Heydorn and H. C. Takacs 150
Crop Acreage Estimation Using a Landsat-Based Estimator as an Auxiliary Variable ... R. S. Chhikara, J. C. Lundgren, and A. G. Houston 157
A Review of Three Discrete Multivariate Analysis Techniques Used in Assessing the Accuracy of Remotely Sensed Data from Error Matrices ... R. G. Congalton and R. A. Mead 169
Landsat Large-Area Estimates for Land Cover ... G. A. May, M. L. Holko, and N. Jones, Jr. 175

A Tribute to the Late R. Jeffrey Lytle



(February 10, 1941–September 4, 1985)

This issue is dedicated to the memory of R. Jeffrey Lytle, whose accomplishments were so widely known and respected in the scientific community and who so ably served on the Administrative Committee of the IEEE Geoscience and Remote Sensing Society; we all share in the loss of our esteemed colleague and friend.

Jeff was born in Columbus, Ohio, and passed away in Walnut Creek, California. He fought cancer valiantly and, true to his nature, was optimistic to the very last.

Jeff attended Purdue University and received his B.S., M.S., and Ph.D. degrees in electrical engineering. Most of his professional career was spent at the Lawrence Livermore National Laboratory where he was Group Leader of the Electromagnetic and Acoustic Sensing Group in the Engineering Research Division. As Group Leader, he encouraged his team members to be innovative and bold in their approach to research. Jeff was instrumental in developing very advanced electromagnetic applications to

geophysical investigation. One technique developed by Jeff, geotomography, earned him a world-wide reputation.

Prior to his death, he was elected Fellow to the Institute of Electrical and Electronic Engineers. Jeff was a Registered Geophysicist in the state of California, an active member in the Society of Exploration Geophysicists, and served as Vice President of the IEEE Geoscience and Remote Sensing Society.

Jeff always had time to listen to new ideas, and his enthusiasm for developing novel methods was infectious. He was a very trustworthy and honest person in all his interactions. A compassionate man, he was very active with young people, involved in church activities, and family oriented. Jeff will be sorely missed by many of his close friends and associates. Jeff is survived by his wife, Glenda, and three children, Ivan, Janette, and Bobby.

FAWWAZ T. ULABY
Editor

Foreword

BACKGROUND

EARLY JOINT RESEARCH by the United States Department of Agriculture (USDA) and the National Aeronautics Space Administration (NASA) pioneered the use of remotely sensed multispectral data for agricultural applications. Initially these data were provided through an aircraft-based research program and multispectral cameras on manned spacecraft which were used to assess the utility of low-spatial-resolution imagery from space. In 1970, the severe infestation of Southern Corn Blight in the U.S. Corn Belt provided the opportunity for the first real-time large-scale experiment involving multispectral analysis and machine processing; the Corn Blight Watch Experiment conducted jointly by NASA and the USDA in 1971.

In 1972, massive grain purchases in the U.S. disrupted U.S. commodity markets which, together with the highly marginal (and apparently worsening) global food supply of the early 1970's, created a strong perceived demand for better information on global crop production. This led to the formation of the multi-agency Large Area Crop Inventory Experiment (LACIE) to evaluate Landsat data for this purpose. The LACIE baseline approach used Landsat data to estimate crop acreage and meteorologically driven yield models to estimate crop yield. Landsat data acquisition and analysis was conducted by NASA, yield estimation by the U.S. Department of Commerce (USDC), and the sampling and aggregation, which combined the acreage and yield estimates, was conducted jointly by NASA and the USDA, as was the accuracy assessment process. Simultaneously with LACIE, the USDA Statistical Reporting Service (SRS), which is responsible for domestic crop estimates, developed an analysis approach that used Landsat data to refine the accuracy and spatial detail of existing estimates based on ground data acquired by the SRS in its annual June Enumerative Survey. In addition, a number of research projects within NASA, the USDA, and their associated university communities investigated applications of Landsat data to a wider variety of problems, including forestry, range management, and agricultural hydrology.

Building on this research base, Secretary of Agriculture Bergland initiated discussions with the USDC, the U.S. Department of Interior (USDI), and NASA in September 1977 that led to the establishment of the AgRISTARS program in FY 1980; the so-called Secretary's Initiative identified eight priority areas (projects) where remote sensing offered potential for improved information. Under AgRISTARS, commodity forecasting research was expanded from the wheat emphasis of LACIE to include all major grains. The AgRISTARS program also funded research in the utilization of remote sensing data to: produce crop and land use statistics in both the with and without ground

truth cases; measure soil moisture and snowpack properties, model snowmelt runoff, provide information on resource status and condition; and to conduct forest inventories and condition assessments.

SIGNIFICANT DATES LEADING UP TO AGRISTARS

| | |
|--------------|---|
| Early 1960's | Development of multispectral scanners. |
| 1965 | Establishment of organized remote sensing research program in scientific community to explore applications for agriculture. |
| 1966 | Development of first digital processing system to analyze CCT's from airborne scanners. |
| 1966 | First computer-aided classification of wheat using airborne multispectral scanner data and digital analysis system. |
| 1967 | Definition of spectral bands, etc. for first earth resources satellite to be launched in 1972. |
| 1969 | Apollo Multiband Camera Experiment. |
| 1971 | Corn Blight Watch Experiment. |
| 1972 | Landsat I launched. |
| 1973 | Joint Canadian study and initial LACIE proposal. |
| 1975 | LACIE tri-agency project officially authorized. |
| 1978 | LACIE ended. |
| 1980 | AgRISTARS program initiated. |

OBJECTIVES AND PROGRAM STRUCTURE

The AgRISTARS program was organized into eight projects each with its own set of objectives, funding, and management. The projects typically were staffed by more than one participating agency and in most cases used a common data system. Periodic progress reviews, conducted by program management, cut across all projects. The overall goal of the program was to determine the feasibility of integrating aerospace remote-sensing technology into existing and future remote-sensing systems. The overall approach was a balanced program of research, development, testing, and evaluation of techniques to improve information for USDA program needs. The projects included:

- 1) early warning and crop condition assessment;
- 2) inventory technology development—originally for foreign commodity production forecasting;
- 3) yield model development;
- 4) soil moisture;
- 5) domestic crops and land cover;
- 6) renewable resources inventory (forestry);
- 7) conservation and pollution; and
- 8) supporting research.

Participating agencies included: the USDA, NASA, the USDC, the USDI, and the U.S. Agency for International Development (USAID), which participated as an *ex-officio* observer.

AgRISTARS rapidly evolved into an "umbrella" program for remote-sensing research in renewable resources accounting for about 75 percent of federally funded research in this area during the 1980-1983 period. The program included optical as well as passive and active microwave systems, and conducted research with field, aircraft, and space data sources.

RESULTS

The early warning/crop condition assessment research provided empirical models for detecting and estimating the yield impacts of stress conditions associated with moisture, flooding, insect damage, winterkill, and hot dry winds. The project also pioneered the use of the NOAA-7 AVHRR data for large-area assessments. Important results obtained in crop identification/area estimation research included the separation of corn and soybeans and small grains as a class, greatly improving processing speed and cost by full automation of classification procedures, and further development of data compression techniques to reduce data volume. In addition, significant basic research was conducted in quantifying soil background effects, the use of active microwave systems in crop identification, and estimating the leaf area index from spectral data for input into process level productivity models. Results in domestic crops and land cover statistics research included the development, testing, and evaluation of operational procedures for estimating crop acreages over large areas. These estimates were made for major crops in seven states and are provided annually to the USDA Crop Reporting Board for inclusion in their official estimates. Work was initiated in the highly diversified irri-

gated crop lands of California with encouraging results. Full land-cover surveys were conducted in Kansas, Missouri, and Arkansas—the first applications of Landsat data on this scale. Yield modeling research developed a series of new empirical models suitable for use with remote-sensing data (corn, soybeans, wheat, and barley). Plant process/simulation models were developed and/or tested for wheat and barley. Conservation/pollution research developed techniques for measuring snow pack properties to estimate water content, modeled snowmelt runoff for U.S. river basins, found an extreme sensitivity of runoff models to assumed soil moisture levels, and developed procedures for monitoring high sediment loads in reservoirs and rivers.

The papers included in this issue do not provide comprehensive coverage of program accomplishments although all of the major research areas are represented. The interested reader should obtain a copy of one of the AgRISTARS Annual Reports which includes a full listing of all program publications and reports. A single reference that provides a reasonable coverage of program highlights, in abstract and short paper format, is the *Proceedings of the 1985 International Geoscience and Remote Sensing Symposium*, held at Amherst, Massachusetts. An AgRISTARS Annual Report can be obtained from the Remote Sensing Branch, Statistical Reporting Service, U.S. Department of Agriculture, Washington, DC 20250.

HOWARD C. HOGG
Guest Editor

REFERENCES

- [1] C. E. Caudill and R. E. Hatch, "Overview of the AgRISTARS program," plenary paper, presented at the Int. Geosci. Remote Sensing Symp., Amherst, MA, Oct. 7-9, 1985.
- [2] H. C. Hogg and M. Trichel, "Utility of Landsat data in meeting USDA information requirements," Staff Rep., NASA Headquarters, Jan. 1984.



Howard C. Hogg received the B.S. and M.S. degrees in agricultural economics from Oregon State University in 1958 and 1959, respectively, and the Ph.D. degree in resource economics from the University of Hawaii in 1965.

He is currently a Visiting Fellow at the World Resources Institute, Washington, DC. Prior to joining the staff at WRI, he spent 20 years with the Federal Government, first in the U.S. Department of Agriculture (1965-1980) and then in the National Aeronautics and Space Administration (1980-1985). His last assignment at NASA was Discipline Chief for the AgRISTARS Program. Throughout his Federal career, which included assignments in several foreign countries, he specialized in natural resource problems and issues including the development of large-scale data and analytical systems. He has published about 50 articles in journals, conference proceedings, and agency reports.

Dr. Hogg is a member of the American Agricultural Economics Association and the International Association of Agricultural Economists.

Hydrologic Research Before and After AgRISTARS

EDWIN T. ENGMAN

Abstract—Hydrologic research prior to AgRISTARS had followed a rather defined path in which the knowledge curve with time resembles a staircase, rather than a constant incline. AgRISTARS did not introduce remote sensing to hydrology. Some aspects of land-cover analysis, snow area, and floodplain delineation were being studied. However, the concentrated effort of remote-sensing applications to hydrology did help add another step to the knowledge curve.

I. INTRODUCTION

THIS PAPER has two objectives. First, I will try to describe the status of hydrologic research and knowledge when the AgRISTARS program was begun. The three papers that follow this one will highlight some of the work that has been accomplished in modeling, snow hydrology, and water quality. In essence, the first part of this paper is the yardstick by which to evaluate progress in AgRISTARS. The second goal of this paper is to project where future steps in the knowledge curve may lead us. Remote sensing is a fairly new tool in hydrology. I will try to convince the reader that this is not simply a fad but will have a major role in future hydrologic applications.

II. BRIEF HISTORY

Hydrology's historical roots are based on ancient observations and man's attempts to manage water for survival. Chow [1] has broken the history of hydrology down into eight epochs. This is in concert with most other descriptions of man's increase in knowledge—typically an exponential curve. In the *Period of Speculation* (ancient–1400), Plato, Homer, and Aristotle recognized some form of hydrologic cycle. Although these early philosophers and scientists did not have a quantitative understanding of hydrology, a great number of practical hydraulic structures, such as aqueducts and irrigation systems, illustrated man's desire and need to control water resources as a prerequisite for civilization as we know it. During the Renaissance, in the *Period of Observation* (1400–1600), Palissy and Leonardo da Vinci described a hydrologic cycle in which water moved from the oceans to rain on the land and returned to the oceans. Quantitative hydrology probably began during the *Period of Measurement* (1600–1700) in which scientists such as Perrault, Mariotte, and Halley made measurements of different hydrologic components. It is interesting to note that Perrault and Mariotte were physicists and Halley an astronomer (no, not an astrologer!). The *Period of Experimentation* (1700–1800) gave us

a long list of familiar names that includes Pitot, Bernoulli, D'Alembert, and Chézy with discoveries that bear their names. According to Chow [1], the nineteenth century, which he called the *Period of Modernization* (1800–1900), saw the establishment of the science of hydrology as we now know it. Many significant advances to hydrology were accomplished in this century, especially in the areas of groundwater and surface water. The foray into quantitative hydrology was extended in the *Period of Empiricism* (1900–1930). A lack of good scientific understanding of hydrology led to a large number of empirical formulas developed to solve site-specific problems. It is interesting that most references associated with this epoch are institutions (Bureau of Reclamation, Miami Conservancy District, etc.) rather than people. This is not the case for the *Period of Rationalization* (1930–1950). Here we find the true gurus of modern hydrology. People like Sherman, Horton, Theis, Gumble, Hazen, Bernad, and Einstein published their research and developed procedures that are still very much in use today.

Chow's last epoch is the *Period of Theorization* (1950 to date, e.g., 1964). Here hydrologists attempted to use theoretical approaches to solve hydrologic problems. This work provided a great deal of insight into the complexities of hydrology but did not do a great deal for the practicing hydrologist.

Were this list to be updated to 1985, several additional periods could be added—the period of the computer, the period of multidisciplinary research, the period of systems analysis, the period of environmental quality, the period of modeling, the period of stochasticism versus determinism, etc. I think we could also add a period of remote-sensing applications to this list.

The interesting thing to notice about the post-1964 epochs is that they generally widen the breadth of hydrology as a science. Environmental quality research may be an example of this. However, other areas, such as the period of the computer, certainly have also increased the depth of our knowledge. The period of remote sensing also has increased the depth of our knowledge.

III. EFFECTIVENESS OF NEW METHODS

One interesting aspect of recent hydrologic research is that although we feel we know more about the physical process, use sophisticated analysis techniques, and can produce very elaborate output, we have not been able to demonstrate consistently improved accuracy or reproducibility.

The volume of published techniques that are available for use (e.g., the rational formula and SCS technique) is

Manuscript received April 26, 1985; revised June 25, 1985.

The author is with the U.S. Department of Agriculture, Agricultural Research Service, Beltsville, MD 20705.

IEEE Log Number 8406232.

not in proportion to their use [2]. In addition, newer or complex (sophisticated?) methods have not been adopted widely by practicing engineers. Presumably, this is because the newer techniques have not been shown to give demonstrably better results and, in general, their use requires more data and usually a large computer.

An interagency work group of the Hydrology Committee of the Water Resources Council [3] was assigned the task of developing consistent national guidelines for defining peak flow frequencies at ungaged stream locations. The many differing procedures used in practice and the lack of agreement about their use precluded selecting procedures to include in a national guide without developing objective information about procedure performance.

In a recent paper, Naef [4] addressed the success of models in reproducing measured discharge. His conclusions are based on two projects: the World Meteorological Organization Intercomparison of Conceptual Models used in operation hydrological forecasting [5], and on a study of rainfall runoff models using data from small basins in Switzerland. The results show that simple models can give satisfactory results; however, neither the simple nor the more complex models tested were free from failure in certain cases because none of them adequately describe the rainfall-runoff process. In addition, it could not be proved that complex models give better results than simpler ones.

A third study by Loague and Freeze [6] presented model-performance calculations for three event-based rainfall-runoff models on three data sets involving 269 events from small upland catchments. The models include a regression model, a unit-hydrograph model, and a quasi-physically based model. The results of the study show surprisingly poor model efficiencies for all models on all data sets on an event-by-event bases. The poor performance of the quasi-physically based model could probably be ascribed to a combination of model error and input error. They speculated that the primary barrier to the successful application of physically based models in the field may lie in the scale problems that are associated with the unmeasurable spatial variability of rainfall and soil hydraulic properties. The fact that simpler less-data-intensive models provided as good or better predictions than a physically based model is food for thought.

If one accepts these studies as indicators of the effectiveness of recent hydrologic research results, one should ask, Why? Why is it that more complex and more physically based models do not give us better results? There is perhaps no clear answer, but I would speculate that lack of the proper amounts and types of data may be a large part of the answer. I will try to show how remote sensing may provide some new types of data that will help make the complex models easier to use as well as improve their performance. For example, remote sensing may be the only viable approach to handle spatial variability of watershed properties because the basic data are spatial in nature. In this paper I will try to show how the period of remote sensing may develop into a very large and significant step in the knowledge curve. This will be based on

the uniqueness of remote sensing to obtain spatially distributed information as well as some entirely new forms of measurement.

IV. DEVELOPMENT OF REMOTE SENSING

Remote sensing as it is generally known today is an outgrowth of photogrammetry. Strictly defined, remote sensing involves the collection of data by systems which are not in direct contact with the item being measured. Early remote sensing emphasized interpretation of photos and descriptive analysis of the subject. The launching of the Landsat A (later renamed Landsat 1) satellite in July 1972 started the modern era of remote sensing. The availability of so many data on a repetitive basis covering four spectral bands, all areas of the Earth, and a relatively fine resolution was the impetus for a great deal of research. It is with this background that this paper addresses remote-sensing applications to hydrology. Two major subjects are addressed—1) current applications of remote sensing to hydrology and modeling, and 2) future directions for remote sensing in hydrology.

A. Current Applications

Landsat data have become a common source of information in hydrology. These data, like other remote-sensing applications, are generally used in a fairly simple extension of photogrammetry. However, the unique characteristics of specific spectral bands and the temporal sequence of the data extend their usefulness beyond photo interpretation.

B. Land Use and Runoff Coefficients

Land use or cover is an important aspect of hydrologic processes, particularly infiltration, erosion, and evapotranspiration. Because of this, any process-oriented model (as opposed to a "black-box model") incorporates some land-use data or parameters. Distributed models, in particular, need specific data on land uses identified by location within the watershed. Most of the work to date on adapting remote sensing to hydrologic modeling has been with the Soil Conservation Service (SCS) runoff curve number [7]. The runoff curve number (*RCN*) is a coefficient developed from a hydrologic characterization of the soil and the land cover. The *RCN* may be further adjusted by antecedent precipitation to account for very wet or dry conditions. The importance of land cover can be demonstrated by comparing predicted runoff for a condition where only the land use changes. For example, consider a *B* soil and a 10-cm rain; the calculated runoff for good pasture condition would be approximately 0.25 cm, whereas, if that same field were planted in a small grain with straight rows, the runoff calculated by the SCS procedure would be approximately 2.8 cm.

A number of studies have demonstrated the feasibility of developing the land use categories from Landsat. First, suburban and urban areas were studied because the greatest contrast would be available between the impervious and other more pervious areas. In a study on the Upper Anacostia River Basin in Maryland, Ragan and Jackson

[8] demonstrated the suitability of using Landsat-derived land use data for calculating synthetic flood-frequency relationships. The Landsat-derived results were compared to relationships developed from a conventional approach using air photos.

In early work with remote-sensing data, Jackson *et al.* [9] demonstrated that land cover (particularly percent imperviousness) could be used effectively in the U.S. Army Corps of Engineers [10] STORM model. In connection with the same study, Jackson and Ragan [11] used Bayesian decision theory to demonstrate that computer-aided analysis of Landsat data was highly cost effective.

Slack and Welch [12] demonstrated that SCS *RCN*'s could be developed in a cost-effective manner for a primarily agricultural watershed in Georgia. Ragan and Jackson [8] modified the land-cover requirements for the SCS procedure for suburban areas so that Landsat data could be used. The *RCN*'s developed from the Landsat data closely matched those obtained from a conventional approach based on air-photo analysis. Synthetic flood frequencies developed from the two procedures were essentially identical. Bondelid *et al.* [13] developed a software package and user's manual to estimate *RCN*'s efficiently from Landsat data.

C. Snow Hydrology and Water Supply Forecasting

Water supply forecast models for the western United States have typically been of the multiple-regression form.

$$Y = a + b_1x_1 + b_2x_2 + b_3x_3 + \dots + b_nx_n$$

where Y is the runoff volume for the forecast period, X_1, \dots, X_n are the snow water contents at each of n snow courses. The coefficients a and b_1, \dots, b_n are developed from empirical data. Other variables, such as fall precipitation, base flow, etc., have been included in specific models. The areal extent of snow cover has not generally been used because data to define it have not been available except in certain case studies.

Leaf [14] used aerial photographs to develop relationships between snow cover and accumulated runoff for some Colorado watersheds. He also showed that sequential photos showing snow-cover depletion relationships could be used to help estimate the timing and magnitude of snow-melt peaks.

Since about 1973, the National Oceanic and Atmospheric Administration (NOAA) weather and Landsat satellites have provided a visible and infrared data base of snow cover. With these data available, procedures for analyzing the data have been developed [15]. NOAA has been using satellite data to map mean monthly snow cover over the Northern Hemisphere [16].

Some of the first applications of satellite data were done by Rango *et al.* [17]. They developed a regression model for snow melt in the Indus River basin. This study demonstrated the utility of satellite snow-cover data for large areas with little or no data base. Aircraft and Landsat snow-cover data were combined to develop a long-term data base in California. The addition of snow-cover area

considerably reduced the seasonal runoff forecast error for the King's and Kern River Basins [17].

In the Pacific Northwest, satellite snow-cover data are presently being used operationally in the Streamflow Synthesis and Reservoir Regulation (SSARR) model. In test cases for five basins over a six-year period, the addition of satellite snow-cover data to the model resulted in a definite but statistically insignificant improvement [18].

Landsat imagery was used to calculate snow-cover areas for six basins in Colorado over the period of 1973–1978 [19]. They concluded that forecast error can be reduced on the order of 10 percent by using snow-cover data derived from the satellite.

In California, two areas were studied by comparing satellite-derived snow-cover areas with conventional snow data and by incorporating snow-cover areas into the State's forecasts [20]. Results indicated potential improvement in the forecast accuracy by using snow-cover area, particularly in areas where conventional snow data were limited.

Martinec [21] developed a snowmelt runoff model that uses snow-cover area and temperature as input data. Rango and Martinec [22] have demonstrated that this model can be successfully used on basins as large as 500 km² by using Landsat data to determine the snow-cover area. Using this approach they were able to simulate seasonal volumes within 5 percent of actual values and were able to explain approximately 85 percent of the variation in daily runoff for basins in the Wind River Mountains in Wyoming.

D. Flood and Floodplain Mapping

The area inundated by floods and floodplains can be effectively mapped with remotely sensed data. Satellite data such as that from Landsat can be used to define coverage of a large river basin but may have some limitations on small basins because of resolution. Infrared photography, thermal infrared data, and multispectral scanner data have all been successfully used to map the areal extent of flooding. These applications depend upon measuring changes in reflectivity caused by standing water, high soil moisture, moisture-stressed vegetation, and changes from ambient temperatures. Flooding effects last for some time after inundation and can be detected up to two weeks after the passage of a flood. A number of studies using Landsat data and infrared photography have been reported in a series of papers related to this subject which can be found in the *Water Resources Bulletin*, vol. 10, no. 5, 1974. In spite of the coarser resolution (900 m versus 80 m for Landsat), the NOAA satellite thermal infrared sensor has proved effective in measuring areas of flood inundation [23], [24]. In addition, the NOAA satellites have the advantage of more frequent coverage (twice daily average versus 18-day coverage for Landsat).

Floodplains have been delineated using remotely sensed data and inferring the extent of the floodplain from vegetation changes or some other features commonly associated with floodplains. Rango and Anderson [25] have developed a list of indicators that can be used to infer floodplains from Landsat data. In a more recent study,

Sollers *et al.* [26] examined multispectral aircraft and satellite classifications of land cover features indicative of flood plain areas. They concluded that satellite data can be used to delineate flood-prone areas in agricultural and limited development areas but may not give good results in areas with a heavy forest canopy. The remotely sensed data may best be used for preliminary planning and for monitoring flood plain activities with time.

V. FUTURE DIRECTIONS FOR REMOTE SENSING IN HYDROLOGY

To date, most remote-sensing applications have consisted of fairly direct extensions of photogrammetry. However, using information from specific spectral bands to infer land-use properties is an example of remote-sensing information used as a unique data source or measurement. The spectral classification used by Bondelid *et al.* [13] is an example of this. Fortunately, we appear to be on the threshold of major new breakthroughs in the uses of remote sensing data. These fall into four areas:

1) Measuring System States: Use of electromagnetic radiation outside of the visible range such as thermal infrared and microwave for their unique responses to properties important to hydrology.

2) Area versus Point Data: The use of data representing an area in which the spatial variability of specific parameters of the area have been integrated.

3) Temporal Data: The potential for frequent measurement to develop time series of changes in given parameters and to monitor the dynamic properties in hydrology.

4) New Data Forms: The merging of several data sets of different wavelengths, polarizations, look angles, etc. to provide specific measurements of hydrologic parameters developed from the unique characteristics of remote sensing.

Each of these areas presents a unique opportunity for hydrologists to apply remote sensing in ways other than simple extensions of photogrammetry. Remote sensing can produce a complex measurement that is simultaneously observing several factors. It is also giving us a view that is uncommon to our past thinking in that it looks at a relatively large area and somehow integrates information from the entire scene. The challenge is to learn how to use this information and to understand it. To do this we must develop new concepts and challenge our usual way of conceptualizing hydrologic processes. Some areas of current research and areas of opportunity are discussed below.

A. Monitoring System States

One of the more exciting aspects of remote sensing for hydrologists is the potential for measuring and monitoring the state of the hydrologic system. The major state variables that appear to be useful are the soil moisture, snow water content, snowpack condition, frozen soils, and temperature. For the most part, hydrologists have modeled the hydrologic system pretty much as a "black box," using only input data (usually rainfall and maybe potential evap-

oration) and the output hydrograph. The unit hydrograph is a good example of a hydrologic "black box." The development of the comprehensive hydrologic model such as the Stanford Model [27] exposed the interior of the black box and subdivided the rainfall-runoff process into a number of physical processes. However, from a systems point of view, this type of model was still pretty much a black box because there were no provisions for monitoring or measuring any system states.

Attempts to use ancillary data such as soil moisture to improve model performance have not been very successful. For the most part this is because existing models represent the soil in a way to make the model work and have not considered the possibility of independent determination of soil moisture or soil parameters. Morton [28] makes the point that our models attempt to make reality conform to our own concepts. He presents the argument that the commonly used simulation models require assumptions that cannot be supported by theory or empirical studies. For the most part, he claims, the simulation models stress mathematical tractability and attempt to make reality conform to conventional wisdom. Morton [28] proposes an analytical approach based on spatial averages of the major water balance components. He suggests independent estimates of areal evapotranspiration because spatial estimates of changes in storage (soils, swamps, rocks) are too costly to contemplate even for a small basin. However, this may not be the case with remote sensing inasmuch as spatial changes in basin storage in the form of soil moisture can be measured.

Snow, the amount and its condition, are important inputs to models that predict the timing and amount of snowmelt runoff. Like soil moisture, microwave data appear very promising to the snow hydrologist. Not only can a microwave sensor be an all-weather instrument because it penetrates cloud cover, it can also penetrate the snow pack, which presents one with the opportunity of inferring many of the properties of the snow pack and the underlying soil. These include depth and water content as well as the degree of ripeness, crystal size, and the presence of liquid water in a melting snow pack. As with soil moisture, the microwave measurement reflects several characteristics at once.

Frozen soils are another system state that, if known, would be extremely useful to hydrologists. With microwave remote sensing we can differentiate between frozen and nonfrozen soils. For a given soil moisture, the dielectric constant changes dramatically when the soil water changes from a frozen to a liquid state. Thus we have the potential for determining remotely whether or not a soil is frozen. This should greatly benefit the people responsible for flood forecasting, particularly in the upper mid-western United States. However, I am not sure that we know how to use this information. How many of our prediction models are truly distributed so that they can use information that tells us the soils in certain areas of a watershed are frozen? How do we change our runoff coefficients or infiltration models to account for frozen soils?

How can we treat areas that are partially frozen and partially frost free (like south-facing slopes)? Can we determine what type of frost is present (concrete versus columnar) and assign infiltration rates to each? These are questions that must be answered before we realize the benefits possible from this measurement.

Surface temperatures are an additional system state that may prove useful to hydrologists. Satellite measurements of surface temperature fields offer the potential for energy budget studies over large complex areas. Dodd [29] used Heat Capacity Mapping Mission (HCMM) data in combination with a numerical model of the boundary layer proposed by Carlson and Boland [30] to estimate the spatial distribution of thermal inertial, moisture availability, and the sensible and evaporative heat fluxes. The approach was tested over two urban areas, Los Angeles and St. Louis. Recent research by Price [31] suggests the potential for using remotely sensed thermal data for assessing the surface moisture budget. In this study analytical expressions were derived, with a diurnal correction, that relate mean evaporation rate and a soil moisture parameter to surface temperature of bare soils. The possibility of determining the spatial distribution of evaporative flux or moisture availability for complex areas has many potential uses in hydrology, agriculture, forestry, and climatology. Much work needs to be done, particularly in improving the boundary layer models and understanding the edge effects caused by land use changes and the spatial variation of roughness length.

Using system-state data will require new models developed to incorporate the new data types. Such models would structurally resemble contemporary simulation models but would be more capable of accounting for spatial variability and changes. Also, the subprocess algorithms (infiltration, evapotranspiration, etc.) would be designed to use remote-sensing data as well as the more typical inputs. Research being done at the Remote Sensing Systems Laboratory at the University of Maryland in developing a remote-sensing-based hydrologic model [32] has demonstrated the potential. This model is similar in structure to other watershed models such as the Stanford Model, but more of its parameters are physically based in the sense that data to describe them can be obtained through remote sensing. Another feature of this model is the use of a geographic information system (GIS) as a data management tool to produce the input data in a useable format. The GIS assimilates remote-sensing data and the historically more common point data and provides a spatially distributed framework for the model.

B. Area versus Point Data

Remote sensing measures spatial information rather than point data. To some, this is a deficiency because they would like to reproduce the point data they are comfortable with. I would suggest this is because our concepts and models have been developed from a point concept, i.e., raingage, soil column, and soil moisture access tube. Apparently there is much more information in a remote-

sensing scene, and it may be much more valuable than a point measurement. We simply have to learn what information is there and how to use it. This may require developing new concepts and models to accommodate this type of information. As a mental exercise, consider how you would develop a hydrologic model if you had only remotely sensed data, had no schooling in traditional hydrology, and had no awareness of raingages, soil column models, and similar point concepts or measurements. The high degree of understanding we have developed for the movement of water down through a soil profile is a case in point. I suggest that by concentrating on details only in the vertical direction, you have been looking at the wrong question. It seems to me that variability in the horizontal plane may be hydrologically made more significant than anything we have been studying in the last few decades. Remote sensing, and its ability to measure the response from an area, is potentially one way to approach this problem.

C. Temporal Data

Remote-sensing data from a satellite platform can provide unique time series data for hydrologic use. The actual frequency of observation can vary from continuous to once every two weeks or so, depending upon the sensors and type of orbit. This approach is appealing because it may be a very cost-effective method to monitor various hydrologic states over very large areas.

Most continuous simulation models are mass balance-type models, taking rainfall (or snowmelt) as input and after storage and losses, routing it to stream flow. The stored water defines the state of the system and, as such, controls the rate of sequential processes and events. Since each successive computation is based on the previous state of the system, errors in the predicted output often get larger with time. How well could we improve our prediction if we could check our system periodically and update our predictions? Repetitive measures of soil moisture used as feedback to the model could do this. Improved prediction accuracy may have large tangible benefits.

A recent study by Jackson *et al.* [33] demonstrated how possible applications of repetitive remote measurements of soil moisture might be used. They discussed how these areal data may be used to calibrate soil and vegetation parameters and to correct errors resulting from point measurements of precipitation. In the study they demonstrated how soil moisture observations are useful in calibration and updating the state of the system. However, it was also pointed out that the model structure itself may preclude a valid analysis of the value of soil-moisture measurements or the frequency needed to improve the simulations. One must carefully choose the model to be used in this type of study; it may be necessary to develop a new model or make significant modifications to existing models.

D. New Data Forms

The spatial and temporal possibilities of remote-sensing data coupled with direct measurement of hydrologic state

variables may lead to an entirely new type of hydrologic data or model parameters. The use of remote sensing to determine land use for the SCS RCN and other runoff coefficients was reviewed in an earlier section. Although used as an extension of photogrammetry, these examples did illustrate the use of characteristics of specific spectral bands to infer the land-use properties. We may be able to determine runoff characteristics directly because a remote-sensing measurement potentially can integrate several features into one response.

The response of different wavelengths is determined by the surface and near surface of the target. This measured response is a composite response of several individual features. For example, microwave brightness temperature is affected by surface roughness, grain size of the soil, vegetation cover, and soil moisture. Each of these has a different effect, and this effect varies with wavelength, angle of incidence, and polarization. Therefore, any one microwave measurement is an integrated measure of these effects as well as a spatial sample. These features are the same watershed characteristics that are used to describe the hydrologic characteristics of a watershed, i.e., soil cover or management practice and antecedent moisture.

It is possible that remote sensing in the microwave area can give us a direct measure of runoff potential or a runoff coefficient. Blanchard *et al.* [34] have had some success in determining a SCS RCN for some watersheds in Texas. In their study using an airborne passive microwave imaging scanner, they investigated the relationship between RCN and the antenna temperature differences for two flights over the same watersheds. Recent research by Zevenbergen *et al.* [35] showed high correlations between Landsat-derived soils or vegetation indices and RCN for rangelands. This work suggests that a soil-cover complex may be a good estimate of potential runoff in natural range areas. This type of study suggests that we should consider the remote-sensing measurement as a direct measure of runoff potential in the same sense as an infiltrometer directly measures infiltration. Use of several different wavelengths, polarizations, etc., may provide all the information we need to predict runoff for a fairly large area. To do so may require that hydrologists develop some new concepts or models to use this type of information.

The spatial and temporal measurement of soil moisture may lead to an entirely new types of hydrologic data or model parameters. The key to this approach would be to examine changes in a watershed state with time series remotely sensed data. Observations of how a watershed soil moisture changes during a drying cycle of several days (10 or so) may provide new insight into the storage changes in a watershed. It may also give one insight into the hydrologic performance, rather than hydrologic characteristics, of soils. The difference between hydrologic performance and characteristics would be that a hydrologic characteristic would be analogous to a lab measurement which has no context with spatial variability or topographic location within a basin. The hydrologic performance of a soil, on the other hand, would be a quantifiable

characteristic that reflects not only the physical characteristics of the soil but also how it behaves hydrologically with the basin. Its spatial distribution with respect to elevation, flowing streams, and other soils would combine to define its hydrologic performance.

VI. FUTURE CONSTRAINTS

All these potential approaches to improving our hydrologic knowledge exist. There have been enough data, truck experiments, aircraft flights, and space platforms to whet our appetites. Unfortunately, we apparently are caught in a Catch-22 situation. We need to be able to demonstrate that these remote sensing data will indeed improve our hydrologic knowledge and improve hydrologic applications in order to justify specific instrumentation on some type of aircraft or space platform. However, we need these platforms and instruments to demonstrate the utility of the data.

What is needed is a commitment to put some of these instruments into space [36] so that the hydrologic procedures can be developed. Our work to date has highlighted the potential for remote sensing in hydrology. Improved performance of our hydrologic procedures and models is pretty much at a standstill because of a lack of the proper types and amounts of data. The integrated Earth observation system being planned by NASA [37] would go a long way to provide these types of data. We need to encourage the development of this program and even speed up its development (planned for flight in the 1990's). I think we know enough about wavelengths, incident angles, and resolution to come up with a sound HYDROSAT package. It may not be the optimal system, and undoubtedly the characteristics of future systems will change from what we learn. In the meantime we need to anticipate how we could use such data with aircraft experiments and simulated data.

REFERENCES

- [1] V. T. Chow, Ed., *Handbook of Applied Hydrology*. New York: McGraw-Hill, 1964.
- [2] R. H. McCuen, and W. J. Rawls, "Classification of evaluation of flood flow frequency estimation techniques," *Water Res. Bull.*, vol. 15, no. 1, pp. 88-93, 1979.
- [3] Water Resources Council, Hydrology Committee, "Estimating peak flow frequencies for natural ungaged watersheds—A proposed nationwide test," U.S. Water Resources Council, Washington, DC, 1981.
- [4] F. Naef, "Can we model the rainfall-runoff process today?" *Hydrologic Sci. Bull.*, vol. 26, no. 3, pp. 281-289, 1981.
- [5] World Meteorological Organization, "Intercomparison of conceptual models used in operational hydrological forecasting," WMO Operational Hydrology Rep. 7, 1975.
- [6] K. M. Loague and R. A. Freeze, "A comparison of rainfall-runoff modeling techniques on small upland catchments," *Water Resources Res.*, vol. 21, no. 2, pp. 229-248, 1985.
- [7] U.S. Soil Conservation Service, *SCS National Engineering Handbook, Section 4: Hydrology*, U.S. Dep. of Agriculture, Washington, DC, 1972.
- [8] R. M. Ragan and T. J. Jackson, "Runoff synthesis using Landsat and the SCS model," *Proc. ASCE*, paper 15387, vol. 106, no. HY5, pp. 667-678, 1980.
- [9] T. J. Jackson, R. M. Ragan, and W. N. Fitch, "Test of Landsat-based urban hydrologic modeling," *ASCE J. Water Resources, Planning and Management Division*, vol. 103, no. WR1, pp. 141-158, 1977.
- [10] U.S. Army Corps of Engineers, "Urban storm water runoff STORM,"

- Hydrologic Eng. Center, Davis, CA, Computer Program 723-58-L2520, 1976.
- [11] T. J. Jackson and R. M. Ragan, "Value of Landsat in urban water resources planning," *ASCE J. Water Resources, Planning and Management Division*, vol. 103, no. WR1, pp. 33-46, 1977.
- [12] R. B. Slack and R. Welch, "Soil conservation service runoff curve number estimates from Landsat data," *Water Resources Bull.*, vol. 16, no. 5, pp. 887-893, 1980.
- [13] T. R. Bondelid, T. J. Jackson, and R. H. McCuen, "A computer based approach for estimating runoff curve numbers using Landsat data," *AgRISTARS Conservation and Pollution Tech. Rep. CR-R1-04040*, 1981.
- [14] C. F. Leaf, "Aerial photographs for operational streamflow forecasting in the Colorado Rockies," in *Proc. 37th Western Snow Conf.* (Salt Lake City, UT), 1969.
- [15] A. Rango and K. I. Itten, "Satellite potentials in snowcover monitoring and runoff prediction," *Nordic Hydrology*, vol. 7, pp. 209-230, 1976.
- [16] D. R. Wiesnet and M. Matson, "Monthly winter snowline variation in the Northern Hemisphere from satellite records, 1966-1975," *NAT. Environ. Satellite Service*, Washington, DC, NOAA Tech. Memo NESS 74, 1975.
- [17] A. Rango, J. F. Hannaford, R. L. Hall, M. Rosenzweig, and A. J. Brown, "The use of snow covered area in runoff forecasts," NASA Goddard Space Flight Center, Greenbelt, MD, Document X-913-77-48, 1977.
- [18] J. P. Dillard and C. E. Orwig, "Use of satellite data in runoff forecasting in the heavily forested, cloud covered Pacific Northwest," in *Proc. Workshop on Operational Applications of Satellite Snowcover Observations*, NASA Conf. Pub. 2116, pp. 127-150, 1979.
- [19] B. A. Shafer and C. F. Leaf, "Landsat derived snowcover as an input variable for snowmelt runoff forecasting in central Colorado," in *Proc. Workshop on Operational Applications of Satellite Snowcover Observations*, NASA Conf. Pub. 2116, pp. 151-169, 1979.
- [20] A. J. Brown, J. F. Hannaford, and R. L. Hall, "Application of snow covered area to runoff forecasting in selected basins of the Sierras, Nevada, California," in *Proc. Workshop on Operational Applications of Satellite Snow Cover Observations*, NASA Conf. Pub. 2116, pp. 185-200, 1979.
- [21] J. Martinec, "Study of snowmelt-runoff process in two representative watersheds with different elevation range," in *Results of Research and Experimental Basins, Proc. Wellington Symp.*, publ. 96, pp. 29-39, 1970.
- [22] A. Rango and J. Martinec, "Application of a snowmelt-runoff model using Landsat data," *Nordic Hydrology*, vol. 10, pp. 225-238, 1979.
- [23] C. P. Berg, M. Matson, and D. R. Wiesnet, "Assessing the Red River of the north 1978 flooding from NOAA satellite data," in *Proc. Pecora 5 Symp.* (Sioux Falls, SD), pp. 309-315, 1979.
- [24] G. Tappan, N. C. Howath, P. C. Doraiswamy, T. Engman, and D. W. Goss, "Use of NOAA-N satellites for land/water discrimination and flood monitoring," *AgRISTARS Rep. EW-L3-04394*, 1983.
- [25] A. Rango and A. T. Anderson, "Flood hazard studies in the Mississippi River Basin using remote sensing," *Water Resources Bull.*, vol. 10, no. 5, pp. 1060-1081, 1974.
- [26] S. C. Sollers, A. Rango, and D. L. Henninger, "Selecting reconnaissance strategies for flood plain surveys," *Water Resources Bull.*, vol. 14, no. 2, pp. 359-373, 1978.
- [27] N. H. Crawford and R. K. Linsley, "Digital simulation in hydrology: Stanford watershed model IV," Stanford University, Tech. Rep. no. 39, 1966.
- [28] F. I. Morton, "Integrated basin response—A problem of synthesis or a problem of analysis," in *Proc. Canadian Hydrology Symp.* (Associate Committee on Hydrology, Natl. Res. Council, Canada), pp. 361-363, 1982.
- [29] J. K. Dodd, "Determination of surface characteristics and energy budget over an urban-rural area using satellite data and a boundary layer model," Master's thesis, The Pennsylvania State Univ., 1979.
- [30] T. N. Carlson and F. E. Boland, "Analysis of urban-rural canopy using a surface heat flux/temperature model," *J. Appl. Meteorol.*, vol. 17, no. 7, pp. 998-1013, 1978.
- [31] J. C. Price, "Use of remotely sensed infrared data for inferring environmental conditions from surface characteristics and regional scale meteorology," in *Proc. 1981 Int. Geosci. Remote Sensing Symp.* (Washington, DC), pp. 1195-1201, 1981.
- [32] J. R. Groves and R. M. Ragan, "Development of a remote sensing based continuous streamflow model," in *Proc. 17th Int. Symp. Remote Sensing Environ.* (Ann Arbor, MI), pp. 447-456, 1983.
- [33] T. J. Jackson, T. J. Schumge, A. D. Nicks, G. A. Coleman, and E. T. Engman, "Soil moisture updating and microwave remote sensing for hydrologic simulation," *Bull. Int. Assoc. Scientific Hydrology*, vol. 26, no. 3, pp. 305-319, 1981.
- [34] B. J. Blanchard, J. W. Rouse, Jr., and T. J. Schumge, "Classifying storm runoff potential with passive microwave measurements," *Water Resources Bull.*, vol. 11, no. 5, pp. 892-907, 1975.
- [35] A. W. Zevenbergen, "Runoff curve numbers for rangeland from Landsat data," Hydrology Lab. Tech. Rep. HL85-1, 1985.
- [36] A. Rango, "Assessment of remote sensing input to hydrologic models," *Water Resources Bull.*, 1985.
- [37] NASA, "National Aeronautics and Space Administration, Earth observing system," Goddard Space Flight Center, Greenbelt, MD, NASA Tech. Memo. 86129, 1984.

*



Edwin T. Engman received the B.E. and M.S. degrees in agricultural engineering from Cornell University, Ithaca, NY, and the Ph.D. degree in civil engineering from Pennsylvania State University, University Park, PA.

Before assuming his current position in 1976, he spent 13 years with the Agricultural Research Service as a Research Hydrologist in Vermont and subsequently as the Director of the Northeast Watershed Research Center in Pennsylvania. In addition, he worked for two years as a Principal Hydrologist with the NUS Corporation in Maryland. Since 1976, his research has concentrated on remote-sensing applications in water resources, emphasizing use of microwave data for soil-moisture studies.

Passive Microwave Soil Moisture Research

THOMAS SCHMUGGE, MEMBER, IEEE, PEGGY E. O'NEILL, MEMBER, IEEE, AND JAMES R. WANG

Abstract—During the four years of the AgRISTARS Program, significant progress was made in quantifying the capabilities of microwave sensors for the remote sensing of soil moisture. In this paper we discuss the results of numerous field and aircraft experiments, analysis of spacecraft data, and modeling activities which examined the various noise factors such as roughness and vegetation that affect the interpretability of microwave emission measurements. While determining that a 21-cm wavelength radiometer was the best single sensor for soil moisture research, these studies demonstrated that a multisensor approach will provide more accurate soil moisture information for a wider range of naturally occurring conditions.

I. INTRODUCTION

AT THE START of the AgRISTARS Program in 1980, much was known about the basic sensitivity of microwave sensors to soil moisture variations, although the importance of other soil and scene parameters had not yet been determined. Therefore, the major thrust of the AgRISTARS Soil Moisture Program was to quantify these noise sources and to demonstrate the utility of microwave sensors to soil moisture research. The basis for microwave remote sensing of soil moisture is the strong dependence of the soil's dielectric properties on its moisture content due to the large contrast between the dielectric constant of water (~ 80) and that of dry soil (~ 3). The dependence of the dielectric constant on moisture content was modeled as a function of soil texture by Wang and Schmugge [1]. Subsequent improvements in our understanding of the dielectric properties of soils were made in this program and were recently reported by the University of Kansas group [2], [3]. This dependence of the soil's dielectric properties on moisture content can be observed with either passive or active microwave sensors through its effect on the soil's emissivity and reflectivity. The progress made with active microwave sensors will be documented in another paper in this issue [4].

The change in the soil's dielectric constant based on its water content produces a change in its emissivity from about 0.95 when dry to 0.6 or less when wet, which implies a change of about 30 percent in the natural emission from the soil. At microwave wavelengths, the intensity of this emission is essentially proportional to the product of the temperature and the emissivity of the surface (Rayleigh-Jeans approximation). This product is commonly referred to as the microwave brightness temperature (T_B).

The brightness temperature observed by a radiometer at a height H above the ground is

$$T_B = \tau(H) * (rT_{\text{sky}} + (1 - r) T_{\text{soil}}) + T_{\text{atm}} \quad (1)$$

where r is the surface reflectivity and $\tau(H)$ is the atmospheric transmission. The first term is the reflected sky brightness temperature which depends on wavelength and atmospheric conditions; the second term is emission from the surface ($1 - r = e$, the emissivity); and the third term is the contribution from the atmosphere between the surface and the receiver. At the longer wavelengths best suited for soil moisture sensing, the atmospheric effects are minimal. Thus, (1) can be written as

$$T_B = (1 - r) T_{\text{soil}} = eT_{\text{soil}} \quad (2)$$

Thermal microwave emission from soils is generated within the soil volume. The amount of energy generated at any point within the volume depends on the soil dielectric properties (or soil moisture) and the soil temperature at that point. As the energy propagates upward through the soil from its origin, it is affected by the dielectric gradients along the path of propagation. In addition, as the energy crosses the surface, it is reduced by the effective transmission coefficient (emissivity) of the surface, which is determined by the average dielectric characteristics of the soil in a transition layer just below the surface. It is the thickness of this layer which determines the actual soil moisture sampling depth and it is the properties of this layer which have the dominant effect on the emitted intensity. Theoretical studies [5], [6] have indicated that this transition layer is a few tenths of a wavelength thick or about 2 to 5 cm at a 21-cm wavelength. The field verification of this depth was done as part of the AgRISTARS program and will be described in Section II.

Field and aircraft experiments up to 1980 had demonstrated the basic sensitivity of radiometric measurements to surface layer soil moisture. These experiments also indicated that there are a number of factors other than soil moisture which influence the intensity of the emission from the soil; these include, among others, surface roughness, vegetation cover, and soil texture. A review of the approximate status of microwave sensing of soil moisture was given in the paper by Schmugge [7] presented at the ERIM Symposium of that year. Thus, at the beginning of the AgRISTARS program we were able to identify a number of questions which should be addressed in the program. Those relevant to passive microwave systems are:

Manuscript received April 1, 1985; revised August 1, 1985.
The authors are with the Space and Earth Sciences Directorate, NASA
Goddard Space Flight Center, Greenbelt, MD 20771.
IEEE Log Number 8406231.

What are the optimum wavelengths or combination of wavelengths for microwave and thermal IR systems?

What is the soil moisture sampling depth as a function of wavelength?

Can moisture gradient information be obtained by multiwavelength systems?

What are the limits on the accuracy of the soil moisture estimation imposed by:

- surface roughness
- vegetative cover
- soil heterogeneity
- incident angle dependence
- surface cover heterogeneity
- atmospheric effects for space systems
- mixed scene in the large footprint of spaceborne sensors.

In the course of the four years that the AgRISTARS program was active, measurements and analyses were performed which addressed, at least indirectly, all these questions except the last two. As discussed above, it was felt that the atmospheric effects are not significant at the microwave wavelengths relevant for soil moisture sensing. The studies of the effects of mixed scenes within a spaceborne radiometer footprint were scheduled for later in the program and were not performed. There had been one such study done prior to the AgRISTARS program [8]. In this paper, we will summarize the progress made in addressing these questions through the field and aircraft measurements, analysis of spacecraft data, and modeling studies.

II. FIELD MEASUREMENTS

A. Bare Soil

The purpose of the field measurements program is to perform detailed studies of the basic interaction of the electromagnetic radiation with the soil surface and the dependence of the subsequent emission on various soil properties. Field measurements have the advantage that only a small plot (e.g., 20 × 20 m) is observed which can be relatively well documented. As a result, the effects of changes in the surface parameters can be studied under calibrated conditions. Field programs have been performed by the Remote Sensing Center of Texas A&M University during several years of the AgRISTARS program and as a cooperative effort of GSFC and the USDA Hydrology Laboratory of the Beltsville Agricultural Research Center (BARC) during the four years 1979–1982.

One of the early significant results of these experiments was the verification that the soil moisture sampling depth was only a few tenths of a wavelength. This was done by the group at TAMU by studying the drydown of a moist soil with both radiometric and gravimetric (0–2, 0–5, 0–9-cm layers) measurements of the surface soil moisture [9]. Initially, the three layers dry at the same rate, but after three days they begin to diverge with the surface layer drying faster. These observations were compared with the

temporal variation of surface soil moisture estimated from the radiometric measurements made at 1.4, 5.0, and 10.7 GHz. Again, results at the three frequencies indicate drying at the same rate initially but then diverging after only about 2 days. The two higher frequency estimates show a dry value of about 8 percent on day 12, which the lowest frequency and the 0–2-cm gravimetric measurement did not reach until day 14. This result indicates that the sampling depth for the 1.4-GHz radiometer is between the 2- and 5-cm level.

Bare soil measurements were made at BARC as functions of angle between 10° and 70° at both *L* (1.4 GHz) and *C* (5 GHz) bands for several years over bare fields having two different soil textures [10]–[12]. Examples of the data are given in Fig. 1 for *L*- and *C*-bands at 10°. These plots show emissivity and normalized brightness temperature (NTB) versus soil moisture in a 0–2.5-cm layer. NTB is obtained by multiplying the emissivity by 300, so that the plots can be compared more directly with the observations. The data are from two fields with different soil textures. Most of the data were from a sandy loam (sand = 68 percent, clay = 11 percent) field which had a relatively smooth surface and the remainder were from a loam (sand = 34 percent, clay = 24 percent) plot which had a somewhat rougher surface. The data from the two soils are represented by different symbols (* = sandy loam and x = loam). The dashed curves are the calculated emissivities from the Fresnel equations for the two soils assuming a smooth surface. The lower one is for the sandy loam. The solid line is the regression fit to these data. At *L*-band, the calculated emissivities are at most 0.05 below the observed regression line, with much of the data lying above the calculated curves. We believe that the higher observed values are primarily due to the surface roughness of these fields which tends to increase the emissivity of the surface [13]. The range of emissivities is about the same for the calculations (0.6 to 0.9) and the observations (0.63 to 0.95). The *C*-band data behave similarly with several important differences. While the emissivities for the wet soils are about the same at the two wavelengths, they are higher at *C*-band for dry soils. This results from the fact that the sampling depth at the shorter wavelength is shallower than the soil layer measured (0 to 2.5 cm). For example, at a soil moisture of 10 percent in this layer, the *C*-band is responding to the drier soil closer to the surface. As a result, the slope and intercept of the regression line are greater at *C*-band.

For a smooth surface the emissivity in the vertical polarization will increase with increasing incidence angle out to Brewster's angle (θ_B) where the emissivity is one. The effect of soil moisture is to increase the value of θ_B ($\theta_B = \tan^{-1} \sqrt{K}$, where K is the dielectric constant) from about 62° for a dry soil to 79° for a wet soil. The net result of this is to decrease the sensitivity of the vertical polarization to soil moisture variations at the off-nadir angles.

The results of the statistical analyses of these data are presented in Table I. The values presented are the slope and intercept of the regression, the rms difference be-

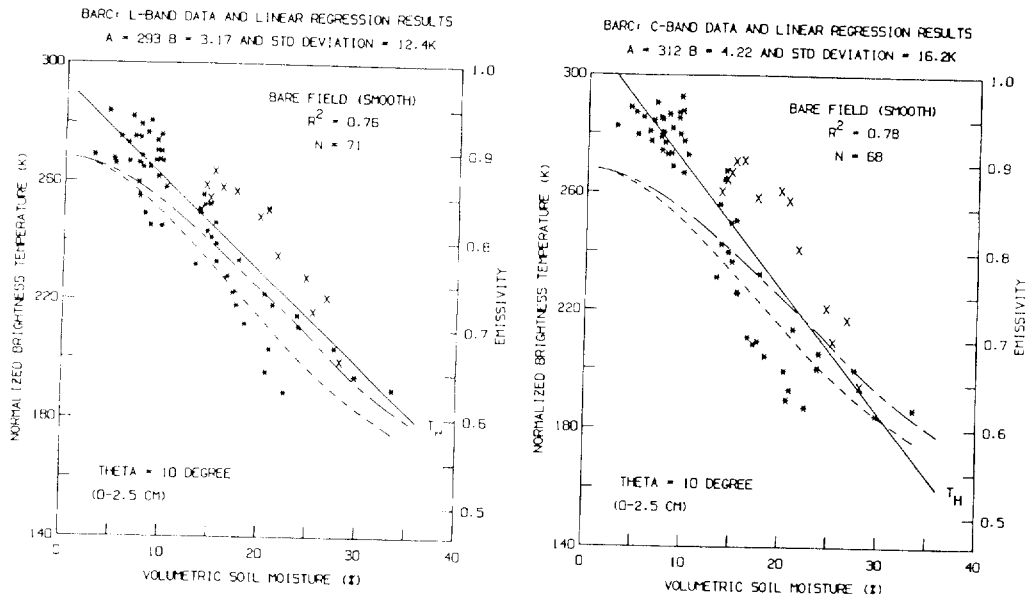


Fig. 1. Field measurements of normalized brightness temperature (NTB) or emissivity for bare smooth fields at L- and C-bands for an incidence angle of 10° . The values of the regression results are also given. A: intercept, B: slope and the rms deviation from the regression.

TABLE I

| ANGLE | L-BAND (HORIZONTAL) | | | | | L-BAND (VERTICAL) | | | | | C-BAND (HORIZONTAL) | | | | | C-BAND (VERTICAL) | | | | |
|-------|---------------------|----------------|----------------|------------------|-----------------|-------------------|-----|------|------|------|---------------------|-----|------|------|------|-------------------|-----|------|------|------|
| | N | A ¹ | B ² | STD ³ | RR ⁴ | N | A | B | STD | RR | N | A | B | STD | RR | N | A | B | STD | RR |
| 10 | 71 | 293 | 3.17 | 12.4 | 0.76 | 71 | 294 | 3.00 | 11.3 | 0.78 | 68 | 312 | 4.22 | 16.2 | 0.78 | 68 | 312 | 4.06 | 15.6 | 0.77 |
| 20 | 71 | 288 | 3.24 | 12.4 | 0.77 | 71 | 294 | 2.88 | 11.2 | 0.77 | 68 | 310 | 4.37 | 17.6 | 0.76 | 68 | 312 | 3.98 | 16.1 | 0.76 |
| 30 | 71 | 281 | 3.30 | 12.4 | 0.78 | 71 | 293 | 2.69 | 10.5 | 0.77 | 68 | 307 | 4.58 | 18.4 | 0.76 | 68 | 314 | 3.80 | 15.2 | 0.76 |
| 40 | 69 | 271 | 3.30 | 12.8 | 0.77 | 71 | 291 | 2.36 | 10.1 | 0.73 | 68 | 301 | 4.70 | 19.6 | 0.75 | 68 | 315 | 3.40 | 13.4 | 0.77 |
| 50 | 69 | 255 | 3.21 | 12.8 | 0.76 | 70 | 287 | 1.87 | 8.9 | 0.69 | 66 | 288 | 4.66 | 21.0 | 0.72 | 68 | 314 | 2.75 | 10.7 | 0.77 |
| 60 | 69 | 228 | 3.02 | 13.1 | 0.73 | 71 | 277 | 1.15 | 6.8 | 0.59 | 68 | 266 | 4.52 | 22.8 | 0.67 | 68 | 305 | 1.81 | 6.9 | 0.78 |
| 70 | 71 | 188 | 2.49 | 12.4 | 0.67 | 70 | 249 | 0.05 | 6.3 | 0.00 | 68 | 232 | 3.92 | 23.1 | 0.59 | 68 | 276 | 0.30 | 4.7 | 0.17 |

BRIGHTNESS TEMPERATURES NORMALIZED TO: 300.0 K. THE SURFACE ROUGHNESS PARAMETER, H = 0.00

¹A = intercept

²B = slope

³STD = standard error

⁴RR = r-squared value

tween the data and the regression line, and the r -squared value of the regression. There are several factors which should be noted:

- 1) the monotonic decrease in sensitivity for the vertical polarization with increasing angle, which is due to the Brewster angle effect;
- 2) the almost constant slope and r -squared values for the horizontal polarization out to 50° ; and
- 3) the similar behavior at C-band with the difference that the slope and intercept are higher due to the shallower sampling depth at this frequency.

B. Vegetation-Covered Soil

A vegetation layer covering the soil will absorb and scatter some of the microwave radiation incident on it. The

absorption is primarily due to the water content in the vegetation. The precise sources for the scattering are not well understood at the present time and are the subject of much current research, both experimental and theoretical.

The radiation measured by a radiometer can be expressed as the sum of three terms: the emission from the soil reduced by the vegetation and the emissions from the vegetation, both direct and that reflected from the soil surface. The strength of the emission from the vegetation will be proportional to its absorption, which is described by the optical depth (τ):

$$\tau = at \sec(\theta) \quad (3)$$

where t is the canopy thickness and a is the volume absorption coefficient which depends on the real and imag-

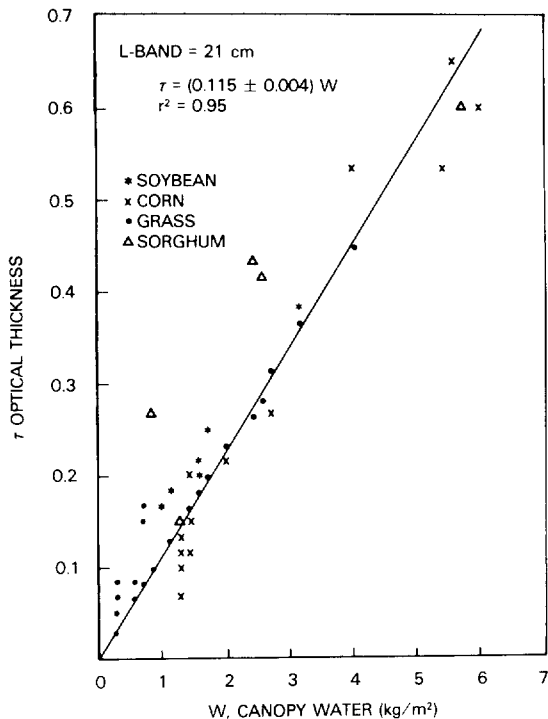


Fig. 2. Variation of optical depth (τ) determinations with vegetation water content for corn-, grass-, and soybean-covered fields [16].

inary parts of the canopy dielectric constant. Brunfeldt and Ulaby [14] have shown that the dielectric constant for the leaf portion of the canopy can be expressed in terms of its fractional volume and its dielectric constant. The fractional volume of the leaf portion of the canopy can be estimated from the leaf thickness and the leaf area index (LAI) for the canopy. The leaf dielectric constant is a strong function of plant water content. The stalk and fruit portions of the canopy are more difficult to estimate because their dimensions are comparable to the sensor wavelengths. However, since water is the dominant dielectric component of the vegetation, the optical thickness can be parameterized in terms of the canopy water content (W) given in units of kilograms per square meter to a first approximation [15].

Values for the optical depth can be estimated by comparing the observed radiation from a vegetated field with that expected for a bare field either from a model or from observations of the field after the vegetation has been stripped off. A summary of optical depth measurements obtained by these approaches is given in Fig. 2 plotted versus canopy water content [16]. It is clear that there is a strong linear dependence of the optical depth on the canopy water content.

In an analysis of the expected emission over a vegetated canopy, Jackson *et al.* [15] have shown that by assuming that the plant and soil temperatures are approximately equal the observed emissivity can be written as

$$e = T_B/T_s = 1 + (e_s - 1) \exp(-2\tau) \quad (4)$$

where e_s is the bare soil emissivity and T_s is the soil temperature. Thus, the sensitivity to soil moisture variations

is reduced by this exponential factor

$$de/dsm = \exp(-2\tau) de_s/dsm \quad (5)$$

where sm is the volumetric soil moisture. An optical thickness of about 0.7 reduces the sensitivity of microwave radiometers to soil moisture to ~ 25 percent that of bare soil. In Table I the sensitivity was $\sim 3.2K$ per unit soil moisture; thus, the presence of vegetation would reduce that to $0.8K$ per unit soil moisture which is about the limit of useful sensitivity for soil moisture measurement. This level of optical thickness is attained by a mature corn canopy, making soil moisture detection very difficult through a crop cover of this density.

C. Multiwavelength Measurements

Several experiments involved microwave measurements made at wavelengths greater than 21 cm, i.e., at 50 cm at BARC [11] and at 40 cm by a JPL group [17]. As expected, the longer wavelengths showed a greater ability to penetrate vegetation and a deeper soil moisture sampling depth. However, it was found in both experiments that the sensitivity to soil moisture variations was less at the 50-cm wavelengths than at the shorter wavelengths. For the BARC data, the sensitivity of the 50-cm brightness temperatures to soil moisture was approximately one-half that observed in the 21-cm data. For the wettest fields, the emissivity was up to 0.1 higher than that observed at either the 21- or 6-cm wavelengths. The reasons for this decreased sensitivity have not been determined. Because of this result and the problems of increased interference from man-made sources of radiation and poorer spatial resolution for a given antenna size, further studies at the longer wavelengths were not pursued.

III. AIRCRAFT EXPERIMENTS

As discussed in the previous section, microwave sensors mounted on truck platforms are used to develop soil moisture estimation algorithms based on remotely sensed data, since they allow the evaluation of factors such as soil type, roughness, and vegetation under well-controlled conditions. At the same time, complementary research has been conducted with aircraft sensors in order to examine the effects of large area coverage, scene heterogeneity, and instrument sensitivity at the lower resolutions typical of aircraft systems. While results from these experiments generally verify the basic relationships between sensor measurements and soil moisture derived from theory and the small-scale ground-based studies, they also demonstrate the limited utility of a single-sensor approach to soil moisture prediction for a wide variety of naturally occurring conditions.

A. Bare Fields

Most of the aircraft experiments utilized the sensor package flown on NASA research aircraft (primarily the C-130), which included microwave radiometers at 1.4 and 5 GHz, and microwave scatterometers at 13.3, 4.75, 1.6, and 0.4 GHz. Cameras, a thermal infrared radiometer, and a

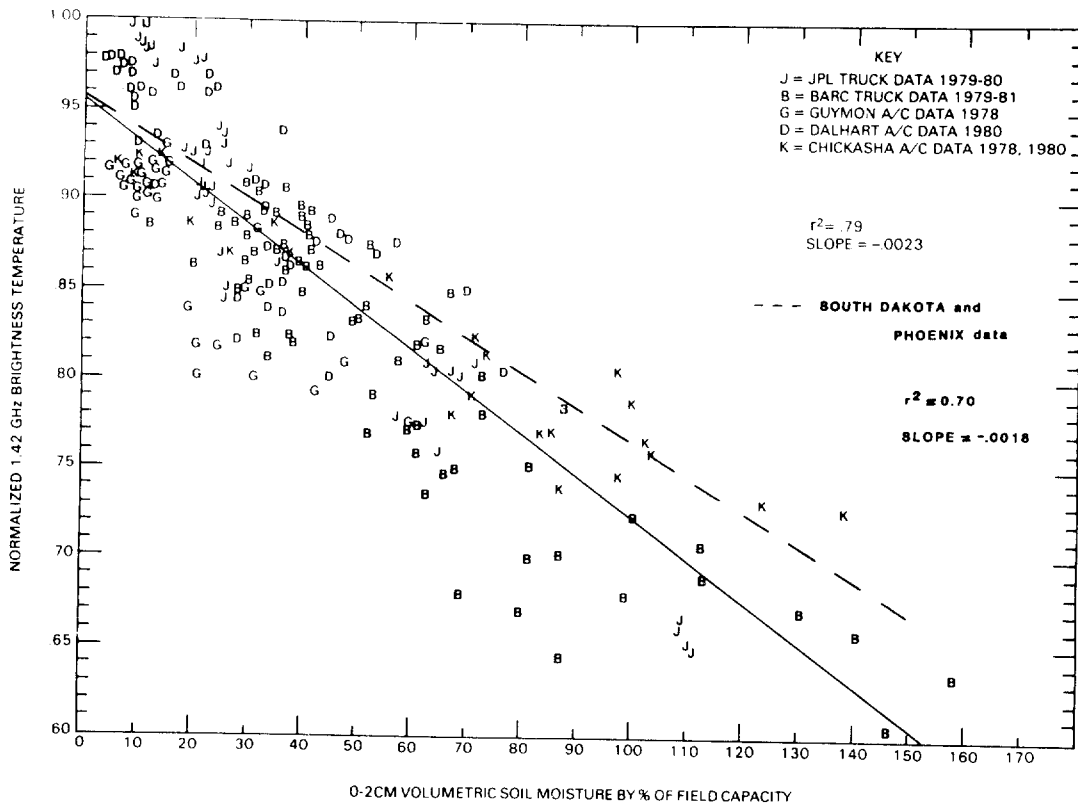


Fig. 3. Summary of truck and aircraft results at L-band for several different measurement campaigns comparing emissivity with volumetric soil moisture [28].

visible/infrared scanner were also available aboard this aircraft. Flights took place between 1976 and 1980 at a number of agricultural sites across the country, such as Hand County, South Dakota; Colby, Kansas; Chickasha, Oklahoma; Guymon, Oklahoma; Dalhart, Texas; and Taylor Creek, Florida. Field cover conditions ranged from bare and grassland pasture to crops such as wheat, milo, alfalfa, corn, and citrus trees.

In examining the data from bare and minimally vegetated fields, researchers noted strong correlations between the microwave brightness temperature and near-surface soil moisture (typically 0–2 cm or 0–5 cm depth). An example of this relationship with data from several of the aircraft experiments is presented in Fig. 3. The solid regression line is the combined result of three aircraft and two ground-based experiments, while the dashed line represents aircraft data from South Dakota and Phoenix. Normalized T_B is calculated by dividing the observed T_B by the soil temperature, and is an approximation to the soil's emissivity. At the high soil moisture levels indicated, measurements from aircraft radiometers showed higher emissivities than those from truck sensors, due to soil texture, roughness, and vegetation cover differences between the two types of test sites. (The truck experiments involved carefully prepared plots of sandy soil with smooth, bare surfaces.) Even though these factors were not corrected for in this comparison, the relationship between microwave emissivity and surface soil moisture is still quite strong.

As roughness and vegetation increased beyond minimal levels, the microwave sensitivity to soil moisture decreased, especially at higher frequencies. Even small amounts of vegetation masked underlying soil moisture variations at frequencies higher than C-band [18]. Based on an evaluation of coincident data from the different instruments, the 1.4-GHz radiometer operating at a nadir look angle was determined to be the best *single* sensor for soil moisture determination in bare fields [18]–[20].

A problem with evaluating the accuracy of soil moisture estimation algorithms derived from remotely sensed data lies in the variability of point samples of soil moisture which are averaged together to determine mean moisture levels on a per field basis. Using 1.4-GHz passive data for bare and pasture fields, numerous researchers were able to estimate volumetric soil moisture with a standard error of 4–6 percent [18], [23]–[25]. However, this level of error is approximately the same as the variation in the ground samples of soil moisture [24]. In fact, Mo and Schmutge [26] were able to reproduce the scatter in microwave observations of soil moisture in South Dakota solely through introducing error into the soil moisture measurement (with a coefficient of variation of 0.25) though a Monte Carlo simulation technique. Both studies illustrate the uncertainty in assessing the accuracy of remote sensing techniques with "ground truth" that is inherently noisy. Although an L-band radiometer has a sensitivity to surface soil moisture of 2–3K per percent volumetric soil moisture for minimally vegetated fields [27], [28], differences in

soil properties such as soil type, bulk density, and surface roughness over the larger areas typical of aircraft and satellite systems may permit quantification of only 4–5 levels of soil moisture. Relative changes in moisture content for the same site over time from repeat microwave measurements should have a better resolution.

B. Roughness

Although it is clear from the previous discussion that microwave radiometers can estimate soil moisture content for smooth, bare fields, the presence of variations in surface cover conditions such as roughness and vegetation can greatly reduce microwave sensitivity to soil moisture and introduce scatter into the emissivity/soil moisture relationship [27]. Since very few agriculturally or hydrologically important areas are always smooth and bare, it is imperative to develop techniques for removing the effects of roughness and vegetation from microwave estimates of soil moisture, preferably in a manner compatible with a remote sensing approach.

Choudhury *et al.* [13] determined that the rough surface reflectivity could be related to the smooth surface reflectivity (R_0) in the following way:

$$R = R_0 \exp(-h \cos^2 \theta) \quad (6)$$

where the h parameter is related to height variations of the soil surface. The effect of increasing h values (i.e., roughnesses) on the passive microwave response to soil moisture is to decrease the sensitivity of the microwave emissivity to the moisture variations by the “ $\exp(-h)$ ” factor in the same fashion as the vegetation in (5). Jackson *et al.* [29] used representative values of h based on the observed range of bulk density and soil moisture in their test fields and were able to reduce the standard error of their soil moisture estimate by a few percent. While this procedure is an improvement over ignoring the effects of surface roughness, it is of limited usefulness in an operational sense.

Theis *et al.* [30] used one possible approach in analyzing their aircraft data, which contained 1.6-GHz scatterometer data taken coincidentally with 1.4-GHz radiometer data. Noting that the influence of surface roughness was substantial at large incidence angles while the sensitivity of the radar backscatter (σ°) to soil moisture remained about the same, the researchers plotted σ° versus volumetric soil moisture at a 40° look angle and determined the σ° intercept for a 0-percent soil moisture level. They then used this intercept as a “quantification” of the degree of roughness in combination with the 1.4-GHz emissivity to estimate soil moisture directly. With the roughness compensation supplied by the L -band scatterometer, they were able to improve the R^2 value to 0.95, compared to $R^2 = 0.69$ obtained when predicting soil moisture from the passive data alone. Although conducted on a limited data set, the encouraging results from this study clearly point out the potential of multisensor techniques for improving microwave estimates of soil moisture.

A comparison of the different experiments raises a ques-

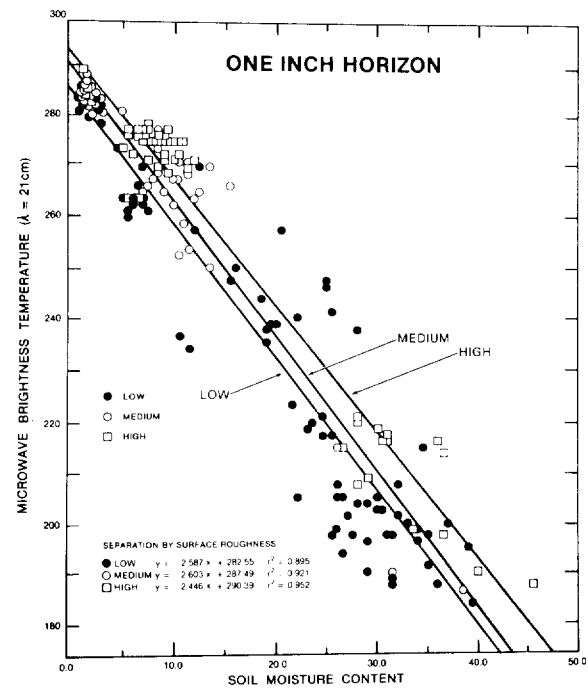


Fig. 4. L -band aircraft results over the Hand County, South Dakota, test site. The data were segregated into 3 qualitatively different roughness categories based on ground photographs.

tion about the actual magnitude of roughness effects under normal agricultural conditions. Owe and Schmugge [19] in the analysis of 1.4-GHz aircraft data obtained over an agricultural site found that on the average the roughness effects were not large (Fig. 4). They segregated the data into three roughness categories based on ground photographs of the individual fields and found that the regression slopes for T_B versus surface soil moisture were not significantly altered by the roughness but that the roughest fields were about 8K higher than the smoothest. These fields covered the range of roughnesses that might normally occur in an area which is mostly planted in small grains or in pastures. These results point out that while roughness can have a very significant effect, its naturally occurring range may not be as great as the extremes observed in prepared plots for truck measurements.

C. Vegetation

The dominant factor affecting the accurate interpretation of microwave data in terms of soil moisture information is the presence of vegetation. A vegetation canopy over a soil volume attenuates the emission of the soil and adds to the total radiative flux from the scene with its own emission (assuming that scattering is minimal at low frequencies). As frequency and incidence angle increase, the microwave sensitivity to the soil moisture underneath the vegetation is greatly reduced, depending on the canopy type and water content. Ulaby *et al.* [31] found that the vegetation loss factor was twice as great at 5 GHz than at 1.4 GHz using aircraft radiometer data from Colby, Kansas; this result was confirmed by the flights over native grass pastures at Chickasha as shown in Fig. 5 [18]. Theis *et al.* [20] noted that the effect of vegetation was much

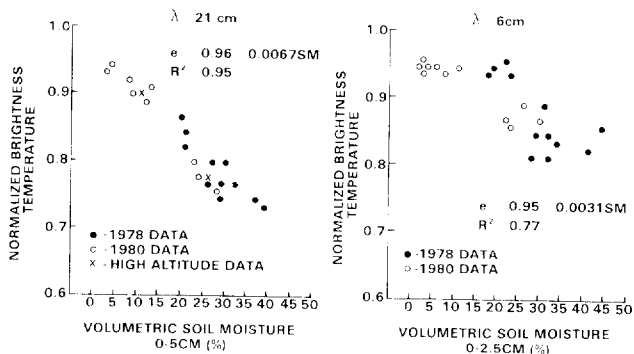


Fig. 5. Comparison of L- and C-band emissivities measured from an aircraft platform with ground measurements of soil moisture for native grass pastures in Oklahoma [18]. Note the 50-percent decrease in sensitivity at C-band.

more significant on the microwave response to soil moisture than surface roughness, especially as the plant wet biomass increased to the level of dense corn.

In an attempt to quantify the effect of vegetation on radiometric measurements of soil moisture and thus extend the usefulness of the microwave approach to a wider range of agricultural conditions, Theis *et al.* [20] calculated the perpendicular vegetation index (PVI) from visible/near-infrared data acquired at the same time as the microwave data. The PVI, which is the perpendicular distance of measured values of reflectance from the bare soil reflection line on a plot of MSS band 5 (0.6–0.7 μm) versus MSS band 7 (0.8–1.1 μm), is directly related to plant biomass in that higher PVI values correspond to higher biomass [32]. They then used the PVI in combination with 1.4-GHz emissivity values to estimate surface soil moisture directly for every test field at Guymon and Dalhart except for dense corn (PVI > 4.3). With only remotely sensed information, they were able to improve their estimates of the 0–2-cm soil moisture from $R^2 = 0.09$ to $R^2 = 0.75$ for vegetated fields. Jackson *et al.* [15] also utilized a combination of emissivity and wet biomass values to predict soil moisture under a variety of vegetation layers. Although the actual levels of biomass were known in this controlled study, the investigators expressed their belief that the same information could be obtained through visible/infrared remote sensing. Since vegetation in a given area does not change as fast as surface soil moisture, some repeat reflectance data could be used in conjunction with more frequent passive microwave measurements to estimate soil moisture through vegetation. Although the timely acquisition and registration of different types of data might present some operational challenges, the multisensor technique appears to be significantly better for soil moisture determination over a range of surface conditions than the use of a single sensor alone.

Ulaby *et al.* [33] arrived at a similar conclusion after examining active and passive microwave data from the Colby experiment. They found that the 1.4-GHz radiometer produces lower estimation errors at low soil moisture levels, while the 4.75-GHz scatterometer is more accurate at soil moistures greater than 70 percent of field capacity.

Taking advantage of the complementary nature of the two systems, a combination of a radiometer and a radar will reduce soil moisture prediction errors to less than ± 30 percent of true percent of field capacity, even under a lossy corn canopy.

In analyzing aircraft radiometer and radar data in the context of simple vegetation canopy emission and scattering models, vegetation loss factors (which describe the amount of soil signal attenuation) were found to be greater for the passive data than the active at a given wavelength [33]. This is primarily due to radiation (scattered or emitted) from the vegetation which is reflected by the soil surface. As soil moisture increases, the amount of energy reflected from the surface increases. Thus, in the passive case the increased reflectivity counteracts the decrease in emission for wet soils [34].

IV. SPACECRAFT RESULTS

Most measurements by orbiting microwave radiometers for soil moisture estimation were made at frequencies greater than 5 GHz, with a short Skylab mission with a 1.4-GHz radiometer during the summer of 1973 being the only exception. Results from these measurements have been reported by Schmugge *et al.* [35], Blanchard *et al.* [21], Eagleman and Lin [36], Allison *et al.* [37], and Wang [38]. The work of Allison *et al.* was based on ESMR-5 (19.3-GHz Electronically Scanning Microwave Radiometer on board Nimbus-5 satellite) observations of the great eastern Australian floods during January–March 1974. Because of the frequent, wide-swath coverage of ESMR-5, they were able to observe the development and subsidence of the flooded region day and night over the entire two-month period. The studies by Schmugge *et al.* and Blanchard *et al.* were also based on the ESMR-5 observations, while those by Eagleman and Lin used the Skylab 1.4-GHz radiometer measurements. Since soil moisture ground truth was difficult to acquire in large-area measurements, the Antecedent Precipitation Index (API) was used and determined to be a good indicator of soil moisture content [21]. It was found that over a region with sparse vegetation cover like western Texas and Oklahoma, microwave emission strongly correlated with API [21], [36]. Wang [38] has extended the analyses to examine the effect of vegetation cover over a large scale.

In contrast to studies of the vegetation effect from truck and aircraft platforms, large-area observations and analyses of this effect with satellite sensors are quite limited. Eagleman and Lin [36] have pointed out the microwave signature of vegetation cover in their analyses of the Skylab 1.4-GHz radiometer data. More recently, Wang [38] has used the data obtained from both the Skylab radiometer and the two lowest frequency channels of the Scanning Multichannel Microwave Radiometer (SMMR) to study the vegetation effect in more detail. Two areas, Region A in western Texas and Region B in eastern Texas and Oklahoma, were chosen for the analyses. The biomass distribution of vegetation cover in Texas has been analysed by

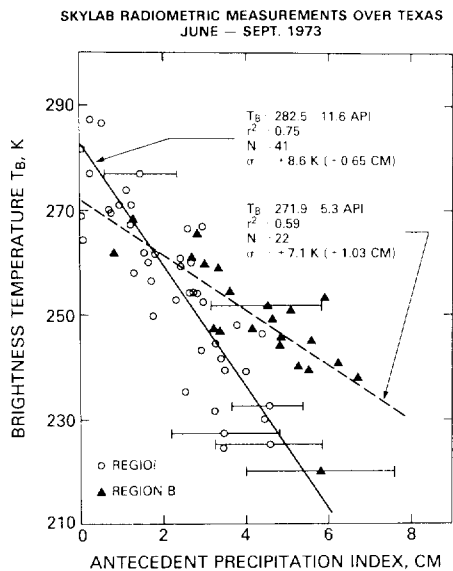


Fig. 6. Comparison of microwave brightness temperatures measured by the Skylab 1.4-GHz radiometer with the antecedent precipitation index (API) for two regions in Texas [38].

Newton *et al.* [8] using Landsat imagery and by Gregor and Norwine [39] using NOAA satellite imagery. Both of these studies have shown a gradual increase in vegetation biomass from western to eastern Texas. Therefore, the microwave signatures from regions *A* and *B* are expected to be different. Both Skylab radiometer and SMMR measurements with ground resolution cells falling in these two regions were used to correlate with API, which was calculated from the daily average total precipitation in cm from the weather stations falling within the resolution cell of each radiometric measurement.

Fig. 6 shows a scatter plot between the T_B 's measured from the Skylab 1.4-GHz radiometer and the corresponding API's for both regions *A* and *B*. Applying linear regressions to each of the two data groups results in r -squared values of 0.75 and 0.59 for regions *A* and *B*, respectively. Two main features of interest are observed in this figure. First, the radiometric measurements over region *B* with dense vegetation cover result in a shallower slope compared to that of region *A* with sparse vegetation cover. This is in agreement with the results of measurements at ground level and aircraft altitudes described earlier. Secondly, the large API values of about 6 cm are the results of heavy rainfalls on the days immediately before the microwave radiometric measurements. The moisture content of surface soils under this condition is generally at field capacity. The radiometric measurements over such soils should give T_B 's of about 190–200K when there is no vegetation cover [12]. The extension of the region *A* regression line to API = 6 cm in the figure gives a T_B of about 210K. This is in a reasonable agreement with the values obtained from either the ground level or aircraft experiments considering the fact that some areas within the ground resolution cell of the Skylab radiometer are covered with vegetation. A vegetation-covered soil is generally associated with a higher T_B .

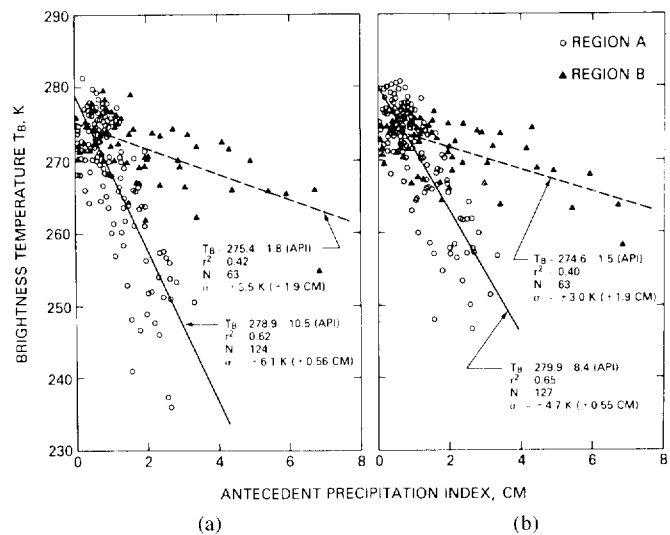


Fig. 7. Comparison of microwave brightness temperatures measured by the Nimbus-7 SMMR instrument with API for the same two regions of Texas from June to September 1979; (a) 6.6-GHz results, (b) 10.7-GHz results.

Fig. 7(a) and (b) show the scatter plot between T_B 's and API's for both the 6.6- and 10.7-GHz SMMR frequencies. The microwave radiometric responses over the two regions are quite different at both frequencies. Linear regressions applied to the four data groups corresponding to two regions and two frequencies give the correlation coefficients and regression slopes indicated in the figure. Clearly, the slopes derived from region *B* are much shallower compared to those from region *A*, showing the effect of vegetation. The presence of this vegetation effect introduces ambiguity in soil moisture determination. For a T_B measurement from either Fig. 6 or Fig. 7, the estimated API value would depend on whether the land within the radiometer resolution cell is covered with vegetation or not. To overcome this problem, it is necessary to have some recent estimate on the biomass of vegetation cover [15] such as the approach used by Theis *et al.* [20] as described earlier.

Radiometric measurements generally can be made to an accuracy of ± 3 K or less [11]. The large scatter of the data points in Fig. 7 is largely caused by the inhomogeneity of surface cover and rainfall distribution within the resolution cells of the sensors. The statistics of the measurements in both figures are characterized by the standard errors of estimates (SEE) derived from the regression analyses using either T_B or API as independent variables in each data group. At 1.4-GHz, the derived SEE's of API are 0.65 cm and 1.03 cm for regions *A* and *B*, respectively. For 6.6- and 10.7-GHz measurements, the derived SEE's are 0.56 and 0.55 cm, respectively, for region *A*. For region *B*, the estimated SEE's are 1.90 cm at both frequencies. These results suggest that for measurements over sparsely vegetated terrain like region *A*, it is possible to determine at least 5 moisture levels within the API range of 0–6 cm. For measurements over terrain with dense vegetation cover like region *B*, it is still possible to estimate 4–5 moisture levels at the 1.4-GHz frequency. At 6.6- or 10.7-GHz fre-

quencies, however, it will be difficult to determine more than 3 moisture levels.

V. MODELING RESULTS

A. Roughness

Experimentally, the effects of surface roughness on the radiometric response to soil moisture were observed as early as 1974 in a field experiment done at Texas A&M University [42]. They observed a significant increase in emissivity with increasing surface roughness and thus a decrease in the sensitivity to soil moisture. This effect was also observed in field measurements at BARC, although data from the aircraft experiments indicate that the impact of roughness arising from normal agricultural practices may be less severe.

Attempts to model the effects of surface roughness have been slow in coming. As mentioned earlier, Choudhury *et al.* [13] related rough and smooth surface microwave reflectivities by an exponential factor h . Using this expression, they found that they could fit the observed data with an empirical value for h , but that h did not scale properly with wavelength or the rms surface height variations. This discrepancy occurred because the model did not consider the incoherent part of the scattered field which depends on the horizontal scale of the surface height variations. Working independently, Tsang and Newton [43] and Fung and Eom [44] developed models which include both the rms surface height and the horizontal correlation length (l). Both groups found that their formulations can give good agreement with both active and passive microwave measurements.

B. Sensitivity Analysis

Based on the model of Mo *et al.* [16], Jack Paris at the 1982 Soil Moisture Project Review presented an analysis of the effects that vegetation and surface roughness have on the radiometric sensitivity to soil moisture. From (5) and (6) we have

$$\begin{aligned} \Delta NTB/\Delta SM &= (\Delta NTB/\Delta SM)_{\text{bare}} \exp(-h) \exp(-2\tau) \\ &= (\Delta NTB/\Delta SM)_{\text{bare}} \exp(-h - 2\tau) \end{aligned}$$

where the emissivity is expressed in terms of NTB for convenience in comparing to radiometer noise levels. On a h versus τ plot the locus of points having equal sensitivity reduction will be a straight line of the form $h + 2\tau = \text{constant}$. This result is illustrated in Fig. 8 showing the range of sensitivity reduction which can be expected as a function of h and τ . The range of h values observed by Choudhury *et al.* [13] in their analysis of both field and aircraft data was from 0 to 0.6. Therefore, even for the roughest fields it should still be possible to sense moisture variations through optical thicknesses up to 0.5, at which level the sensitivity is reduced to 20 percent of the bare field value. Fortunately, for vegetated fields surface roughness tends to be reduced as the sharp edges are eroded with time so that heavier vegetation canopies (up to 0.7) can be penetrated. At this reduction level the range of NTB

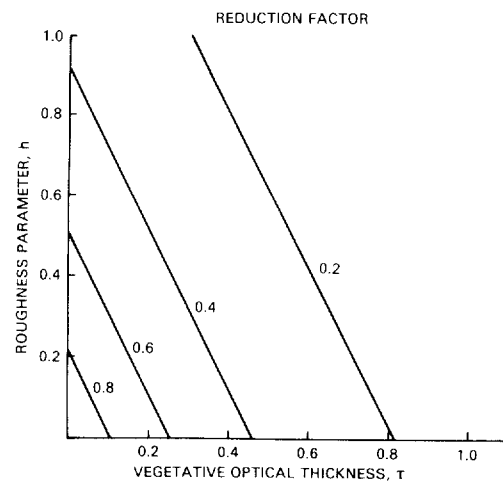


Fig. 8. Nomograph of the sensitivity reduction factor as a function of the roughness parameter (h) and the vegetative optical thickness (τ). This factor when multiplied by the bare field sensitivity yields the reduced sensitivity under the conditions h and τ .

from wet to dry is about 20K which is the range of brightness temperature that was observed by the Kansas group in aircraft data over a corn field. This level of sensitivity would be adequate if there were no other sources of uncertainty present; however, with additional uncertainties in soil temperature and soil texture, it may only be possible to distinguish between wet and dry conditions under very dense vegetation.

C. Other Research

In this paper we have only presented modeling results which are directly related to some of the measurement programs. There have been other theoretical activities which are of a more fundamental and esoteric nature. These include the work of Tsang *et al.* [45] showing the correspondence between active and passive microwave observations and the work of Kong *et al.* [46] on the emission from furrowed fields.

These modeling activities are important because they provide the physical framework for interpreting the experimental results and for extending these interpretations to a wider range of observational conditions. As noted earlier, this modeling involves the extensive use of empirical parameters because of the difficulty in determining the relevant quantities from first principles or direct measurements, e.g., the scattering of microwave radiation from vegetation or from rough soil surfaces. In dealing with natural systems such as soils and plants, we are confronted with a high degree of naturally occurring variability which makes the sampling of these quantities difficult. Thus, the use of empirical parameters based on remotely sensed observations which tend to average out this variability may be the most appropriate approach to take.

VI. CONCLUSIONS

Significant progress was made during the AgRISTARS Soil Moisture Project in quantifying the capabilities of microwave sensors for the remote sensing of soil moisture.

The use of the 21-cm wavelength as the best single channel for radiometric observations of soil moisture was verified. There were no indications that radiometric observations at multiple microwave wavelengths yield significant additional information about the moisture conditions in the soil volume beyond that obtained from a single wavelength alone. In fact, other remote sensing approaches used in conjunction with L-band passive data are more successful than multiple wavelength microwave radiometry in providing accurate soil moisture information over a wider range of conditions, e.g., the use of visible/near-infrared for vegetation estimates and active microwave for roughness estimates.

In addition to examining combinations of different sensors for soil moisture research, the studies conducted under the AgRISTARS Program also improved our understanding of the various noise factors which affect the interpretability of microwave emission data. Researchers verified experimentally the magnitude of the soil moisture sampling depth, while surface roughness was explained theoretically in terms of two measurable parameters, the surface height variance and the horizontal correlation length. Absorption of soil emission by vegetation was quantified, and although scattering of energy within vegetation canopies was observed in some instances [47], this effect is less important than absorption effects for microwave radiometry. Our knowledge of the impact of soil texture variations became more refined [3], with more recent work [48] confirming the importance of soil properties such as density and soil structure. Based on a consideration of these results, we feel that it should be possible to measure the soil moisture of the surface layer (0–5 cm) to an accuracy of ± 5 -percent absolute about 90 percent of the time where vegetation permits, the major difficulty being when the soil surface has just been worked and is extremely rough and of low density.

It is important to realize that while remote sensing measurements will not provide as accurate or as deep a measurement of soil moisture as can be obtained by conventional in situ measurements, they do provide a means for getting repetitive measurements over large areas of the moisture condition of the surface soil layer. This type of information has not been conventionally available in the past, and thus, a major task for the near future is the demonstration of the utility of surface soil moisture in determining such things as the partitioning of energy at the land surface and its effect on surface runoff. An opportunity for this will be the field experiments planned in the International Satellite Land Surface Climatology Program (ISLSCP). Successful demonstration of the utility of microwave remotely sensed soil moisture information in these experiments will be necessary before passive sensors requiring large antennae are flown in space as part of a proposed space platform.

REFERENCES

- [1] J. R. Wang and T. J. Schmugge, "An empirical model for the complex dielectric permittivity of soils as a function of water content," *IEEE Trans. Geosci. Remote Sensing*, vol. GE-18, pp. 288–295, 1980.
- [2] M. T. Hallikainen, F. T. Ulaby, M. C. Dobson, M. A. El-Rayes, and L. Wu, "Microwave dielectric behavior of wet soil—Part I: Empirical models and experimental observations," *IEEE Trans. Geosci. Remote Sensing*, vol. GE-23, pp. 25–34, 1985.
- [3] M. C. Dobson, F. T. Ulaby, M. T. Hallikainen and M. A. El-Rayes, "Microwave dielectric behavior of wet soil—Part II: Dielectric mixing models," *IEEE Trans. Geosci. Remote Sensing*, vol. GE-23, pp. 35–46, 1985.
- [4] M. C. Dobson and F. T. Ulaby, "Active microwave soil moisture research," *IEEE Trans. Geosci. Remote Sensing*, this issue, pp. 23–36.
- [5] T. T. Wilheit, "Radiative transfer in a plane stratified dielectric," *IEEE Trans. Geosci. Electron.*, vol. GE-16, pp. 138–143, 1978.
- [6] E. G. Njoku and J. A. Kong, "Theory for passive microwave sensing of near-surface soil moisture," *J. Geophys. Res.*, vol. 82, pp. 3108–3118, 1977.
- [7] T. J. Schmugge, "Soil moisture sensing with microwave techniques," in *Proc. 14th Int. Symp. Remote Sensing Environ.* (San Jose, Costa Rica, Apr. 1980, 23–30), pp. 487–505.
- [8] R. W. Newton, B. V. Clark, J. F. Paris, and W. M. Pritchard, "Orbiting passive microwave sensor simulation applied to soil moisture estimation," Texas A&M Remote Sensing Center. Final Rep. RSC-3753 on NASA Grant NSG-5266, p. 208, 1980.
- [9] R. W. Newton, Q. R. Black, S. Mankanvand, A. J. Blanchard, and B. R. Jean, "Soil moisture information and thermal microwave emission," *IEEE Trans. Geosci. Remote Sensing*, vol. GE-20, pp. 275–281, 1982.
- [10] J. R. Wang, J. E. McMurtrey, E. T. Engman, T. J. Jackson, and T. J. Schmugge, "Radiometric measurements over bare and vegetated fields at 1.4 GHz and 5 GHz frequencies," *Remote Sensing Environ.*, vol. 12, pp. 295–311, 1982.
- [11] J. R. Wang, T. J. Schmugge, J. E. McMurtrey, W. I. Gould, W. S. Glazar, and J. E. Fuchs, "A multifrequency radiometric measurement of soil moisture content over bare and vegetated fields," *Geophys. Res. Lett.*, vol. 9, pp. 416–419, 1982.
- [12] J. R. Wang, P. E. O'Neill, T. J. Jackson, and E. T. Engman, "Multifrequency measurements of the effects of soil moisture, soil texture and surface roughness," *IEEE Trans. Geosci. Remote Sensing*, vol. GE-21, pp. 44–50, 1983.
- [13] B. J. Choudhury, T. J. Schmugge, R. W. Newton, and A. Chang, "Effect of surface roughness on the microwave emission from soils," *J. Geophys. Res.*, vol. 84, pp. 5699–5706, 1979.
- [14] D. R. Brunfeldt and F. T. Ulaby, "Measured microwave emission and scattering in vegetation canopies," *IEEE Trans. Geosci. Remote Sensing*, vol. GE-22, pp. 520–524, 1984.
- [15] T. J. Jackson, T. J. Schmugge, and J. R. Wang, "Passive microwave sensing of soil moisture under vegetation canopies," *Water Res. Res.*, vol. 18, pp. 1137–1142, 1982.
- [16] T. Mo, B. J. Choudhury, T. J. Schmugge, J. R. Wang, and T. J. Jackson, "A model for microwave emission from vegetation-covered fields," *J. Geophys. Res.*, vol. 87, pp. 11229–11237, 1982.
- [17] E. G. Njoku and P. E. O'Neill, "Multifrequency microwave radiometer measurements of soil moisture," *IEEE Trans. Geosci. Remote Sensing*, vol. GE-20, no. 4, pp. 468–475, 1982.
- [18] T. J. Jackson, T. J. Schmugge, and P. E. O'Neill, "Passive microwave remote sensing of soil moisture from an aircraft platform," *Remote Sensing Environ.*, vol. 14, pp. 135–151, 1984.
- [19] M. Owe and T. J. Schmugge, "Microwave radiometer response to soil moisture at the 21 cm wavelength," presented at the Amer. Soc. Agronomy, Annual Meeting (Washington, DC), 1983.
- [20] S. W. Theis, B. J. Blanchard, and R. W. Newton, "Utilization of vegetation indices to improve microwave soil moisture estimates over agricultural lands," *IEEE Trans. Geosci. Remote Sensing*, vol. GE-22, pp. 490–496, 1984.
- [21] B. J. Blanchard, M. J. McFarland, T. J. Schmugge, and E. Rhoades, "Estimation of soil moisture with API algorithms and microwave emission," *Water Res. Bull.*, vol. 17, pp. 767–774, 1981.
- [22] T. J. Jackson, "Profile soil moisture from surface measurements," *J. Irrigation Drainage Div.*, *ASCE*, vol. IR-2 pp. 81–92, 1980.
- [23] Q. R. Black and R. W. Newton, "Airborne microwave remote sensing of soil moisture," AgRISTARS Tech. rep. SM-TI-40457, 1981.
- [24] M. Owe, E. B. Jones, and T. J. Schmugge, "Soil moisture variation patterns observed in Hand County, South Dakota," *Water Res. Bull.*, vol. 18, pp. 949–954, 1982.
- [25] H. K. Burke and J. H. Ho, "Analysis of soil moisture extraction algorithm using data from aircraft experiments," ERT Inc., Concord, MA. Final Rep. Cont. NAS5-26361, Doc. P-A826, 1981.
- [26] T. Mo and T. J. Schmugge, "Monte Carlo simulation of the effect of

- soil moisture variation on the microwave emission from soils," *IEEE Trans. Geosci. Remote Sensing*, vol. GE-21, pp. 473-479, 1983.
- [27] T. Schmugge, "Remote sensing of soil moisture with microwave radiometers," *Trans. ASAE*, vol. 26, pp. 748-753, 1983.
- [28] P. E. O'Neill, "Microwave remote sensing of soil moisture: A comparison of results from different truck and aircraft platforms," *Int. J. Remote Sensing*, vol. 6, no. 7, pp. 1125-1134, 1985.
- [29] T. J. Jackson, P. O'Neill, J. Wang, and J. Shiue, "Evaluation of a pushbroom microwave radiometer aircraft soil moisture remote sensing system," paper 84-2516, presented at the ASAE (New Orleans, LA), Dec. 11-14, 1984.
- [30] S. W. Theis, B. J. Blanchard, and A. J. Blanchard, "Utilization of active microwave roughness measurements to improve passive microwave soil moisture estimates over bare soils," in *Proc. IGARSS'84* (Strasbourg, France), Aug. 27-30, 1984.
- [31] F. T. Ulaby, M. Razani, and M. C. Dobson, "Effects of vegetation cover on the microwave radiometric sensitivity to soil moisture," *IEEE Trans. Geosci. Remote Sensing*, vol. GE-21, pp. 51-61, 1983.
- [32] A. J. Richardson and C. L. Wiegand, "Distinguishing vegetation from soil background information," *Photogrammetr. Eng.*, vol. 48, pp. 1541-1552, 1977.
- [33] F. T. Ulaby, M. C. Dobson, and D. R. Brunfeldt, "Improvement of moisture estimation accuracy of vegetation-covered soil by combined active/passive microwave remote sensing," *IEEE Trans. Geosci. Remote Sensing*, vol. GE-21, pp. 300-307, 1983.
- [34] A. K. Fung and H. J. Eom, "A comparison between active and passive sensing of soil moisture from vegetated terrains," *IEEE Trans. Geosci. Remote Sensing*, vol. GE-23, pp. 768-775, 1985.
- [35] T. J. Schmugge, J. M. Meneely, A. Rango, and R. Neff, "Satellite microwave observations of soil moisture variations," *Water Res. Bull.*, vol. 13, pp. 265-281, 1977.
- [36] J. R. Eagleman and W. C. Lin, "Remote sensing of soil moisture by a 21 cm passive radiometer," *J. Geophys. Res.*, vol. 81, pp. 3660-3666, 1976.
- [37] L. J. Allison, T. J. Schmugge, and G. Byrne, "A hydrological analysis of east Australian floods using Nimbus-5 electrically scanning radiometer data," *Bull. Amer. Met. Soc.*, vol. 60, pp. 1414-1427, 1979.
- [38] J. R. Wang, "The effect of vegetation on soil moisture sensing observed from orbiting microwave radiometers," *Remote Sensing Environ.*, vol. 11, pp. 141-151, 1985.
- [39] D. H. Gregor and J. Norwine, "A gradient model of vegetation and climate utilizing NOAA satellite imagery," NASA Johnson Space Flight Center, Houston, TX, AgRISTARS FC-JI-04176, JSC-17435, 1981.
- [40] C. J. Tucker, J. H. Elgin, and J. E. McMurtrey, "Relationship of crop irradiance to alfalfa agronomic values," *Int. J. Remote Sensing*, vol. 8, pp. 69-76, 1980.
- [41] C. J. Tucker, J. R. G. Townshend, and T. E. Goff, "African land-cover classification using satellite data," *Science*, vol. 227, no. 4685, pp. 369-375, 1985.
- [42] R. W. Newton and J. Rouse, "Microwave radiometer measurements of moisture content," *IEEE Trans. Antennas Propagat.*, vol. AP-28, pp. 680-686, 1980.
- [43] L. Tsang and R. W. Newton, "Microwave emission from soils with rough surfaces," *J. Geophys. Res.*, vol. 87, pp. 9017-9024, 1982.
- [44] A. K. Fung and H. J. Eom, "An approximate model for backscattering and emission from land and sea," Remote Sensing Lab., Univ. of Kansas, AgRISTARS Rep. SM-K1-04049, 1981.
- [45] L. Tsang, A. J. Blanchard, R. W. Newton, and J. A. Kong, "A simple relation between active and passive microwave remote sensing measurements of earth terrain," *IEEE Trans. Geosci. Remote Sensing*, vol. GE-20, pp. 482-484, 1982.
- [46] J. A. Kong, S. L. Lin, and S. L. Chuang, "Microwave thermal emission from periodic surfaces," *IEEE Trans. Geosci. Remote Sensing*, vol. GE-22, pp. 377-382, 1984.
- [47] P. E. O'Neill, T. J. Jackson, B. J. Blanchard, J. R. Wang, and W. I. Gould, "Effects of corn stalk orientation and water content on passive microwave sensing of soil moisture," *Remote Sens. Environ.*, vol. 16, pp. 55-67, 1984.
- [48] T. J. Jackson, P. E. O'Neill, G. van der Kolf, G. J. Koopman, and J. R. Wang, "Effects of soil properties on the microwave emission of soils," *Pres. 4th Int. Symp. Remote Sensing Soil Survey, Int. Soc. Soil Sci.* (Wageningen and Enschede, The Netherlands, March 4-8, 1985).

*



Thomas Schmugge (M'83) received the B.S. degree in physics from the Illinois Institute of Technology in 1959 and the Ph.D. degree in physics from the University of California, Berkeley, in 1965.

From 1964 to 1970, he was a member of the Physics Department at Trinity College, Hartford, CT. He began his work on the use of microwave techniques for remote sensing in 1970 as a National Academy of Sciences Senior Research Associate at the NASA Goddard Space Flight Center, Greenbelt, MD. Since that time, he has been at Goddard working primarily on the application of passive microwave techniques for the remote sensing of soil moisture and snow. He is also involved in the development of techniques for using remotely sensed data to estimate areal averages of the evapotranspiration flux. He was the Project Scientist for the Soil Moisture Project in the AgRISTARS Program. Currently, he is a Senior Scientist in the Hydrological Sciences Branch at Goddard and is the Project Scientist for the First ISLSCP Field Experiment that is part of the International Satellite Land Surface Climatology Project.

*



Peggy E. O'Neill received the B.S. degree in geography from Northern Illinois University in 1976 and the M.A. degree in geography from the University of California, Santa Barbara, in 1979.

Since 1980, she has been employed as a Physical Scientist in the Hydrological Sciences Branch at the NASA Goddard Space Flight Center, Greenbelt, MD. Her major areas of research include analysis of microwave remote-sensing techniques for the determination of soil and vegetation properties.

Ms. O'Neill is a member of the American Water Resources Association, the American Geophysical Union, and the Remote Sensing Society.

*

James R. Wang received the B.S. degree in physics from the University of Washington, Seattle, and the M.S. and Ph.D. degrees in physics from the University of Chicago, Chicago, Ill.

Prior to joining the NASA Goddard Space Flight Center, Greenbelt, MD, in 1977, he was employed by Columbia University, New York, NY; Computer Sciences Corporation, Silver Spring, MD; and Lockheed Electronics Company, Houston, TX. His research interests include the applications of both active and passive techniques for the remote sensing of geophysical parameters such as soil moisture, water vapor, and precipitation.

Active Microwave Soil Moisture Research

M. CRAIG DOBSON, MEMBER, IEEE, AND FAWWAZ T. ULABY, FELLOW, IEEE

Abstract—This paper summarizes the progress achieved in the active microwave remote sensing of soil moisture during the four years of the AgRISTARS program. Within that time period, from about 1980 to 1984, significant progress was made toward understanding 1) the fundamental dielectric properties of moist soils, 2) the influence of surface boundary conditions, and 3) the effects of intervening vegetation canopies. In addition, several simulation and image-analysis studies have identified potentially powerful approaches to implementing empirical results over large areas on a repetitive basis. This paper briefly describes the results of laboratory, truck-based, airborne, and orbital experimentation and observations.

I. INTRODUCTION

THE OBJECTIVE of the AgRISTARS soil moisture project was to develop and evaluate the technology to make both remote and ground measurements of soil moisture. The attainment of this objective was viewed as a precursor to using soil-moisture information in application models for predicting crop yield, plant stress, and watershed runoff. This paper summarizes the advances made during the AgRISTARS program with respect to the sensing of soil moisture using active microwave techniques; a companion paper in this issue deals with passive microwave techniques [1].

Prior to the AgRISTARS program, the capability of active microwave techniques to sense near-surface soil moisture had been, for some years, an area of considerable research interest. A number of field experiments had been conducted, most of which used truck-mounted FM-CW scatterometers. The systems had been used as spectrometers over the 1- to 18-GHz frequency band in order to investigate the spectral properties of radar response to first-order soil properties such as soil moisture, and to the random component of soil roughness induced by agricultural tillage practices [2]–[4]. These efforts identified radar sensitivity to near-surface soil moisture as a function of surface roughness and soil texture for various combinations of the radar sensor parameters of frequency, polarization, and angle of incidence with respect to nadir [5], [6]. In general, the studies concentrated on nonvegetated soil surfaces and approached the problem from an analytical viewpoint, i.e., as an optimization problem, with the objective of identifying sensor parameters having maximal sensitivity to and correlation with near-surface soil moisture but also having minimal sensitivity to sur-

face roughness and agricultural canopy cover. The resulting recommendations for a C-band radar (at about 5 GHz) operating at angles of incidence in the 10° to 20° range have not been substantively altered by the findings of subsequent investigations.

Research undertaken as part of the AgRISTARS program was directed at verifying these preliminary findings and extending them via a parametric analysis of each of the scene variables expected to affect the radar backscattering from an agricultural setting. The scene variables examined include soil-moisture profile and sampling depth, soil bulk density, soil surface boundary conditions (such as random surface roughness, row direction effects related to ridge/furrow tillage practices, and local slope as related to local angle of incidence), vegetation canopies, and geographic conditions (such as variability in local topography, soil texture, field size and shape, and the presence of nonagricultural features such as urban areas, forests, and water bodies). The preceding variables were examined (sometimes not definitively) through a series of laboratory and field experiments generally coupled with concurrent modeling efforts. A summary of the significant results of these investigations is presented in the ensuing sections.

II. SOIL DIELECTRIC PROPERTIES

The dielectric properties of moist soils are quintessential in determining the microwave scattering and absorption by a soil medium. Whereas the relative permittivity of dry soil constituents is typically about 3 and depends upon packing density, the permittivity of water is about 80. Although naturally occurring soils are spatially and temporally complex media, it has proved convenient to examine the dielectric behavior of relatively simple and “homogeneous” test soils in the laboratory. This simplification is justified when applying soil dielectric properties to scattering and emission models at the microscale level; it breaks down at larger scales (related to sensor resolution) only because the true variance in the spatial and temporal properties is exceedingly difficult to quantify.

In general, a soil medium can be treated as a volume consisting of variable fractions of soil solids, aqueous fluids, and air. Soil solids are characterized by the distribution of particle sizes (texture) and the mineralogy of their constituent particles (particularly the clay fraction). Several laboratory studies have been conducted to investigate the effects of soil moisture, bulk density, and soil texture on the net dielectric behavior of the soil medium using either guided-wave or free-space transmission techniques

Manuscript received July 8, 1985; revised September 12, 1985.

The authors are with the Radiation Laboratory, Department of Electrical Engineering and Computer Science, University of Michigan, Ann Arbor, MI 48109.

IEEE Log Number 8406230.

[7]–[9]. In particular, these studies sought to quantify the role of dielectrically bound water (not necessarily chemically bound water), whose quantity is strongly dependent upon soil texture and mineralogy. The results both of the studies and of subsequent analyses [10] indicate the following.

1) The dielectric constant of dry soil is independent of frequency over the microwave region and is primarily dependent upon soil bulk density.

2) The addition of water to a dry soil medium results in an increase in the dielectric constant that is smaller in magnitude for initial increments of “bound water” than for subsequent additions of “bulk water.”

3) The quantity of “bound water” is controlled by soil texture and mineralogy (being roughly proportional to the soil clay fraction), which results in profound differences among soil types with respect to the dielectric constant at a given moisture content.

4) The observed differences among soil types are frequency dependent and are greatest at the lower frequencies (those less than approximately 3 GHz), where the effects of the effective salinity of soil fluids exert significant influence.

5) The frequency dependence of soil dielectric properties is generally of the Debye type and is similar in form to that observed for water.

6) Because the dielectric constant of moist soils is proportional to the number of water dipoles per unit volume, the preferred measure for soil moisture is volumetric.

The study by Wang and Schmugge [7] at 1.4 and 5 GHz resulted in an empirical formulation for the calculation of the soil dielectric constant as a function of soil moisture and soil texture. A later study by Dobson *et al.* [9] over the frequency range from 1 to 18 GHz resulted in both multifrequency empirical formulations and a physically based theoretical model that explicitly treats a number of soil physical properties including soil bulk density, specific surface area, cation exchange capacity, volumetric soil moisture, and the quantity and dielectric nature of “bound water.” An example of the frequency response of soil dielectric properties is shown for silt in Fig. 1.

The scientific rationale for conducting the dielectric investigations was clearly twofold: first, to gain a fundamental understanding of the basic property governing microwave sensor response and, second, to provide an accurate data base for the derivation of dielectric properties as needed inputs to increasingly accurate and demanding microwave emission and scattering models. In parallel with the soil dielectric work, preliminary investigations have sought to determine the dielectric properties of common components of vegetation canopies such as fruit, stalks, and leaves [11]. These efforts have been complicated by the fact that the canopy elements are commonly similar to a wavelength in size, they assume preferred orientations in nature, and they may be irrevocably altered by the sample-preparation process.

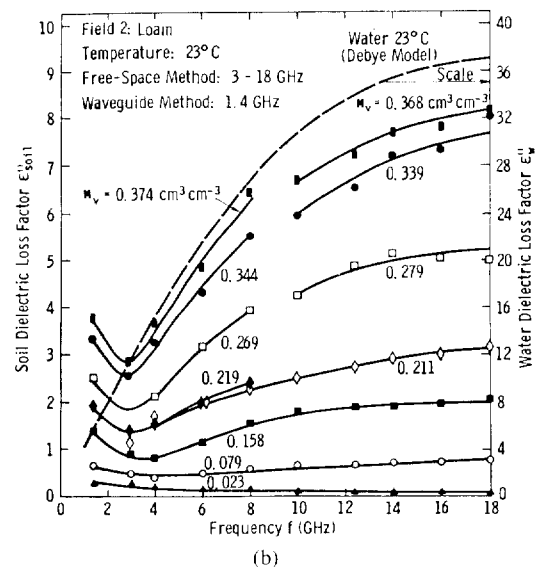
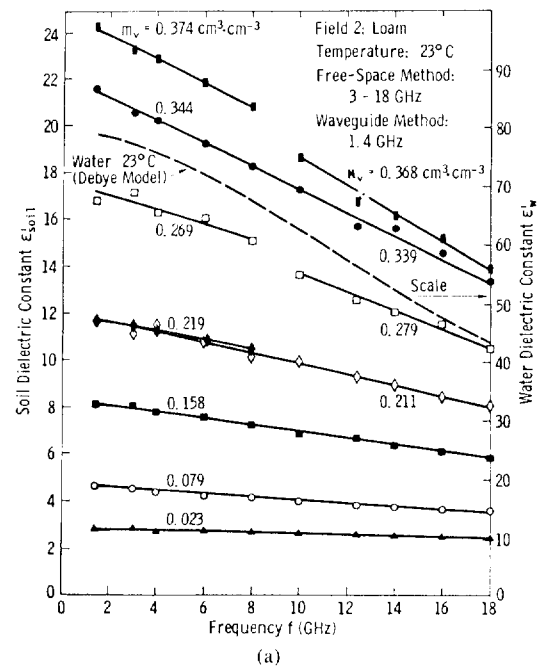


Fig. 1. Measured (a) real part and (b) imaginary part of the dielectric constant as a function of frequency with volumetric wetness as a parameter.

III. NONVEGETATED SOIL

The microwave energy incident upon the soil surface may be scattered, transmitted, or absorbed; the relative quantities of each of these processes and their directional characteristics are determined by the intrinsic dielectric properties of the soil medium and by the boundary conditions at the air–soil interface. Boundary conditions of interest include the small-scale random surface roughness generated by agricultural tillage practices, azimuthally dependent ridge/furrow patterns, and the slope of a terrain element, which affects the local angle of incidence.

A radar measures that quantity of the incident power which is backscattered, and, in the general case, this quantity can consist of both a coherent component (from

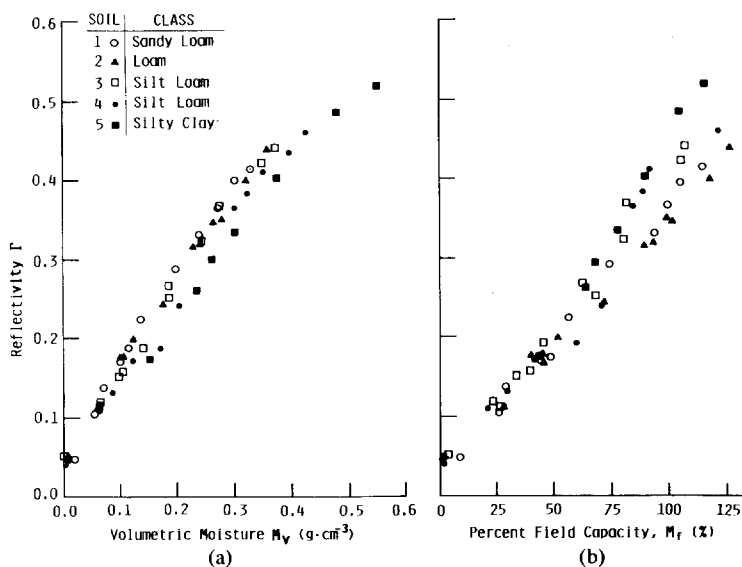


Fig. 2. Power reflection coefficient at nadir at 1.4 GHz versus (a) true volumetric soil moisture M_v , and (b) percent of field capacity M_f .

specular reflection) and an incoherent component (from scattering). Although both terms are strongly dependent upon the Fresnel power reflection coefficient determined by the dielectric properties of the soil (as modified by surface roughness), the coherent component is more strongly dependent upon the angular properties of both the scene (roughness and local angle of incidence) and the sensor (beamwidth). Hence, the coherent component can dominate the integrated response at near-nadir angles, especially for systems having large beamwidths. For applications in which the purpose is to identify the backscattered signal that would be derived by an orbital synthetic-aperture radar (SAR) processed to have an effective pencil beam, the effective weighting by the antenna pattern of the measurement system (truck-mounted or airborne scatterometer) must be taken into account. A procedure was implemented to retrieve the “true” backscattering coefficient from the truck-mounted scatterometer data, which was experimentally obtained at angles near nadir [12].

A. Soil Properties

Recent investigations have yielded considerable insight into the nature of the soil bulk properties that control the radar backscattering response. The studies have explored the role of soil moisture and profile shape, soil bulk density, and soil texture [5], [6], [13]–[16]. However, the effects of organic constituents, clay mineralogy, and stony soil inclusions remain largely unexplored.

1) *Near-Surface Moisture Profile*: For the simplest case, that of a semi-infinite internally homogeneous soil layer bounded by a smooth surface, the power reflection coefficient at nadir is determined from the dielectric constant by

$$\Gamma = \left| \frac{\sqrt{\epsilon} - 1}{\sqrt{\epsilon} + 1} \right|^2 \quad (1)$$

where $\epsilon = \epsilon' - j\epsilon''$. By applying (1) to dielectric data measured at 1.4 GHz for several different soil textures, Dobson *et al.* [10] found that values of Γ range between 0.04 for dry soil and 0.52 for saturated soil, which corresponds to a difference of 11 dB, as shown in Fig. 2. However, field experimentation with both truck-mounted and airborne scatterometers at this frequency exhibited a dynamic range of 12 to 15 dB over the same moisture range [5].

A comparison of scattering-model calculations with scatterometer-measured data from plots of smooth, bare soil led to the postulation of two possible explanations for the apparent discrepancy: 1) the existence of subsurface effects and 2) an impedance-matching layer at the surface. Allen *et al.* [17] discounted subsurface effects due to soil-moisture profile shape (i.e., increasing soil moisture versus depth for a dry surface layer) because these effects would typically lead to an increase in the reflection coefficient calculated for a dry surface. Assuming the existence of a transition zone (in which the upper millimeters of soil are considerably drier on a volumetric basis than the average of the top several centimeters) functioning as an impedance-matching layer, Allen *et al.* [17] compared field backscattering measurements to the solutions of a Kirchhoff scattering model using both Wilheit’s [18] method for calculating the reflection coefficient from a layered medium and an iterative solution to the Riccati equation. This assumption yielded good fits to the measured data and indicated that the thickness of the transition layer is inversely related both to near-surface soil moisture and to frequency. From the standpoint of field measurements, this result emphasizes the need to pay critical attention to the moisture profile at the surface (at a subcentimeter level) in order to produce exact model calculations of the backscattering from dry soils.

2) *Soil Moisture Response*: Before the advent of the AgRISTARS program, extensive measurement programs

were conducted by the University of Kansas using truck-mounted scatterometer systems to observe test plots of nonvegetated soil with distinctive surface roughnesses and soil textures [2]–[5]. For a given soil condition (roughness or texture), radar backscattering was found to be linearly dependent upon the volumetric moisture M_v in the upper 2 to 5 cm of soil and to have linear correlation coefficients ρ typically on the order of 0.9

$$\sigma^0(\text{dB}) = A + B M_v. \quad (2)$$

For a given sensor combination of frequency, polarization, and angle of incidence, the empirically derived regression coefficients A and B were found to be dependent upon soil surface roughness and soil texture, wherein A is primarily controlled by surface roughness, and B is primarily controlled by soil texture. For the prairie mollisols examined in these studies, polarization had no statistically discernible effect on the sensitivity term B . Both combinations of like linear polarizations (HH and VV) yielded equivalent A , whereas cross-polarization produced a substantially lower value of A . In addition, the sensitivity term B was observed to be dependent upon both frequency and angle of incidence, gently decreasing with either increasing frequency or angle of incidence.

Subsequent studies by independent groups using ground-based scatterometers in the United States, France, and Japan [16], [19], [20] have verified many of these results. However, the results obtained by Hirose *et al.* [20] based on 9-GHz observations of Kanto loam represent a notable exception: they found that the cross-polarized sensitivity to near-surface volumetric soil moisture was four times that of the like-polarized backscattering. This result was attributed to the effects of multiple surface scattering; however, a similar effect has not been observed for very rough mollisols [5], [21].

Several investigators have reported the results of airborne scatterometer observations designed to sense soil moisture. These experiments were conducted during a series of overflights in 1978 and 1980 [21], [22]. Typically, these experiments used fan-beam Doppler scatterometers, operating at P -, L -, C -, and Ku -bands, mounted aboard a NASA Johnson Space Center C-130 aircraft. Multitemporal observations of test areas in Kansas, Oklahoma, and Florida yielded fairly robust data sets in terms of soil moisture, vegetation cover, and surface roughness conditions. Analyses of these data support the conclusions reached on the basis of the more geographically limited truck-mounted scatterometer observations.

Calculations of the power reflection coefficient from the measured dielectric data shown in Fig. 2 indicate that the backscattering coefficient (in square meters times reciprocal square meter) should be linearly dependent upon soil moisture at moisture levels below saturation. Near saturation, the backscattering should level off, apparently becoming less sensitive to added increments of water. Because all of the field measurements of backscattering to date have reported σ^0 in decibels, empirical regressions have taken the form given by (2). The scattering typically

inherent in the field measurements makes it difficult to substantiate this expectation. However, field measurements have shown the saturation effect at high moisture contents, and these studies demonstrate that supersaturated and flooded soils behave as specular surfaces, which yield lower backscattering at off-nadir angles than non-saturated (but wet) soils [6], [23].

3) *Soil Bulk Density*: The dielectric studies of moist soils show that, for a given gravimetric soil moisture (the ratio of water mass to dry soil mass), the effect of increased soil bulk density should be to increase the reflection coefficient due both to increased soil solids and to water dipoles per unit volume of soil. Because the contribution of the dry soil solids is small relative to that of the water component, the effects of density on dielectric properties (and hence on the reflection coefficient) are largely accounted for by expressing soil moisture on a volumetric basis (the ratio of water volume to moist-soil volume). The significance of soil bulk density effects has proved to be very difficult to verify by field measurements, due to 1) spatial variance in bulk density, 2) the temporal dynamics of bulk density, particularly for certain clay-rich soils, and 3) the great difficulty in obtaining an accurate determination of field bulk density for very thin layers of near-surface soil. The issue of soil bulk density effects has been addressed recently by several studies [10], [15], which conclude that very careful attempts should be made to quantify soil bulk density in the field in order to avoid mistaking the density effects on sensor response for soil texture or roughness effects on sensor response.

4) *Soil Texture*: Because most of the ground- and aircraft-based scatterometer studies of moist soils were purposely chosen to cover test sites having lateral homogeneity of soil type and texture, the effects of soil texture and mineralogy on radar backscattering are less understood than properties such as surface roughness. The effects of soil texture are best inferred from dielectric studies and, as observed by Dobson and Ulaby [6], during truck-mounted scatterometer measurements.

The dielectric data strongly suggest that the first monolayer of water surrounding the surface of a soil particle is largely irrotational under an impressed microwave field and hence is characterized by a relatively low dielectric constant that is dissimilar to either bulk water or ice [9]. The quantity of water that is dielectrically "bound" is determined by soil-particle size distribution (texture) and mineralogic composition via the specific surface area of the soil. The data also suggest that additional volumetric increments of water (beyond the "bound" component) exhibit dielectric properties that appear to be independent of soil texture *per se* but are dependent upon the effective salinity of the soil solution (which may be controlled by texture and mineralogy).

Attempts to compare early field investigations of different soils led to the development of a normalized soil-moisture index known as *percent of field capacity*, which is defined as the ratio of the gravimetric soil moisture to the moisture at a soil's field capacity. In practice, field capac-

ity is typically defined on the basis of laboratory measurements of soil water retention at an arbitrarily defined value of $\frac{1}{3}$ -bar matric potential. This index was an attempt to account for the soil properties governing the apportionment of soil fluids into "bound" and "bulk" water. The application of this index to empirical comparisons of airborne radiometer [13] and truck-mounted scatterometer data [5] with soil moisture as observed for two different soil types yielded relationships that were apparently independent of soil type. Further work by Dobson and Ulaby [6], comparing the backscattering from three smooth soil surfaces having distinctive soil textures yielded the same result, but also showed that the expression of soil moisture in terms of matric potential produced linear relationships that were independent of soil texture. The linear relationship between matric potential and reflectivity [16] or backscattering [14] has also been noted by more recent investigations, which, unfortunately, have dealt with single soil textures only.

In partial contradiction to the preceding observations, an analysis of the dielectric data brings into question the physical basis of the percent-of-field-capacity index (and hence its geographical extensibility) on the basis that the index functions as a surrogate for accurate volumetric soil moisture information by partially accounting for the inter-soil variability in soil bulk density [10]. Hence, to some extent, the use of percent-of-field capacity may be useful, though not rigorously correct. As a consequence, it is believed that the best physical descriptor of soil moisture is volumetric, and the evidence to date indicates that the inter-soil variability in radar sensitivity to M_v is related to the soil-specific nature of the characteristic curve relating matric potential to M_v . However, this should be examined specifically by additional experimentation.

B. Boundary Conditions

The nature of the boundary at the air-soil interface determines both the amplitude and the phase properties of the reflection and transmission by the soil medium. The nature of the effects upon radar backscattering caused by soil surfaces can be subdivided into three categories:

- 1) effective local angle of incidence related to terrain slope,
- 2) small-scale surface roughness with laterally random size distributions, and
- 3) azimuthally dependent and generally periodic roughness patterns induced by agricultural tillage practices.

For a given sensor combination of frequency, polarization, and angle of incidence (relative to the mean surface), boundary conditions do not significantly affect the sensitivity to soil moisture but do add a bias term to the response.

1) *Local Slope*: The effects of a variable local angle of incidence can be inferred from an examination of Fig. 3, which shows the angular behavior of σ^0 for five nonvegetated soil surfaces as measured by a truck-mounted scat-

terometer. The angular dependence of the cross-polarized return is far less than that shown for like polarization. For a given frequency and polarization, the bias in σ^0 caused by the variation in local angle of incidence related to topographic relief is seen to be a function of angle of incidence, local slope, and the random roughness of the soil surface as seen in Fig. 4, whereby the smoother surfaces yield a greater bias per degree of angular uncertainty.

2) *Random Surface Roughness*: Examples of the measured effects of small-scale random surface roughness on radar backscattering are shown in Figs. 3 and 4 for non-vegetated soil surfaces that were specifically prepared for this purpose. The data used to derive Fig. 3 have been deconvolved to remove the coherent portion of the net measured backscattering related to the antenna pattern of the measurement system [12]. The angular effects of variable surface roughness are seen to decrease rapidly with frequency, as even the smoothest surface observed (rms height is 1.1 cm) is no longer smooth by the Rayleigh criterion at frequencies above 3.4 GHz. The observed crossover in the angular responses for the various surfaces over the angular range from about 7 to 15° has been interpreted [5] as the optimal angular range for soil-moisture sensing with a minimal dependence on agronomically induced random surface roughness (certain geologic surfaces can be much rougher). Even within this angular range, however, it can be seen that roughness effects can be a significant source of error in soil-moisture determination from like-polarized backscattering for a particular field unless:

- 1) the roughness itself is concurrently extracted via multifrequency or multipolarized observation (like- and cross-polarized returns), or
- 2) soil moisture is estimated via a change-detection approach because surface roughness varies slowly with time for agricultural fields in the absence of tillage operations.

The preceding approach seems to be tractable because the backscattering behavior of randomly rough surfaces is shown to be well described by current scattering models. These models take two general forms with some modifications. The Kirchhoff model with the scalar approximation, or physical optics model [25], is used to describe the exponentially decaying angular dependence characteristic of smooth surfaces. The Kirchhoff model with the stationary-phase approximation, or geometric-optics model, is applied to relatively rough surfaces that display a slowly varying angular dependence near nadir.

The like-polarized backscattering coefficient of an isotropically rough surface consists of both a coherent term, σ_{ppc}^0 , which is important only at angles near normal incidence, and a noncoherent term σ_{ppn}^0 , which is important at all angles

$$\sigma^0(\theta) = \sigma_{ppc}^0(\theta) + \sigma_{ppn}^0(\theta), \quad p = v \text{ or } h. \quad (3)$$

The coherent scattering coefficient is given by the ap-

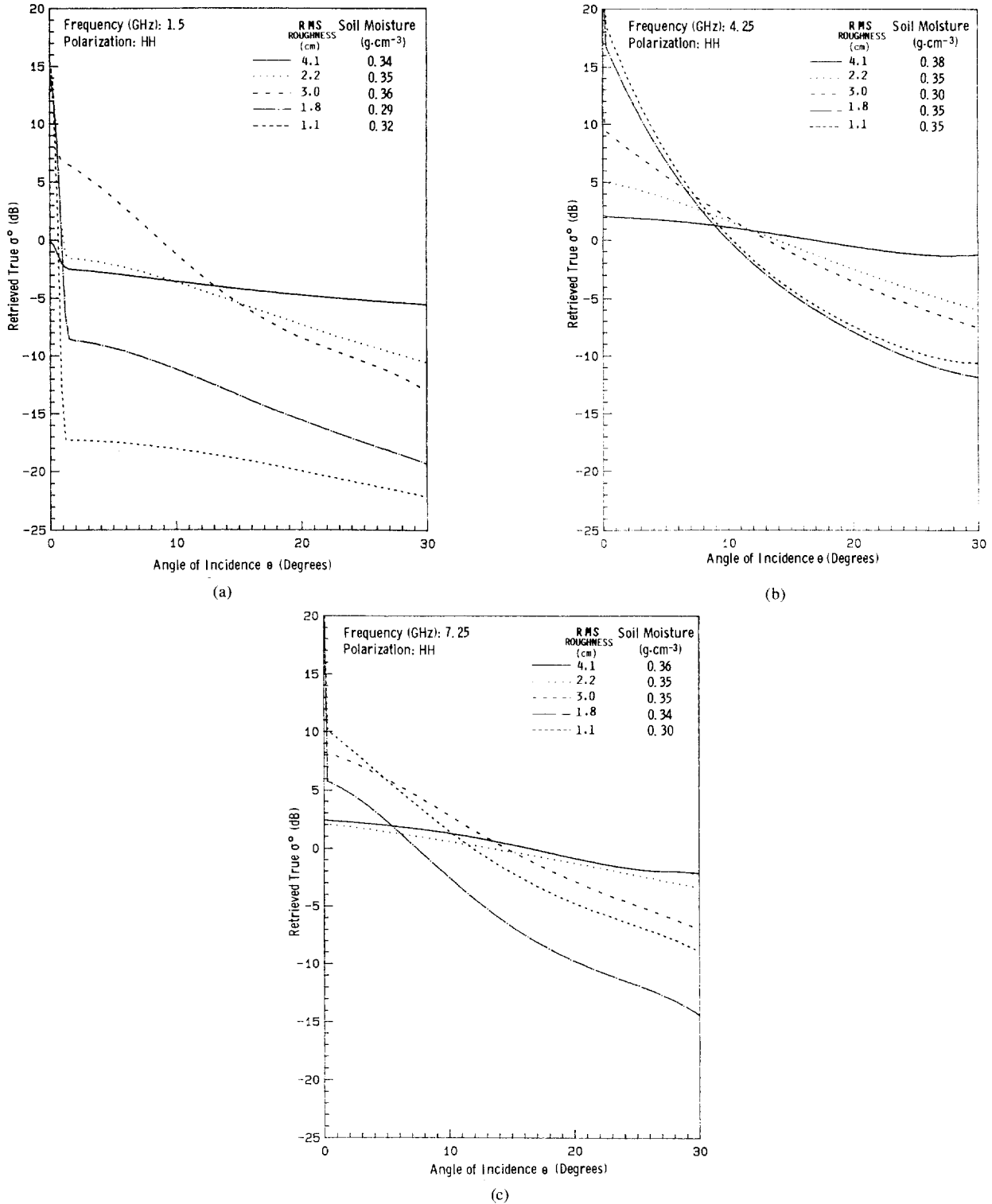


Fig. 3. Angular pattern of retrieved true σ^0 for five soil surfaces with different roughness scales (σ from 1.1 to 4.6 cm) at (a) 1.5 GHz, (b) 4.25 GHz, and (c) 7.25 GHz (from [12]).

proximate expression [24]

$$\sigma_{ppc}^0(\theta) \approx \frac{\Gamma_p(\theta)}{B^2} \exp(-4K^2\sigma^2) \exp(-\theta^2/B^2) \quad (4)$$

where

$$B^2 = (kR_0\beta)^{-2} + (\beta/2)^2.$$

$\Gamma_p(\theta)$ is the Fresnel reflectivity for polarization p at incidence angle θ , $k = 2\pi/\lambda$, σ is the surface rms height, R_0 is the range from the antenna to the center of the illuminated area, and β is the one-sided beamwidth of the antenna for a nonimaging scatterometer or its pixel-equivalent for an imaging system.

For the noncoherent component, the physical optics

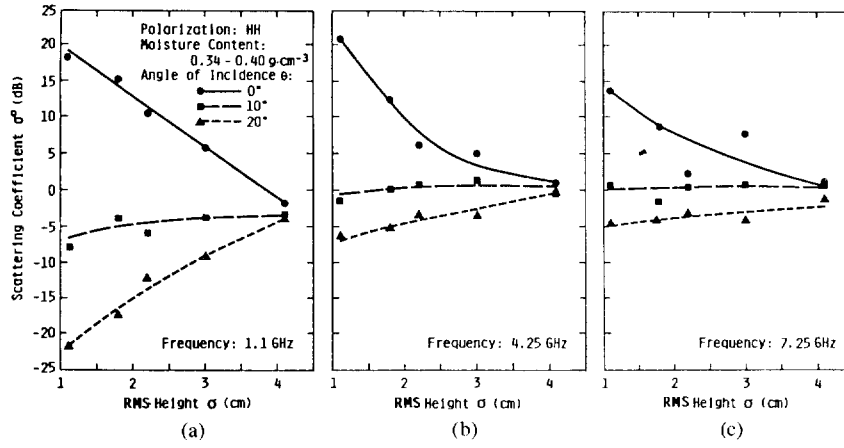


Fig. 4. Scattering coefficient dependence on rms height and angle of incidence at (a) 1.1 GHz, (b) 4.25 GHz, and (c) 7.25 GHz.

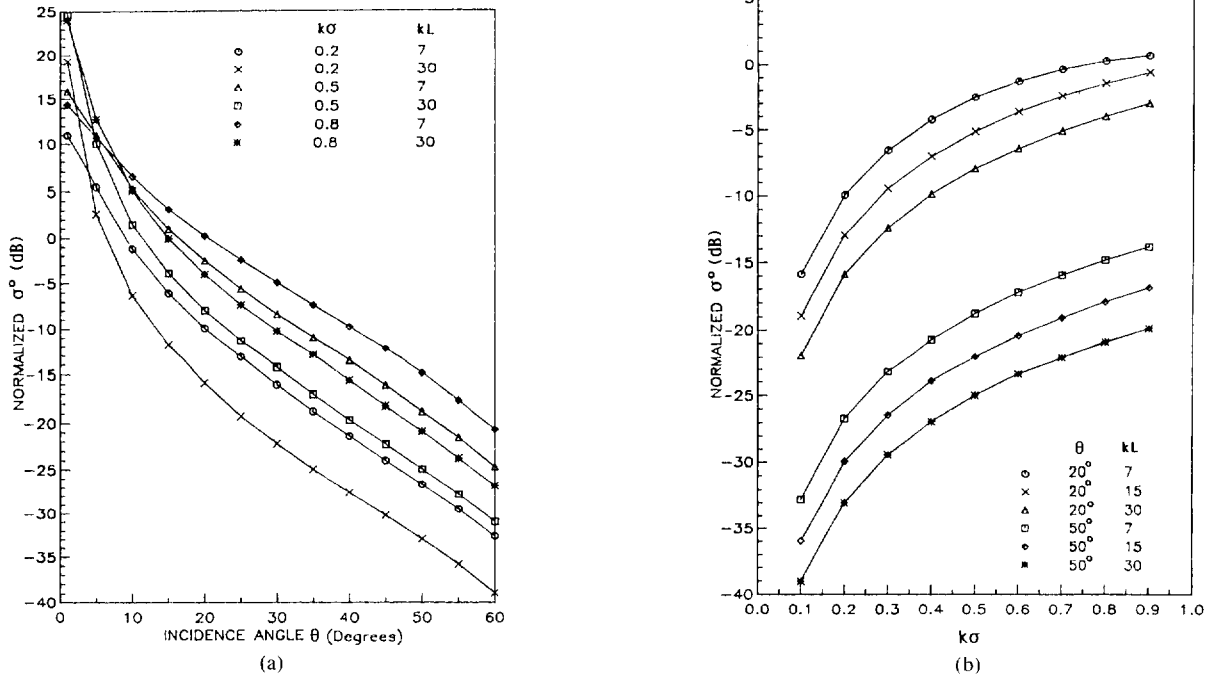


Fig. 5. Computed normalized backscattering using the scalar approximation as a function of (a) incidence angle and (b) $k\sigma$.

model gives [25]

$$\begin{aligned} \sigma_{ppn}^0(\theta) = & 2 k^2 \cos^2 \theta \Gamma_p(\theta) \exp[-(2k\sigma \cos \theta)^2] \\ & \cdot \sum_{n=1}^{\infty} [(4k^2 \sigma^2 \cos^2 \theta)^n / n!] \\ & \cdot \int_0^{\infty} \rho^n(\xi) J_0(2k \xi \sin \theta) \xi d\xi \end{aligned} \quad (5)$$

where $J_0(\cdot)$ is the zeroth-order Bessel function of the first kind and $\rho(\xi)$ is the surface correlation function. Fig. 5 shows plots of $\sigma_{ppn}^0(\theta)/\Gamma_p(\theta)$ as a function of θ and $k\sigma$ for an exponential surface correlation function $\rho(\xi) = e^{-\xi/L}$, where L is the correlation length of the surface. The geometric optics model gives the same expression for HH and

VV polarizations [25]

$$\sigma_n^0(\theta) = \frac{\Gamma(0) \exp(-\tan^2 \theta / 2m^2)}{2m^2 \cos^4 \theta} \quad (6)$$

where m is the rms slope and $\Gamma(0)$ is the Fresnel reflectivity evaluated at normal incidence. Plots of $\sigma_n^0(\theta)/\Gamma(0)$ versus θ are shown in Fig. 6.

3) *Periodic Row Directional Effects:* Agricultural crops are generally planted in parallel rows in either a rectangular format or in concentric rings (as in the case of some center-pivot irrigation systems). Soil tillage is also conducted by parallel operations using farm implements, which typically produce nonrandom and periodic ridge/furrow boundary conditions that modulate the small-scale and isotropic roughness components. The periodic com-

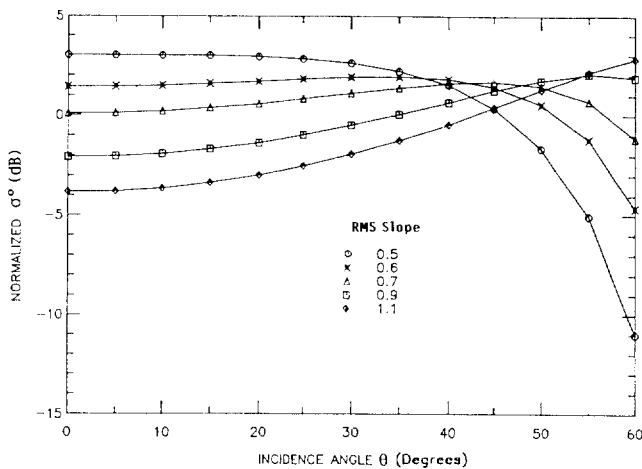


Fig. 6. Computed normalized backscattering using the stationary-phase approximation (geometric-optics model) as a function of incidence angle and rms slope.

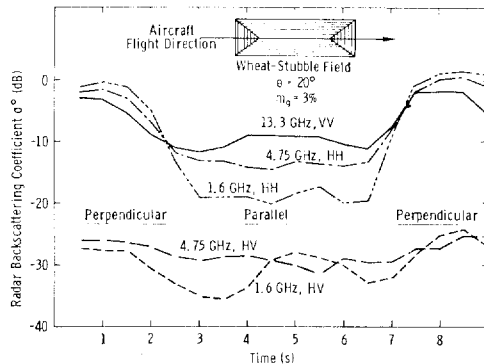


Fig. 7. Scatterometer time response measured for a wheat-stubble field whose row pattern is shown in the insert. The observation angle was 20° .

ponents of surface roughness are of particular interest to the soil-moisture estimation problem because they have been observed to exert a considerable angular effect on radar backscattering [26]. Of major concern is the azimuthal dependence of the radar backscattering from ridge/furrow patterns. Examples of this type of dependence include the "bowtie" effect commonly seen on radar images of rectangularly tilled agricultural fields and in the airborne Doppler scatterometer time traces shown in Fig. 7. In certain respects, this phenomenon is analogous to the "cardinal direction" effect observed in radar images of urban scenes in which radar view angles orthogonal to cultural features yield very high levels of backscattering.

Observations of agricultural fields with truck-mounted and airborne scatterometers [21], [26], [27] and Seasat L-band SAR [28] suggest that radar is most sensitive to azimuthal viewing geometry for angles within 15° of orthogonal to the row direction and that this sensitivity decreases in an exponential fashion as view angle becomes parallel to row direction. Because many, but not all, agronomically important areas are planted in a rectangular grid pattern with a north-south and east-west orientation, an operational orbital radar intended for soil moisture sensing should have an orbital inclination greater than 15° from polar orbit in order to minimize these effects at most latitudes.

Scatterometer observations have shown that the azimuthal effects of ridge/furrow patterns are also dependent upon the degree of isotropic small-scale surface roughness present, angle of incidence with respect to the ridge/furrow profile shape, frequency, and polarization. These effects are accurately described by a modified form of the scattering models previously introduced, which treats the periodic surface modulation as modifying the local angle of incidence for finite elements within the integrated illumination area [27]. In functional form, the backscattering coefficient $\sigma^0(\theta, \psi)$ of a periodic surface observed at an incidence angle θ (relative to the mean surface) and azimuth angle ψ (relative to the row direction) is related to $\sigma^0(\theta')$, the backscattering coefficient at the local angle of incidence θ' , by an integral of the form

$$\sigma^0(\theta, \psi) = \frac{1}{A} \iint_{\text{Illuminated Area}} \sigma^0(\theta') dA \quad (7)$$

where A is the illuminated area. The preceding form is given here simply to indicate that $\sigma^0(\theta, \psi)$ depends on the full angular range of $\sigma^0(\theta')$; the actual transformation involves the various polarization states of $\sigma^0(\theta')$, which leads to a more complicated integral [27] than that given in (7). Many of the row-direction effects can be summarized using the look-direction modulation function $M(\theta)$ defined as the difference in σ^0 (in decibels) between parallel and perpendicular observations with respect to row direction as follows:

- 1) $M(\theta)$ is greatest for fields having the least random roughness and decreases rapidly as the surface becomes electromagnetically rough at a given frequency.
- 2) Related to the preceding, $M(\theta)$ decreases rapidly with increasing frequency.
- 3) $M(\theta)$ has a local maximum for local angles of incidence that are tangential to furrow slopes; this angle is typically in the 20° to 40° range and depends upon the field-specific tillage practices in use.
- 4) Importantly, the cross-polarized scattering coefficient is relatively insensitive to row direction effects and is typically found to be less than 2 dB for the reported measurements and models. The larger variance seen in the 1.6-GHz HV response shown in Fig. 7 has been attributed to poor polarization-isolation of the antennas.

IV. VEGETATED SOIL

Remotely sensing the moisture of the soil beneath a vegetation canopy has been the subject of keen interest and moderate experimental attention for the past 10 years. Early work, based largely on truck-mounted scatterometer measurements, sought to identify those sensor combinations of frequency and angle of incidence least sensitive to the presence of agricultural canopies. The studies concluded that the optimum parameters for moisture sensing should be frequencies of less than 6 GHz and angles of incidence of less than 20° in order to minimize both the direct backscattering by the vegetation and the effec-

tive attenuation loss related to the two-way transmission through the canopy [29]. Subsequent studies using truck-mounted scatterometer data as well as data obtained by the airborne Doppler scatterometers have provided both simple empirical models and more robust theoretical models for the effects of agricultural canopies [30]–[32]. To date, most of the work has treated the vegetation canopy as an isotropic medium of disperse scattering elements with properties linked to bulk biophysical parameters such as crop type and wet and dry biomass; some rigorous studies of the role of canopy structure (the size, shape, and orientation distributions of canopy elements) have been undertaken [33], but further work is needed.

A. Bulk Canopy Biophysical Properties

In general, the radar backscattering from a vegetated soil surface consists of three components: 1) a soil surface component, 2) a vegetation component, and 3) a surface-vegetation interaction component.

$$\sigma_{\text{total}}^0 = \sigma_{\text{surface}}^0 + \sigma_{\text{vegetation}}^0 + \sigma_{\text{interaction}}^0. \quad (8)$$

For an isotropic canopy characterized by an optical depth τ , the surface term is given by

$$\begin{aligned} \sigma_{\text{surface}}^0(k\sigma; kL; \epsilon; \theta; \psi, \tau) \\ = T^2(\theta, \tau) \sigma_{\text{soil}}^0(k\sigma; kL; \epsilon; \theta; \psi; 0) \end{aligned} \quad (9)$$

where $T(\theta, \tau)$ is the one-way transmissivity of the vegetation layer

$$T(\theta, \tau) = \exp(-\tau \sec \theta). \quad (10)$$

The vegetation layer is treated as a uniform “cloud” of identical water particles, with the resulting scattering being entirely due to volume scattering, in which case there is no need to account for the scattering at the diffuse air-vegetation boundary. A full theoretical treatment of the vegetation term by Eom and Fung [32] permits multiple scattering within the vegetation layer. However, due to the small magnitude of the single-scattering albedo typically ascertained for crop canopies at frequencies below 6 GHz (on the order of 0.1), empirical model evaluations have generally simplified the treatment of this term by considering only single scattering. This simplification results in the “cloud model” developed by Attema and Ulaby [30], which is only applicable to like-polarized returns

$$\sigma_{\text{vegetation}}^0 = \frac{3 \kappa_s \cos \theta}{4 \kappa_e} [1 - T^2(\theta, \tau)] \quad (11)$$

where κ_s is the volume scattering coefficient and κ_e is the extinction coefficient of the vegetation layer. A Rayleigh scattering phase function was assumed in the derivation leading to (11). Both parameters, which are dependent upon the biophysical properties of the canopy, are assumed to be polarization- and direction-independent. The surface-vegetation interaction term is determined by multiple reflection between the canopy and the surface, and its magnitude can be estimated approximately by

$$\begin{aligned} \sigma_{\text{interaction}}^0 \approx \frac{3}{4} (1 + \cos^2 2\theta) \kappa_s T^2(\theta, \tau) \Gamma_p(\theta) \\ \cdot \exp[-(2k\sigma \cos \theta)^2]. \end{aligned} \quad (12)$$

This term is thought to become significant for sensor configurations for which the transmission loss is small and when there is significant scattering from either the vegetation volume or the soil surface. The surface-vegetation interaction term can be the dominant term in cross-polarized return.

Empirical evaluations of scatterometer data with respect to (8) have generally ignored the contribution of the interaction term and have sought to define the remaining model coefficients based upon multifrequency or multian-gle curve-fitting solutions for single-target observations [34] or have sought to define crop averages for the vegetation term and loss over a growing season [35]. Attempts to estimate the canopy loss factor on the basis of measurements of the dielectric properties of the vegetation have resulted in good fits to the measured data [11], [36]. In addition, several recent attempts have been made to define the loss parameter directly from one-way canopy transmission measurements using scatterometers at C- and X-bands [36], [37] and radiometers at S- and C-bands [38].

The one-way canopy loss as derived from radiometer observations of test plots of wheat, corn, and soybeans is shown in Fig. 8 as a function of crop-development stage. These values were obtained through a comparison of the apparent brightness temperatures of test plots in their natural state with those of adjacent plots in which the underlying soil surface was covered with a reflective material (wire mesh screens) or microwave absorber. Temporal behavior is clearly related to changes in vegetation biomass and to the appearance of distinctive canopy structural elements; the exact nature of these relationships remains to be determined. In general, the studies conducted to date show that

- 1) both the canopy loss and the vegetation volume scattering coefficient are linked to the canopy’s biophysical properties, and especially, but not exclusively, to canopy type, canopy structure, and the water volume fraction within the canopy;
- 2) the canopy loss and the volume scattering coefficient increase with frequency;
- 3) the vegetation term in (8) tends to dominate the net return as either frequency or incidence-angle increases; and
- 4) the interaction term functions to enhance radar sensitivity to the moisture contained in the soil beneath a vegetation canopy.

For purposes of soil-moisture sensing, it is preferable that the sensing systems exhibit no sensitivity to canopy biophysical parameters. If this cannot be the case, it is pertinent to define how much the canopy’s effects reduce radar sensitivity to near-surface soil moisture for canopy conditions typical of an agricultural setting. The effects of

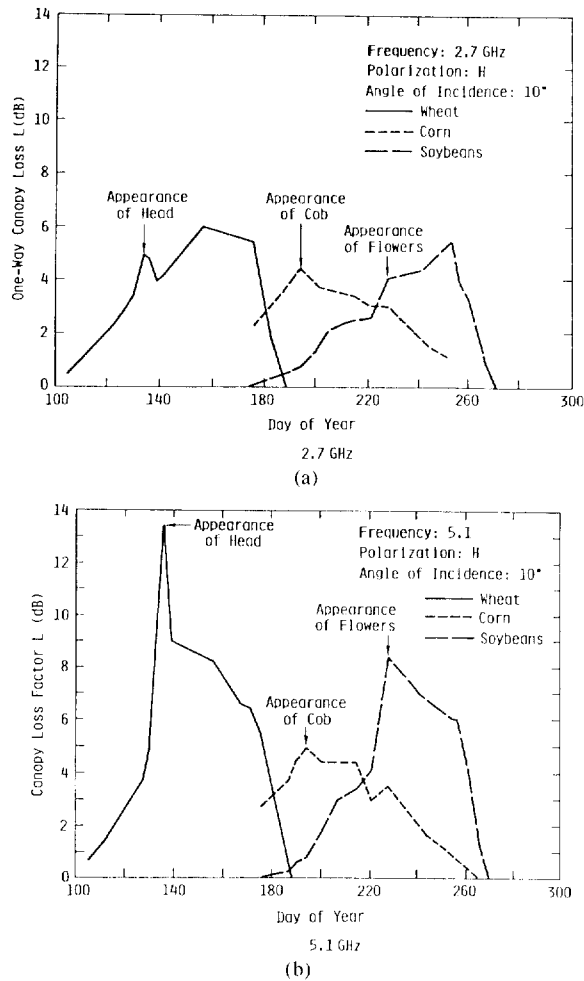


Fig. 8. Comparison of canopy attenuation for various crops at (a) 2.7 GHz and (b) 5.1 GHz.

canopies of corn, soybeans, wheat, and milo (sorghum) on radar sensitivity to soil moisture at the sensor configuration deemed least sensitive to surface-boundary conditions (C-band at 10° to 20° angles of incidence) have been examined empirically using multiyear scatterometer observations [35]. Data obtained over the period from crop emergence to crop harvest were used to define average canopy loss and $\sigma_{\text{vegetation}}^0$ for each crop type through a linear regression approach that assumed σ_{soil}^0 to be that calculated from measured soil moisture by

$$\sigma_{\text{soil}}^0 = 0.025 \exp(0.034 M_f), \quad \text{m}^2 \cdot \text{m}^{-2} \quad (13)$$

where M_f is the 0–5-cm percent of field capacity. Equation (13) results from the linear regression of 181 observations of bare soil plots with rms surface-height variations ranging from 0.7 to 4.3 cm at C-band with HH polarization and a 10° angle of incidence; the linear correlation coefficient was found to be 0.85 [39]. Assuming a negligible interaction term (see 12), the average canopy effects yield the responses shown in Fig. 9. It is apparent from Fig. 9 that at low soil-moisture levels (less than 50 percent of field capacity) the backscattering contributions from the crop canopy itself dominates the total return, whereas at higher moistures, the canopy loss causes a reduction in the

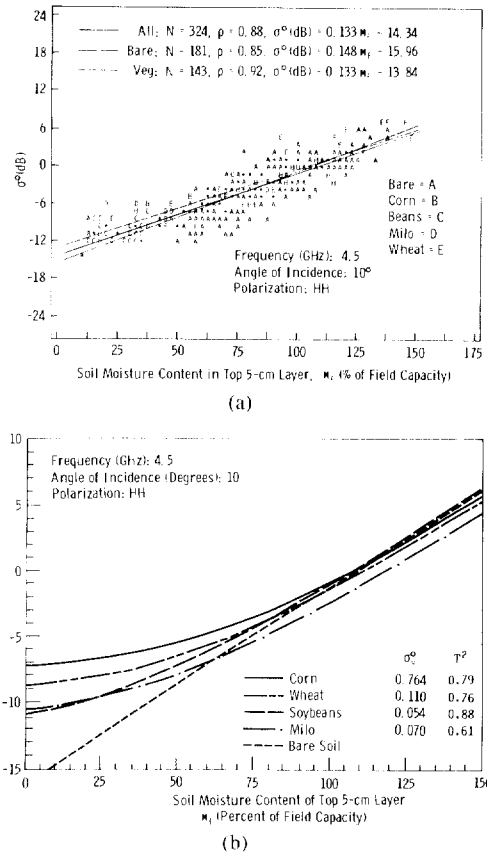


Fig. 9. (a) Linear regression of σ^0 (in decibels) versus M_f for bare fields, vegetation-covered fields, and both types combined; (b) variation of canopy backscattering coefficient with soil-moisture content for bare soil and individual crop types.

net backscattering of between 0.7 and 2.0 dB for corn and milo, respectively, as compared to that from bare soil alone. Application of the regression procedure to all 143 observations of the various crops at this sensor combination yielded a general algorithm for estimating the moisture of soil beneath agricultural crop canopies with a linear correlation coefficient of 0.91 [39].

$$\begin{aligned} \sigma^0 &= \sigma_v^0 + T^2 \sigma_{\text{soil}}^0 \\ &= 0.066 + 0.75 \sigma_{\text{soil}}^0, \quad \text{m}^2 \cdot \text{m}^{-2}. \quad (14) \end{aligned}$$

In an analysis of the prediction errors arising from the use of generalized algorithms such as (13) for bare soil or (14) for vegetated soil, Ulaby *et al.* [35] concluded that it would be difficult to estimate soil moisture with any good degree of accuracy for low soil-moisture conditions (less than about 50 percent of field capacity) from a single sensor observation unless the presence of a canopy cover is known *a priori* or from other sensor observations (visible/IR or some other microwave frequency, polarization, or angle). On the other hand, for soil moisture conditions greater than 50 percent of field capacity, it is estimated that the 90-percent probability confidence interval would yield an uncertainty of ± 15 percent of true field capacity, which corresponds to an uncertainty in volumetric moisture of about ± 0.02 and $0.05 \text{ cm}^3 \cdot \text{cm}^{-3}$ for sands and silty clay soils, respectively. It is interesting to note that

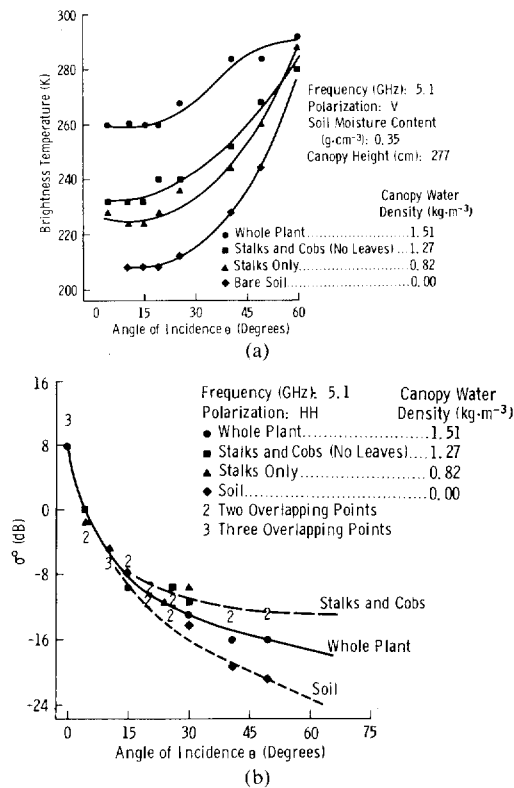


Fig. 10. Effect of a mature corn canopy undergoing progressive stages of defoliation on (a) emission and (b) backscattering at C-band.

of the 583 discrete moisture observations made in Kansas between May and November, 80 percent had 0- to 5-cm moisture values in excess of 50 percent of field capacity.

B. Canopy Structure

The canopy structure is the complex spatial organization of discrete canopy components such as stalks, leaves, and fruit. Each component has a characteristic size, shape, orientation, and location distribution. In part because canopy structure is exceedingly difficult to quantify under natural field conditions, very few experiments have been conducted to examine its effects upon radar backscattering with respect to frequency, angle, and polarization. As a consequence, the impact of the variability of canopy structure upon radar sensitivity to soil moisture over time or between species cannot be specifically addressed. Nevertheless, several very interesting studies have been conducted and can be classed into two groups: transmission measurements [36], [37] and defoliation experiments.

The transmission measurements examined the vertical structure of wheat (grain heads versus stalks and leaves) with respect to polarization and local angle of incidence at X-band and demonstrated that in certain cases the layered structure of the canopy is important because canopies having strong angular properties (such as vertical stalks) can couple differentially at HH and VV polarizations [36], [37].

The defoliation experiments examined the backscattering and emission from canopies from which successive layers or types of canopy components had been progressively removed (by cutting). Fig. 10 is an example of a

corn canopy monitored with a scatterometer and a radiometer (both at 5.1 GHz) through successive defoliation stages until only the bare soil surface remained. For the radiometer, the canopy brightness temperature is dominated by the vegetation contribution at all angles; the increment in brightness temperature over that observed for the bare soil case is roughly proportional to the overlying water density of the canopy. In sharp contrast, the radar backscattering is observed to be insensitive to the presence of the corn canopy at incidence angles of less than 15° . At higher angles, the backscattering contribution of the canopy increases and is dominated by the return from the vertically aligned stalks and cobs, whereas the canopy loss component is apparently dominated by the leaves. Observations such as these strengthen the argument for using incidence angles near nadir for radar sensing of soil moisture.

V. SOIL MOISTURE RETRIEVAL

The ultimate objective of the soil-moisture research conducted under the auspices of the AgRISTARS program is to develop the algorithms and methodology necessary for retrieving soil-moisture estimates on an areal basis for applications in hydrologic and agronomic monitoring and assessment. The sensitivity of radar backscattering to scene parameters including soil moisture, soil texture, soil density, surface roughness, surface slope, crop-canopy cover, and row-directional effects has been examined, either independently or in combination, by means of scatterometer studies of individual test plots in which the scatterometers were capable of relatively fine spatial resolution. The next logical step, then, in the analysis is to examine the combined effects of all scene variables on the capacity of radar to accurately estimate soil moisture for an imaging system with a coarser resolution, such as an orbital SAR.

Experimental work in this area has been limited to the L-band and HH-polarized SAR systems carried by Seasat in 1978 [28] and SIR-B in October of 1984. The data produced by the SIR-B mission are currently under investigation by several research groups. Although the scatterometer studies indicate that this frequency and polarization combination is less than satisfactory for purposes of soil-moisture sensing, primarily because of the pronounced dependence upon surface roughness and row-directional effects, the Seasat data were found to be highly correlated with near-surface soil moisture ($\rho = 0.84$) for agricultural test field in the Great Plains for which concurrent ground truth was available [28]. In addition, a qualitative analysis of several Seasat scenes over Iowa revealed a dramatic sensor sensitivity to antecedent rainfall events, although corresponding ground truth was not available to resolve the question of whether the sensor response was driven by free water present on the crop canopies or by soil moisture (or both) [40].

Because orbital sensors with the scatterometer-defined optimal sensor configuration (i.e., C-band at 10° to 20° angles of incidence) are not yet available, the expected

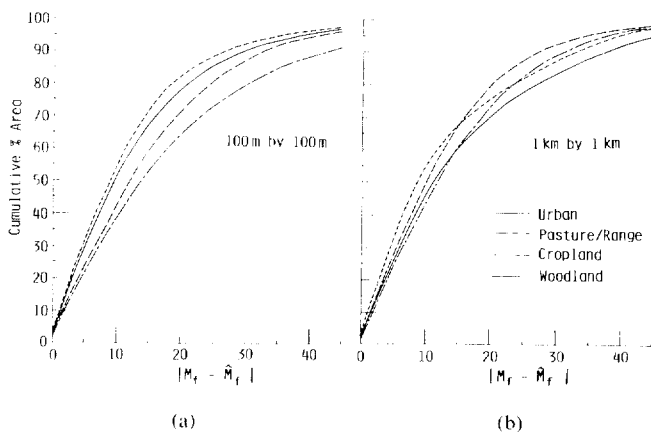


Fig. 11. Cumulative percent area of all moisture-dependent pixels (excludes cultural features, water, and woodland) in each subregion as a function of absolute moisture classification error for (a) 100 m \times 100 m radar resolution and (b) 1 km \times 1 km radar resolution. M_r represents the true moisture and \hat{M}_r the moisture estimated by the radar (from [42]).

performance of such systems has been tested via simulation studies that incorporate all known sensor and scene characteristics [41]–[43]. These studies have sought to define both sensor characteristics (i.e., resolution, antenna size, power requirements, and data rate) and the influence of scene confusion factors (i.e., topographic effects, variable canopy cover, and the complex spatial distributions of water bodies, forests, and urbanized areas) on the accurate retrieval or soil moisture from a SAR image.

The simulation studies are based upon digital terrain models in which each terrain element is characterized as to land-cover category, soil properties, and crop row direction. Typically, meteorologic events are used to simulate dynamics in the near-surface soil-moisture distributions over the test region as a function of time and local evapotranspiration demands. At selected time intervals, the backscattering properties of each subresolution element are defined by a Monte Carlo procedure based upon the scatterometer studies and estimates of “true” natural scene variability. The effects of signal scintillation (fading), shadowing, and layover are also incorporated into the image-formation model.

Early simulations of a 20 km \times 20 km, largely agricultural test region indicated that 0- to 5-cm soil moisture (expressed as a percent of field capacity) could be retrieved with an accuracy of ± 20 percent for 90 percent of the agricultural area using a C-band SAR with HH polarization at 7° to 17° angles of incidence and resolutions of 100 m \times 100 m [41], [42]. The simple retrieval algorithm required only the range position of the image pixel and the magnitude of the backscattered signal as input. A subsequent simulation for a much larger area, ≈ 100 km \times 120 km, which included more diverse topographic and land-cover conditions [43], reached much the same conclusion but more fully addressed the effects of scene confusion factors on the expected retrieval accuracy using a very simple “blind” algorithm dependent only upon range. The

results are summarized as follows (Fig. 11):

- 1) retrieval accuracy is optimized when radar resolution is smaller than the expected field-size dimensions of agricultural fields,
- 2) retrieval accuracy is optimized when radar resolution is coarser than local topographic variation in hilly areas,
- 3) the effects of row direction on retrieval accuracy are small, provided that the orbital trajectory yields azimuth view angles not orthogonal to row direction, and
- 4) retrieval accuracy can be improved by about 10 percent when multirate change detection is used to provide updates.

The rationale for the postulated effectiveness of multirate change detection is based upon a simple consideration of scene-confusion factors and scene dynamics. For practical purposes, topography is constant, surface roughness decays slowly with time (except at critical points in the local crop calendar such as planting and harvest periods), and the interfield variance in canopy cover varies over periods of weeks for most canopies.

A change-detection approach applied to Seasat imagery over a test site in southwestern Kansas shows the technique to be effective for discriminating fields subjected to irrigation or tillage operations from larger spatial scale variations related to antecedent rainfall events [44]. The use of spatial filtering techniques on multirate “difference” images permits the ready distinction of these two general types of scene dynamics.

VI. CONCLUSIONS

During the period of the AgRISTARS program, significant progress was made toward understanding the fundamental processes of target/sensor interaction, quantifying the effects of bulk scene properties and air-soil boundary conditions, developing both empirical and theoretical backscattering and emission models, and evaluating the potential performance of “optimal” orbital radar in terms both of sensor requirements and of possible soil-moisture retrieval methodologies. The research to date indicates that estimates of soil moisture in the 0- to 5-cm layer can be retrieved with reasonable accuracy for most requirements over agricultural areas from multirate and single-sensor observations. Such a system should operate at C-band over angles of incidence from about 10° to 20°. There is strong—but not conclusive—evidence to indicate that HV polarization will yield superior performance to HH polarization for soil-moisture retrieval.

There are, however, many pieces of the puzzle remaining to be fitted by means of further experimental investigation. For example, the precise physical role of soil texture as related to volumetric water content and soil matric potential with respect to radar backscattering is undefined at present. The utility of high-quality, cross-polarized

backscattering in minimizing the effects of surface boundary conditions (i.e., topographic slope, small-scale roughness, and row direction) needs to be examined. The theoretical backscattering models must be rigorously tested using data sets that provide sufficient physical characterization of the dielectric and roughness properties of soil. The effects of complex vegetation canopies on radar backscattering are only marginally understood and need further study. Finally, the confusion effects of complex geographical distributions of land-cover categories need to be better defined on the basis of the analysis of calibrated imagery.

REFERENCES

- [1] T. J. Schmugge, P. E. O'Neill, and J. R. Wang, "Passive microwave soil moisture research," *IEEE Trans. Geosci. Remote Sensing*, this issue, pp. 12-22.
- [2] F. T. Ulaby, "Radar measurements of soil moisture content," *IEEE Trans. Antennas Propagat.*, vol. AP-22, pp. 257-265, 1974.
- [3] F. T. Ulaby, J. Cihlar, and R. K. Moore, "Active microwave measurement of soil water content," *Remote Sensing Environment*, vol. 3, pp. 185-203, 1974.
- [4] F. T. Ulaby and P. P. Batlivala, "Optimum radar parameters for mapping soil moisture," *IEEE Trans. Geosci. Electron.*, vol. GE-14, pp. 81-93, 1976.
- [5] F. T. Ulaby, P. P. Batlivala, and M. C. Dobson, "Microwave backscatter dependence on surface roughness, soil moisture, and soil texture: Part I—Bare soil," *IEEE Trans. Geosci. Electron.*, vol. GE-16, pp. 286-295, 1978.
- [6] M. C. Dobson and F. T. Ulaby, "Microwave backscatter dependence on surface roughness, soil moisture, and soil texture: Part III—Soil tension," *IEEE Trans. Geosci. Remote Sensing*, vol. GE-19, pp. 51-61, 1981.
- [7] J. R. Wang and T. J. Schmugge, "An empirical model for the complex dielectric permittivity of soil as a function of water content," *IEEE Trans. Geosci. Remote Sensing*, vol. GE-18, pp. 288-295, 1980.
- [8] M. Hallikainen, F. T. Ulaby, M. C. Dobson, M. El-Rayes, and L. K. Wu, "Microwave dielectric behavior of wet soil, Part I: Empirical models and experimental observations," *IEEE Trans. Geosci. Remote Sensing*, vol. GE-23, pp. 25-34, 1985.
- [9] M. C. Dobson, F. T. Ulaby, M. T. Hallikainen, and M. A. El-Rayes, "Microwave dielectric behavior of wet soil, Part II: Dielectric mixing models," *IEEE Trans. Geosci. Remote Sensing*, vol. GE-23, pp. 35-46, 1985.
- [10] M. C. Dobson, F. Kouyate, and F. T. Ulaby, "A reexamination of soil textural effects on microwave emission and backscattering," *IEEE Trans. Geosci. Remote Sensing*, vol. GE-22, pp. 530-535, 1984.
- [11] F. T. Ulaby and R. P. Jedlicka, "Microwave dielectric properties of plant materials," *IEEE Trans. Geosci. Remote Sensing*, vol. GE-22, pp. 406-414, 1984.
- [12] F. T. Ulaby, C. T. Allen, and A. K. Fung, "Method for retrieving the true backscattering coefficient from measurements with a real antenna," *IEEE Trans. Geosci. Remote Sensing*, vol. GE-21, pp. 308-313, 1983.
- [13] T. J. Schmugge, "Effect of texture on microwave emission from soils," *IEEE Trans. Geosci. Remote Sensing*, vol. GE-18, pp. 353-361, 1980.
- [14] R. Bernard, P. Martin, J. L. Thony, M. Vauclin, and D. Vidal-Madjar, "C-Band radar for determining surface soil moisture," *Remote Sensing Environment*, vol. 12, pp. 189-200, 1982.
- [15] J. R. Wang, "Passive microwave sensing of soil moisture content: Soil bulk density and surface roughness," *Remote Sensing Environment*, vol. 13, no. 4, pp. 329-344, 1983.
- [16] W. P. Waite, A. M. Sadeghi, and H. D. Scott, "Microwave bistatic reflectivity dependence on the moisture content and matric potential of bare soil," *IEEE Trans. Geosci. Remote Sensing*, vol. GE-22, pp. 394-405, 1984.
- [17] C. T. Allen, F. T. Ulaby, and A. K. Fung, "A model for the radar backscattering coefficient of bare soil," Remote Sensing Lab., University of Kansas Center for Research, Lawrence, KS, AgRISTARS SM-K1-04181, 1982.
- [18] T. T. Wilheit, Jr., "Radiative transfer in a plane stratified dielectric," *IEEE Trans. Geosci. Electron.*, vol. GE-16, pp. 138-143, 1978.
- [19] T. LeToan and M. Pausader, "Active microwave signatures of soil and vegetation-covered surfaces. results of measurement programs," in *Proc. ISP Int. Colloq. Spectral Signatures of Objects in Remote Sensing* (Avignon, France, Sept. 8-11, 1981), pp. 303-314.
- [20] H. Hirose, S. Komiyama, and Y. Matsuzaka, "Cross-polarized radar backscatter from moist soil," *Remote Sensing Environment*, vol. 7, pp. 211-217, 1978.
- [21] G. A. Bradley and F. T. Ulaby, "Aircraft radar response to soil moisture," *Remote Sensing Environment*, vol. 11, pp. 419-438, 1981.
- [22] T. J. Jackson, A. Chang, and T. J. Schmugge, "Aircraft active microwave measurements for estimating soil moisture," *Photogrammetr. Eng.*, vol. 47, pp. 801-805, 1981.
- [23] M. C. Dobson, H. J. Eom, F. T. Ulaby, and A. K. Fung, "Active and passive microwave sensitivity to near-surface soil moisture and field flooding conditions," presented before Microwave Signatures in Remote Sensing, URSI Commission F (Toulouse, France), Jan. 16-20, 1984.
- [24] A. K. Fung and H. J. Eom, "Coherent scattering of a spherical wave from an irregular surface," *IEEE Trans. Antennas Propagat.*, vol. AP-31, pp. 68-72, 1983.
- [25] F. T. Ulaby, R. K. Moore, and A. K. Fung, *Microwave Remote Sensing: Active and Passive*, vol. III. Dedham, MA: Artech House, 1985.
- [26] F. T. Ulaby and J. E. Bare, "Look-direction modulation function of the radar backscattering coefficient of agricultural fields," *Photogrammetr. Eng.*, vol. 45, pp. 1495-1506, 1979.
- [27] F. T. Ulaby, F. Kouyate, A. K. Fung, and A. J. Sieber, "Backscattering model for a randomly perturbed periodic surface," *IEEE Trans. Geosci. Remote Sensing*, vol. GE-20, pp. 518-528, 1982.
- [28] A. J. Blanchard and A. T. C. Chang, "Estimation of soil moisture from Seasat SAR data," *Water Res. Bull.*, vol. 19, pp. 803-810, 1983.
- [29] T. F. Bush and F. T. Ulaby, "An evaluation of radar as a crop classifier," *Remote Sensing Environment*, vol. 7, pp. 15-36, 1978.
- [30] E. A. W. Attema and F. T. Ulaby, "Vegetation modeled as a water cloud," *Radio Sci.*, vol. 13, pp. 357-364, 1978.
- [31] F. T. Ulaby, C. T. Allen, G. Eger, III, and E. Kanemasu, "Relating the microwave backscattering coefficient to leaf area index," *Remote Sensing Environment*, vol. 14, pp. 113-133, 1984.
- [32] H. J. Eom and A. K. Fung, "A scatter model for vegetation up to Ku-band," *Remote Sensing Environment*, vol. 15, pp. 185-200, 1984.
- [33] R. H. Lang and J. S. Sidhu, "Electromagnetic backscattering from a layer of vegetation: A discrete approach," *IEEE Trans. Geosci. Remote Sensing*, vol. GE-21, no. 1, pp. 62-71, 1983.
- [34] T. Mo, T. J. Schmugge, and T. J. Jackson, "Calculations of radar backscattering coefficient of vegetation-covered soils," *Remote Sensing Environment*, vol. 15, pp. 119-133, 1984.
- [35] F. T. Ulaby, A. Aslam, and M. C. Dobson, "Effects of vegetation cover on the radar sensitivity to soil moisture," *IEEE Trans. Geosci. Remote Sensing*, vol. GE-20, pp. 476-481, 1982.
- [36] F. T. Ulaby and E. A. Wilson, "Microwave attenuation properties of vegetation canopies," *IEEE Trans. Geosci. Remote Sensing*, vol. GE-23, pp. 746-753, Sept. 1985.
- [37] C. T. Allen and F. T. Ulaby, "Modeling the polarization dependence of the attenuation in vegetation canopies," in *1984 IEEE Int. Geosci. Remote Sensing Symp. (IGARSS'84) Dig.* (Strasbourg, France), Aug. 27-30, 1984.
- [38] D. R. Brunfeldt and F. T. Ulaby, "Measured microwave emission and scattering in vegetation canopies," in *1983 IEEE Int. Geosci. Remote Sensing Symp. (IGARSS'83) Dig.*, vol. II (San Francisco, CA), Aug. 31-Sept. 2, 1984.
- [39] F. T. Ulaby, G. A. Bradley, and M. C. Dobson, "Microwave backscatter dependence on surface roughness, soil moisture, and soil texture, Part II: Vegetation-covered soil," *IEEE Trans. Geosci. Remote Sensing*, vol. GE-17, pp. 33-40, 1979.
- [40] F. T. Ulaby, B. Brisco, and M. C. Dobson, "Improved spatial mapping of rainfall events with spaceborne SAR imagery," *IEEE Trans. Geosci. Remote Sensing*, vol. GE-21, pp. 118-122, 1983.
- [41] F. T. Ulaby, M. C. Dobson, J. Stiles, R. K. Moore, and J. C. Holtzman, "A simulation study of soil moisture estimation by a space SAR," *Photogrammetr. Eng.*, vol. 48, pp. 6545-6560, 1982.
- [42] M. C. Dobson, F. T. Ulaby, and S. Moezzi, "Assessment of radar resolution requirements for soil moisture estimation from simulated satellite imagery," Remote Sensing Lab., Univ. of Kansas Center for Research, Lawrence, KS, 1982, RSL Tech. Rep. 551-2.

- [43] M. C. Dobson, S. Moezzi, F. T. Ulaby, and E. Roth, "A simulation study of scene confusion factors in sensing soil moisture from orbital radar," Remote Sensing Lab., Univ. of Kansas Center for Research, Lawrence, KS, 1983, RSL Tech. Rep. 601-1.
- [44] B. Brisco, F. T. Ulaby, and M. C. Dobson, "Spaceborne SAR data for land-cover classification and change detection," in *1983 IEEE Int. Geosci. Remote Sensing Symp. (IGARSS'83) Dig.* (San Francisco, CA), Aug. 31-Sept. 2, 1983.

*



M. Craig Dobson (M'83) was born in Rochester, NY, on October 25, 1951. He received the B.A. degree in anthropology and geology in 1973 from the University of Pennsylvania and the M.A. degree in geography in 1981 from the University of Kansas.

He has been a Senior Associate Research Engineering with the Department of Electrical Engineering and Computer Science at the University of Michigan since September 1984. Prior to that, he was an Associate Research Scientist with the

Remote Sensing Laboratory at the University of Kansas Center for Research, Inc. For the past ten years, his research interests have been in the area of microwave remote sensing of renewable resources and include the dielectric properties of natural media, backscattering and emission from terrain, and radar image analysis and simulation.

Mr. Dobson is a member of the American Society of Photogrammetry.



Fawwaz T. Ulaby (M'68-SM'74-F'80) was born in Damascus, Syria, on February 4, 1943. He received the B.S. degree in physics from the American University of Beirut, Lebanon, in 1964 and the M.S.E.E. and Ph.D. degrees in electrical engineering from the University of Texas, Austin, in 1966 and 1968, respectively.

From 1968 to 1984, he was with the Electrical Engineering Department at the University of Kansas, where he was the J. L. Constant Distinguished Professor, and the University of Kansas Center for Research, where he was Director of the Remote Sensing Laboratory. He is currently with the Radiation Laboratory and the Department of Electrical and Computer Engineering, University of Michigan, Ann Arbor. His current research interests involve microwave propagation and active and passive microwave remote sensing. Along with R. K. Moore and A. K. Fung, he is a coauthor of the three-volume series *Microwave Remote Sensing: Active and Passive*, Reading, MA: Addison-Wesley. In addition, he is coeditor of the *Manual of Remote Sensing*, 2nd ed., vol. I, American Society of Photogrammetry.

Dr. Ulaby is a member of Eta Kappa Nu, Tau Beta Pi, and Sigma Xi. He has been named the Executive Editor for IEEE TRANSACTIONS ON GEOSCIENCE AND REMOTE SENSING, 1984-1985, and was the Geoscience and Remote Sensing Society's Distinguished Lecturer for 1984. He was named an IEEE Fellow in 1980 "for contributions to the application of radar to remote sensing for agriculture and hydrology," received the GRS Society's Outstanding Service Award in 1982, and its Distinguished Service Award in 1983. In 1984, he also received a Presidential Citation for Meritorious service from the American Service of Photogrammetry. He received the University of Kansas Chancellor's Award for Excellence in Teaching in 1980, the University of Kansas Gould Award for "distinguished service to higher education" in 1973, and the Eta Kappa Nu MacDonald Award as an "outstanding electrical engineering professor in the United States of America" in 1975.

Soil Water Modeling and Remote Sensing

THOMAS J. JACKSON

Abstract—Soil water modeling research conducted as part of the AgRISTARS Soil Moisture project was reviewed along with other relevant studies. Research was categorized as follows: reviews of models, development of simulation models, integrating remotely sensed data and models, surface versus profile soil moisture, and estimating soil water properties. This review and evaluation found that some of the major objectives of the program were satisfied and that several of the results represent significant contributions to the science.

I. INTRODUCTION

SOIL WATER modeling research was one of the principal areas of the AgRISTARS Soil Moisture Project. Much of this program was adopted from the Plan for Research for Integrated Soil Moisture Studies (PRISMS) developed by the Soil Moisture Working Group [1]. There were three research directions related to soil moisture modeling identified in this report:

- 1) Evaluate the models that are currently in use because these will help define the type of data that is needed.
- 2) Develop new models or adapt existing models to better utilize remotely sensed data.
- 3) Since remote sensing methods of estimating soil moisture provide information on the surface layer, develop methods for extrapolating this information through the root zone.

In addition, it was also recognized that remote-sensing soil-moisture research could be conducted using simulation models and that there was a need for the development of sophisticated physically based models with this capability. Another problem related to modeling was how to deal with the spatial variability of large sensor resolution units when modeling soil water.

Over the course of the AgRISTARS project, all of the problems mentioned above were addressed. All of the modeling research was pertinent to the program and some results have had impact on the science of soil water modeling. In this review, the results of soil water modeling studies conducted during the AgRISTARS project will be described. For the purpose of organization, I have subdivided the material as follows:

- 1) reviews and comparisons of soil water budget models;
- 2) development of sophisticated models for simulation studies;

- 3) integration of remotely sensed data and soil water models;
- 4) profile soil moisture from surface layer measurements; and
- 5) estimating soil water properties.

Although the primary purpose of this review is to present the results of AgRISTARS funded research, it will include several studies that were conducted independently because they clearly address the same objectives. In some cases these independent efforts have produced more relevant results than the AgRISTARS-supported research.

II. SOIL WATER BUDGET MODELING

Soil water modeling was included as part of a survey conducted by Schmugge *et al.* [2] at the outset of the AgRISTARS project. They reviewed all methods that could be used to estimate soil moisture including *in situ*, remote sensing, and modeling.

The basic conservation of mass equation describing soil moisture is:

$$SM_t = SM_{t-1} + P - R - L - E - T + C - Q$$

where

| | |
|------------|---|
| SM_t | is the soil moisture volume at time t ; |
| SM_{t-1} | is the soil moisture volume at previous time; |
| P | is the precipitation; |
| R | is the surface runoff; |
| L | is the net lateral subsurface outflow; |
| E | is the evaporation or condensation; |
| T | is the transpiration; |
| C | is the capillary rise from lower levels; and |
| Q | is the percolation. |

Schmugge *et al.* [2] found that the published soil moisture models varied in the level of detail used to represent the physical system and the temporal definition of the driving forces. The important differences between models they identified were the 1) method used for computing the potential evapotranspiration, 2) method used for computing infiltration and runoff, 3) temporal definition of evaporative demand and precipitation, 4) consideration of saturated and unsaturated levels, 5) number of soil layers used, 6) method used for computing soil evaporation and plant transpiration, and 7) consideration of the thermal properties of the soil system.

The state of the art in soil water profile modeling at the time of the Schmugge *et al.* [2] survey included models

Manuscript received June 1, 1985; revised August 20, 1985.
The author is with the U.S. Department of Agriculture, ARS Hydrology Laboratory, Beltsville, MD 20705.
IEEE Log Number 8406229.

that could simulate water movement and heat transfer very well using theoretical functions for bare soils. However, root water extraction was and still is very difficult to model theoretically and has only been treated empirically.

Kanemasu *et al.* [3] reviewed all aspects of soil moisture as related to crop yield modeling. They found that most crop yield models utilized a soil water component or a surrogate variable such as precipitation or API; however, the level of detail used was variable. They recommended that in order to evaluate the sensitivity of crop yield models to the soil moisture component, it is necessary to use a model that includes a plant stress component.

The authors concluded from a review of the literature that crop yield sensitivity to soil moisture was related to climate. Under drier climatic conditions, crop yield is much more sensitive to soil moisture, presumably because under wetter conditions there is less variability in soil moisture. They also noted that good estimates of soil properties such as field capacity were also very important.

Next Kanemasu *et al.* [3] considered the use of two types of soil moisture observation information, profile and surface. Profile soil moisture would have a variety of uses in models. First, it could be used to correct estimates of soil moisture (updating). This would prevent the compounding of errors in simulation that might result from errors in the inputs such as precipitation. Second, observed profile soil moisture could be used to define model relationships. Estimating parameters such as field capacity can be difficult due to either the lack of data or spatial variability. By using comparisons between observed and simulated values of soil moisture, the best value of the parameter could be determined. A third use of soil moisture would be in estimating initial conditions for simulation. Finally, frequent observations of profile moisture could be used to estimate evapotranspiration (ET) directly. With the exception of ET estimation, the frequency of observation would be between one to three days. In order to use surface moisture for any of these same applications, much more frequent observations would be required.

Kanemasu *et al.* [3] suggest that surface moisture, if monitored daily, could provide information for models of:

- 1) runoff problem areas,
- 2) water erosion problem sites,
- 3) spatial variability of rainfall and subsequent spatial variations in surface evaporation,
- 4) watershed management,
- 5) mandatory minimum tillage and conservation monitoring,
- 6) remote resolution of irrigation frequency and rates on larger systems (e.g., center pivots),
- 7) remote resolution of irrigation frequency and rotation patterns in large surface irrigation projects such as in the Soviet Union and China,
- 8) pollution and saline deep reclamation,
- 9) environmental impact data (strip mine seepage, etc.),
- 10) planting data models,

- 11) trafficability, and
- 12) thermal inertia.

Hildreth [4] compared the characteristics of eight soil water profile models. His criteria for selecting these from the many described in the literature included: it must be adaptable for multiple locations and crops, some testing must have been conducted using field observations, and the computer program must be available.

The models Hildreth [4] evaluated fell into three categories based upon the method used to determine soil water changes. These categories were budget, semidynamic, and dynamic. Budget models used an accounting procedure with empirical functions which approximated the actual processes. The dynamic models attempted to utilize the precise theoretical relationships as much as possible. The semidynamic approach falls somewhere between the two extremes. A summary of the characteristics of these models is presented in Table I. His evaluation also included a comparative summary of some of the significant features and limiting factors of each model. These are presented in Table II.

The principal recommendation of Hildreth's study [4] was that all of these models should be evaluated using the same data set. It was intended that data collected in an experiment conducted in Kansas would be used; however, Arya and Hildreth [5] found that the quality of these data was very poor and the evaluation was never completed.

One model that has received significant attention as part of the AgRISTARS project is the Soil-Plant-Atmosphere-Water (SPAW) model originally developed by Saxton *et al.* [6]. Fig. 1 is a flow chart of this model. It incorporates some physically based and some empirical components. SPAW was later modified to include a means for estimating crop water stress and the effect of stress on the canopy development [7]. This model was then tested over large areas of several states.

In a related study Calder *et al.* [8] conducted an evaluation of 35 different formulations of soil water deficit models. These were all evaluated using neutron probe observations of soil moisture at six grassland sites. They began by using a very simple formulation and then made improvements in meteorological inputs and/or the soil water functions to assess the effects on predictions. Fig. 2 is reproduced from their paper and shows the characteristics of the models and the expected trend in the accuracy.

Calder *et al.* [8] found that successive improvements to the soil characterization resulted in improved predictions, as might be expected. What was somewhat surprising was that increasing the detail of the meteorological input did not always result in improved predictions. The authors suggest that the daily time step and the low variability of evaporation demand in the United Kingdom probably affect these results.

This study represents a very systematic approach to determining the incremental value of additional input data and model complexity on the ultimate decision variable, the soil water deficit. However, part of the problem with

TABLE I
SUMMARY OF SOIL WATER PROFILE MODELS [4]

| Type | Name | Characteristics | Potential evapotranspiration function | Crops | Soil | Input | Output |
|--------------|---|---|---|-------------------------------------|---|--|---|
| Budget | CMI (Hill version) two layers | $\Delta SM=P-ET$ Top layer evaporates first at potential rate | Thornthwaites empirical function; average temperature, day length | Average vegetation | Variable field capacity and wilting point used | Precipitation, daily temperature | Compares measured and predicted SM; determines difference, plot predicted SM vs. depth. Outputs PET and AET. |
| Budget | Baier and Robertson six layers | $\Delta SM=P-ET-R-Q$ converts layers to zones with standard percent of total water | Empirical | Spring wheat, soybeans, fallow | Total available water, eight drawdown tables, field capacity, wilting point | Complete meteorological data, initial SM, root distribution | Daily output of AET, PET, water balance comparative data on observed and predicted SM. |
| Budget | Feyerherm six layers | Similar to Baier and Robertson | Similar to Baier and Robertson | Winter and spring wheat | Specific table and total water | Similar to Baier and Robertson | Similar to Baier and Robertson. |
| Budget | Kanemasu five layers | Similar to Baier and Robertson but more flexible | Energy balance, empirical coefficients, and leaf area index | Wheat, corn soybeans, sorghum | Similar to Baier and Robertson | Complete meteorological data, more extensive soil and plant data needed than Baier and Robertson | Complete water balance, AET, PET, soil evaporation SM by layer. |
| Budget | SIMBAL (Stuff) 10 layers (needs updating) | $\Delta SM=P-ET+C$ +tile drainage | Pan evaporation | Corn | Field capacity and wilting point. Needs special data | Precipitation and pan evaporation, needs depths to tile and water table | Similar to Baier and Robertson with more water balance information. |
| Semi-dynamic | Saxton variable | $\Delta SM=P-ET-R+Q-C$ Soil moisture redistribution accomplished by simplified dynamic flow equation | Pan evaporation, empirical relationships | Specified by tables or functions | Depends on moisture-tension and moisture conductivity functions | Complete meteorological data or pan evaporation, extensive plant and canopy data, much of which is not readily available | Compact daily output of water balance, crop stress, AET, PET and pan evaporation. |
| Dynamic | Hanks variable | $\Delta SM=P-ET-R+Q-C$ Dynamic water flow and variable time step, limited plant capability | Arbitrary, PET or AET | Depends on root and soil data | Depends on moisture-tension and moisture conductivity functions | Precipitation and pan evaporation, limited root distribution and crop cover data | Limited water balance at end of each input period; plot SM vs. depth. |
| Dynamic | Van Bavel variable | $\Delta SM=P-ET-R+Q-C$ Dynamic water flow equation, dynamic plant-soil-atmosphere interaction; very flexible, uses CSMPIII, shading output, SM vs. time and depth also available | Evaporation only, energy balance and leaf area index; uses empirical coefficients | Given by canopy, root and soil data | Given by moisture-tension and moisture conductivity functions used | Complete meteorological data, detailed plant soil and atmospheric data needed | Flexible time increments for all output; calculates crop water use as a function of crop change and SM change |

the apparent inconsistency of the conclusions of this study may be that all of the models used fall under the budget category described above and may not be able to benefit from detailed input data.

Jackson *et al.* [9] considered the impact of soil moisture observations on hydrologic modeling. As described above for crop yield models, they recognized two primary uses—calibration and updating model predictions. They evaluated the sensitivity of one model by updating surface soil moisture using observed data and found that under the tested conditions observed soil moisture was of limited value. However, this study dealt only with the simulation of annual runoff. It is very likely that simulations of daily runoff would be much more sensitive to soil moisture.

Peck *et al.* [10] conducted a survey of the possible use of remote sensing in hydrologic modeling. One of the subjects they considered was soil moisture. Six hydrologic models were described and the soil moisture accounting component was outlined. In a subsequent study, Peck *et*

al. [11] considered how remotely sensed data, including soil moisture, might be used in these models. Each model was evaluated to determine if it could use soil moisture observations in its current configuration or by minor modification 1) as an input, 2) an update, or 3) to calibrate.

None of the models calibrated by Peck *et al.* [11] could currently utilize soil moisture observations nor could they be adapted easily to use the data as input. However, most of the models could utilize the data for update and calibration.

The studies summarized above constitute a fairly good survey or review of soil water modeling and how soil moisture observations might be used in models and/or applications. However, I do not think that a true evaluation of these models has been completed. The study which had been planned by Arya and Hildreth [5] would probably have answered many questions concerning model sensitivity and accuracy as related to soil moisture. As mentioned, the study conducted by Calder *et al.* [8] is along

TABLE II
SOIL WATER MODEL COMPARATIVE SUMMARY FROM [4]

| Model | Significant features | Limiting factors |
|---------------------|---|--|
| CMI (Hill Version) | Uses readily available meteorological data Requires minimum input data Long usage | Determines average weekly changes for general crop/land Two-layer model Runoff only when profile filled Limited number of processes modeled |
| Baier and Robertson | Uses readily available meteorological data with options to use more if available Takes into account freezing soil and snow Used extensively in Canada | Developed for Canadian soils, crops, and climate |
| Feyerherm | Uses readily available meteorological data | No profile printout Crop and soil specific |
| Kanemasu | Tested for several crops Five layers | Soil and crop specific Uses solar radiation only Many empirical constants |
| SIMBAL | For poorly drained soil Small amount of input data needed | Crop and soil specific; highly empirical; many coefficients Uses pan evaporation |
| Saxton | Includes data for wide range of soils Calculates stress Has feedback Represents many processes | Needs crop data not readily available Uses pan evaporation |
| Hanks | Dynamic model Extensively tested and used Prints depth profile | Needs hydrologic data for specific soil Needs evapotranspiration estimates Needs canopy and root depth |
| Van Bavel | Dynamic and flexible Ease of programming and use Calculates evaporation and transpiration directly from meteorological data Several new approaches | Not tested Complex Uses flexible and easy computer language which may not be readily available |

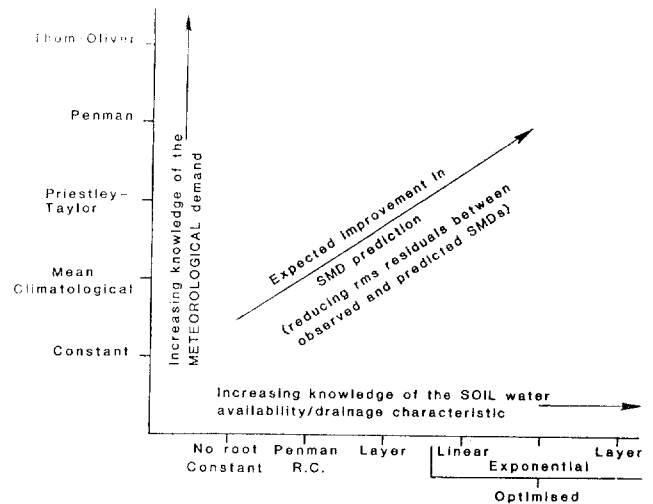


Fig. 2. Effects of increasing the meteorological and/or soil water functions on the accuracy in estimating the soil water deficit (SMD) from [8].

tremely difficult to collect data at the level of spatial and temporal resolution that is needed as input to physically based emission models. However, it is quite simple given the appropriate soil water model to simulate these data.

In order to be useful in this type of study, the model should be soundly based in theory and include all possible factors that affect both water movement and heat transfer. Such models should be extremely accurate if the physical system and the input data can be described in enough detail.

Van Bavel and Lascano [12] proposed a model for bare soils that could simulate water and energy balance. Lascano and Van Bavel [13] used a version of this model called CONSERVB to simulate a set of detailed field observations over a 30-day period. Their results showed good agreement between the predicted and observed soil moisture. The model was able to predict the measured value within one standard deviation of the observed value. The model also predicted the temperature profile very well.

Camillo and Schmutge [14] also developed a computer model that simulated both moisture and heat flow in bare soils by solving the partial differential equations describing the physical processes. Comparisons to analytical solutions and field observations were used to verify the model's performance. The model was also tested using a detailed bare soil data set [15].

An example of the use of a soil water simulation in conjunction with a microwave emission model was presented by Camillo and Schmutge [16]. Using their model described above, the authors simulated the soil and heat balance for a series of soils, initial conditions, and rainfall amounts over time. These detailed descriptions of water and heat were then used as input to a microwave emission model so that a detailed simulation of emission could be generated.

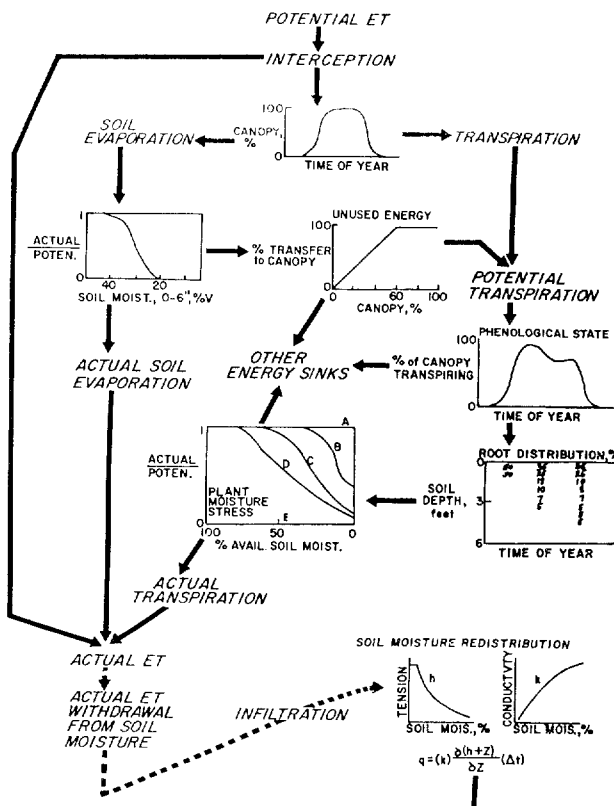


Fig. 1. The SPAW model from [6].

the lines of what should have been performed as part of the AgRISTARS program.

III. SOIL WATER SIMULATION MODELS AS A RESEARCH TOOL

Soil water models can be more useful than field observations as inputs to microwave emission models. It is ex-

IV. INTEGRATION OF REMOTELY SENSED SOIL MOISTURE AND MODELS

All of the research described previously dealt with how the remotely sensed data could be used to estimate soil

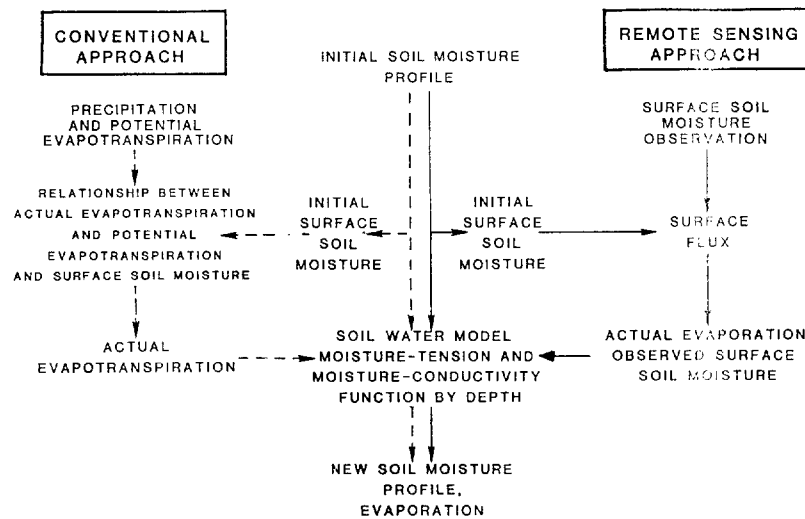


Fig. 3. The general approach used by Bernard *et al.* [18] versus a conventional approach to estimating bare soil evaporation.

moisture within the framework of existing soil water modeling approaches. An alternative to this approach is to develop new models that take advantage of the type of information that remotely sensed soil moisture can provide. Earlier work, such as that conducted by Idso *et al.* [17], focused on the use of thermal infrared data in conjunction with energy budget models to estimate soil moisture and evapotranspiration. Bernard *et al.* [18] suggested that if direct estimates of surface soil moisture were available, these could be used to determine the actual evapotranspiration through relationships between potential and actual evapotranspiration or as the upper boundary layer condition in soil water models.

Meylan *et al.* [19] point out that difficulties in specifying the upper boundary condition are a limiting factor in soil water modeling. They suggested that the use of frequent surface soil moisture measurements could improve the model simulation. These authors outlined a physically based water and heat transfer model that would utilize thermal infrared and passive microwave data as inputs. The model would also require measured soil water characteristics for the soil and meteorological data (precipitation, insolation, temperature, humidity, and pan evaporation). From the soil and meteorological observations, the soil temperature and moisture profiles would be computed. Remotely sensed data would then be used to adjust the simulations and to independently estimate evapotranspiration. To date, the authors have not published any simulation or test results using this model.

Another French research group has conducted a much more comprehensive and thorough evaluation of the use of microwave remote sensing in soil water simulation. Bernard *et al.* [18] developed an approach for modeling soil water and estimating evapotranspiration under bare soil conditions. Their method is based on Richards' equation for one dimensional isothermal water movement. It requires as input the moisture-tension and moisture-conductivity relationships and initial conditions, in addition to estimates of surface soil moisture. Fig. 3 illustrates the

general operation of a procedure employing remotely sensed surface soil moisture and compares it to a conventional approach. Here the conventional approach used is similar to that employed in the SPAW model outlined in Fig. 1 under bare soil conditions. The authors evaluated this approach by using field observations of all inputs, soil moisture, and evaporation. Observed surface soil moisture was used to simulate microwave observations. Comparisons between measured evaporation and simulated evaporation indicated that the model was very accurate under the tested conditions. These tests conducted on a bare light clay indicated that the procedure would be accurate for estimating cumulative evaporation if the surface moisture was measured once every three days. Daily evaporation could be determined accurately with two daily measurements of surface soil moisture, one in the early morning and the other in the early evening.

Prevot *et al.* [20] followed up on the approach described above by conducting a field experiment that would provide all the data required for testing the model. They collected all meteorological data, soil moisture, and radar data required over a one-month period. The results of this investigation showed that the remote sensing approach could be used to determine the soil water balance and evaporation with the same accuracy as neutron probe methods. The authors found that this approach actually worked better if rainfall observations were not used. They attribute this to the structure of the model and the radar measurement frequency.

Smith and Newton [21] also developed a physically based soil water simulation model that utilizes remotely sensed data. Their general approach is similar to that of Bernard *et al.* [18] in that microwave emission is used to estimate surface soil moisture which in turn is used to determine the surface flux that drives the model. The focus of this work was to predict profile moisture; further details are provided in the next section.

The general approach used by Bernard *et al.* [18] shows a great deal of original thinking. The basic concept in-

volved is not that complex; however, the linking of all the components into a prediction process is. A major drawback to all of the research conducted to date is that the useful procedures are designed for bare soils. These techniques should be expanded to vegetated fields.

V. ESTIMATING PROFILE SOIL MOISTURE FROM SURFACE LAYER MEASUREMENTS

Remote sensing of soil moisture usually provides a measure of surface moisture. If these techniques are to be of value in applications, methods must be developed to predict profile soil moisture using the surface data. The solution to this problem was identified as major objective in AgRISTARS Soil Moisture project. Although some efforts have used simple procedures, most have involved the use of soil water modeling.

Jackson [22] pointed out that the problem could be solved using several levels of data collection and model sophistication. A single surface layer measurement every n days represents the simplest sensor configuration and the least costly alternative. From this option the frequency of surface measurements can be increased, ancillary meteorological data can be used, and sophisticated models can be employed. All of these alternatives for improvement will, of course, involve greater costs.

The simplest approach to the problem is to develop a regression equation to predict profile soil moisture from surface layer measurements. Biswas and Dasgupta [23] presented the results of one investigation using data collected at depths of 7.5, 15, 30, 45, and 60 cm. They found good correlations in almost all cases. The coefficient of determination decreased as the depth of the profile layer from the surface increased. One problem they detected was that there was no clear relationship between the regression parameters and site variables.

Blanchard [24] evaluated linear correlations between soil layers on 16 small watersheds located in Oklahoma. Data were available every two weeks for several years. Because the data were collected using neutron probes, the first surface layer available was 0–22.8 cm. His results also showed that this approach produced high correlations between the surface layer and the profile moisture to a depth of 50 or 60 cm, although the decrease at deeper depths was very small. He found better results on rangelands than on croplands.

Smith and Newton [21] used a data set generated by a detailed simulation model to evaluate the relationship between different surface layer thickness soil moistures and those in a 100-cm profile. They found that this approach worked well during a dry down and would be better approximated using a nonlinear function.

Arya *et al.* [25] evaluated the regression approach using field observations of surface and profile soil moisture. Fig. 4 shows the results for different field conditions that were observed for the 0–5 cm and 5–45 cm soil moisture values. It is apparent in these figures that the surface soil moisture exhibits a very large dynamic range while the profile soil moisture exhibits much smaller variations. This

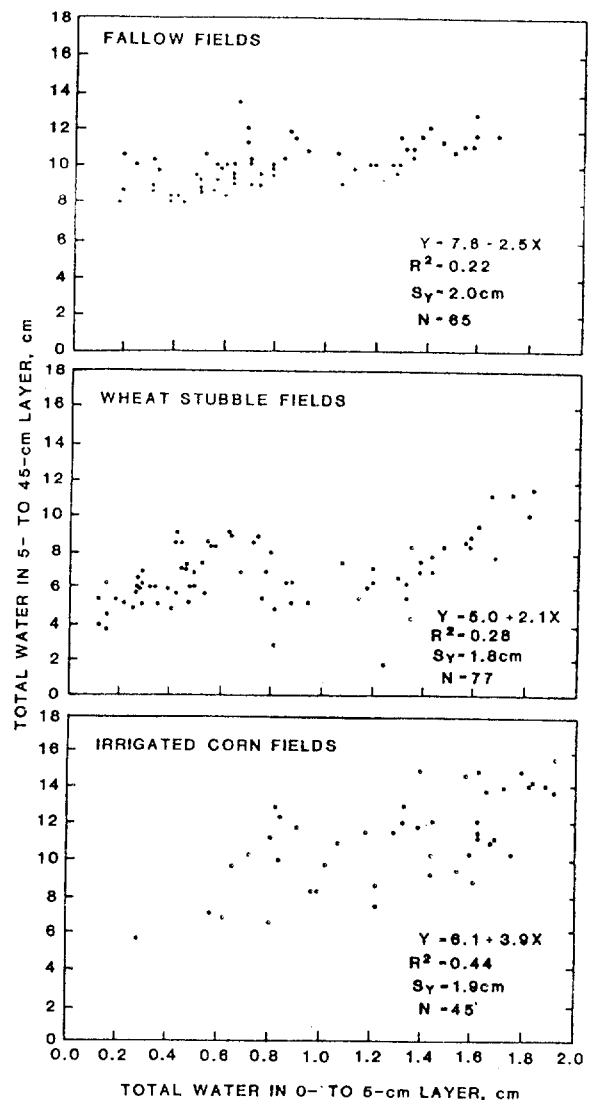


Fig. 4. Relationship between the 0–5-cm and 5–45-cm soil water as a function of field cover from [25].

is more significant in fields that are dominated by soil evaporation, such as fallow and stubble fields. The corn fields show a much stronger relationship. Fig. 5 is adapted from Arya *et al.* [25] and shows the correlation between the surface layer of a given thickness and a varying profile depth soil moisture. Results are presented separately for fallow and corn fields. This figure illustrates the following points:

- 1) Correlation decreases as the profile depth increases.
- 2) The correlation between the surface and profile moisture is larger for planted fields than for fallow fields.
- 3) Increasing the thickness of the surface layer improves the relationship between the surface and the profile moisture.

The reason why simple regression relationships can be used, under some conditions, to predict profile moisture from surface layer measurements is that the laws of physics link all layers of the soil together. If these relationships are approximately linear then the regression approach will work. Kondratyev *et al.* [26] approached the problem with

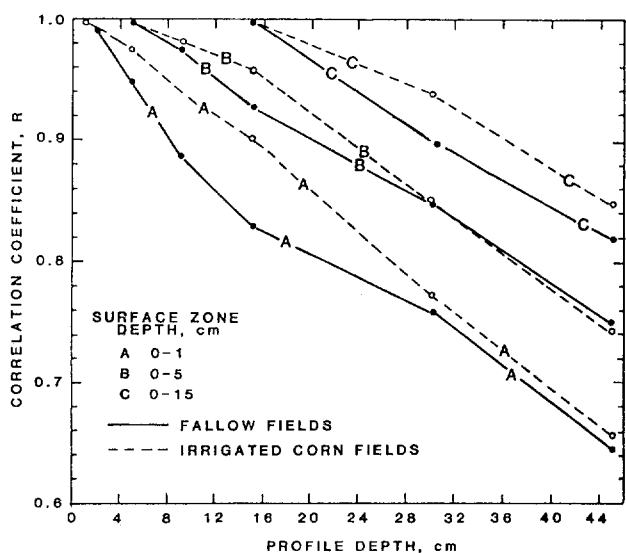


Fig. 5. Correlation between various surface depth soil moistures and profile depths from [25].

a more sophisticated yet simple approach. They used an equation that for a given soil moisture described the gradient of soil moisture with depth. This gradient is related to the wilting point profile of the soil. The authors report that the method has been tested and performed very well. A recent report [27] states that the method is being used operationally in conjunction with passive microwave remote sensing.

Jackson [22] developed and numerically evaluated a method that was based on the assumption that the soil profile was in the state of hydraulic equilibrium. Under this assumption, the laws of physics specify that all points in the soil column must have the same hydraulic potential, which is made up of its matric potential and gravitational potential (i.e., depth below the surface). By specifying the moisture-tension (matric potential) relationship for each soil layer, the observed surface soil moisture can be used to predict the profile soil moisture.

Using a detailed soil moisture simulation model and representative meteorological and soils data, Jackson [22] simulated data to evaluate his approach. His results, based upon the standard error of estimate in predicting the profile soil moisture, showed that the accuracy of the predictions increased at the thickness of the surface layer increased. However, beyond approximately 10 cm the improvement was marginal. Other analysis showed that this approach worked better on soils with higher water conductivities (i.e., sands). Another series of simulations analyzed the effect of time of day on the predictions. Fig. 6 shows the results obtained. As we would expect, the approach works best when the soil is most likely to be in hydraulic equilibrium (predawn).

Smith and Newton [21] evaluated the method proposed by Jackson [22] using a data set simulated by a detailed model and an actual set of observed meteorological data collected over a 30-day period. They found that the soil moisture in at least the surface 20 cm could be accurately predicted using the surface 0-5 cm average soil moisture.

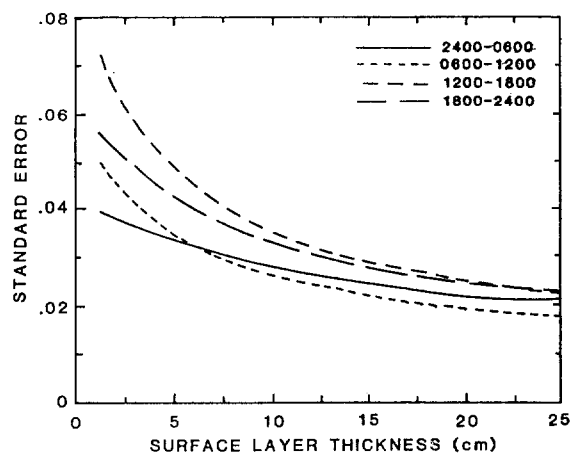


Fig. 6. Error of estimating profile soil moisture from surface soil moisture as a function of the time of day from [22].

Poor results were obtained for predictions of the 20-50 cm soil moisture. It should be noted that Smith and Newton [21] did not consider the effects of time of day on the results. Improved predictions would be found if predawn surface soil moisture was used.

All of the methods discussed so far for predicting profile soil moisture have been very simple and are based on relating the surface moisture at that instant in time to the profile moisture. If the data are available on a frequent basis, the change in surface soil moisture provides additional information for assessing the profile moisture. Arya *et al.* [25] developed a relatively simple algorithm that combines the rate of change of the surface moisture and flux at the bottom of the surface zone, estimated from soil hydraulic properties, to determine the profile soil moisture. The one drawback to this procedure may be that it requires a moisture gradient in the surface zone (0-5 cm). The authors propose that if the 0-5 cm soil moisture was available, the 0-2 cm moisture could be predicted using an empirical equation. From the 0-2 and 0-5 cm soil moistures, the gradient could be approximated. Comparisons between predictions made using this approach and both field and simulated data showed good agreement.

In a previous section, the model developed by Bernard *et al.* [18] was described. This method can also predict profile moisture. It utilizes the change in surface moisture in conjunction with a soil water simulation model. Smith and Newton [21] utilized a similar but more sophisticated surface flux-modeling approach. They modified a physically based soil water simulation model so that it was driven by the surface layer soil moisture. This approach was based on hourly observations of surface moisture and it is unlikely that such a sophisticated approach would work with less frequent observations.

Unfortunately, all of these more sophisticated methods have only been evaluated for bare soils. Vegetation presents a problem in soil water modeling because of the difficulty in specifying root water extraction. Camillo and Schmutge [28] concluded a study to determine if profile moisture could be predicted from surface measurements in vegetated fields. They found that the matric potential

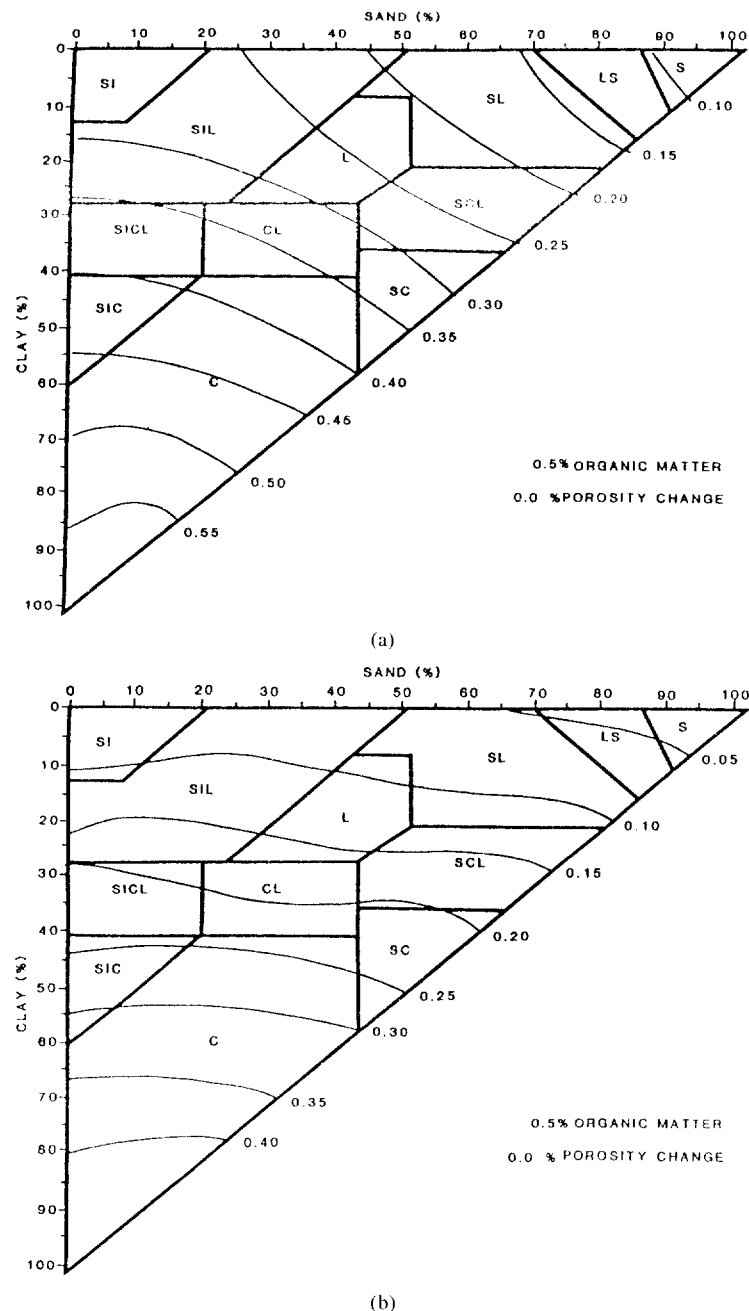


Fig. 7. Estimating (a) 0.3-bar and (b) 15-bar volumetric soil moisture as from the percent sand and clay from [31].

profile could be predicted from the root density profile. Once vegetation reaches maturity, the root density profile is constant. Given the root density profile, the surface soil moisture, and the profile hydraulic properties, the profile soil moisture can be predicted. Limited tests with laboratory and field data indicated that the method has potential.

VI. ESTIMATING SOIL WATER PROPERTIES FOR MODELING

A recurring problem in all the research dealing with remote sensing of soil moisture is accounting for the effects of soil properties. The most useful types of information in most cases are the relationships between soil moisture and

matric potential (suction or tension) and soil moisture and hydraulic conductivity. Moisture-matric potential functions can be used to estimate widely used model parameters, such as field capacity and wilting point. Over the course of the AgRISTARS project a number of significant results were published that describe methods for estimating soil water characteristics without resorting to sampling.

Clapp and Hornberger [29] published one of the first generalized approaches for determining soil water characteristics. Their approach only requires the soil texture. However, it does not consider the effects of factors such as bulk density and it utilizes empirical equations.

Arya and Paris [30] developed a procedure for predict-

ing the soil water characteristics that utilizes particle size distribution and bulk density as inputs. Their approach is founded in theory but requires the acceptance of several assumptions concerning the shape and size of particles, especially in the clay fraction. Tests against laboratory data showed good agreement between the predictions and lab results.

Rawls *et al.* [31] developed a series of regression equations for predicting the soil moisture at specific matric potential values. These equations can be used with 3 different levels of input data:

- 1) Percent sand, silt, and clay, organic matter, and bulk density.
- 2) Same as 1, but it also uses a measured 15-bar water content.
- 3) Same as 2, but it also uses a measured 0.33-bar water content.

In addition, this publication also summarizes the average values of the following soil properties by texture class based on over 5000 samples: total porosity, 0.33- and 15-bar soil water values and the saturated hydraulic conductivity. Fig. 7 from Rawls *et al.* [32] is a simple graphical procedure for estimating the 0.33- and 15-bar matric potential water contents based on the sand and clay fractions and porosity. In this same paper the authors also present a method for accounting for different tillage treatments on soil water characteristics.

Another soil property of interest is the bulk density. Rawls [33] presented a method for predicting the bulk density from the particle size distribution and the organic matter content for natural undisturbed soils. Average values of organic matter content for different soil texture classes were summarized.

VII. SUMMARY

Prior to the AgRISTARS Project, the basic questions related to remote sensing of soil moisture and soil water modeling were: 1) What type of data do we need? 2) What can we do with the projected data products? 3) How can surface measurements be extrapolated to develop profile soil moisture?

The first question concerning what type of data do we need was addressed through reviews of existing soil water models and soil water components of crop yield and hydrologic models. These reviews are useful, however, they are qualitative. We still need a qualification of the sensitivity of these models to their soil water component. The study that was planned but never completed as part of AgRISTARS [5] would have provided most of this information. This quantitative comparison should be completed and should take into consideration the approach used by Calder *et al.* [8].

What can we do with the projected data? The efforts by Bernard *et al.* [18] show that frequent surface soil moisture observations could be extremely valuable if new approaches to modeling are developed that take full advantage of the data. However, these methods still need

additional research to account for all the components of the water balance and verification under a wide range of conditions.

The final questions concerning extrapolating surface observations to the profile was one of the most critical. If we could do this, that data could be used in almost every application. Experimental and theoretical analyses have shown that useful information on the upper portion of the soil profile, approximately 40 cm, can be extracted from soil moisture measurements.

The research on soil water modeling conducted during the AgRISTARS project has brought us closer to the answers to the questions listed above. However, there are several additional steps that should be taken to finalize these studies. These include a quantitative comparison of soil water models and further verifications of surface-profile extrapolation techniques. In addition, a significant effort should be made to develop a model, or utilize the same model, as that presented by Bernard *et al.* [18]. This effort should involve a greater amount of ground data collection and wider range of conditions than has been evaluated to date.

REFERENCES

- [1] Soil Moisture Working Group, "Plan of research for integrated soil moisture studies," NASA Scientific and Technical Information Office, Oct. 1980.
- [2] T. J. Schmugge, T. J. Jackson, and H. L. McKim, "Survey of methods for soil moisture determination," *Water Res. Research*, vol. 16, no. 6, pp. 961-979, Dec. 1980.
- [3] E. T. Kanesmasu, A. Feyerherm, J. Hanks, M. Keener, D. Lawlor, P. Rasmussen, H. Reetz, K. Saxton, and C. Wiegand, "Use of soil moisture information in crop yield models," AgRISTARS Rep. SM-M0-00462, July 1980.
- [4] W. W. Hildreth, "Comparison of the characteristics of soil water profile models," AgRISTARS Rep. SM-L0-00490, Jan. 1981.
- [5] L. M. Arya and W. W. Hildreth, "Agricultural soil moisture experiment: Evaluation of 1978 Colby data collected for comparative testing of soil moisture models," AgRISTARS Rep. SM-L1-04047, May 1981.
- [6] K. E. Saxton, H. P. Johnson, and R. H. Shaw, "Modeling evapotranspiration and soil moisture," *Trans. ASAE*, vol. 17, no. 4, pp. 673-677, 1974.
- [7] K. E. Saxton and G. C. Bluhm, "Predicting crop water stress by soil water budgets and climatic demand," *Trans. ASAE*, vol. 24, no. 1, pp. 105-109, 1982.
- [8] I. R. Calder, R. J. Harding, and P. T. W. Rosier, "An objective assessment of soil-moisture deficit models," *J. Hydrol.*, vol. 60, pp. 329-355, 1983.
- [9] T. J. Jackson, T. J. Schmugge, A. D. Nicks, G. A. Coleman, and E. T. Engman, "Soil moisture updating and microwave remote sensing for hydrologic simulation," *Hydro. Sci. Bull.*, vol. 26, no. 3, pp. 305-319, 1981.
- [10] E. L. Peck, R. S. McQuivey, T. N. Keefer, E. R. Johnson, and J. L. Erikson, "Review of hydrologic models for evaluating use of remote sensing capabilities," AgRISTARS Rep. GP-G1-04102, Mar. 1981.
- [11] E. L. Peck, T. N. Keefer, and E. R. Johnson, "Strategies for using remotely sensed data in hydrologic models," AgRISTARS Rep. CP-G1-04151, July 1981.
- [12] C. H. M. Van Bavel and R. J. Lascano, "CONSERVB. A numerical method to compute the soil water content and temperature profiles under a bare surface," Texas A&M Univ., College Station, TX, Remote Sensing Center Tech. Rep. RSC-134, Dec. 1980.
- [13] R. J. Lascano and C. H. M. Van Bavel, "Experimental verification of a model to predict soil moisture and temperature profiles," *Soil Sci. Soc. Amer. J.*, vol. 47, pp. 441-448, 1983.
- [14] P. Camillo and T. J. Schmugge, "A computer program for the simulation of heat and moisture flow in soils," AgRISTARS Rep. SM-G1-04086, May 1981.
- [15] P. J. Camillo, R. J. Gurney, and T. J. Schmugge, "A soil and atmo-

- spheric boundary layer model for evapotranspiration and soil moisture studies," *Water Res. Research*, vol. 19, no. 2, pp. 371-380, Apr. 1983.
- [16] P. J. Camillo and T. J. Schmugge, "Correlating rainfall with remotely sensed microwave radiation using physically based models," *IEEE Trans. Geosci. Remote Sensing*, vol. GE-22, no. 4, pp. 415-423, July, 1984.
- [17] S. B. Idso, R. J. Reginato, and R. D. Jackson, "An equation for potential evaporation from soil water and crop surfaces adaptable to use by remote sensing," *Geophys. Res. Lett.*, vol. 4, pp. 187-188, 1977.
- [18] R. Bernard, M. Vauclin, and D. Vidal-Madjar, "Possible use of active microwave remote sensing data for prediction of regional evaporation by numerical simulation of soil water movement in the unsaturated zone," *Water Res. Research*, vol. 17, no. 6, pp. 1603-1610, Dec. 1981.
- [19] P. Meylan, C. Morzier, and A. Musy, "Determination of changes in the hydrologic and thermal profiles of soil by simulation and remote sensing," *Tech. Trans., AgRISTARS Rep. SM-J1-00800*, Feb. 1981.
- [20] L. Prevot, R. Bernard, O. Taconet, D. Vidal-Madjar, and J. L. Thony, "Evaporation from a bare soil evaluated using a soil water transfer model and remotely sensed surface soil moisture data," *Water Res. Research*, vol. 20, no. 2, pp. 311-316, Feb. 1984.
- [21] M. R. Smith and R. W. Newton, "The prediction of root zone soil moisture with a water balance-microwave emission model," *AgRISTARS Rep. SM-T3-04425*, May 1983.
- [22] T. J. Jackson, "Profile soil moisture from surface measurements," *J. Irrig. Drain. Div. ASCE*, vol. 106, no. IR2, pp. 81-92, June 1980.
- [23] B. C. Biswas and S. K. Dasgupta, "Estimation of soil moisture at deeper depth from surface layer data," *Mausam*, vol. 30, no. 4, pp. 511-516, 1979.
- [24] B. J. Blanchard, "Correlation of spacecraft passive microwave system data with soil moisture indices (API)," *Remote Sensing Center, Texas A&M Univ., College Station, TX, RCS-3622-2*, 1979.
- [25] L. M. Arya, J. C. Richter, and J. F. Paris, "Estimating profile water storage from surface zone soil moisture measurements under bare field conditions," *Water Res. Research*, vol. 19, no. 2, pp. 403-412, Apr. 1983.
- [26] K. Ya. Kondratyev, V. V. Melentyev, Yu. I. Rabinovich, and E. M. Shulgina, "Passive microwave remote sensing of soil moisture," in *Proc. 11th Symp. Remote Sensing Environ.* (Environmental Research Inst. of Michigan, Ann Arbor), 1977.
- [27] N. A. Armand, V. N. Oleksich, V. G. Shinkaryuk, and A. M. Shutko, "Remote determination of the moisture content of soils in the irrigated lands of Moldavia," *Gidromekh. Melior* (NASA Tech. Transl.), pp. 58-60, 1981.
- [28] P. Camillo and T. J. Schmugge, "Estimating soil moisture storage in the root zone from surface measurements," *Soil Sci.*, vol. 135, no. 4, pp. 245-264, Apr. 1983.
- [29] R. B. Clapp and G. M. Hornberger, "Empirical equations for some soil hydraulic properties," *Water Res. Research*, vol. 14, no. 4, pp. 601-604, Aug. 1978.
- [30] L. M. Arya and J. F. Paris, "A physico empirical model to predict the soil moisture characteristic from particle-size distribution and bulk density data," *Soil Sci. Soc. Amer. J.*, vol. 45, pp. 1023-1030, 1981.
- [31] W. J. Rawls, D. L. Brakensiek, and K. E. Saxton, "Estimation of soil water properties," *Trans. ASAE*, vol. 25, no. 5, pp. 1316-1320, Oct. 1982.
- [32] W. J. Rawls, D. L. Brakensiek, and B. Soni, "Agricultural management effects on soil water processes Part I: Soil water retention and Green and Ampt infiltration parameters," *Trans. ASAE*, vol. 26, no. 6, pp. 1747-1752, Dec. 1983.
- [33] W. J. Rawls, "Estimating soil bulk density from particle size analysis and organic matter content," *Soil Sci.*, vol. 135, no. 2, pp. 123-125, Feb. 1983.

*



Thomas J. Jackson received the Ph.D. degree in civil engineering from the University of Maryland, College Park, in 1976.

He is a hydrologist with the Hydrology Laboratory of the U.S. Department of Agriculture, Agricultural Research Services, Beltsville, MD. His research focuses on the application of remote sensing to water management in hydrology and agriculture. He has conducted studies utilizing Landsat data in hydrologic modeling and microwave measurements for soil moisture monitoring.

Progress in Snow Hydrology Remote-Sensing Research

ALBERT RANGO

Abstract—Snow hydrology research conducted as part of the AgRISTARS Conservation and Pollution Project was reviewed along with other relevant studies. The major areas of emphasis were visible snow cover analysis, snowmelt-runoff modeling, and microwave snow investigations. Results from these areas of investigation were very positive and contributed greatly to our scientific understanding. Based on the AgRISTARS results, specific components of additional snow research have been defined that will permit future operational applications.

I. INTRODUCTION

THE AGRICULTURE and Resources Inventory Surveys Through Aerospace Remote Sensing (AgRISTARS) program provided major support for NASA and USDA snow hydrology research related to remote sensing for the period 1980–1984. AgRISTARS was the vehicle to continue work started in the 1970's that showed the potential for remote sensing of snow for hydrologic purposes.

Significant knowledge on snow-hydrology remote sensing started to be accumulated soon after the first Landsat and NOAA satellites were launched in 1972. The first snow parameter of interest to be extracted from satellite data was the areal extent of snow cover using visible imagery and photointerpretation methods. Several Federal and state water resources agencies participated in a project on the operational applications of satellite snow-cover observations. The satellite snow-cover data were successfully tested primarily in empirical seasonal runoff estimation methods. For example, three years of testing in California resulted in the reduction of seasonal streamflow forecast error from 15 to 10 percent on three study basins [1]. Potential benefits of these types of improved satellite snow-cover based predictions across the 11 western states total \$10 million for hydropower and \$28 million for irrigation annually [1], assuming an operational remote-sensing capability. These results were based on empirical techniques and little testing of snow cover data in hydrologic models was performed.

Before AgRISTARS was begun, investigators began to examine the potential use of snow cover in existing hydrologic models because of the potential demonstrated in the interagency project [1]. Only a few models like the Streamflow Synthesis and Reservoir Regulation (SSARR)

model and the Snowmelt-Runoff Model (SRM) had provisions to make use of measurement of the portion of the basin or elevation zone covered by snowpack. The major differences between the two models were simplicity (SRM) and that SSARR would simulate the snow-covered area if it was not measured, whereas SRM required an actual snow-cover measurement to operate. Investigators at NASA decided to test the applicability of using satellite data in SRM and chose two remote basins in the Wind River mountains of Wyoming. Landsat photointerpretation was used to extract snow extent as a decimal fraction by elevation zone. Snow-cover depletion curves were then used to derive daily snow-cover values for input to SRM for simulation purposes. Both seasonal volume and daily streamflows were simulated quite accurately (96 and 84 percent, respectively) [2], [3].

During this early work with visible snow-cover data, additional research was being conducted to evaluate the utility of the microwave spectral region for snow measurements. All types of data collection were attempted including the use of microwave sensors on trucks, airplanes, and satellites. Much of the early truck and aircraft work was reported in [4], [5]. Most of these studies involved passive microwave techniques as opposed to active microwave investigations. The utilization of satellite microwave sensors for snow measurements was first attempted and reported by Rango *et al.* [6]. The Nimbus-6 Electrically Scanning Microwave Radiometer was used to separate snow-covered and snow-free areas and to map snow-covered area on a continental basis. Additionally, on the Canadian high plains significant relationships between dry snow depth or water equivalent and microwave brightness temperature were obtained, and the presence of melt-water in the snowpack was easily detected [6]. These early positive results provided the impetus to include microwave studies with the snow-cover and snowmelt runoff research in the Conservation and Pollution Project (CPP) of AgRISTARS.

II. SNOW COVER AND SNOWMELT RUNOFF RESEARCH

A. Snow Cover Delineation

The mapping of snow-cover extent was found to be very efficient when photointerpretation was used in the previously reported demonstration project [1]. As a result, photointerpretation of snow cover was employed for AgRISTARS using a zoom transfer scope whenever snow-cover data was needed for modeling. Because it was so

Manuscript received May 15, 1985.

The author is with the U.S. Department of Agriculture, ARS Hydrology Laboratory, Beltsville, MD 20705.

IEEE Log Number 8406224.

easy on the basins used, not much effort in the way of development of improved snow-mapping techniques was conducted in AgRISTARS. The digital snow-mapping approach, although potentially useable, was not employed.

Despite the exclusive use of photointerpretation, several research and/or technical problems remain for snow-cover mapping. Although generally of minimal importance for most basins studied in the CPP (the exception is the Dischma basin), photointerpretation is very difficult to employ effectively in small basins or in basins with snow-packs that ablate in a discontinuous fashion as opposed to a regular ablation that allows a contiguous snow line to be drawn. The digital approach would be much preferred in such situations. The potential for digital snow-mapping techniques was established in the 1970's (e.g., [7]); however, the approach is not used operationally except in Norway with NOAA polar orbiting data [8]. There is a definite need to develop the digital approach for widespread application to problem basins as well as for use when a large number of basins are studied.

Additionally, cloud cover remains a problem for snow mapping. In order to avoid this hinderance, the optimum approach would be to develop an active microwave system for snow mapping under all-weather conditions. Foster [9] discovered a way to increase the number of useable visible image snow scenes (while waiting for development of an all-weather system) as part of the CPP. Because snow has such a high reflectivity, it can reflect enough moonlight at night to allow snow mapping if the satellite sensors are sensitive enough to low light levels. Nighttime snow mapping would increase the chances of obtaining cloud-free imagery. Although Landsat sensors are not sensitive enough to map snow at night, the Defense Meteorological Satellite Program (DMSP) satellites have more sensitive sensors allowing mapping by moonlight as demonstrated by Foster [9]. Using the DMSP capability, it is projected that five additional images per month can be obtained that are suitable for snow mapping. At present, however, special arrangements are necessary in order to obtain DMSP data.

The final snow-cover mapping problem is that no complete operational delivery system exists for a type of information that has been shown to have numerous proven operational applications. Much more effort should be devoted to this seemingly trivial task which has many complex aspects.

B. Snowmelt-Runoff Modeling

The SRM was developed by Martinec [10] and utilized with visual ground observations and aircraft photography to obtain the required snow-cover input data. The availability of satellite snow-cover observations permitted application on much larger and a greater number of basins than previously tested. These new applications entailed adapting the model to accept more data input and to run on a larger computer than previously. As a result a user manual was developed to assist users in widespread application of the model with remote-sensing data [11].

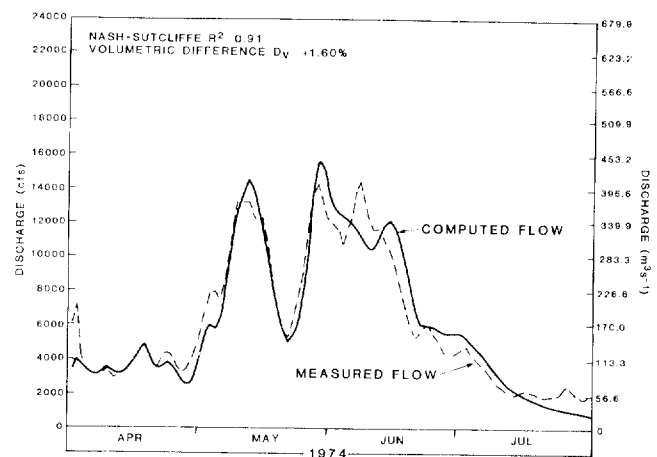


Fig. 1. Discharge simulation for the Kings River basin (3999 km²), California, using the snowmelt-runoff model.

In AgRISTARS it was decided that SRM utility should be tested using satellite data in a wide variety of basins to see if further model adaptation work was required. Several western United States basins were selected (that were of particular interest to the Soil Conservation Service (SCS)) as well as some internationally diverse basins. Three basins were selected and tested by the SCS [12], [13] in the Rio Grande basin of Colorado—South Fork of the Rio Grande (559 km²), Conejos River (730 km²), and the Rio Grande above Del Norte (3419 km²). Additionally, the Kings River (3999 km²) in California, the Dischma basin (43.3 km²) in Switzerland, and the Okutadami River (422 km²) in Japan were selected for testing. Combined with basins tested earlier the size (area) of the basins of SRM application ranged from 2.65 to 3999 km².

Although the basins tested had a wide diversity of conditions and data quality, the original statistical results reported for Wyoming [2], [3] held consistent and were actually somewhat improved. For the six basins tested in AgRISTARS, the seasonal volume simulation accuracy was 97 percent (volumetric difference) and the daily flow accuracy was 86 percent (R^2 value). Fig. 1 shows the SRM simulated hydrograph for the 1974 snowmelt season for the Kings River.

Consideration of the AgRISTARS results indicates that snow-covered area from satellites can be used very efficiently by SRM to simulate flow on a wide variety of mountain snowmelt basins. The results merit the expenditure of effort to convert SRM from the simulation to the forecasting mode and to link the model to an operational snow cover data stream. Finally from the results reported, it is apparent that other watershed models could advantageously incorporate snow cover data for improved simulation or prediction.

C. Indirect Water Equivalent Estimates

An indirect approach to estimating the snow water equivalent in a basin is possible using visible imagery and a grid system superimposed over the basin. To achieve this, air temperatures are extrapolated to the mean elevation of each grid unit in the basin, melting-degree days are

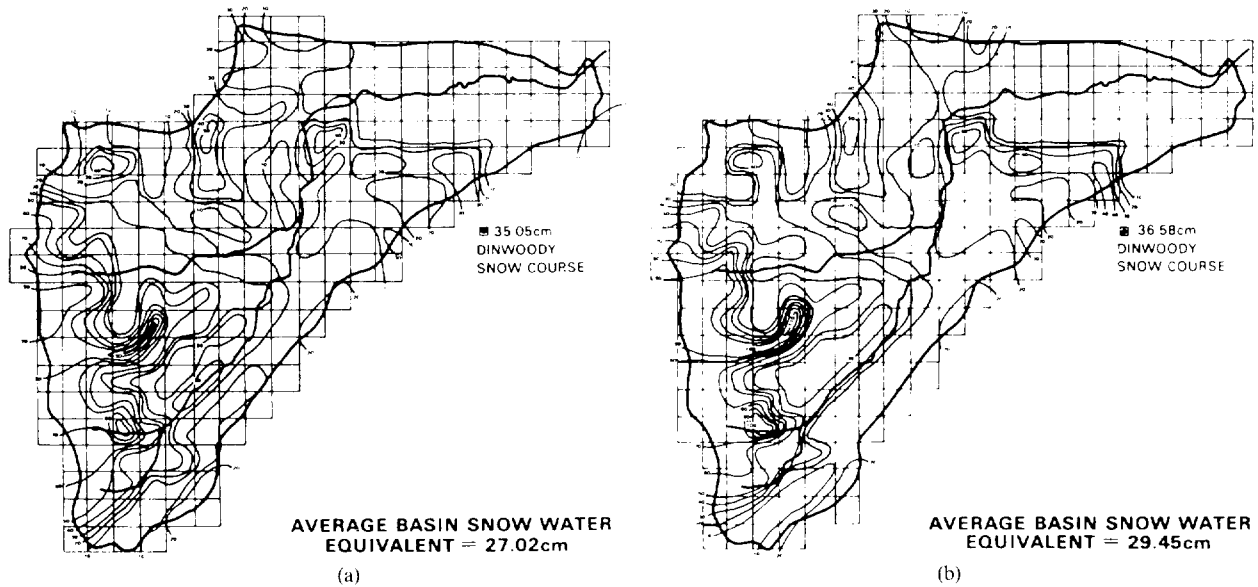


Fig. 2. Isopleths of snow water equivalent in the Dinwoody Creek basin (228 km^2), Wyoming for (a) April 1 and (b) May 1, 1976, obtained from a snowmelt model and Landsat observations from [14].

calculated, and daily grid snowmelt values are calculated and summed from the date of estimated maximum snowpack water equivalent accumulation (near the beginning of the snowmelt period). The end date for summing the snowmelt totals is the day snow cover leaves the grid based upon satellite observations. The total snowmelt is corrected by subtracting snowfall amounts during the period to yield the maximum snow water equivalent for each grid unit [14].

This approach was developed and applied on the Dinwoody Creek basin (228 km^2) in Wyoming with a 1-km grid and Landsat imagery. The temperature lapse rate and degree day factor values were taken from the values used in SRM runs on the basin. Fig. 2 shows the resulting areal distribution of snow water equivalent values for April 1 and May 1, 1976 [14]. Similar maps were produced for April 1 and May 1, 1974.

The utilization of this method provides areal snow water equivalent maps that can be used only in retrospective analysis because the final product is only available after the snow has disappeared. The product can be used for several purposes. Because winter precipitation measurements are notoriously in error, the maps could be used to correct the measurements for use in water balance studies. Analysis over several years will identify persistent areas of heavy snow accumulation in the basin which could be used to focus watershed management treatment activities for improving water yield. The location of recurring snow accumulation patterns can also be used as an aid in the establishment of new point measurement sites, e.g., in the SnoTel network, so that they can be more representative of conditions in a particular area of a basin. Finally, the areal water equivalent estimates available in this approach can be used in conjunction with methods under development for remote measurement of water equivalent using

microwave techniques that will be described in Section III of this paper. Because of the spatial capabilities of the microwave remote sensing measurements, this grid-based method could be used to improve the required ground truth data by adding appropriate areal information to the scarce point measurements.

III. MICROWAVE ANALYSIS OF SNOW CHARACTERISTICS

In the microwave wavelength region, several very significant and important advantages are evident for the snow hydrologist. Emission and reflection of microwave radiation from snow and ice surfaces is strongly affected by subsurface properties, thereby permitting the possibility of inferring information with depth. The other important advantage of the microwave region is that, depending on wavelength, microwave radiation will penetrate clouds and most precipitation, thus providing an all-weather observational capability. This is very significant in snow regions where clouds frequently obscure the surface.

Passive microwave resolution from space is inherently poor because of the large antenna sizes required, but improvements in the next few years are foreseen. Using active microwave techniques, resolution from space can be as good as 10 m, which is more than sufficient for detailed analysis of snow and ice properties. Microwave interaction with snow is extremely complex, especially in the active microwave case, and the result is that data interpretation is extremely difficult. This basic complexity is further confused by the rapid changes in snow characteristics, such as crystal size and liquid-water content, that are possible under varying climatic conditions. The dielectric constants of water and ice are so drastically different that even a little melting will cause a strong microwave response. Because of the uncertainties in the microwave interac-

TABLE I
RESPONSE OF MICROWAVE EMISSION OF SNOW DUE TO VARIOUS PHYSICAL
CONDITIONS FROM [16]

| Physical condition | Microwave emission response |
|----------------------|--|
| Physical temperature | Increases linearly as temperature increases. |
| Snow particle radius | Decreases as radius increases. |
| Snow depth | Decreases as depth increases until saturation depth which is a function of wavelength. |
| Snow wetness | Increases rapidly in presence of free water. |
| Background surface | Affects the signature for thin and dry snow conditions. |

tions, significantly more ground information is needed for microwave snow studies than for comparable visible, near infrared, and thermal infrared studies.

Prior to the start of AgRISTARS enough microwave snow data had been collected and analyzed to establish that prospects were good for acquiring hydrologically meaningful snow information. During AgRISTARS, increased effort was devoted to additional data collection from truck, aircraft, and satellite platforms for analysis and use with models. A good survey of truck, aircraft, and satellite microwave snow experiments is given by Foster *et al.* [15]. Table I from Burke *et al.* [16] summarizes the general response of microwave emission due to various physical conditions associated with the snowpack. The truck and aircraft data collected in AgRISTARS have been used primarily to develop and verify radiative transfer models. The passive microwave satellite data from Nimbus-5, -6, and -7 have been used in empirical studies of snow over large areas.

The empirical studies over large areas that were begun on the Canadian high plains before AgRISTARS were extended to similar areas with low vegetation cover in the U.S. and Russia during the project. The Nimbus satellite microwave data continued to show significant relationships between snow depth and 0.81-cm brightness temperatures with R^2 values of the same order (0.70–0.80) as found in the Canadian study area. The relationships were specific to each study area and could not be transferred from one area to another. In examination of these data, it was found that where the snowpack undergoes considerable freezing and thawing that the horizontal polarization is better suited than the vertical polarization for detecting variations in snow depth. The ice lenses, layers, and surface crusts associated with the freeze/thaw cycles are transparent to the horizontally polarized data but tend to dampen the vertical polarization response [15].

A limiting factor to these empirical studies is the effect of high vegetation on the snow microwave response. The microwave brightness temperature of a snow scene increases as the vegetation cover density over the snowpack increases. The emissivity of the vegetation tends to overwhelm the scattering effect of the underlying snow. Hall *et al.* [17] used a simple model to remove the effects of forest trees from the typical brightness temperature-snow

depth regression relationship. The simple model was based on the percent forest cover and the brightness temperature of the forest trees in the absence of snow. The residual brightness temperature after correction was found to be correlated with the snow water equivalent under the canopy.

A microscopic scattering model was developed by Chang *et al.* [18] and used to simulate the effect of varying snow water equivalent on microwave brightness temperature [19]. In the model the intensity of microwave radiation emitted from a snowpack depends upon physical temperature, grain size, density, depth or snow water equivalent, and underlying surface conditions beneath the snow. Fig. 3 shows model-generated curves for 0.81-cm wavelength relating brightness temperature to snow water equivalent as a function of snow grain size [19]. These particular curves are for a dry snow condition, unfrozen ground, and an incidence angle of 50° . Fig. 4 is a plot of model predictions of snow water equivalent using truck-acquired passive microwave data versus measured snow water equivalent. The agreement is quite good when typical grain sizes from the study site are known. Fig. 5 shows the scattering of the Nimbus-7 Scanning Multichannel Microwave Radiometer (SMMR) 0.81-cm brightness temperature versus snow depth for the Russian test site previously mentioned [19]. A linear regression technique for relating brightness temperature to snow depth yields $R^2 = 0.75$. The data display considerable scatter which is probably due to inhomogeneity within each footprint and assumptions made in interpreting the data. The microwave model was also used to generate a depth versus brightness temperature curve which fits well with the observations and the empirical relationship in Fig. 5.

The shallow snow depths in the study shown in Fig. 5 are indicative of the depths necessary for insulating winter wheat seedlings from extreme winter temperatures prevalent in wheat growing areas like this one in Russia. Early knowledge of the snow depth during the winter months is, therefore, critical in predicting the forthcoming winter wheat yield. Testing of the model in deeper mountain snowpacks with aircraft and truck (see Fig. 4) data indicates that it can also be used in situations to improve snowmelt runoff forecasts.

Several other results from AgRISTARS are significant for microwave snow applications. Snow boundaries can generally be defined in the 0.81-cm data because of the sharp decrease in brightness temperature when going from a land to snow surface [16]. In estimating snow water equivalent, the radiation from dry snow is strongly influenced by grain size so that some independent means for obtaining grain size estimates needs to be developed. Regarding the state of the underlying soil, the presence of frozen ground can be detected by using the polarization ratio at about 3-cm wavelength [19]. Because liquid water in the snowpack coats the snow grains and causes a significant increase in internal absorption of the microwave radiation and a decrease in volume scattering or an in-

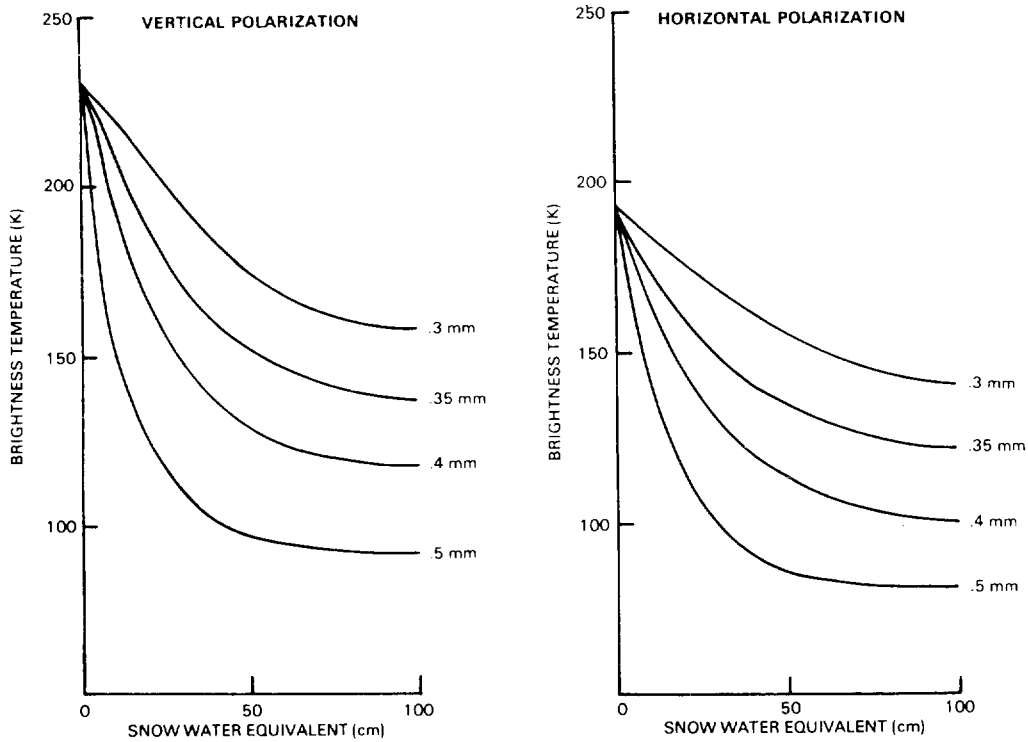


Fig. 3. Microscopic scattering model-generated calculations relating 0.81-cm brightness temperature to snow water equivalent over unfrozen soil for several crystal radii (incidence angle is 50°) from [19].

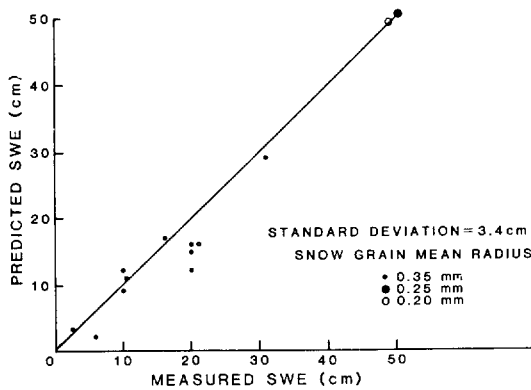


Fig. 4. Comparison between microwave model predictions of snow water equivalent at 0.81 cm and field measurements.

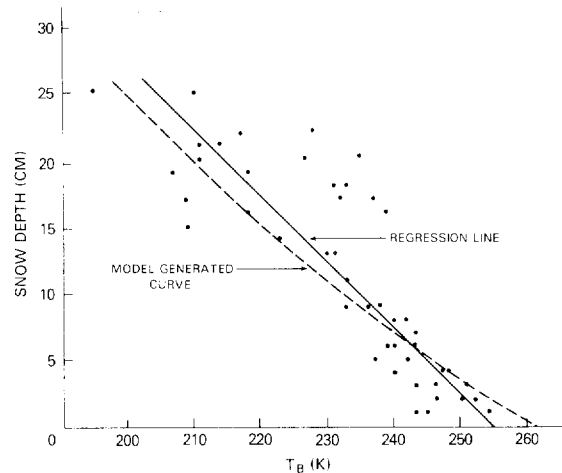


Fig. 5. Comparison between empirical relationship of snow depth versus brightness temperature from Nimbus-7 SMMR 0.81-cm data and model calculations over Russia from [19].

crease in the snow emissivity, the onset of snowmelt is easily detected [15].

To summarize our capabilities for collecting snow data with microwave techniques it should be helpful to consider the major snow characteristics. Also the capabilities are evaluated with a space platform in mind, but it is important to remember that there are certain advantages to aircraft data collection, primarily improved resolution. The measurement of snow areal extent is feasible using passive microwaves on a global, regional, or even large catchment basis and really needs very little development to be operational. For measurement of snow extent on small basins, active microwave techniques should work equally well, but, thus far, there have been few attempts to acquire relevant 0.81-cm radar data from aircraft or spacecraft. Re-

garding snow water equivalent, empirical relationships can be derived for specific large, flat, and low vegetation areas and likely used to estimate water equivalent (or depth) with passive microwave data. The use of radiative transfer models make the use of the microwave data more widely applicable but additional and difficult to obtain input information is required, e.g., snow grain size. Again, the active microwave region shows significant promise, however, it has not been exploited to any great degree. The sensitivity of both active and passive microwaves to liquid water in the snowpack has been shown in numerous ex-

periments [20]. The onset of snowmelt should be observed equally well with either technique. It remains to be seen if quantitative measures of the liquid water in the snowpack can be extracted. Finally, using multiple wavelength bands, inference of the condition of the underlying soil seems possible but further work will be required.

So despite many positive results, much snow research needs to be done in the passive microwave area but particularly in the active region. How should this important research proceed? This topic was comprehensively addressed during AgRISTARS, and a detailed research plan was completed [21]. Starting on this plan of research now should permit completion of an operational approach to microwave snow measurements by 1995.

IV. CONCLUSION

The results of research on snow hydrology completed during AgRISTARS have important applications for the organizations involved, particularly USDA and NOAA. One major application is seasonal and short-term streamflow estimation in areas with a significant snowmelt-runoff component. Remote sensing can be used now to obtain the areal extent of snow in a basin, and models exist to estimate runoff based on the input of this snow cover data. Because of very positive research results in AgRISTARS, it seems that researchers will be able to develop microwave remote-sensing techniques to measure or detect snow water equivalent or depth, the presence of liquid water in the snowpack, and the hydrologic condition of the soil beneath the snowpack. In order to make forecasts, the remote-sensing information will have to be input to an appropriate hydrologic model, such as SRM or SSARR, capable of producing seasonal and daily flow estimates. These estimates would be used as input for water management in the areas of irrigation, flooding, water supply, and hydropower.

Aside from the uses of remote sensing for crop-condition assessment developed in other AgRISTARS projects, the advances in snow hydrology have direct applications for crop-yield estimates. First, the predicted water supply for irrigated areas has a direct bearing on the forecast crop yield in irrigated regions. Second, measurement of onsite snow water equivalent in agricultural fields can be used to figure the potential soil moisture recharge resulting from the melting snow. This will have a direct effect on crop growth in both irrigated and nonirrigated fields. Finally, the depth of snow and associated insulating effect will be important for winterkill estimates which comprise part of crop-yield estimation.

The results presented in this paper document a very positive AgRISTARS effort, yet there are real problems in getting these advances implemented in an operational way. This problem persists despite the fact that an extremely positive benefit/cost ratio of 75:1 for using just snow cover extent in snowmelt-runoff forecasts was shown before the start of AgRISTARS in a conservative study [1]. It appears that no government or private agency is currently

capable of making snow extent data available in an operational time frame or format to capitalize on the benefit/cost ratio. Secondly, no government research organization seems amenable to mounting the solid research program necessary to bring the microwave snow capabilities up to an operational level. A modest undertaking over a 5-10-year period would result in a very positive return even if only parts of the effort were successful. As stated before, the plan to direct this research already exists. AgRISTARS should not be the completion point, but only a successful beginning for snow-hydrology research.

REFERENCES

- [1] A. Rango, "Operational applications of satellite snow cover observations," *Water Res. Bull.*, vol. 16, no. 6, pp. 1066-1073, 1980.
- [2] A. Rango and J. Martinec, "Application of a snowmelt-runoff model using Landsat data," *Nordic Hydrology*, vol. 10, pp. 225-238, 1979.
- [3] A. Rango, "Remote sensing of snow covered area for runoff modeling," in *Proc. Oxford Symp.*, IAHS-AISH Pub. 129, pp. 291-297, 1980.
- [4] A. T. C. Chang, A. Rango, and J. C. Shiue, "Remote-sensing of snow properties by passive microwave radiometry: GSFC truck experiment," NASA Conf. Pub. 2153, pp. 169-185, 1980.
- [5] A. T. C. Chang, J. L. Foster, D. K. Hall, and A. Rango, "Monitoring snowpack properties by passive microwave sensors on board aircraft and satellites," NASA Conf. Pub. 2153, pp. 235-248, 1980.
- [6] A. Rango, A. T. C. Chang, and J. L. Foster, "The utilization of spaceborne microwave radiometers for monitoring snowpack properties," *Nordic Hydrology*, vol. 10, pp. 25-40, 1979.
- [7] A. Rango and K. I. Itten, "Satellite potentials in snowcover monitoring and runoff prediction," *Nordic Hydrology*, vol. 7, pp. 209-230, 1976.
- [8] T. Anderson and H. Odegaard, "Application of satellite data for snow mapping," Norwegian National Committee for Hydrology, Rep. 3, 1980.
- [9] J. L. Foster, "Night-time observations of snow using visible imagery," *Int. J. Remote Sensing*, vol. 4, no. 4, pp. 785-791, 1983.
- [10] J. Martinec, "Snowmelt-runoff model for stream flow forecasts," *Nordic Hydrology*, vol. 6, no. 3, pp. 145-154, 1975.
- [11] J. Martinec, A. Rango, and E. Major, "The snowmelt-runoff model (SRM) user's manual," NASA Ref. Pub. 1100, 1983.
- [12] E. B. Jones, B. A. Shafer, A. Rango, and D. M. Frick, "Application of a snowmelt model to two drainage basins in Colorado," in *Proc. 49th Ann. Western Snow Conf.*, pp. 43-54, 1981.
- [13] B. A. Shafer, E. B. Jones, and D. M. Frick, "Snowmelt runoff modeling in simulation and forecasting modes with the Martinec-Rango model," NASA Contractor Rep. 170452, 1982.
- [14] J. Martinec and A. Rango, "Areal distribution of snow water equivalent evaluated by snow cover monitoring," *Water Res. Research*, vol. 17, no. 5, pp. 1480-1488, 1981.
- [15] J. L. Foster, D. K. Hall, A. T. C. Chang, and A. Rango, "An overview of passive microwave snow research and results," *Rev. Geophys. Space Phys.*, vol. 22, no. 2, pp. 195-208, 1984.
- [16] H. K. Burke, C. J. Bowley, and J. C. Barnes, "Determination of snowpack properties from satellite passive microwave measurements," *Remote Sensing Environ.*, vol. 15, pp. 1-20, 1984.
- [17] D. K. Hall, J. L. Foster, and A. T. C. Chang, "Measurement and modeling of microwave emission from forested snowfields in Michigan," *Nordic Hydrology*, vol. 13, pp. 129-138, 1982.
- [18] A. T. C. Chang, P. Gloersen, T. Schmugge, T. T. Wilheit, and H. J. Zwally, "Microwave emission from snow and glacier ice," *J. Glaciology*, vol. 16, pp. 23-29, 1976.
- [19] A. T. C. Chang, J. L. Foster, D. K. Hall, A. Rango, and B. K. Hartline, "Snow water equivalent estimation by microwave radiometry," *Cold Regions Sci. Tech.*, vol. 5, pp. 259-267, 1982.
- [20] W. H. Stiles, F. T. Ulaby, and A. Rango, "Microwave measurements of snowpack properties," *Nordic Hydrology*, vol. 12, no. 3, pp. 143-166, 1981.
- [21] NASA "Plan of research for snowpack properties remote sensing (PRS)²," Recommendations of the Snowpack Properties Working Group, Goddard Space Flight Center, Greenbelt, MD, 1982.



Albert Rango received the B.S. and M.S. degrees in meteorology from Pennsylvania State University and the Ph.D. degree in watershed management from Colorado State University.

He has served on the faculty at Pennsylvania State University and has been a private water resources consultant. From 1972 to 1982, he was employed by the NASA Goddard Space Flight Center in Greenbelt, MD, where he was Head of the Hydrological Sciences Branch. In 1983, he was appointed Chief of the Hydrology Laboratory of

the Agricultural Research Service in Beltsville, MD. His special areas of research interest are in the applications of remote sensing to snow hydrology, soil moisture, and hydrological modeling. His experience includes serving as project leader for two interagency remote-sensing demonstration projects on the operational applications of satellite snow-cover data and the utilization of hydrologic land use data in flood flow frequency simulation. At present, he is president-elect of the American Water Resources Association and U.S. National Representative to both the International Commission on Snow and Ice and the International Committee on Remote Sensing and Data Transmission of the International Association of Hydrological Sciences.

Early Warning and Crop Condition Assessment Research

GLENN O. BOATWRIGHT AND VICTOR S. WHITEHEAD

Abstract—The Early Warning Crop Condition Assessment Project of AgRISTARS was a multiagency and multidisciplinary effort. Its mission and objectives were centered around development and testing of remote-sensing techniques that enhance operational methodologies for global crop-condition assessments. The project developed crop stress indicator models that provide data filter and alert capabilities for monitoring global agricultural conditions. The project developed a technique for using NOAA-*n* satellite advanced very-high-resolution radiometer (AVHRR) data for operational crop-condition assessments. This technology was transferred to the Foreign Agricultural Service of the USDA. The project developed a U.S. Great Plains data base that contains various meteorological parameters and vegetative index numbers (VIN) derived from AVHRR satellite data. It developed cloud screening techniques and scan angle correction models for AVHRR data. It also developed technology for using remotely acquired thermal data for crop water stress indicator modeling. The project provided basic technology including spectral characteristics of soils, water, stressed and non-stressed crop and range vegetation, solar zenith angle, and atmospheric and canopy structure effects.

I. INTRODUCTION

THE EARLY WARNING and Crop Condition Assessment (EW/CCA) Project was one of eight projects in the AgRISTARS' program. Its mission and objectives (develop and test remote-sensing techniques that enhance operational methodologies for crop-condition assessment) were in response to the initiatives issued by the Secretary of Agriculture. The project was managed by the USDA-ARS but was a multiagency multidisciplinary effort in which funds and personnel were provided by the USDA-ARS, the USDA-SRS, the NASA-JSC, and the USDC-NOAA. The EW/CCA project conducted basic research at various ARS research locations and provided resources to industry, universities, and other government agencies for early warning and crop-condition assessment technology development.

Early in the program the project concentrated on crop-stress indicator models for monitoring large areas. Later in the program stress models were evaluated and verified, field experiments were conducted to relate plant stresses to remotely sensed characteristics, studies were pursued to better understand and utilize NOAA-AVHRR satellite data, and the transfer of technology to potential users was emphasized.

Manuscript received May 20, 1985; revised August 20, 1985.

The authors are with the U.S. Department of Agriculture, Agricultural Research Services, and the NASA Johnson Space Center, Houston, TX 77058.

IEEE Log Number 8406225.

Many of the tasks undertaken by the Houston EW/CCA unit involved bringing existing research technology to a point where it could be used in an operational environment. In most cases the technology had to be modified and adapted before it could be transferred and implemented for operational applications.

Early warning/crop condition assessment implementation plans were developed each year in anticipation of resource increases that never materialized. In fact, yearly resource reductions resulted in the termination of some tasks prior to their completion.

Although many aspects of the EW/CCA project could be emphasized, this paper emphasizes crop-stress indicator models, environmental satellite studies, and condition assessments. Other individual EW/CCA studies are being documented.

II. CROP STRESS INDICATOR MODEL DEVELOPMENT

Meteorologically driven crop-stress indicator models were developed or modified [6], [12], [16], [17], for wheat, maize, grain sorghum, and soybeans. These models provide early warning alerts of potential or actual crop stresses due to water deficits, adverse temperatures, and water excess that could delay planting and harvesting operations. The stress indicator models were intended to be data filters and alert mechanisms for large-area monitoring rather than stand-alone systems. All stress indicator models require daily precipitation, maximum and minimum temperature, and evapotranspiration estimates as inputs. The stress indicator models require accurate crop phenology and water budget subroutines because parameter thresholds are crop specific and crop stage dependent. Consequently, they are best executed in conjunction with agrometeorological crop models.

The maize stress-indicator model is used to describe parameter and threshold values used by the stress-indicator models. Fig. 1 illustrates specific threshold values for soil moisture and air temperature. Hazardous alerts are provided when soil water is deficient or in excess and when high or low air temperature exceeds the threshold values. The threshold values are crop stage dependent for both soil water and temperature parameters. The models provide running sums for both hazardous and optimum growing conditions. Fig. 2 summarizes the maize stress model output of optimum, adequate, and hazard days during 1979 and 1980 seasons for a crop reporting district in Missouri.

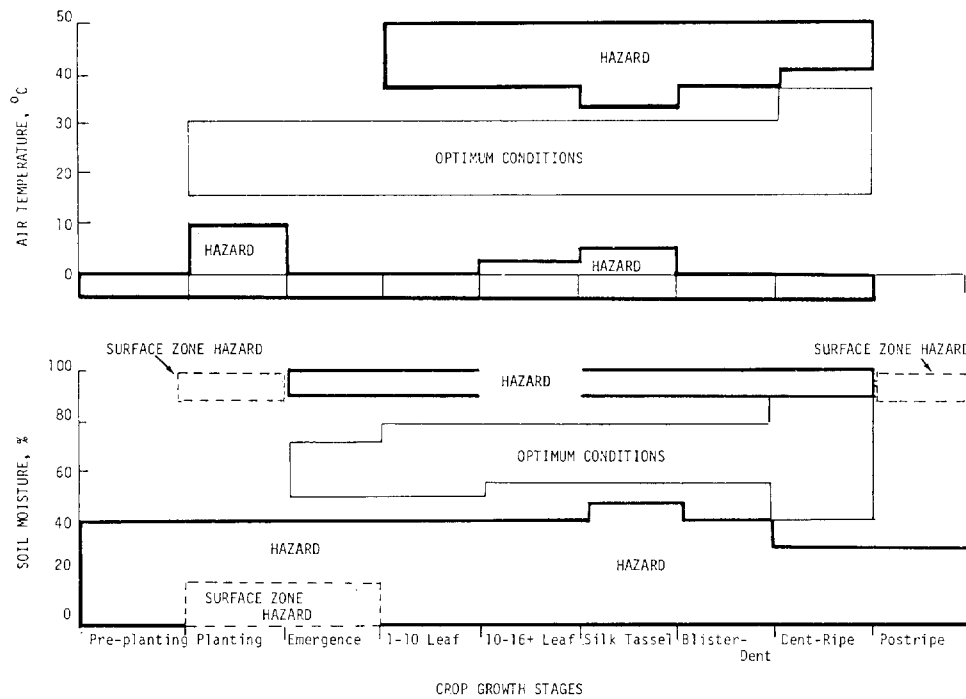


Fig. 1. Parameters and threshold values for a maize stress indicator model that proves daily hazardous and/or optimum flags for moisture and temperature conditions at various crop phenology stages.

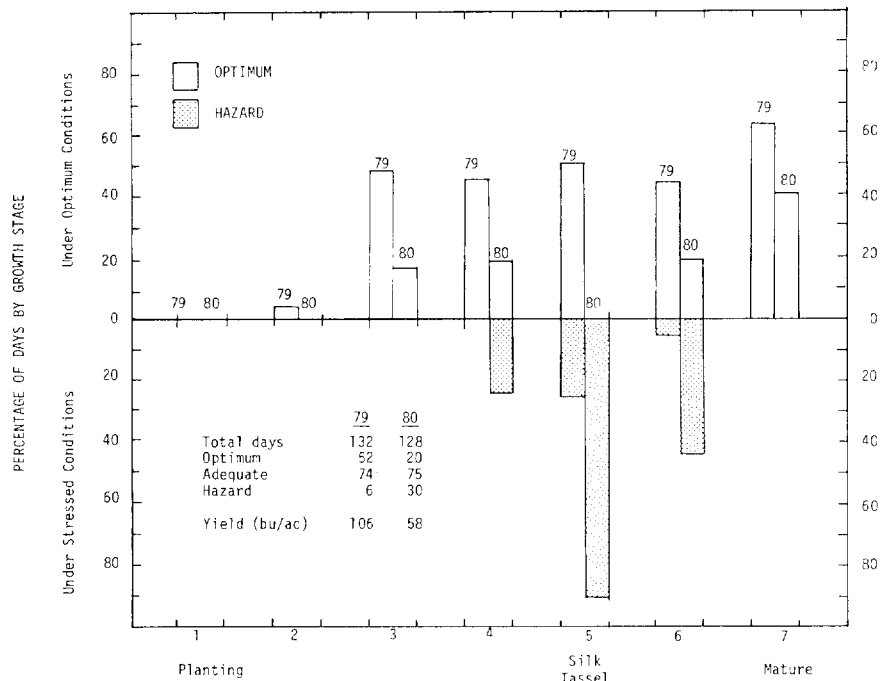


Fig. 2. Comparison of 1979 and 1980 stress alerts from the maize stress indicator model for a crop reporting district in Missouri.

In 1979, only 6 hazardous days were recorded whereas, in 1980, the model alerted 30 hazardous days. Maize yields were 106 and 58 bushels per acre for 1979 and 1980, respectively. These results show that there is a strong relationship between model results and maize yield as estimated by SRS for the crop reporting district.

The phenology [16] of the maize model was evaluated using ground-based plant-growth observations. The re-

sults (Fig. 3) show that predicted growth stage lagged by about 8 days during the early part of the growing season. However, during the critical tassel-silk stage the model was only about 4 days slow. One should remember that ground observations were made at the crop reporting district (CRD) level and one would expect that phenology within a CRD would vary up to 7-8 days.

Test results for the phenology component [12] of the

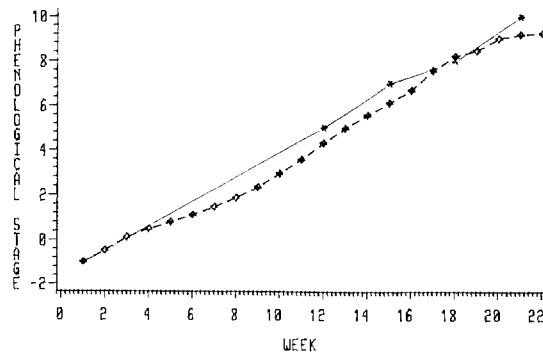


Fig. 3. Test results of the maize phenology model. S.W. Crop Reporting District, Missouri.

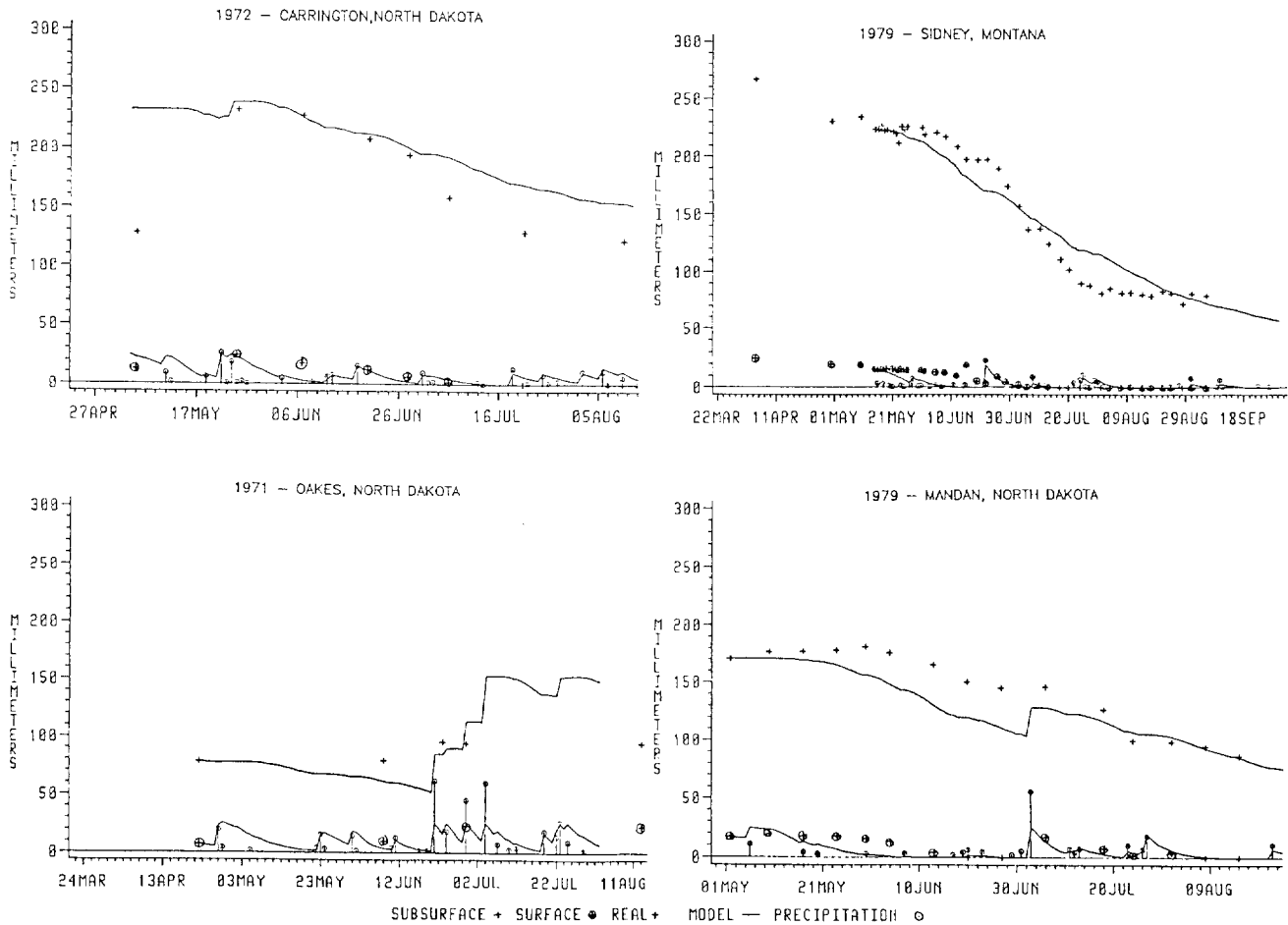


Fig. 4. Solid line shows ground truth, dashed line model results. Soil water budget model test results for four experimental field sites.

wheat stress indicator model suggest that adjustments are needed at spring greenup. These adjustments can be made if soil temperature data are available to establish when spring regrowth begins [4].

The soil water budget model [4] was tested using ground truth from experimental field plots in North Dakota and Montana. The results (Fig. 4) show that the model tracks profile soil water fairly well when initializing parameters (surface and subsurface available water holding capacity and initial soil water) were known and accurately set. Other data sets, not shown in this paper, indicate that dur-

ing the hot dry summer periods, the model may overestimate the amount of available profile water.

Indicator models for monitoring wheat winterkill [1] and for assessing potential wheat yield reductions [13] were modified and/or developed. Considerable field research was conducted to establish the parameters and threshold values.

All models discussed in this section have been transferred to USDA-FAS and are currently being used by the Foreign Crop Condition Assessment Division.

Parameter and threshold values were established for po-

tential wheat stripe rust epidemics and for losses caused by harvest delays [2], [3]. Although these models have not been completed, additional information can be obtained from the Pathology Department, Montana State University, and from the USDA-ARS Northern Plains Research Center, Mandan, ND.

III. ENVIRONMENTAL SATELLITE AND SPECTRAL STUDIES

Perhaps the most significant contribution made by the EW/CCA project was the early research associated with NOAA-*n* environmental satellite data. In 1980, NOAA-6 and NOAA-7 Advanced Very High Resolution Radiometer (AVHRR) data were analyzed to relate vegetation characteristics and satellite-derived vegetative index numbers. Correlation analysis [7] indicated a good relation between Landsat and NOAA-6 data, $r = 0.86$ (Fig. 5). Environmental satellite vegetative index number (VIN = channel 2-channel 1) trajectories computed for two geographic grids in southeast and south-central South Dakota are shown in Fig. 6. Changes in greenness between the two I, J grids, during the summer of 1981, correspond quite well to amounts of precipitation recorded at nearby weather stations. Results like these and problems that developed with Landsat 3, promoted the USDA-FAS to request that the EW/CCA project develop a NOAA-*n* AVHRR data processor for operational crop-condition assessments.

Since 1982, NOAA has provided a weekly worldwide depiction of a vegetative index based upon research conducted by the EW/CCA project.

The EW/CCA research unit developed a four-year data base for an established geographical grid covering the U.S. Great Plains. Each cell represents an area of approximately 25×25 nautical miles. The grid cells contain vegetative index numbers (VIN's), daily precipitation, maximum temperature, minimum temperature, evapotranspiration, and solar radiation. Historical and seasonal VIN trajectories for individual grid cells (Fig. 7) and for country and/or crop reporting districts (Fig. 8) suggest that NOAA-AVHRR satellite data provide valuable information for local, regional, and global crop condition assessment purposes. Data presented in Table I show that wheat and corn yields for Burleigh, Morton, and Oliver counties in North Dakota were greater in 1982 than in 1983. VIN's shown in Fig. 7 indicate that greenness within the counties was much greater in 1982 than in 1983. In three Nebraska counties, wheat yields were greater in 1983 than in 1982. In contrast, yields for corn and soybeans were greater in 1982 than in 1983. VIN trajectories for grids within these three counties show that greenness during the growing season for wheat was greater in 1983 than in 1982, but during the corn and soybean growing season the reverse was true.

Considerable research was conducted to develop a practical method for automatically screening cloud-contaminated pixels from NOAA-AVHRR satellite data. The initial cloud screening technique applied calibration

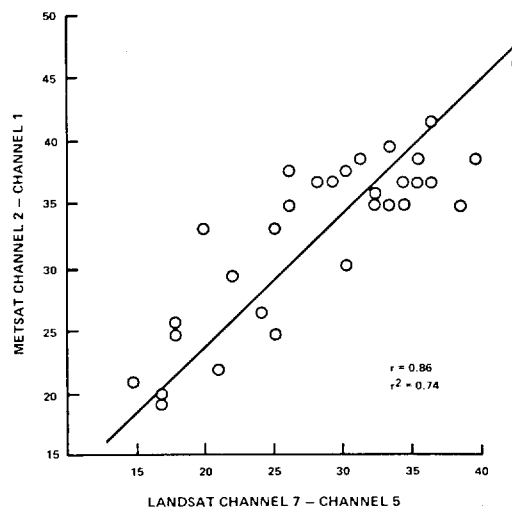


Fig. 5. Correlation analyses between Landsat MSS and NOAA-6 AVHRR data.

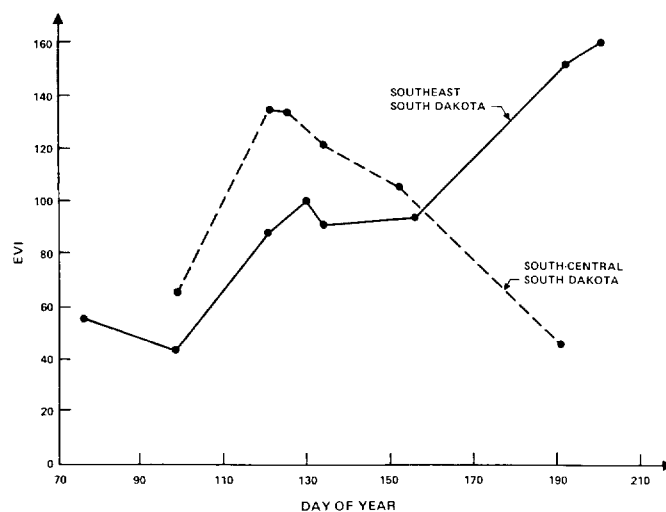


Fig. 6. Environmental satellite vegetative index (EVI) trajectories during the summer of 1981 for two geographic grid cells in South Dakota.

coefficients supplied in the header of the digital tapes to channels 1 and 2. All pixels with values greater than 25-percent albedo in either channel were screened out and not used in the VIN computation. A second cloud screening technique [11] utilized data from channels 3 and 4. Threshold values computed from these channels improved the ability to screen and remove cloud contamination pixels. A third approach involved the development of a hierarchical classification of NOAA-7 AVHRR data into clouds, haze, water, bare soil, and vegetation. Channels 1 and 2 were used to detect clouds and to classify cloud-free data into water, bare soil, and vegetation. Channels 3 and 4 were used to detect the presence of haze. Although these techniques improved the ability to screen and remove cloud-contaminated pixels, they were not implemented because channel 3 became unstable as the satellite aged.

In the most recent cloud-screening technique, developed by EW/CCA, threshold values for channels 1 and 2 depend on solar zenith angle. Consideration of sun angle

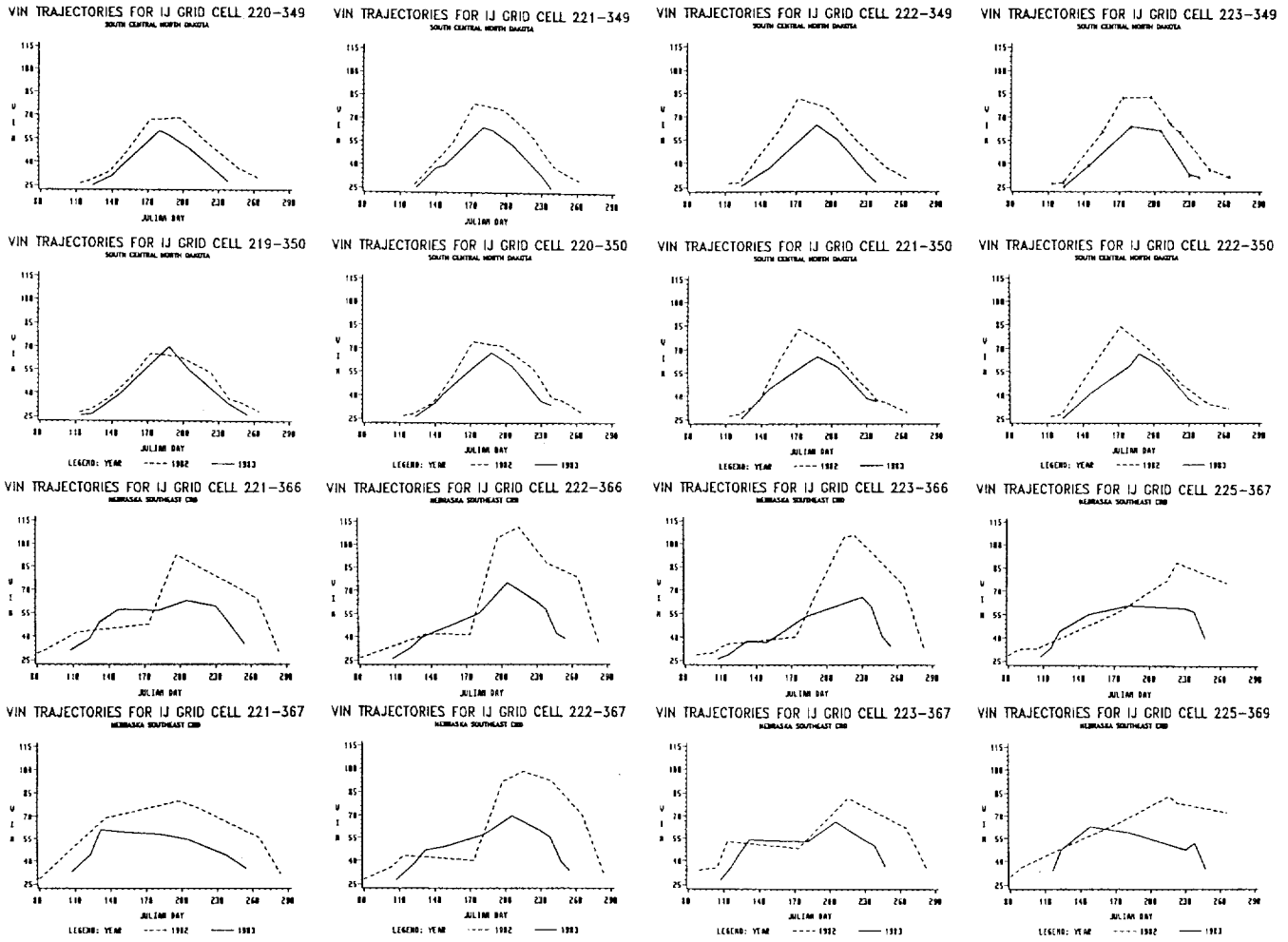


Fig. 7. Comparison of 1982 and 1983 vegetative index numbers (VIN's) for individual 25 x 25 nautical mile grid cells in North Dakota and Nebraska.

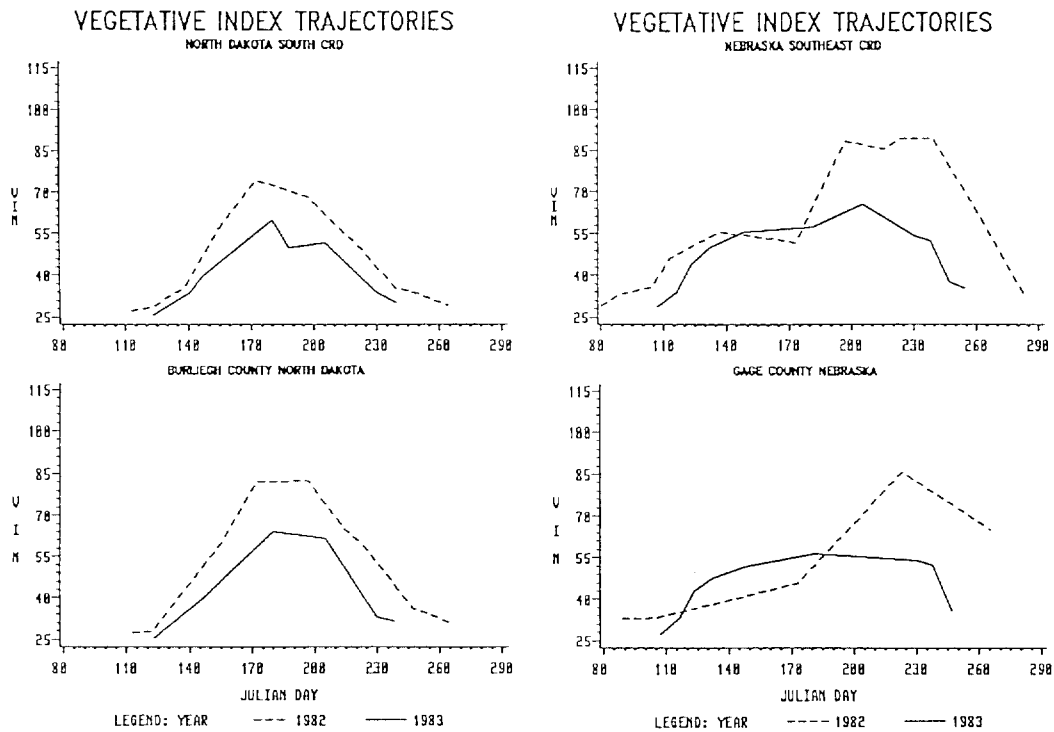


Fig. 8. Comparison of 1982 and 1983 vegetative index numbers (VIN's) for counties and crop reporting districts in North Dakota and Nebraska.

TABLE I

STATISTICAL REPORTING SERVICE COUNTY YIELD ESTIMATES, DIFFERENCES IN YIELDS (1982-1983), AND IDENTIFICATION OF I,J GRIDS LOCATED IN VARIOUS COUNTIES IN NEBRASKA AND NORTH DAKOTA

| STATE | COUNTY | CROP | COUNTY YIELDS Bu./Ac. | | DIFFERENCE Percent | GRID CELL | |
|--------------|----------|----------|-----------------------|-------|--------------------|-----------|---|
| | | | 1982 | 1983 | | I | J |
| North Dakota | Burleigh | Wheat | 39.2 | 33.9 | -14% | 223-349 | |
| | Burleigh | Corn | 55.0 | 40.5 | -26% | 223-350 | |
| | Morton | Wheat | 26.5 | 23.1 | -13% | 220-350 | |
| | Morton | Corn | 52.2 | 50.5 | -03% | 221-350 | |
| | Oliver | Wheat | 30.6 | 24.5 | -20% | 222-349 | |
| North Dakota | Oliver | Corn | 50.0 | 51.9 | +04% | 221-349 | |
| Nebraska | Nemaha | Wheat | 29.1 | 40.2 | +27% | 225-367 | |
| | Nemaha | Corn | 96.5 | 42.7 | -56% | 225-367 | |
| | Nemaha | Soybeans | 35.1 | 24.3 | -31% | 225-367 | |
| | Saline | Wheat | 27.3 | 39.7 | +31% | 223-366 | |
| | Saline | Corn | 117.2 | 100.3 | -15% | 223-366 | |
| | Saline | Soybeans | 34.3 | 29.3 | -15% | 223-366 | |
| | Fillmore | Wheat | 28.3 | 47.2 | +40% | 222-366 | |
| | Fillmore | Corn | 126.6 | 116.7 | -08% | 222-366 | |
| | Fillmore | Soybeans | 41.4 | 38.2 | -08% | 222-366 | |

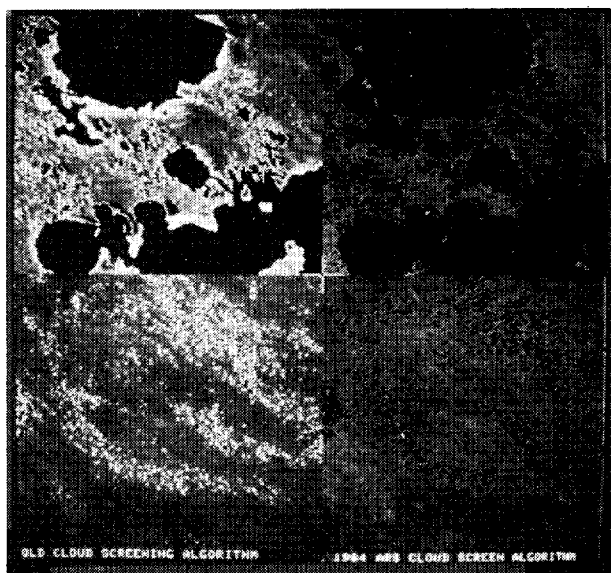


Fig. 9. Comparison between the old and the new cloud screening techniques developed by EW/CCA.

automatically corrects for latitude and time of year or seasonal changes. This new cloud screening technique stabilized I,J grid VIN trajectories and permitted the use of VIN's from grids when only a few pixels within the grid are retained and used. We recommend that vegetative index numbers not be computed when more than 80 percent of the pixels within the grid are screened out.

Fig. 9 illustrates the improvement achieved when using the new technology compared to the original technique delivered to the USDA-FAS. This new cloud screening technology has not been published. However, it has been transferred to the USDA-FAS and is currently being used in their operational system.

The increase of atmospheric haze caused by volcanic particulates and reaction products, as measured by the NOAA-7 AVHRR data, is shown in Fig. 10. Ground-observed prevailing nadir atmospheric transmission decreased approximately 11 percent after the El Chicon volcano eruption [14]. The decrease in atmospheric

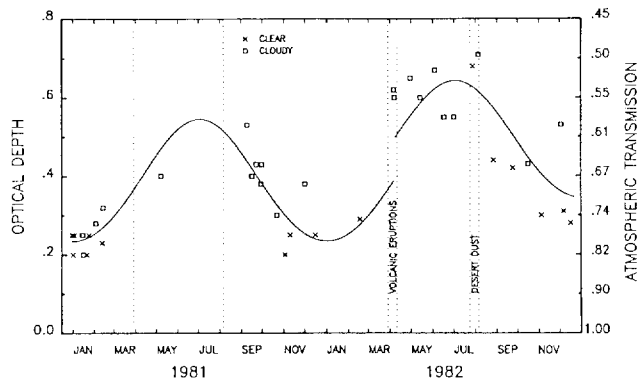


Fig. 10. Prevailing nadir atmospheric transmission, ground-measured, and NOAA AVHRR minimum digital counts before and after the El Chicon Volcano eruptions.

transmission agreed with increases of NOAA-7 AVHRR digital count minimum values in the visible and infrared bands obtained over the Gulf of Mexico. These results demonstrate the importance of transient atmospheric haze effects relative to early warning crop stress monitoring.

The effects of solar illumination, view angle, and non-Lambertian surfaces [9] on NOAA-AVHRR sensor data are summarized in Fig. 11. Results of this study indicated that useful greenness information can be derived using up to approximately 512 pixels either side of nadir. The findings also show that solar zenith corrections are not necessary when computing VIN's and that increased shadowing with increasing view angles play a significant role in the interpretation of data from non-Lambertian surfaces.

The effects of scan angle were studied using consecutive day NOAA-AVHRR data. To assure that information collected on consecutive days came from the same ground location, the data were rectified [5]. A very large data set was assembled to include data collected throughout the season from locations across the U.S. Fig. 12 demonstrates the change in channel and VIN values between consecutive day satellite passes, as the scan angle increases both east and west of nadir. Data depicted in the lower half of Fig. 12 were used to develop equations that model scan angle effects for the center 1024 pixels of the scan. Individual channel data or computed VIN's can be corrected for scan angle effects. The models are more effective when channel values are corrected before VIN's are computed.

IV. CROP CONDITION ASSESSMENT

Soil water, when in limited supply or in excess, is a major factor in crop condition and production. The EW/CCA project was involved in numerous tasks to detect, monitor, and determine the degree of stress associated with various soil water conditions for several crops. Research tasks ranged in scope from basic research to technology transfer for operational applications.

Canopy temperatures, obtained by infrared thermometry along with wet- and dry-bulb air temperatures and an estimate of net radiation were used in equations derived from energy balance considerations to calculate a crop

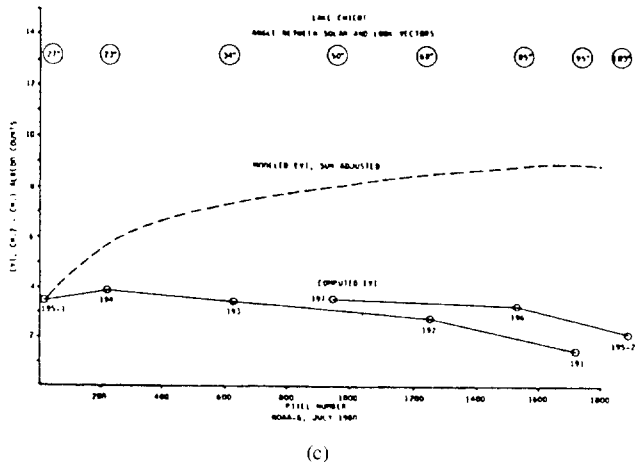
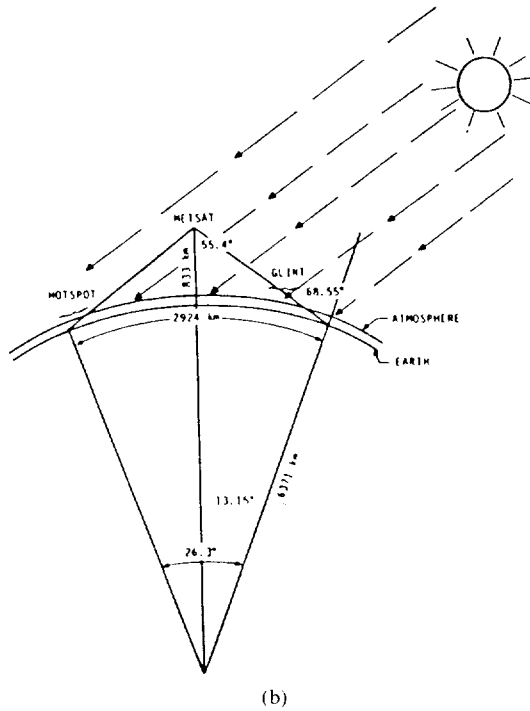
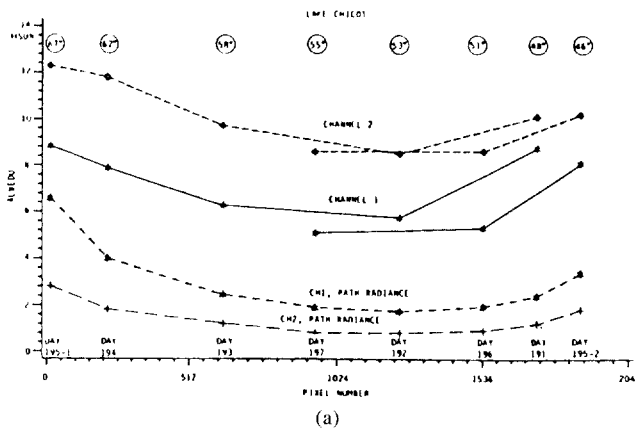


Fig. 11. Geometric and solar correction of the NOAA AVHRR data. (a) Radiance values as influenced by scan angle (pixel number) for channels 1 and 2 of the NOAA-6 AVHRR sensor. (b) Geometric relationship between the Sun the AVHRR scanning limits with respect to the Earth. (c) Modeled EVI's (Lambertian surface) and computed NOAA-6 derived EVI's illustrate the atmospheric and illumination geometry effects. Simulated data were derived using Dave's data set.

water stress index (CWSI). The CWSI (Fig. 13), closely paralleled a plot of the extractable soil water in the 0-to 1.1-m soil zone. Although the CWSI [8] was developed using wheat plot data, the concepts led to the development of an index using NOAA-AVHRR data for large-area application.

The satellite-derived stress index (SDSI) requires day/night canopy temperature measurements for individual satellite pixels and air temperature measurements obtained from meteorological stations. The stress index is computed using the following equation:

$$SDSI = \frac{DT - AT}{DT - NT}$$

where

- DT* is the satellite acquired daytime maximum temperature,
- AT* is the meteorological station daytime maximum temperature, and
- NT* is the satellite-acquired nighttime minimum temperature.

The numerator is a function of evapotranspiration. The denominator is a function of vapor pressure deficit, and indicator of potential evapotranspiration. The SDSI parameter approximates the pattern of crop water stress index [8]. Where high values of SDSI co-exist with large values of VIN's, it is interpreted as an indicator of crop water stress. At this time the relationship is subjective in interpretation, but an effort is in progress to quantify the parameter. Fig. 14 illustrates, in image form, the relationship between VIN's and the SDSI. Dark portions in the stress image indicate areas of low stress, light portions in the VIN image indicate areas of high vegetation. The scatter plot in Fig. 15 represents a multitude of land uses, such as water, bare soil, pasture, stream bed vegetation, and various crops. Although considerable scatter of data points exist, there is a strong correlation between VIN values and the SDSI. The stress index would provide more consistent results if the spatial distribution of meteorological air temperature data were better.

Hot dry winds, such as a sukovey in the U.S.S.R., can cause a significant decrease in yield of spring and winter wheat. The Yield Reduction Model [13] was used over three major winter wheat producing provinces in the North China Plains. Results from the model (Fig. 16) suggest that the potential for yield reduction was greater in 1982 than in 1983. Reports from China also verify that poorer yields were obtained in 1982 than in 1983.

Landsat MSS studies were conducted, across the U.S. Great Plains, to determine the feasibility of monitoring rangelands to predict the potential for water stress in adjacent croplands. The hypothesis was that water often becomes limiting in rangeland areas before adjacent croplands show symptoms of water deficit. Results from these studies suggest that Landsat acquisitions are too infrequent for reliable prestress indicators for adjacent crops. However, vegetation greenness indexes [10] computed for

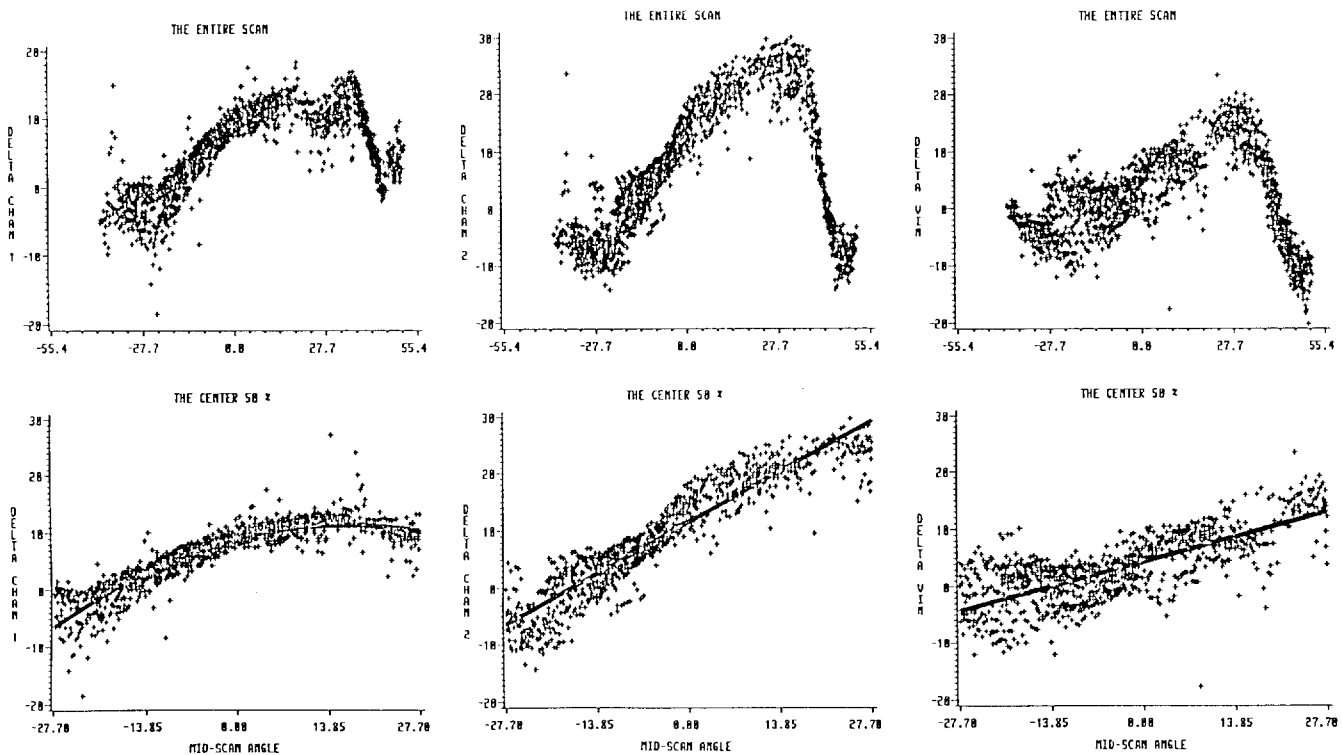


Fig. 12. Changes in NOAA AVHRR channel values and vegetative index numbers between consecutive day satellite passes as the scan angle increases both east and west of nadir: Center 1024 pixels to be modeled for scan angle corrections.

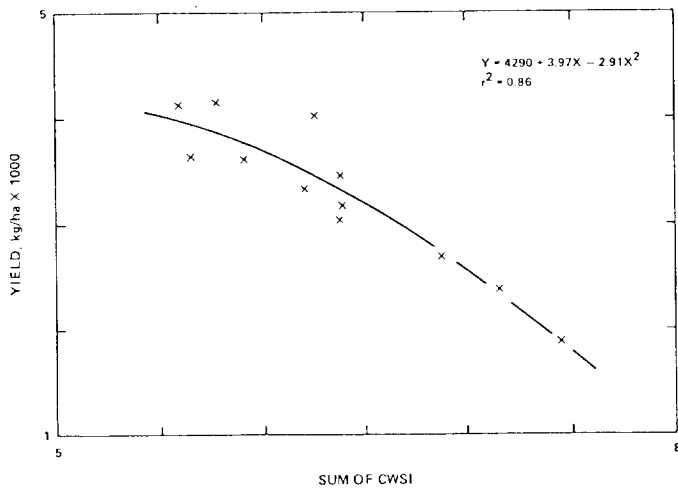


Fig. 13. The CWSI as a function of Julian days for wheat plot A, which received a single-post emergence irrigation. Circles represent the calculated CWSI data points and the hand drawn solid line show data point trends. The plus symbols represent the extractable water used from the 0- to 1.1-m depth. Ordinate values also represent extractable water used.

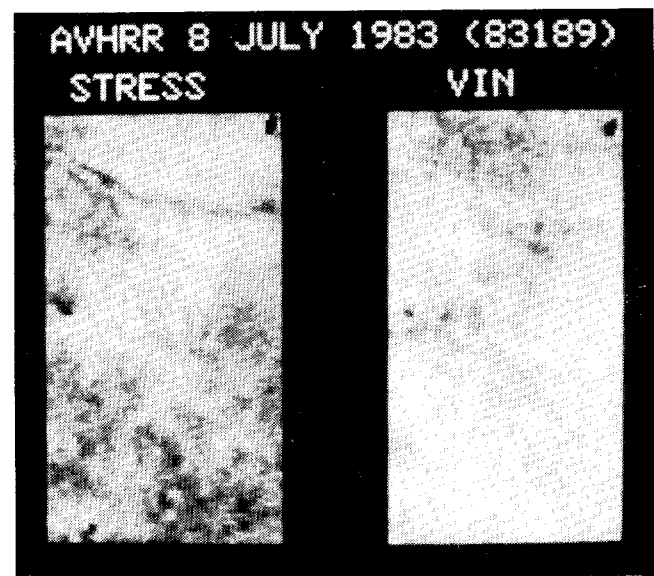


Fig. 14. Comparison of satellite derived vegetative index image and thermal stress indicator image for Grady County, Oklahoma.

all Landsat MSS pixels within a 5 × 6 mile segment parallel the greenness index of only rangeland pixels within the same segment. Fig. 17 illustrates the changes in greenness within and between years and that the overall greenness of the segment is never significantly different from the greenness of rangeland. Similar results were obtained for all segments studied within the U.S. Great Plains. These results combined with vegetative indices computed from AVHRR data for I,J grid cells (Fig. 7)

suggest that AVHRR data could provide useful information about overall crop conditions for large areas.

Handheld radiometer studies (15) suggest that plant diseases may be monitored from satellite platforms if moisture and temperature conditions could be tracked using meteorologically driven disease indicator models. Decreases in vegetative index numbers can occur because of drought and/or plant disease conditions. Knowledge of

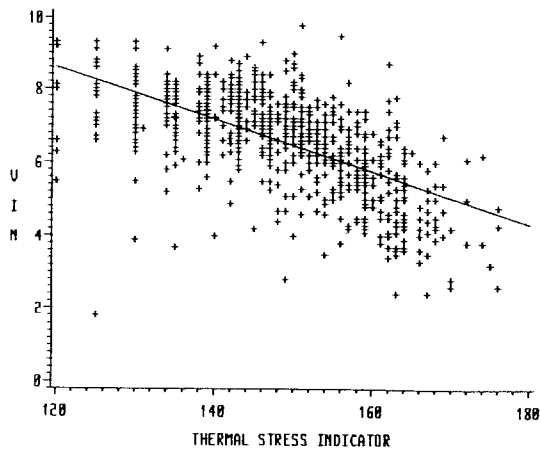


Fig. 15. Scatter plot of satellite derived vegetative index numbers and thermal stress indicator values for Grady County, OK.

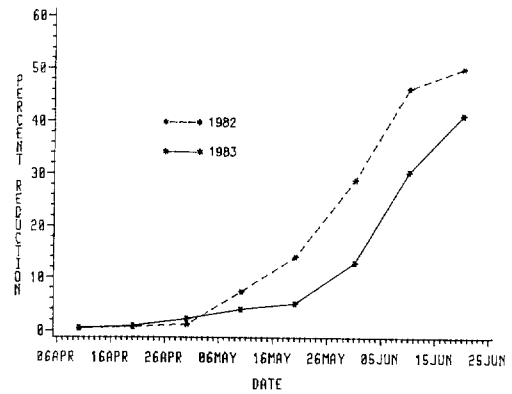


Fig. 16. Comparison of 1982 and 1983 results of the wheat yield reduction model for major wheat growing provinces of China.

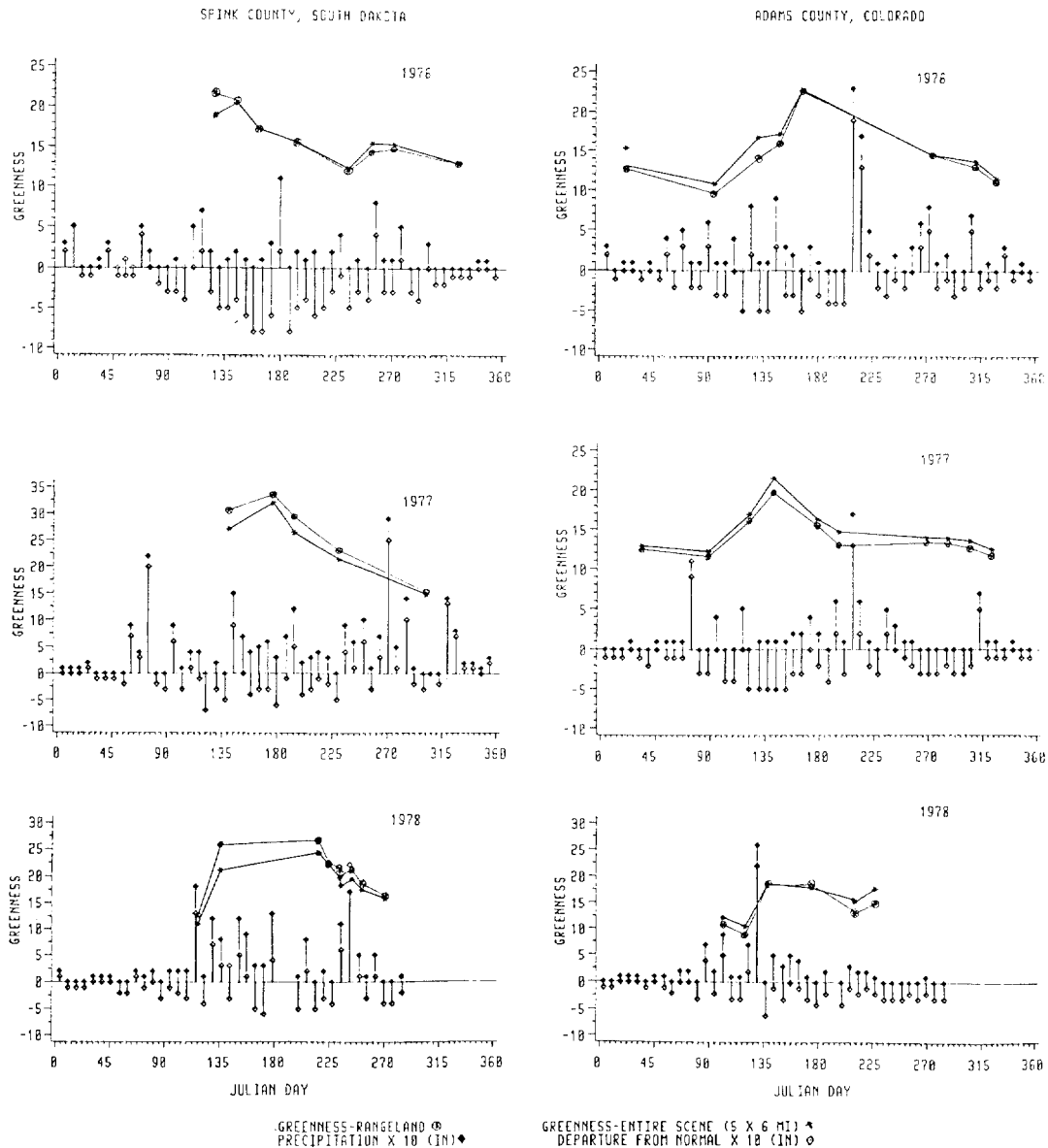


Fig. 17. Seasonal and yearly trajectories depicting rangeland and total scene vegetative indices for 5 x 6 mile segments in South Dakota and Colorado.

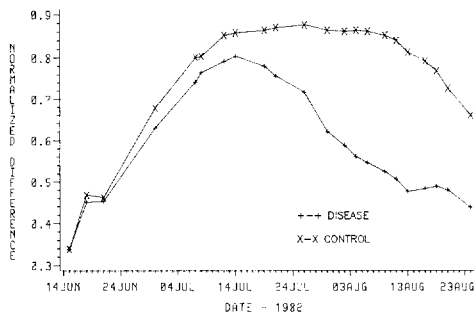


Fig. 18. The effect of stem rust on vegetative index numbers during the growing season for wheat, Montana Rust Disease Study, Exotech Radiometer.

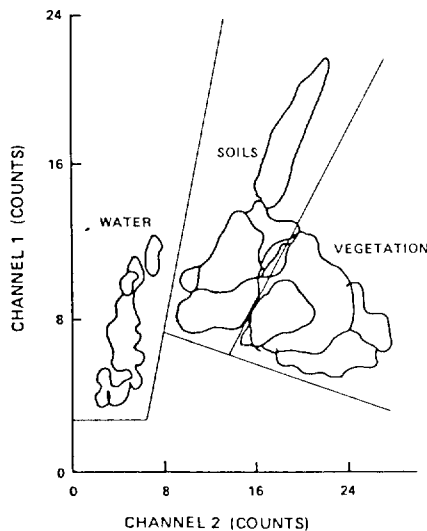


Fig. 19. Flood classifier for delineation of water, vegetation, and soils using NOAA-6 spectral data.

moisture conditions will define which condition exist. Fig. 18 indicates that the vegetative index (normalized difference) began to decrease soon after wheat plants were inoculated with rust spores on June 7 and again on June 18, 1982. After July 14, the normalized difference (ND) of the diseased plants decreased almost linearly (from 0.78 to 0.40), whereas the ND of nondiseased plants remained above 0.80 until August 13 when natural senescence was in progress. Although yield data are not shown in this paper, diseased plots yielded significantly less grain than nondiseased plots.

Plant stress caused by flooding also results in significant crop damage. Thus, a classifier (Fig. 19) and crop damage estimator was developed for monitoring flooded areas. Large river basin flooding is easily detected and monitored using this classifier, however small stream flooding is more difficult because of the AVHRR pixel resolution.

V. CONCLUSIONS AND RECOMMENDATIONS

In the authors' view, the EW/CCA project made major contributions to science and to operational users of remote sensing. Crop-stress indicator models were developed that provide hazardous and optimal alerts for water and temperature factors. These models are used by the USDA-

FAS as data filters and as an alert tool for monitoring global crop conditions.

Environmental satellite research led to the development of a NOAA-AVHRR data processor, making it possible for the USDA-FAS to use the data in their operational crop-condition assessment program. Research increased our knowledge of the spectral characteristics of soils, water, vegetation, crop stresses, and crop types. Research involving the effects of cloud contamination, atmosphere, geometry, canopy structure, solar zenith angle, and scan angle improved our ability to utilize satellite data for agricultural purposes.

Crop-condition assessment studies resulted in the development of crop water stress indexes based on canopy and air temperature differences obtained from either ground or space platforms. A yield-reduction model was developed and transferred to an operational user. Landsat MSS and NOAA AVHRR studies indicate that large-area crop condition monitoring can be achieved without explicit knowledge of vegetative cover. Widespread plant disease (stem rust) monitoring is feasible in conjunction with a disease susceptibility model that uses meteorological data inputs.

The authors recommend that research studies continue which meet the requirements supplied by users. Efforts must be continued to enhance and improve the use of the gridded vegetative indices for the U.S. Great Plains. This implies the development of geographically referenced information systems. The scan angle model should be implemented so that more of the scan swath can be used. We emphasize that participants in the EW/CCA project were truly interdisciplinary scientists and that excellent cooperation was received from all researchers. Continuation of a multidisciplinary team that works in conjunction with the user will significantly enhance the research results and will speed the transfer of technology to operational units. More emphasis and resources should be placed on technology transfer.

ACKNOWLEDGMENT

The authors take this opportunity to express their gratitude to the many government agencies, research scientists, agricultural research centers, universities, industry, and the AgRISTARS management team who supported the Early Warning and Crop Condition Assessment (EW/CCA) Project. The joint cooperation and support from these various groups make it difficult to acknowledge specific contributions made by each organization.

However, resources from the USDC-NOAA were directed toward satellite-derived products such as solar insolation, maximum/minimum temperatures, precipitation, snow cover, basic research using NOAA-AVHRR data, and the development of vegetative index numbers derived from AVHRR data.

The NASA Johnson Space Center provided resources that were directed toward satellite sensor research, software development, studies to enhance the utilization of NOAA-AVHRR data, parameter identification and devel-

opment for modeling winterkill, wheat yield reduction, harvest loss, and potential evapotranspiration.

Resources provided by the USDA-SRS were utilized to establish individual relations between spectral data and plant stresses, spectral characteristics for stressed and nonstressed crops, stress model development, improved understanding and utilization of AVHRR data, software development, and statistical analyses for many of the research tasks.

Resources from the USDA-ARS were divided among several research locations. The unit in Weslaco, Texas, provided basic technology including spectral characteristics of soils, water, and crop and range vegetation, thermal and aridity relationships, atmospheric and cloud effects, spectral inputs to crop models, and spectral components analysis.

The ARS unit in Phoenix, Arizona, conducted basic spectral and thermal studies that contributed to improved understanding of vegetative indices and crop water stress. They established relations of spectral and/or canopy temperatures with yield components, plant stresses, and final yield. These studies provided insight and knowledge into the effects of surface geometry, canopy structure, solar zenith angle, and atmosphere on both spectral and thermal characteristics.

The ARS Hydrology Research unit in Beltsville, Maryland, developed a model for monitoring floods and assessed other hydrologic parameters.

The Crops Research unit in Beltsville and ARS personnel at Bushland and Lubbock, Texas, provided ground based spectral information for major crops under stressed and nonstressed conditions.

The research unit in Mandan, North Dakota, defined parameters and established threshold values for harvest loss modeling, and measured spectral responses of grasslands under different management practices.

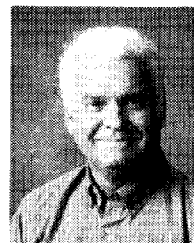
Research conducted at Sidney, Montana, and at Akron, Colorado, provided basic research needed to establish parameter and threshold values for the wheat winterkill and wheat yield reduction models.

The EW/CCA unit in Houston coordinated and managed the project. This unit, composed of scientists from ARS, SRS, NASA, NOAA, and Lockheed Engineering and Management Services Company (LEMSCO), directed resources toward crop stress indicator model development, development and implementation of basic and applied remote-sensing technology, and the transfer of proven technology to users. The Houston unit was collocated with the Foreign Crop Condition Assessment Division of the Foreign Agricultural Service (FAS). The FAS division identified needed technology, provided computer resources, and assisted in technology transfer from the EW/CCA unit in Houston to FAS in Washington.

REFERENCES

- [1] A. C. Aaronson, "The large area operational application of the winterkill model using real time data and evaluation of the results," USDA-FAS Crop Condition Assessment Div., Tech. Memo. 13, 1980.
- [2] A. Bauer, and A. L. Black, "Rain-Induced spring wheat harvest losses," AgRISTARS EW/CCA Rep. EW-U3-04405, Feb. 1983.
- [3] —, "The water factor in harvest-sprouting of hard red spring wheat," AgRISTARS EW/CCA Rep. EW-U3-04406, Feb. 1983.
- [4] G. O. Boatwright, F. W. Ravet, and T. W. Taylor, "Development of early warning models," Ch. 12, ARS Wheat Yield Project, USDA-ARR, to be published.
- [5] J. A. Boatwright and W. M. Bradley, "Image correction and registration utility system (ICARUS) design document," Unnumbered Tech. Rep., LEMSCO; 1984.
- [6] C. J. A. Gay and R. F. Gay, "Early warning soybean stress prediction model," Ph.D. dissertation, Biosystems Research Group Department of Industrial Engineering, Texas A&M Univ., College Station, TE, Oct. 1983.
- [7] T. I. Gray and D. G. McCrary, "Meteorological satellite data: A tool to describe the health of the world's agriculture," AgRISTARS EW/CCA Rep., EW-N1-04042, JSC-17112, Feb. 1981.
- [8] R. D. Jackson, E. B. Idso, R. J. Reginato, and P. J. Pinter, Jr., "Canopy temperature as a crop water stress indicator," *Water Res. Research*, vol. 17, pp. 1133-1138, 1981.
- [9] W. R. Johnson, "Atmospheric effects on metsat data," AgRISTARS EW/CCA Rep., EW-L2-04387, JSC-18589, Jan. 1983.
- [10] R. J. Kauth, and G. S. Thomas, "The tasselled cap—A graphic description of the spectral temporal development of agricultural crops as seen by Landsat," in *Proc. Symp. Machine Processing Remotely Sensed Data* (West Lafayette, IN), vol. 4B, pp. 41-51, 1976.
- [11] M. L. Mathews, "Cloud screening and solar correction investigations on the influence on NOAA-6 advanced very high resolution radiometer derived vegetation assessment," AgRISTARS EW/CCA Rep., EW-L3-04402, JSC-18606, Mar. 1983.
- [12] F. W. Ravet and J. R. Hickman, "A meteorologically driven wheat stress indicator model," USDA-FAS Crop Condition Assessment Div. Tech. Memo. 8, 1979.
- [13] F. W. Ravet, W. J. Cremins, T. W. Taylor, P. Ashburn, D. Smika, and A. Aaronson, "A meteorologically driven yield reduction model for spring and winter wheat," AgRISTARS EW/CCA Rep. EW-U3-04397, JSC-18601, Feb. 1983.
- [14] A. J. Richardson, "El Chicon volcanic ash effects on atmospheric haze measured by NOAA-7 AVHRR data," *Remote Sensing Environ.*, vol. 16, pp. 157-164, 1984.
- [15] E. L. Sharpe, C. R. Perry, A. L. Scharen, G. O. Boatwright, D. C. Sands, L. F. Lautenschlager, C. M. Yahyaoui, and F. W. Ravet, "Monitoring cereal rust development with a spectral radiometer," *Phytopath.*, vol. 75, 1985.
- [16] T. W. Taylor and F. W. Ravet, "A meteorologically driven maize stress indicator model," AgRISTARS EW/CCA Rep. EW-U1-04119, JSC-17399, Apr. 1981.
- [17] —, "A meteorologically driven grain sorghum stress indicator model," AgRISTARS EW/CCA Rep. EW-U1-04208, JSC-17797, Nov. 1981.

*

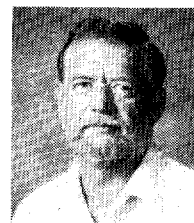


Glenn O. Boatwright received the B.S. and M.S. degrees in soils from Oklahoma A&M in 1954 and 1956, respectively, and the Ph.D. degree in plant and soil science from Montana State University in 1970.

From 1956 to 1972, he was a Research Scientist with the Agricultural Research Service in Mandan, ND, Bozeman, MT, and Gunnison, CO. He was a rancher in Chickasha, OK, from 1972 to 1976. He returned to the Agricultural Research Service in 1976 as a Research Scientist where he

is currently the Early Warning Crop Condition Assessment Project Manager.

*



Victor S. Whitehead was born on September 18, in Taylor, AR. He received the B.A. degree in physics and math from Baylor University, the M.S. degree in meteorology from Texas A&M University, and the Ph.D. degree in engineering sciences from the University of Oklahoma.

Since 1968, he has been employed by the NASA Johnson Space Center in a variety of Earth Observations Program and Remote Sensing Program assignments, including LACIE and AgRISTARS.

Field Spectroscopy of Agricultural Crops

MARVIN E. BAUER, MEMBER, IEEE, CRAIG S. T. DAUGHTRY, LARRY L. BIEHL, MEMBER, IEEE,
EDWARD T. KANEMASU, AND FORREST G. HALL

Abstract—The design, implementation, and results of multisite multiyear experiments to measure and model the multispectral reflectance of agricultural crops in relation to their biophysical characteristics are described. The experimental approach involved multitemporal reflectance measurements together with detailed measurements of the agronomic characteristics of crop canopies. One result of the field measurements and analyses was a quantitative description of the complex relationships among crop canopy, soil, atmosphere, and illumination and sensor geometries. Leaf area index was identified as a key biophysical parameter linking crop physiology and multispectral remote sensing. Quantitative understanding and models of this relationship led to the development of spectral-temporal profile models for crop species identification and development stage estimation. A second key development has been the development of conceptual approaches and models for spectral estimation of leaf area index and light interception of crop canopies as inputs to crop growth and yield models. Other results include quantification of the effects of soil background, cultural practices, moisture stress, and nutrient deficiencies on crop reflectance, and the effects of sun angle and sensor view angle on measured canopy reflectance. The field measurements of canopy reflectance and geometry also provided data bases to test and validate canopy radiation models. In summary, the AgRISTARS field research on agricultural crops has provided a critical link between satellite and leaf spectral data.

Key Words—Multispectral, remote sensing, reflectance, canopy radiation, leaf area index, crop identification, crop-condition assessment, spectral inputs to crop models.

I. INTRODUCTION

TO DEVELOP the full potential of multispectral data acquired from satellites, quantitative knowledge, and physical models of the spectral properties of specific Earth surface features are required. Knowledge of the relationships between spectral-radiometric characteristics and important biophysical parameters of agricultural crops and soils can best be obtained by carefully controlled studies of fields or plots where complete data describing the agronomic-biophysical properties of the crop canopies and soil background are attainable and where frequent timely calibrated spectral measurements can be made [1]. These attributes distinguish field research from other remote-sensing research activities. Although the term field spectroscopy has generally not been applied to this research,

Manuscript received June 16, 1985; revised August 29, 1985.

M. E. Bauer was with the Laboratory for Applications of Remote Sensing, Purdue University, West Lafayette, IN 47907. He is now with the Remote Sensing Laboratory, University of Minnesota, St. Paul, MN 55108.

C. S. T. Daughtry and L. L. Biehl are with the Laboratory for Applications of Remote Sensing, Purdue University, West Lafayette, IN 47907.

E. T. Kanemasu is with the Evapotranspiration Laboratory, Kansas State University, Manhattan, KS 66506.

F. G. Hall was with the NASA Johnson Space Center, Houston, TX 77058. He is now with the NASA Goddard Space Flight Center, Greenbelt, MD 20771.

IEEE Log Number 8406221.

in retrospect it seems to clearly and concisely describe the approach. Definitions of spectroscopy include study of spectra, especially the experimental observation of spectra; production and investigation of spectra; and physics that deals with theory and interpretation of interactions between matter and electromagnetic radiation.

Satellite sensors will ultimately provide the data for most agricultural remote-sensing applications [2], [3], but the spatial and temporal resolution of current satellite data is not well suited for efficiently determining the cause-effect relationships between spectral response and other crop variables. And, while laboratory measurements of leaf and soil reflectance spectra are important elements of a balanced research program, these data cannot be directly extrapolated to crop canopies where there are many interacting variables such as environment and crop geometry. *In situ* spectral measurements of crop canopies provide an essential bridge between the macro observations of agricultural fields by aircraft and satellite sensors and micro observations in the laboratory of leaves and soil samples.

A second key role of field research is in the development and verification of canopy radiation models. These models provide a theoretical basis for remote-sensing experiments, and can greatly enhance the remote-sensing research by extending the field measurements to a wider set of environmental conditions and sensor viewing and illumination geometries than can be obtained by direct measurements [4]. The possibility of inverting such models to estimate agronomically important canopy parameters such as LAI adds to their importance. Accurate measurements of canopy reflectance, as well as the measurements of the model inputs, are required for model verification.

This paper describes field research that was sponsored by the NASA Johnson Space Center, Houston, TX, as part of the AgRISTARS Supporting Research Project. Other, related research has been conducted by the USDA Agricultural Research Service and the NASA Goddard Space Flight Center. The remainder of the paper, which summarizes the field research accomplishments since the LA-CIE field research project [1], is divided into four main sections describing the field research objectives (Section II), development of capability (Section III), experiment design and approach (Section IV), and experiment results (Section V).

II. FIELD RESEARCH OBJECTIVES

The overall objectives of the AgRISTARS Field Research project were to: 1) conduct analyses and develop

physical models of the spectral properties of crops and soils in relation to agronomic and physical properties of the scene, 2) provide candidate models and analysis techniques to other supporting research experiments and AgRISTARS projects, and 3) assess the capability of current, planned, and possible future satellite sensor systems to capture available information for identification and assessment of crops and soils.

Specific objectives included:

- 1) Model the relationship of agronomically important canopy parameters (e.g. leaf area index and development stage) to reflectance properties of crop canopies.
- 2) Determine the effects of plant stresses, particularly moisture and nutrient deficiencies, on the spectral reflectance of crop canopies.
- 3) Quantify the effects of cultural, soil, and environmental factors, on the spectral characteristics of vegetation.
- 4) Quantify the effects of sensor and illumination geometry, and its interaction with canopy geometry, on the spectral reflectance of crop canopies.
- 5) Acquire canopy reflectance measurements, together with measurements of the model input variables, for evaluation and inversion of canopy radiation models.

III. DEVELOPMENT OF CAPABILITY

During the past decade a great deal of capability to acquire meaningful spectral measurements of agricultural crops and soils has been developed, and a substantial number of results are appearing in the scientific literature. The capability and results described in this paper are in large part due to sustained support of the NASA Johnson Space Center over an extended period beginning in the 1970's. The relevancy and critical role of field research in the development of satellite applications of remote sensing has long been recognized [5], but a significant amount of development and testing of instrumentation and measurement procedures for remote-sensing field research has been required.

A. Field Research Instrumentation

Although the importance of quantitative knowledge of crop spectral characteristics was recognized early in the development of contemporary remote sensing, the lack of appropriate field instrumentation severely restricted development of a comprehensive research program. Laboratory measurements of leaves and soil did not represent the complexity and spatial variability of canopies in the field, nor include the effects of illumination and viewing geometry. Aircraft multispectral scanners, while providing excellent data for development of digital image analysis techniques, have not been widely used in field research because of the difficulties of operation on an on-call basis, calibration problems, inflexibility of wavelength band configuration, and large costs of operation and data processing. As a result, researchers requiring *in situ* mea-

surements have turned to multiband and continuous wavelength instruments.

Initial efforts involved extension of laboratory spectroradiometers to field applications. Further efforts led to development of rugged high-resolution field spectrometer systems such as the Exotech 20C operated by Purdue University/LARS and the S-191H operated by the NASA Johnson Space Center. These instruments are capable of accurately measuring spectral reflectance and emitted spectral radiance, and have been used on truck-mounted towers and helicopters. Using these instruments the LACIE Field Measurements project [1] produced spectral data which were calibrated (and, therefore, comparable from time to time and place to place). A large number of spectra for experiments with both controlled plot and commercial fields were acquired, processed, archived, and analyzed over the three-year project, but it became clear that these systems could not economically satisfy the need to acquire data at the number of sites needed to represent the variability in crop, soil, and weather conditions associated with production of major crops.

At the same time it was equally clear that while having the advantage of simplicity and low cost, that the then available multiband radiometers were not adequate. In particular, these instruments were characterized by restricted wavelength coverage and did not include bands in the middle and thermal infrared. In summary, available instruments were either inadequate or too costly to obtain the necessary data. Additionally, there was a critical need for standardized acquisition and calibration procedures to insure the validity and comparability of data.

In response to the need to increase the number of researchers and locations conducting remote sensing field research, researchers at Purdue University began to design a multiband radiometer system especially for agricultural field research. The LACIE Field Research project had demonstrated that a practical means to obtain spectral data from a wide variety of subjects and to increase the number of investigators who could afford to acquire and analyze data was to simplify the instrumentation and reduce the amount of data obtained for each observation. To achieve this, a field-rated multiband radiometer with a limited, but sufficient, number of wavelength bands sampling all important parts of the reflective spectrum from 0.4 to 2.4 μm , plus a thermal infrared band (10.4 to 12.5 μm) was specified. Other design criteria included: comparatively inexpensive to acquire, maintain, and operate; simple to operate, calibrate, and service; rugged, light weight, and portable; complete with data recording and handling hardware and software; and well-documented for use by researchers [6].

The NASA Johnson Space Center sponsored the development of the system and in 1981 purchased 15 of the radiometer units for use at NASA-sponsored research sites. These instruments, together with solid-state data logger, camera, truck or helicopter platform, and reflectance calibration standard, became the primary spectral data acquisition systems of the Field Research segment of

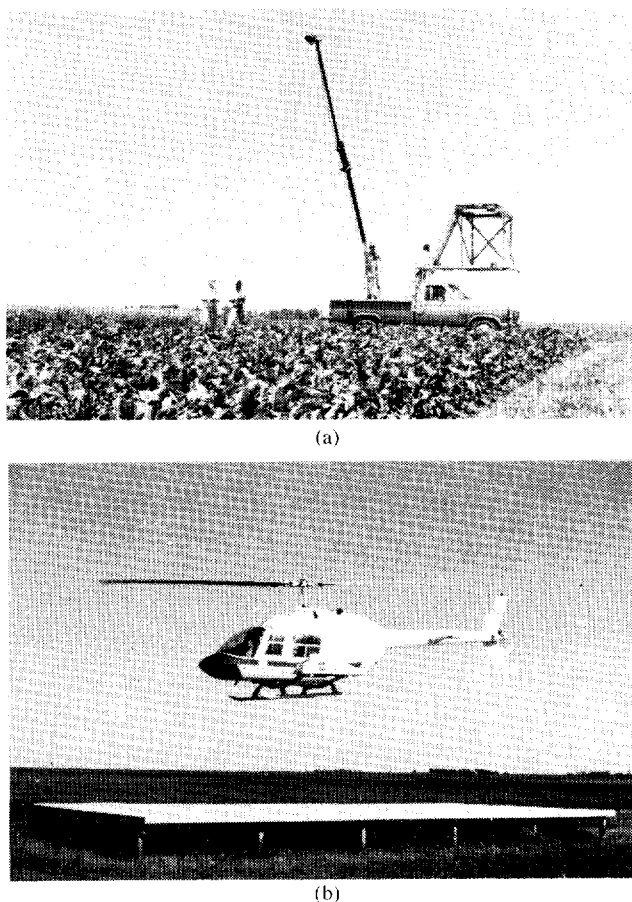


Fig. 1. (a) Truck-mounted multiband radiometer and (b) helicopter-mounted spectrometer systems. The truck-mounted system includes radiometer, 35-mm camera, data logger, and calibration standard. Measurements of 40 to 60 plots/h can be made with this system. The helicopter system, shown hovering over a canvas calibration standard, flies transects, typically 6 miles long, over commercial fields at an altitude of 75 m. With average field sizes, 10 to 30 spectra are acquired of each field.

TABLE I
AgRISTARS FIELD RESEARCH COMMERCIAL FIELD TEST SITES

| Location | Major Crops | Years | Sensors ^a |
|------------------------------|-------------------------------------|---------|---------------------------------------|
| Webster County, Iowa | Corn Soybean | 1979-81 | FSS NS-001 |
| Cass County, North Dakota | Spring wheat Barley Sunflower | 1980-82 | FSS ('80, '81) NS-001 MRS ('82) |
| Wharton County, Texas | Cotton Rice Soybean | 1980 | NS-001 |

^aFSS, helicopter-mounted field spectrometer system; NS-001, thematic mapper simulator; MRS, helicopter-mounted multiband radiometer system.

the AgRISTARS Supporting Research Project (Fig. 1). The locations and crop species for which spectral measurements have been made using these systems are listed in Table I.

B. Measurement Procedures

1) *Calibration of Spectral Data*: One of the key aspects of the approach has been to follow procedures, such

that measurements acquired at different locations and times can be compared and/or combined. Although data from an individual experiment are certainly valuable, it is expected that they will have greater value when data from several sites are combined or when a model is tested against an independent data set. It therefore follows that the spectral and agronomic measurement procedures need to be carefully designed and executed.

The spectral data obtained by the spectroradiometer and multiband radiometer systems are processed into comparable units, reflectance factor. A reflectance factor is defined as the ratio of the radiant flux actually reflected by a sample surface to that which would be reflected into the same sensor geometry by an ideal, perfectly diffuse surface irradiated in exactly the same way as the sample [7].

The field calibration procedure consists of the comparison of the response of the instrument viewing the crop or soil to the response of the instrument viewing a level reference surface. The reference surfaces are 1.2-m² painted barium sulfate panels for truck-mounted systems and a 6 × 12 m white canvas panel for the helicopter-mounted sensors. For small fields of view (less than 20° full angle) the term bidirectional reflectance factor has been used to describe the measurement: one direction being associated with the viewing angle (usually 0° from normal) and the other direction being the solar zenith and azimuth angles.

The spectral data are obtained following well-defined field procedures [7]. Key components of the procedure are:

- frequent observations of the reflectance reference panel (at least every 10 to 20 min),
- instrument aperture is sufficiently distant from the scene (at least 3 m above the top of the canopy),
- collect data when solar elevation angles are above 45°, except for modeling experiments,
- no clouds are in the vicinity of the sun, and
- the reflectance reference surface is viewed in the same manner as the scene.

In addition, the non-Lambertian properties of the reference panels must be taken into account. The reflectance of the barium sulfate panels are compared to that of pressed barium sulfate in the laboratory at Purdue/LARS using a bidirectional reflectometer for illumination zenith angles of 10° to 85°. An extensive set of calibration measurements of reference surfaces are kept.

2) *Sensor Altitude*: Use of portable ground-based sensors for measuring crop reflectance has dictated a need for reliable measurement procedures capable of providing calibrated and reproducible canopy reflectance data. An important aspect of acquiring reproducible data for canopies concerns sensor altitude in relation to canopy type and row spacing. Daughtry *et al.* [8] measured the variation in reflectance of corn and soybean canopies as functions of horizontal distance across rows and vertical distance above the soil. Variation as the sensor was moved across the canopy disappeared as sensor altitude increased and integrated across several rows. Coefficients of variation decreased exponentially as sensor altitude increased.

Sampling schemes employing prior knowledge of row spacing were determined to be more efficient (required fewer measurements for a given level of precision) than random sampling schemes. At altitudes where several rows are included in the field of view, as few as two measurements were required to detect 10-percent differences (as percent of the mean) in reflectance, whereas at lower altitudes 20 to more than 100 measurements would be needed.

3) *Agronomic Measurements*: Equally important to acquiring calibrated spectral measurements is the acquisition of accurate agronomic measurements of the canopies. Particular emphasis has been given to measurements of leaf area index because of its central importance to spectral reflectance, photosynthesis and evapotranspiration of crop canopies. There are a number of satisfactory methods to measure the leaf area of individual leaves and plants; however, to estimate the LAI of canopies, the variability in leaf area among plants within plots is an additional source of experimental error. In support of remote-sensing research, Daughtry and Hollinger [9] examined the magnitude of within plot variability and evaluated several methods for measuring LAI with known precision and probability of detecting differences. The approximate errors, number of plants required, and relative costs of each method were determined.

The results provided direction for the sampling and measurement procedures, plus strong evidence that spectral-agronomic relationships are best developed from controlled plots where plant to plant variability is relatively small (10-percent *CV*) compared to that in fields, and that if a parameter such as LAI is to ever be utilized in crop growth and yield models, it will have to be estimated from remotely sensed spectral data. For example, direct area measurements of all leaves on plants using an electronic area meter (the method resulting in the greatest precision with time requirements comparable to other methods) required measurements of 21, 7, and 2 plants to detect true differences in LAI among treatments of 10, 20, and 50 percent at 0.05 level of significance and 90-percent probability of success. These measurements required 168, 56, and 16 man-minutes, respectively.

IV. EXPERIMENT DESIGN AND APPROACH

Following the approach initiated in the LACIE Field Measurements project, a multistage approach to data acquisition was taken, including areal, vertical, and temporal staging. Areal sampling was accomplished with test sites at multiple locations in the U.S. Great Plains and Corn Belt, plus sites at Corvallis, Oregon, and Obregon, Mexico. The sites were selected to sample a wide range of conditions under which corn, soybeans, and wheat are produced. Vertical staging, or collection of data by different sensor systems and at different altitudes, ranged from mobile (truck) towers to Landsat. Temporally, data were collected, depending on sensor system and location at 5–20 day intervals to sample all important development stages and during 5 years (1980–1984) to obtain a measure

of year-to-year variation in growing conditions and its influence on spectral response.

As established during LACIE [1], two major types of experiments were utilized: 1) controlled experiments involving research plots at agricultural experiment stations and 2) noncontrolled experiments in commercial fields located in AgRISTARS segments. The controlled experiments enable detailed agronomic and frequent spectral measurements to be made of plots with known sources of variation (agronomic treatments). The measurements in commercial fields, although less detailed and frequent, provide a measure of natural variation in the spectral-spatial-temporal characteristics of the crops. Past experience has shown that there are generally too many interacting variables in commercial fields to determine exact causes of observed differences in spectral response. With data from plots where only two to four factors are varied under controlled conditions, it is possible to determine more exactly and understand more fully the relationships of agro-physical and spectral characteristics of the crop canopies.

A. Description of Experiments and Measurements

1) *Controlled Plot Experiments*: With the availability of the multiband radiometer systems described above, numerous experiments involving controlled plots have been conducted during AgRISTARS at the locations listed in Table II. Although space does not permit describing, or even listing all of the experiments, it may be helpful to summarize as examples the objectives, experiment designs, and measurements for two experiments. The first is an example of what has been referred to as a cultural practices experiment, while the second is an experiment involving moisture stress.

a) *Corn cultural practices*: This experiment was conducted during the 1980–1983 growing seasons at the Purdue University Agronomy Farm, West Lafayette, IN. The objectives were to 1) identify the threshold of early season spectral detection of corn, 2) determine the relationship of development stage and amount of vegetation (e.g., LAI) to spectral response, and 3) determine the effect of soil background and cultural practices on spectral response. The treatments, with 1981 planting dates, were: four planting dates (May 8, 29, and June 11, 29); three plant populations (25 000, 50 000, and 75 000 plants/ha); and two soil types (Chalmers, dark color; Fincastle, light color). A split plot factorial experiment design with two replications of each treatment was used. Spectral measurements, along with agronomic characterizations of the canopies and surface soil, were made at approximately weekly intervals throughout the growing season. The spectral measurements were made with an Exotech 100 radiometer in all years; in 1982 and 1983 a Barnes multiband radiometer was added. Radiant temperatures and overhead color photographs of the canopies were obtained simultaneously with the reflectance measurements. The primary agronomic measurements included development stage, percent soil cover, LAI, fresh and dry biomass, and surface soil moisture. Beginning in 1982, canopy trans-

TABLE II
SUMMARY OF CONTROLLED PLOT EXPERIMENTS AT AGRICULTURAL
EXPERIMENT STATIONS USING MULTIBAND RADIOMETERS

| Location | Crop(s) | Years | Primary Objectives/Topics Addressed |
|--|---|---------|---|
| Purdue Univ. W. Lafayette, IN | Corn Soybean Winter wheat | 1979-84 | Spectral estimation of LAI, light interception, and development stage Effects of cultural, soil, and environmental factors Canopy modeling/sensor, illumination and canopy geometry effects |
| Univ. Nebraska Lincoln, NE | Corn Soybean | 1981-84 | Moisture stress effects on crop reflectance and radiant temperature Spectral estimation of LAI and grain yield |
| Univ. Minnesota St. Paul, MN | Corn Soybean | 1982-84 | Effects of tillage methods and residue on crop reflectance |
| Kansas State Univ. Manhattan, KS | Winter wheat Corn | 1981-84 | Spectral estimation of LAI, light interception, and development stage Effects of cultural, soil, and environmental factors |
| S. Dakota State Univ. Brookings, SD | Spring wheat Barley Oats | 1982-84 | Spectral separability of small grains Estimation of LAI |
| Oregon State Univ. Corvallis, OR | Winter wheat Barley | 1982-83 | Spectral reflectance characteristics of small grains |
| Texas A&M Univ. College Station, TX | Rice Sorghum | 1982-84 | Effects of cultural practices on crop reflectance |
| CIMMYT Obregon, Mexico | Spring wheat Winter wheat Sorghum | 1982-84 | Effects of moisture stress and cultural practices on crop growth, yield and reflectance |
| Univ. Kansas Lawrence, KS | Corn | 1982-84 | Synergistic effects of optical plus microwave measurements |
| NASA/GSFC Greenbelt, MD | Corn Soybean Winter wheat | 1982-83 | Canopy modeling/sensor, illumination and canopy geometry effects |

mittance was measured at the soil surface to calculate solar radiation interception. Grain yields were measured at harvest time. Similar experiments have been conducted for soybeans.

b) Corn moisture stress: Moisture stress experiments were conducted on corn and soybeans by the University of Nebraska at the Sandhills Agricultural Laboratory near Tryon, NE, in 1981-1984. Irrigation facilities at this site permit the application of water during prescribed growth stages on either whole plots or on gradient plots. For example, in one experiment gradient irrigation treatments were applied across 24 rows of a plot (row 1 receives full irrigation, row 24 receives no water). One set of plots received gradient irrigation during vegetative, pollination, and grain filling stages. A second set of plots received gradient irrigation during vegetative stages and full irrigation thereafter, while a third set of plots received full irrigation at all stages. This experimental setup provided a wide range of stress conditions during the season. The sandy soils and the relatively low amounts of rainfall received at this site make it an ideal location to study moisture stress effects on the growth and spectral characteristics of agronomic crops without the necessity of installing expensive rainout shelters. Spectral measurements were made with Barnes and Exotech 100A multiband radiometers, supplemented by additional radiant temperature measurements at oblique view angles. Agronomic measurements included development stage, LAI, biomass, canopy structure, leaf water potential, leaf photosynthesis, stomatal resistance, and grain yield. Meteorological data routinely collected at this site include soil

moisture, soil temperature, solar radiation, windspeed and direction, air temperature, relative humidity, and rainfall.

2) *Canopy Modeling Experiments:* Canopy radiation models have an important role in remote sensing research. However, the models require validation before widespread use in simulation and estimation. Providing the data for model verification has been one of the objectives of the AgRISTARS field research project.

An efficient method to validate the models is to compare model estimates and canopy measurements of canopy reflectance as a function of sun angle and view angle for a variety of canopy types at different development stages. And, with the development of satellite sensor systems with off-nadir viewing, there is current major interest in the directional reflectance properties of vegetation. With this background, researchers at Purdue University have developed an approach to efficiently acquire canopy reflectance data as a function of view angle and sun angle.

The approach consists of making measurements from a tower placed in the center of a uniform field. Both a truck-mounted tower and a stationary tower built of construction scaffolding (Fig. 2) have been used. The latter method utilizes a 3-m boom mounted on a center pivot. The boom can be rotated on both its horizontal and vertical axes. Rotating the boom about the pivot provides selection of azimuth positions of 0°, 45°, 90°, 135°, 180°, 225°, 270°, and 315°. At each azimuth, measurements are made at view zenith angles of 70°, 60°, 45°, 30°, 22°, 15°, 7°, and 0° followed by measurements in the opposite direction of 7°, 15°, . . . , 70°. Two full hemispheres of measurements can be obtained in 12 min. Calibration

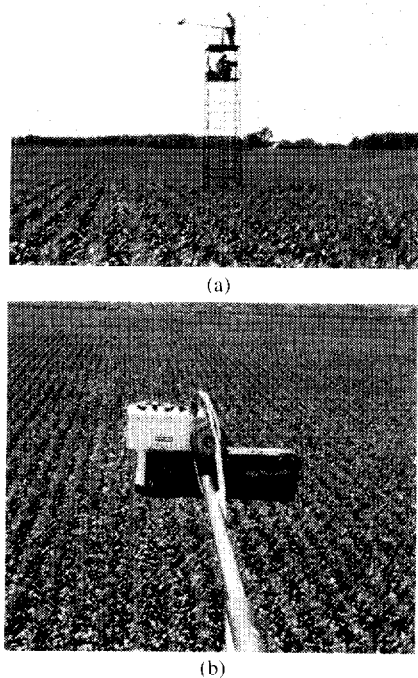


Fig. 2. (a) Tower and (b) radiometer system for making reflectance measurements as a function of view and sun angle. The radiometer and camera mounted on the boom are pointed at zenith view angle of 0° . The boom is on a pivot to enable measurements at different view azimuths and zenith angles.

measurements are made before and after each circuit. To measure the effects of changing sun angle measurements are made at 30- to 60-min intervals throughout the day.

To date measurements have been made on three canopies, soybean, corn, and winter wheat, at major development stages during 1980, 1982, and 1983, respectively. The canopy reflectance measurements have been accompanied by detailed measurements describing the biophysical characteristics of the canopies. These data include leaf area index, total biomass, development stage, percent canopy cover, canopy profile shape, leaf angle distribution, and leaf spectral reflectance and transmittance. Copies of data sets for selected dates have been provided to several investigators for the purpose of evaluating canopy models [10]. The data have been used by Goel *et al.* [11] and Badhwar and Shen [12] to test the inversion of canopy models to predict leaf area index, while Ranson *et al.* [13] have used it to investigate the angular reflectance properties of corn and soybean canopies.

3) *Commercial Field Test Sites*: Measurements were made during AgRISTARS at three commercial field sites (5×6 mile segments) as summarized in Table I using spectrometer or multiband radiometer and multispectral scanner sensors. Each sensor system has unique capabilities for acquiring spectral data. The spectrometer systems produce the highest quality reflectance measurements, but provides only limited measurements of spatial variability. On the other hand, a multispectral scanner in an aircraft provides spatial sampling of the scene and can

obtain data at multiple altitudes, but its spectral coverage is limited to a fixed set of spectral bands. Both systems have the advantage of flexible scheduling and, therefore, provide greater opportunity to obtain cloud-free data at critical crop stages than Landsat provides. However, the processing of data from both systems is relatively expensive, a disadvantage which the multiband radiometer system does not have.

The data collection missions were scheduled at two- to three-week intervals, when possible, coinciding with Landsat overpass dates. Spectral measurements were supplemented by aerial photography and field observations and measurements, including development stage, plant height, presence of stress, plant counts, row width, and grain yield.

B. Data Library

Development of a crops and soils data base for scene radiation research was initiated in 1972 at Purdue University; it has continued to grow and develop as a part of the LACIE and AgRISTARS field research projects [14]. Its purpose is to provide fully annotated and calibrated sets of spectral and agronomic data agricultural remote sensing research.

The data base presently includes more than 300 dates and 180 000 observations of spectroradiometer data, 250 dates and 70 000 observations of multiband radiometer data, and 70 dates and 400 flightlines of multispectral scanner data. These data are supplemented by an extensive set of agronomic and meteorological data acquired during each mission. In addition, the library includes laboratory measurements of over 250 soils from 39 states. With the exception of photography, the data are available on computer tapes.

The data form one of the most complete and best documented data sets acquired for remote-sensing research. It is unique in the comprehensiveness of sensors and missions throughout several growing seasons, and in the calibration of all multispectral data to a common standard. Copies of selected parts of the data have been provided to more than 50 different investigators at universities and government agencies over the past 5 years for research on spectral-agronomic relationships, definition of future sensor parameters, and development of advanced analysis techniques.

V. EXPERIMENT RESULTS

There has been a growing number of published field research results since the beginning of AgRISTARS Supporting Research Project, and although the Project has formally ended, we expect results based on the extensive and comprehensive data sets acquired during the project will continue to be generated. Since it would not be possible to describe in one paper all of the research results based on the data, we have chosen to summarize the results of several key experiments. Complete descriptions of these and other results may be found in the cited references and in agronomic and remote sensing journals.

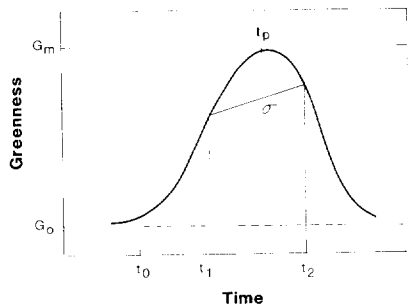


Fig. 3. Temporal profile model of greenness. Key parameters include: spectral emergence date, t_0 ; time of peak greenness, t_p ; maximum greenness, G_m ; and width of the profile, σ .

TABLE III
RELATIONSHIP OF CORN, SOYBEAN, AND SPRING WHEAT DEVELOPMENT STAGES TO CARDINAL POINTS OF TEMPORAL PROFILE

| Cardinal Point | Development Stage | | |
|----------------|-------------------|--------------------|--------------|
| | Corn | Soybean | Spring Wheat |
| t_1 | 12–14 leaves | beginning bloom | jointing |
| t_p | blister | beginning seed | heading |
| t_2 | full dent | beginning maturity | dough |

from Badhwar [15, 16].

A. Spectral-Temporal Profile Modeling

A major breakthrough in capability for crop identification has been development of multitemporal profile models (Fig. 3). Much of the research from initial development to refinement and verification of the models has been with field research data. The present form of the model developed by Badhwar [15] is:

$$G(t) = G_0 + (G_m - G_0)(2\beta e/\alpha)^{\alpha/2} \cdot (t - t_0)^{\alpha} \exp[-\beta(t - t_0)^2]$$

where G_0 is the soil greenness, α and β are crop-specific constants, t_0 is the date of spectral emergence, and G_m is the maximum greenness at time t_p . The model has two inflection points, t_1 and t_2 , which are related to rates of change in greenness. The features G_m , t_p , and σ account for more than 95 percent of the information in the original data, while substantially reducing the dimensionality of the spectral-temporal data. And equally important, the model parameters are related to agrophysical parameters. Application of the model to Landsat MSS [15], [16] and TM [17] data has resulted in accurate crop identification and area estimation. In addition to crop identification the same model form has been used to estimate crop development stages (Table III) [18].

B. Spectral Estimation of Radiation Absorbed by Crop Canopies

Most models of crop growth and yield require an estimate of canopy leaf area index or absorption of solar radiation. Direct measurements of LAI or light absorption can be tedious and time consuming, and are possible only

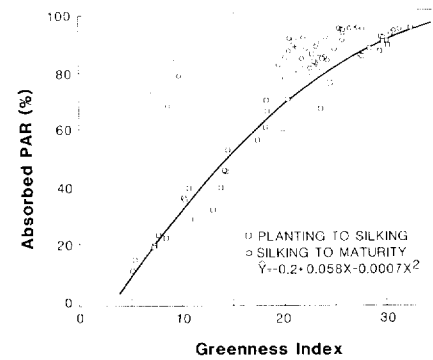


Fig. 4. Relation between absorbed photosynthetically active radiation (APAR) and greenness index for growth (planting to silking) and senescing (silking to maturity) periods of corn development.

for research plots. However, if these parameters could be estimated from remotely sensed spectral data it would enable crop growth and yield models to be implemented over large geographic areas [19]. The objective of experiments on corn [20] and soybeans at Purdue University and winter wheat at Kansas State University [21] has been to model the relationship between photosynthetically active radiation (PAR) absorbed by crop canopies and the spectral reflectance of the canopies.

Absorption of PAR was measured near solar noon in corn canopies planted in a field experiment conducted at the Purdue University Agronomy Farm, at densities of 50 000 and 100 000 plants/ha. Reflectance factor data were acquired with a Landsat MSS band radiometer. From planting to silking, the three spectrally predicted vegetation indices (IR/red ratio, normalized difference, and greenness) examined were associated with more than 95 percent of the variability in absorbed PAR (Fig. 4). The relationships developed between absorbed PAR and the three indices were evaluated with reflectance factor data acquired from corn canopies planted in 1979 through 1982 that excluded those canopies from which the equations were developed. Treatments included in these data were two hybrids, four planting densities (25 000, 50 000, 75 000, and 100 000 plants/ha), three soil types (Typic Argiaquol, Udollic Ochraqulf, and Aeric Ochraqulf), and several planting dates.

Seasonal cumulations of measured LAI and each of the three spectral indices were associated with more than 50 percent of the variation in final grain yields from the test years. Seasonal cumulations of daily absorbed PAR were associated with up to 73 percent of the variation in final grain yields. Absorbed PAR, cumulated through the growing season, was a better indicator of yield than cumulated LAI.

These results, as well as those from the wheat experiments by Kansas State University [21], [22], suggest that APAR may be estimated from canopy spectral reflectance for large areas where direct measurements of LAI would be prohibitive. Thus, estimates of absorbed PAR may be used directly in simple plant productivity models to estimate above ground phytomass production [23] or in more

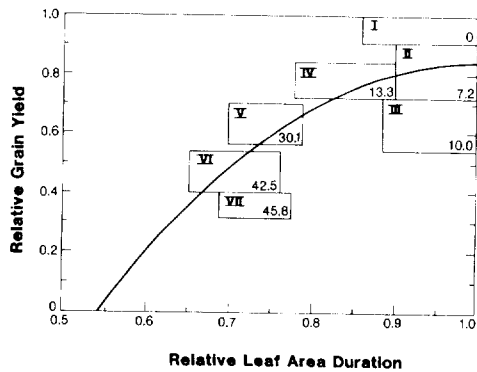


Fig. 5. Influence of canopy temperature on the relationship between relative grain yield and relative leaf area duration for Pioneer 3901 and B73xM017 corn hybrids at Sandhills Agricultural Laboratory in 1982. Temperature regions are accumulated differences (increases) in canopy radiant temperatures between region x and region I (full irrigation/no stress) on seven dates during the growing season.

elaborate crop growth and development simulation models to estimate final crop yields [24].

C. Evaluation of Crop Moisture Stress Effects

The overall objective of field research conducted by the University of Nebraska at the Sandhills Agricultural Laboratory has been to measure and model the effects of moisture stress on the growth, yield, and spectral characteristics of corn and soybeans. In one experiment two hybrids, Pioneer 3901 and B73xM073, were planted at 76 000 plants/ha in 76-cm-wide rows. A gradient irrigation system was used to provide 100, 66, 33, and 0 percent of the maximum water requirements of the crop. A Barnes 12-1000 multiband radiometer was used to make reflectance measurements of the canopies; emitted thermal radiation was measured with this instrument and with an infrared thermometer.

Relative leaf area duration was estimated with an equation incorporating reflectances in TM bands 3, 4, and 5, and explained approximately 50 percent of the variation in grain yields. Periodic canopy temperature measurements accumulated over time accounted for additional variation of grain yields (Fig. 5), with stress causing an elevation in canopy temperatures and reduction in yield [25].

D. Effects of Cultural and Environmental Factors on Crop Reflectance

Understanding the relationship between spectral reflectance and cultural and environmental factors is one of the keys to development and use of remote sensing as a tool for crop monitoring. Multiyear field experiments were conducted by Purdue University to study the effects of cultural practices and soil type on the reflectance characteristics of corn, soybean, and wheat canopies [26]. Treatments included: cultivar, row width, and planting date for soybeans; hybrid, plant population, and planting date for corn; and cultivar, N fertilization, and planting date for wheat. Soil type or soil moisture was an additional factor included in the experiments for both crops. Agronomic

measurements included development stage, LAI, percent soil cover, and biomass. Reflectance factor measurements of the canopies were made with multiband radiometers with wavebands corresponding to the Landsat MSS and TM bands at weekly intervals throughout the growing season.

The results of these experiments [26] indicate that the various cultural practices produced differences in LAI and percent soil cover, which in turn are manifested in the spectral reflectance characteristics of the canopies. Soil color and moisture influenced visible and infrared reflectance early in the growing season. The near infrared/red reflectance ratio and the greenness transformation were useful for predicting LAI and were less sensitive to variations in soil color and moisture than reflectances in single bands. Variations in spectral response were strongly associated with planting date during early to mid-season, with row width and plant population during mid-season to near maturity, and with cultivar and hybrid at maturity (Table IV). Crist [27] has examined the effects of the cultural practices on temporal profiles of greenness and reflectance.

E. Sun Angle-View Angle Effects

The bidirectional reflectance characteristics of vegetation canopies vary with changing sun angle through the day and over the growing season. The measured reflectance is also a function of the view angle and direction. In an investigation at Purdue University, using the measurements approach described above, the effects of sun and view angles on bidirectional reflectance factors of corn canopies ranging in development from the six leaf stage to harvest maturity were examined [28]. For nadir-view angles, there was a strong effect of solar zenith angle on reflectance factor in all spectral bands for canopies with low LAI. A decrease in contrast between bare soil and vegetation due to shadows as solar zenith angle increased appeared to be the major contributor to this change in reflectance factor. Effects of sun angle on reflectance were small for well-developed canopies with high LAI. A moderate increase in reflectance factor was observed at the larger solar zenith angles and was attributed to the presence of specular reflectance.

A strong dependence of reflectance factor on view angle was noted for all of the canopies considered (Fig. 6). For canopies with low LAI, reflectance decreased as view zenith angle increased for visible and middle-infrared wavelength bands which are absorbed by vegetation and increased with view angle for near-infrared wavelengths which are multiply scattered. For higher LAI canopies, reflectance increased as view zenith angle increased. An increase in reflectance at large view zenith angles for some view azimuths indicated a specular component in the reflectance data.

Trends of reflectance with changing sun angle at different view azimuth angles illustrate that the position of the sensor relative to the sun is an important factor for deter-

TABLE IV
PERCENT OF VARIATION IN RED (0.6–0.7 μm) AND NEAR INFRARED (0.8–1.1 μm) REFLECTANCE AND THE GREENNESS TRANSFORMATION OF CORN, SOYBEAN, AND SPRING WHEAT CANOPIES ASSOCIATED WITH SOIL TYPE AND CULTURAL PRACTICES ON SEVERAL DATES (DEVELOPMENT STAGES)

| Agronomic Factor | Spectral Variable | | | | | | | | | | | |
|------------------|-------------------|------|------|------|----------------------|------|------|------|--------------------------|------|------|------|
| | Red Reflectance | | | | Infrared Reflectance | | | | Greenness Transformation | | | |
| | Corn | | | | | | | | | | | |
| | 6/11 | 7/15 | 8/22 | 9/26 | 6/11 | 7/15 | 8/22 | 9/26 | 6/11 | 7/15 | 8/22 | 9/26 |
| Soil type | 56 | 25 | 3 | 2 | 51 | 21 | 5 | – | 16 | – | 2 | – |
| Plant population | – | 8 | 22 | – | 1 | 33 | 36 | 4 | 1 | 31 | 47 | 2 |
| Planting date | 12 | 38 | 7 | 53 | 24 | 8 | 14 | 76 | 39 | 61 | 9 | 82 |
| | Soybean | | | | | | | | | | | |
| | 6/18 | 7/17 | 8/22 | 9/26 | 6/18 | 7/17 | 8/22 | 9/26 | 6/18 | 7/17 | 8/22 | 9/26 |
| Soil type | 13 | 15 | – | – | 15 | 11 | – | – | 2 | – | – | – |
| Planting date | 13 | 63 | 52 | 87 | 44 | 69 | 10 | 85 | 82 | 90 | 12 | 87 |
| Row width | 8 | – | 9 | – | 2 | 5 | 29 | 1 | – | 4 | 29 | – |
| Cultivar | 1 | – | 6 | – | 2 | – | 16 | 10 | – | – | 16 | 8 |
| | Spring Wheat | | | | | | | | | | | |
| | 6/1 | 6/23 | 7/7 | 7/20 | 6/1 | 6/23 | 7/7 | 7/20 | 6/1 | 6/23 | 7/7 | 7/20 |
| Soil Moisture | 2 | 16 | 73 | 52 | 9 | 28 | 69 | 36 | 8 | 41 | 87 | 63 |
| Cultivar | – | 1 | – | 2 | – | 10 | 4 | 4 | – | 9 | 2 | 3 |
| N fertilizer | – | 9 | 3 | 1 | – | 1 | 3 | 4 | – | 6 | 3 | 3 |
| Planting date | 36 | 5 | 7 | 27 | 85 | 35 | 4 | 6 | 42 | 12 | – | 21 |

*Models include variation due to treatments. Total variation is due to blocks, treatments, and experimental error. Interaction terms as well as percentages less than 1.0, are omitted for clarity, but were included in model.

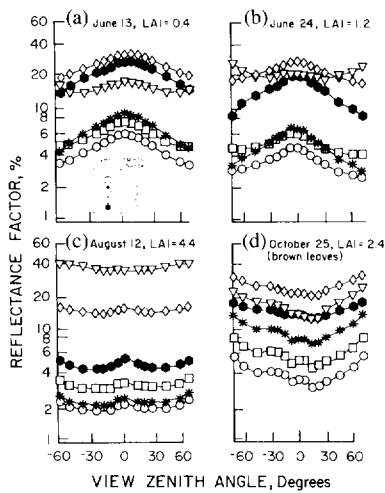


Fig. 6. Effect of view zenith angle on reflectance factors of corn canopies: (a) and (b) sparse, (c) fully-developed, and (d) senescent. Data were acquired near solar noon. Negative and positive view zenith angles indicate that the radiometer was looking east ($\phi_s = 90^\circ$) and west ($\phi_s = 270^\circ$), respectively. TM spectral band numbers are indicated in the legend.

mining the angular reflectance characteristics of corn canopies. Reflectances were greatest for coincident sun and view angles and minimized when the sensor view direction was towards the sun. View direction relative to row orientation also contributes to the variation in reflectance.

F. Inversion of Canopy Reflectance Models

Using data from the sun angle-view angle/canopy modeling experiments at Purdue University [13], Goel and co-

workers have developed the methodology [11] for inverting canopy reflectance models. In their original form, with inputs of leaf reflectance and transmittances, soil reflectance, illumination and view angles, and canopy LAI and leaf area distribution, the models predict canopy reflectance. Goel has shown that the models developed by Suits [29], Verhoef and Bunnik [30], and Norman and Wells [31] can be inverted, i.e., measurements of canopy reflectance can be used to predict agrophysical canopy variables. Spectral prediction of LAI would be a particularly valuable capability. Goel showed that canopy reflectance measurements for a set of several view and sun angles, together with measured (or assumed) leaf and soil reflectances and transmittances are required to achieve accurate LAI estimates. Using a somewhat different approach, Badhwar and Shen [12] have inverted the SAIL model [30] to predict LAI using only nadir view angles.

VI. CONCLUSIONS

The AgRISTARS field research on agricultural crops demonstrated the key role of field spectroscopy in bridging the gap between satellite and leaf spectral data. One result of the field measurements and analyses was a more complete and quantitative description of the complex relationships among plant, soil, and atmospheric variables, and the effects of varying illumination and sensor geometries. Leaf area index was identified as a key biophysical parameter linking crop physiology and multispectral remote sensing. Multitemporal field measurements of can-

opy reflectance were an integral part of the development of spectral-temporal modeling for crop species identification and development stage estimation. Subsequent research led to development of techniques and models to use spectral estimates of leaf area index and light interception by crop canopies as inputs to crop growth and yield models. In addition, the field measurements of canopy reflectance as a function of varying canopy, illumination, and viewing geometry has provided important data for the verification and further development of canopy radiation models.

In conclusion, field spectroscopy is an essential component of the development of remote sensing for monitoring agricultural and natural resources. A sound field research program can provide the basis on which larger scale satellite experiments and operational systems are constructed. Although the research summarized in this paper has contributed substantially to our knowledge and understanding of how biophysical properties are manifested in the spectral characteristics of crop canopies, and how these relationships can be utilized for crop identification and condition assessment, there are still many unanswered questions and problems. The complex and diverse nature of agricultural and natural resources suggests the need for continuing effort to measure and model the spectral-biophysical of vegetation canopies.

ACKNOWLEDGMENT

We are especially grateful to R. B. MacDonald, NASA Johnson Space Center, for the stimulation, challenge, and support he gave to this research, and to B. Robinson, Purdue University, for his unyielding devotion to the development and use of sound measurement procedures and instrumentation. A few of the many other individuals who have contributed to the experiments and results described in this paper include K. Gallo and J. Ranson, Purdue University; G. Asrar, Kansas State University; G. Badhwar, K. Henderson, and D. Pitts, NASA Johnson Space Center; and B. Blad and B. Gardner, University of Nebraska.

REFERENCES

- [1] M. E. Bauer, M. C. McEwen, W. A. Malila, and J. C. Harlan, "Design, implementation, and results of LACIE field research," in *Proc. Large Area Crop Inventory Equipment*, vol. III (NASA Johnson Space Center, Houston, TX), pp. 1037-1066, 1978.
- [2] R. D. Jackson, "Remote sensing of vegetation characteristics for farm management," *Proc. Soc. Photo-optical Instr. Engr.*, vol. 475, pp. 81-96, 1984.
- [3] F. G. Hall, "Remote sensing vegetation at regional scales," *Proc. Soc. Photo-optical Instr. Engr.*, vol. 475, pp. 75-80, 1984.
- [4] J. A. Smith, "Role of scene radiation models in remote sensing," in *Proc. 8th Int. Symp. Machine Processing of Remotely Sensed Data* (Purdue Univ., W. Lafayette, IN), pp. 546-549, 1982.
- [5] R. B. MacDonald, "A summary of the history of the development of automated remote sensing for agricultural applications," *IEEE Trans. Geosci. Remote Sensing*, vol. GE-22, pp. 473-481, 1984.
- [6] B. F. Robinson, M. E. Bauer, D. P. DeWitt, L. F. Silva, and V. C. Vanderbilt, "Multiband radiometer for field research," *Proc. Soc. Photo-optical Instr. Engr.*, vol. 196, pp. 8-15, 1979.
- [7] B. F. Robinson and L. L. Biehl, "Calibration procedures for measurement of reflectance factor in remote sensing field research," *Proc. Soc. Photo-optical Instr. Engr.*, vol. 196, pp. 16-26, 1979.
- [8] C. S. T. Daughtry, V. C. Vanderbilt, and V. J. Pollara, "Variability of reflectance measurements with sensor altitude and canopy type," *Agron. J.*, vol. 74, pp. 744-751, 1982.
- [9] C. S. T. Daughtry and S. E. Hollinger, "Costs of measuring leaf area index of corn," *Agron. J.*, vol. 76, pp. 836-841, 1984.
- [10] G. D. Badhwar, W. Verhoef, and N. J. J. Bunnik, "Comparative study of Suits and SAIL canopy reflectance models," *Remote Sensing Environ.*, vol. 17, pp. 179-195, 1985.
- [11] N. S. Goel and R. L. Thompson, "Inversion of vegetation canopy reflectance models for estimating agronomic variables. V. Estimation of leaf area index and average leaf angle using measured canopy reflectances," *Remote Sensing Environ.*, vol. 16, pp. 69-85, 1984.
- [12] G. D. Badhwar and S. S. Shen, "Techniques for estimation of leaf index using spectral data," in *Proc. 10th Int. Symp. Machine Processing Remotely Sensed Data* (Purdue Univ., W. Lafayette, IN), pp. 333-338, 1984.
- [13] K. J. Ranson, L. L. Biehl, and M. E. Bauer, "Variation in spectral response of soybeans with respect to illumination, view, and canopy geometry," *Int. J. Remote Sensing*, 1985.
- [14] L. L. Biehl, M. E. Bauer, B. F. Robinson, C. S. T. Daughtry, L. F. Silva, and D. E. Pitts, "A crops and soils data base for scene radiation research," in *Proc. 8th Int. Symp. Machine Processing of Remotely Sensed Data* (Purdue Univ., W. Lafayette, IN), pp. 169-177, 1982.
- [15] G. D. Badhwar, "Automatic corn-soybean classification using Landsat MSS data. I. Near-harvest crop proportion estimation," *Remote Sensing Environ.*, vol. 14, pp. 15-29, 1984.
- [16] —, "Use of Landsat-derived profile features for spring small grains classification," *Int. J. Remote Sensing*, vol. 5, pp. 783-799, 1984.
- [17] —, "Classification of corn and soybeans using multi-temporal thematic mapper data," *Remote Sensing Environ.*, vol. 16, pp. 175-181, 1985.
- [18] G. D. Badhwar and K. E. Henderson, "Estimating development stages of corn from spectral data—An initial model," *Agron. J.*, vol. 73, pp. 748-755, 1981.
- [19] C. S. T. Daughtry, K. P. Gallo, and M. E. Bauer, "Spectral estimates of solar radiation intercepted by corn canopies," *Agron. J.*, vol. 75, pp. 527-531, 1983.
- [20] K. P. Gallo, C. S. T. Daughtry, and M. E. Bauer, "Spectral estimation of absorbed photosynthetically active radiation in corn canopies," *Remote Sensing Environ.*, vol. 17, pp. 221-232, 1985.
- [21] G. Asrar, M. Fuchs, E. T. Kanemasu, and J. L. Hatfield, "Estimating absorbed photosynthetic radiation and leaf area index from spectral reflectance in wheat," *Agron. J.*, vol. 76, pp. 300-306, 1984.
- [22] J. L. Hatfield, G. Asrar, and E. T. Kanemasu, "Intercepted photosynthetically active radiation estimated by spectral reflectance," *Remote Sensing Environ.*, vol. 14, pp. 65-75, 1984.
- [23] G. Asrar, E. T. Kanemasu, and M. Yoshida, "Estimates of leaf area index from spectral reflectance of wheat under different cultural practices and solar angle," *Remote Sensing Environ.*, vol. 17, pp. 1-11, 1985.
- [24] G. Asrar, E. T. Kanemasu, R. D. Jackson, and P. J. Pinter, "Estimation of total above-ground phytomass production using remotely sensed data," *Remote Sensing Environ.*, 1985.
- [25] B. R. Gardner and B. L. Blad, "Techniques for remotely monitoring canopy development and estimating grain yield of moisture stressed corn," Center Agric. Meteor. and Climatology, Univ. of Nebraska, Lincoln, NE, Tech. Rep. 83-9, pp. 111-116, 1983.
- [26] M. E. Bauer, C. S. T. Daughtry, and V. C. Vanderbilt, "Spectral-agronomic relationships of maize, soybean, and wheat canopies," in *Proc. Int. Colloquium Spectral Signatures of Objects Remote Sensing* (Avignon, France), pp. 261-272, 1981.
- [27] E. P. Crist, "Effects of cultural and environmental factors on corn and soybean spectral development patterns," *Remote Sensing Environ.*, vol. 14, pp. 3-13, 1984.
- [28] K. J. Ranson, C. S. T. Daughtry, L. L. Biehl, and M. E. Bauer, "Sun-view angle effects on reflectance factors of corn canopies," *Remote Sensing Environ.*, vol. 18, pp. 147-161, 1985.
- [29] G. H. Suits, "The calculation of the directional reflectance of a vegetative canopy," *Remote Sensing Environ.*, vol. 2, pp. 117-125, 1972.
- [30] W. Verhoef, "Light scattering by leaf layers with application to canopy reflectance modeling: The SAIL model," *Remote Sensing Environ.*, vol. 16, pp. 125-142, 1984.
- [31] J. M. Norman and J. M. Welles, "Radiative transfer in an array of canopies," *Agron. J.*, vol. 75, pp. 481-488, 1983.

Marvin E. Bauer (M'86) received the B.S.A. and M.S. degrees from Purdue University and the Ph.D. degree in agronomy from the University of Illinois.

From 1970 to 1983, he was a Research Agronomist at the Laboratory for Applications of Remote Sensing, Purdue University, where he had key roles in the design, implementation, and analysis of data from several major agricultural remote-sensing experiments. He is currently Director of the Remote Sensing Laboratory and a Professor of Remote Sensing at the University of Minnesota.

Dr. Bauer serves as Editor-in-Chief of *Remote Sensing Environment*. He is a member of the American Society of Agronomy, the IEEE Geoscience and Remote Sensing Society, and the American Society of Photogrammetry and Remote Sensing.

*

Craig S. T. Daughtry received the B.S.A. and M.S. degrees from the University of Georgia and the Ph.D. degree in agronomy from Purdue University.

He has been a Research Agronomist at Purdue University's Laboratory for Applications of Remote Sensing since 1976. He has a research background in crop physiology which includes both field and laboratory experiments to evaluate the effects of the environment on yield, photosynthesis, water relations, and chemical composition of several crops. Since joining the LARS staff, he has actively participated in the development of computer-simulation models of corn and soybean growth and yield. His recent research has concentrated on measurements and modeling of the spectral-agronomic relationships of crop canopies and incorporating spectrally derived estimates of canopy leaf area index and light interception into crop growth and yield models.

*

Larry L. Biehl (S'71-M'80) received the B.S. and M.S. degrees in electrical engineering from Purdue University.

He is currently a Research Engineer in the Measurements Program area at the Laboratory for Applications of Remote Sensing, Purdue University. He has participated in Skylab and Landsat MSS and Thematic Mapper Re-

search, and has had major responsibilities in NASA-sponsored field research. These roles have included development and testing of field spectral data acquisition and calibration procedures, data preprocessing, and developing software for effective analysis of spectral data.

*

Edward T. Kanemasu received degrees from Montana State University and the University of Wisconsin.

He joined Kansas State University in 1969 where he is currently a Professor of Agronomy and leader of the Evapotranspiration Laboratory. His primary research interests have been in plant-water relations, evapotranspiration, crop-yield modeling, and remote sensing. He has been an invited lecturer at numerous conferences and symposiums in the U.S. and abroad, and has served on national committees for the USDA, NASA, and several other agencies.

Dr. Kanemasu is a fellow of the American Society of Agronomy and has served as an Associate Editor and Technical Editor, *Agroclimatology and Crop Modeling*, of the *Agronomy Journal*.

*

Forrest G. Hall received the B.S. degree in mechanical engineering in 1963 from the University of Texas, and the M.S. and Ph.D. degrees in physics in 1968 and 1970, respectively, from the University of Houston.

A Mathematical Physicist, he has published models of the lunar atmosphere, microwave sea surface emission properties, and has conducted and published theoretical investigations in stochastic theory. In 1973, he joined the Earth Observations Division at the NASA Johnson Space Center, Houston, TX. He has served as Project Scientist for the Large Area Crop Inventory Experiment (1974-1978) for which he received NASA's medal for Exceptional Scientific Achievement, and as Chief Scientist for the Earth Observations Division (1979-1980). Since 1980, he has served as Manager of the AgRISTARS Supporting Research Project and as Chief of the Earth Sciences Research Branch. In mid-1985, he joined the Laboratory for Terrestrial Physics at the NASA Goddard Space Flight Center, Greenbelt, MD.

Light Interception and Leaf Area Estimates from Measurements of Grass Canopy Reflectance

GHASSEM ASRAR, EDWARD T. KANEMASU, GEORGE P. MILLER, AND R. L. WEISER

Abstract—Grassland is a major component of the Earth's available land. The vast area and remoteness of this ecosystem makes it difficult to assess its condition and monitor productivity by traditional methods. Remote sensing potentially offers a rapid nondestructive approach for monitoring such ecosystems. A study was carried out in a tallgrass prairie site near Manhattan, Kansas, during the 1983 and 1984 seasons to investigate the feasibility of estimating light interception and green leaf area index (LAI) from measurements of canopy multispectral reflectance. Greenness (G_n) index was found to be strongly correlated with intercepted photosynthetically active radiation (PAR). Two methods, a direct regression (RGR) and an indirect approach (IND), were used to estimate LAI from G_n index. The LAI values estimated by RGR method were consistently lower than the measured ones; however, good agreement was obtained between the LAI values estimated by IND method and the measured LAI. This suggests that G_n transformation of canopy spectral reflectance is more closely related to the fraction of intercepted PAR by green foliage than the quantity of green LAI.

I. INTRODUCTION

THE EARTH'S surface includes a wide range of ecosystems and human land-use patterns with varying vegetation covers (cropland, desert, forest, and rangeland). The differences in type and amount of vegetation of these ecosystems are caused primarily by climate and soil. Grassland covers about 17 percent of the Earth's land surface [1] and 28 percent of the land in the United States [2]. The large extent and remoteness of these lands make it difficult to assess their condition and monitor productivity by the traditional methods. Tucker [3] evaluated several techniques for the nondestructive estimation of grassland biomass as an alternative to conventional point-sampled hand clipping. He concluded the choice of which biomass estimation method to use depends on the specific research application. Remotely sensed spectral measurements of reflected and emitted radiation, however, can provide a rapid and nondestructive method for monitoring the changes in grassland ecosystems. This has been demonstrated by Tucker *et al.* [4] who found a strong correlation between integrated normalized difference index based on NOAA-7 satellite imagery and end-of-season above-ground biomass.

Solar radiation provides the energy for photosynthetic activities and hence plant growth. Intraleaf scattering of

solar radiation is important in photosynthesis, since it increases the mean path length of absorbed energy thus facilitating electron capture by plant pigments (chlorophyll and carotenoids). The interception of photosynthetically active radiation (0.4–0.7 μm) is correlated strongly with phytomass production [5]. Since light is primarily intercepted by plant leaves, the duration and magnitude of green LAI is also correlated strongly with phytomass production [6].

Senescence affects the plant pigments by a selective breakdown of chlorophyll and carotenoids [7]. If the leaf and canopy scattering characteristics remain intact as the absorbing pigments are reduced, one would expect a direct relationship between plant senescence and canopy reflectance at wavelengths of strong pigment absorption [8]. This would be opposite to the relationship existing between reflectance and green foliage area during the growth period.

Previous studies [9], [10] have shown the existence of relationships between PAR and canopy spectral reflectance for monocultural crops. Asrar *et al.* [11] developed a procedure for estimating both the PAR absorption and green LAI from measurements of red and near-infrared reflectance in homogeneous plant canopies. This procedure was then evaluated under different management practices and solar illumination angles for different geographical locations [12]. The objective of the current study was to develop a procedure for estimating PAR and LAI from measurements of grass canopy spectral reflectance.

II. SITE DESCRIPTION

The study was conducted during 1983 and 1984 at the Konza Prairie Research Natural Area (KPRNA) located near Manhattan, Kansas (39°9' N, 96°40' W). The predominant soil at this site is a silty clay loam (Udic ustoll), typical of the Flint Hills uplands of Kansas. KPRNA is 3487 ha of unplowed bluestem prairie with big bluestem (*Andropogon gerardii* Vitman), little bluestem (*Andropogon scoparius* Michx.), and Indian grass (*Sorghastrum nutans* (L.) Nash) as the dominant species. Thirty-six other species have been observed in a detailed vegetation composition study [13]. The large number of species and the diversity in their spatial distribution results in a more complex canopy than monoculture crops.

Climate of the prairie uplands is humid subtropical, with temperature ranging from -35° to 47°C annually. Mean

Manuscript received June 16, 1985; revised August 29, 1985. This work was supported by NASA under Contract NAS-167457.

The authors are with the Evapotranspiration Laboratory, Department of Agronomy, Agriculture Experiment Station, Kansas State University, Manhattan, KS 66506.

IEEE Log Number 8406222.

precipitation is 750 mm/year, with variable seasonal distribution resulting in many wet-dry cycles in a normal growing season of 180 days.

III. DATA ACQUISITION

Spectral measurements were conducted on separate sites in 1983 and 1984. Each site was composed of two adjacent transects of the prairie, which were separated by an access road (fire guard). The transects were initially covered with senescent vegetation from previous year(s). Prior to the resumption of growth in early spring, the senescent vegetation was removed from one of the transects by controlled burning. This resulted in two types of surfaces, a bare soil surface that was exposed (burned treatment), and a surface that was covered with senescent vegetation (unburned treatment).

Spectral measurements were continued throughout the entire season on days with clear sky conditions using a truck-mounted assembly equipped with Exotech model 100-A and Barnes Modular Multispectral (MMR) model 12-1000 radiometers. The Exotech radiometer has two wavelength bands in the visible (0.5-0.6 μm and 0.6-0.7 μm) and two in the near infrared (0.7-0.8 μm and 0.8-1.1 μm) regions of the spectrum each with a 15° field of view (FOV). These wavelength bands correspond to the multispectral scanner (MSS) on board Landsat satellites. The Barnes MMR has three wavelength bands in the visible region (0.45-0.52 μm , 0.52-0.60 μm , and 0.63-0.69 μm), two in the near infrared (0.76-0.9 μm and 1.15-1.30 μm), two in the middle infrared (1.55-1.75 μm and 2.08-2.35 μm), and one in the thermal infrared (10.4-12.5 μm) regions each with a 15° FOV. The thermal infrared wavelength band will not be considered in this report. The Barnes MMR wavelength bands 1-4 and 6-7 correspond to wavelength bands 1-5 and 7 of Thematic Mapper (TM) sensor on board Landsats 4 and 5. Both radiometers were mounted in the nadir viewing position 8 m above the soil surface.

Canopy reflectance measurements were replicated 20 times on each transect mostly during midday and referenced to a painted BaSO₄ calibration panel approximately every 15 min. Spectral reflectance and transmittance of individual green and senescent leaves of grass and nongrass vegetation were measured in 0.4-1.1 μm at 0.01- μm intervals with a LiCor model LI-1800 spectroradiometer in 1984.

The components of PAR were measured by two quantum sensors (LiCor model LI-190S) and a quantum line sensor (LiCor model LI-1915) during the 1984 season in both burned and unburned treatments. The measurements started during mid-morning on each date by pointing all three sensors upward, leveling them, and sampling the incoming PAR 10 times. These data were used for intercalibration of the sensors to avoid the error due to variability among the sensors. The two quantum sensors were mounted on a tripod assembly and positioned above the canopy. One sensor was facing upward to record the total (direct + diffuse) incoming PAR, and one sensor was fac-

ing downward to record the reflected PAR from the canopy. The line quantum sensor was placed underneath the canopy, below the last layer of green leaves, to measure PAR transmitted through the canopy. All three sensors were wired into a data logger (Polycorder model 516A) for simultaneous data acquisition. The PAR-sensor assembly was placed at three different locations in each treatment transect. Five sets of measurements were made at each location by transferring the line quantum sensor to different spots in the vicinity of the tripod-assembly. This sequence of measurements were repeated until mid-afternoon for both treatments.

In 1983, four plant samples each 0.1 m², were obtained from three sampling locations that were established each day of reflectance measurements on each treatment transect (total of 12 samples per treatment per date). These sites were then marked to avoid measurements on the same sites later in the season. In 1984, one 0.1 m² plant sample was obtained from nine sampling locations on each of the two treatment transects (total of 9 samples per treatment per date). In the laboratory, the plant samples were separated into green grass leaves, green nongrass leaves, and senescent material. Total green leaf area of both grass and nongrass species was determined using a LiCor model LI-3100 optical area meter.

IV. DATA ANALYSIS

A simple analytical radiation transfer model was used to relate the visible and near infrared canopy reflectance to PAR interception (p) based on the measurements of leaf scattering properties [11]; p is defined by Monsi and Sacki [14] as

$$p = 1 - \exp(-K' \cdot \text{LAI}) \quad (1)$$

where K' is the leaf angle shape coefficient and LAI is the leaf area index. The functional relationship between canopy reflectance (ρ_c) and p was expressed as

$$\rho_c(\lambda) = \frac{(\rho_s(\lambda) \rho_v(\lambda) - 1) + (1 - \rho_s(\lambda)/\rho_v(\lambda)) (1 - p)^{-2K}}{(\rho_s(\lambda) - 1/\rho_v(\lambda) + (\rho_v(\lambda) - \rho_s(\lambda)) (1 - p)^{-2K}} \quad (2)$$

where ρ_s and ρ_v are soil and leaf reflectance at a given wavelength (λ), respectively, and K is a radiation extinction coefficient that depends on foliage scattering property and canopy geometry. K values can be computed from the equations given in [11]. Thus, a set of measured ρ_s and ρ_v values can be used to compute ρ_c from (2) for a range of p values from 0 to 1. A greenness (Gn) transformation given by

$$Gn_e = -0.3974 \rho_{c1} - 0.6849 \rho_{c2} + 0.2564 \rho_{c3} + 0.5543 \rho_{c4} \quad (3)$$

where $\rho_{c1}, \dots, \rho_{c4}$ correspond to wavelength bands of Exotech radiometer, respectively. The values of ρ_c obtained by direct measurements with an Exotech radiometer or simulated using (2) can be used to compute Gn_e .

The coefficients in (3) were derived from a data set obtained from measurements of the grass canopy in 1983 by an Exotech radiometer, and analyzed using a constrained principal component analysis (CPCA) described in [15]. A similar procedure was used to derive a Gn_b index from a data set in which a Barnes MMR radiometer was used

$$Gn_b = -0.044 \rho_{c1} - 0.024 \rho_{c2} - 0.1747 \rho_{c3} + 0.7916 \rho_{c4} + 0.3875 \rho_{c5} - 0.2310 \rho_{c6} - 0.3699 \rho_{c7} \quad (4)$$

where $\rho_{c1}, \dots, \rho_{c7}$ correspond to wavelength bands of Barnes MMR radiometer, respectively. Other spectral transformations such as the near infrared to red ratio (RO) and normalized difference (ND) indices can be computed from the simulated (2) or measured canopy reflectance values by

$$RO = \rho_{cn}/\rho_{cr} \quad (5)$$

and

$$ND = (\rho_{cn} - \rho_{cr})/(\rho_{cn} + \rho_{cr}) \quad (6)$$

where ρ_{cn} and ρ_{cr} are near infrared (0.8–1.1 μm or 0.76–0.90 μm) and red (0.6–0.7 μm or 0.63–0.69 μm) canopy reflectance, respectively.

Measured PAR data can be used to compute a mean daily p value as

$$p = \frac{[\text{PAR}_0 - (\text{PAR}_r + \text{PAR}_t)]}{\text{PAR}_0} \quad (7)$$

where PAR_0 , PAR_r , and PAR_t are the incoming, reflected, and transmitted components, respectively.

V. RESULTS AND DISCUSSION

A. Light Interception

The relationship between measured p values (7) and those computed from (1) depends upon the leaf angle shape coefficient (K') for a given value of LAI. Since direct measurements of leaf angle distribution were not available, we assumed several fixed leaf inclination classes (15°, 30°, 45°, 60°, and 75°) and spherical leaf angle distribution in computing p from (1). Table I presents the linear regression parameters between the measured and computed p values for assumed leaf angle distributions. The highest R^2 and lowest RMSE values were obtained for spherical distribution and 60° fixed leaf inclination angle. Therefore, either one of these leaf angle distributions can adequately characterize the grass canopy. We limit the rest of our discussion to spherical distribution.

The relationships between PAR interception p , RO, ND and Gn transformations for a uniform grass canopy with spherical leaf angle distribution and a solar zenith angle (η) of 30°, computed from (2), (3), (5), and (6) are presented in Fig. 1. The change in RO was not proportional to variation of p over the complete range of p values. RO changed 0.4 unit for one unit change in p for $p < 0.5$;

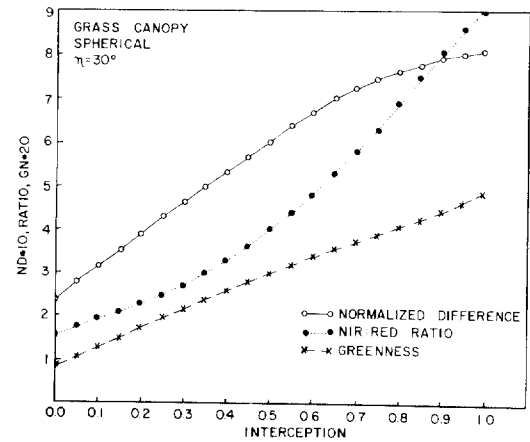


Fig. 1. Relationship between light interception and the spectral indices of RO, ND, and Gn simulated for a grass canopy with spherical leaf angle distribution.

TABLE I
REGRESSION PARAMETERS FOR THE LINEAR RELATIONSHIP BETWEEN MEASURED AND SIMULATED (1) INTERCEPTED PHOTOSYNTHETICALLY ACTIVE RADIATION (IPAR) FOR DIFFERENT LEAF ANGLE DISTRIBUTIONS

| Leaf Angle | B_1^\dagger | R^2 | RMSE |
|------------|---------------|-------|-------|
| Fixed | | | |
| 15° | 1.292 | 0.954 | 0.167 |
| 30° | 1.232 | 0.958 | 0.154 |
| 45° | 1.120 | 0.963 | 0.130 |
| 60° | 1.051 | 0.973 | 0.104 |
| 75° | 1.313 | 0.965 | 0.148 |
| Spherical | 0.998 | 0.974 | 0.097 |

† Simulated IPAR = $B_1 \cdot$ (Measured IPAR)

however, a 1:1 relationship is observed between p and RO for $p > 0.5$. This resulted in an overall nonlinear relationship between p and RO that was also dependent on η [11]. ND changed proportionally with a variation in p for a wide range of p values. The sensitivity of this relationship decreased for $p > 0.75$, but the relationship between p and ND was found to be least sensitive to changes in η [11].

Gn was linearly related to p for $p < 0.9$, but the magnitude of this change was about 0.5 unit of Gn per 1.0 unit of p over this range. The p versus Gn relationship also depended on canopy geometry and solar angle, Fig. 2. The strongest relationship between Gn and p was obtained when it was assumed that leaves form a horizontal green layer with no angular distribution. If a homogeneous and uniform canopy with spherical leaf angle distribution was assumed, then the p versus Gn relationship was also found to depend on η . An increase in η resulted in an increase in the slope of p versus Gn line, due to changes in red and near-infrared reflectance with η . The diurnal variation of the red reflectance was found to be more dependent on solar illumination and canopy geometry than the near-infrared reflectance [16], [17]. This is due to an increased diffusive component of the incoming radiation as a result of longer path length, and increased absorption of short wavelength radiation by vegetation at high solar zenith angles. In spite of the dependency of Gn on η and the canopy

TABLE II
REGRESSION PARAMETERS FOR THE LINEAR RELATIONSHIPS BETWEEN GREENNESS (G_n) AND LIGHT INTERCEPTION (p) BASED ON MEASURED AND SIMULATED CANOPY REFLECTANCE AT DIFFERENT SOLAR ZENITH ANGLES (The G_n values were computed using (3) and (4).)

| Method | Solar Zenith Angle (Deg.) | p | G_n | B_0^\dagger | B_1 | R^2 | RMSE |
|---------------------|---------------------------|-----------|-------------|---------------|-------|-------|-------|
| Exotech Measured | 28-62 | 0.18-0.85 | 0.057-0.240 | -0.121 | 3.468 | 0.732 | 0.114 |
| | Simulated | 30-60 | 0.00-1.00 | -0.125 | 3.853 | 0.915 | 0.088 |
| Barnes Measured | 28-62 | 0.18-0.85 | 0.032-0.357 | -0.275 | 2.748 | 0.817 | 0.095 |

$\dagger p = B_0 + B_1 \cdot G_n$

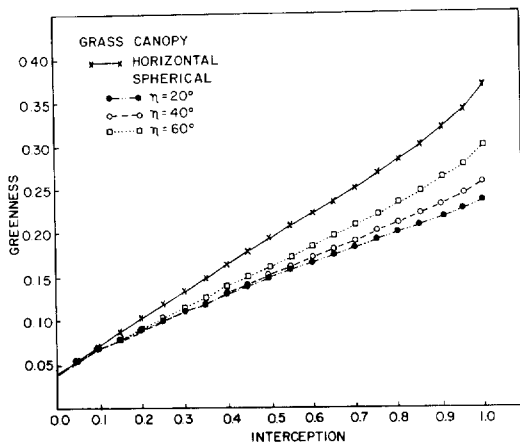


Fig. 2. Relationship between light interception and G_n index simulated for grass canopies with horizontal and spherical leaf angle distributions.

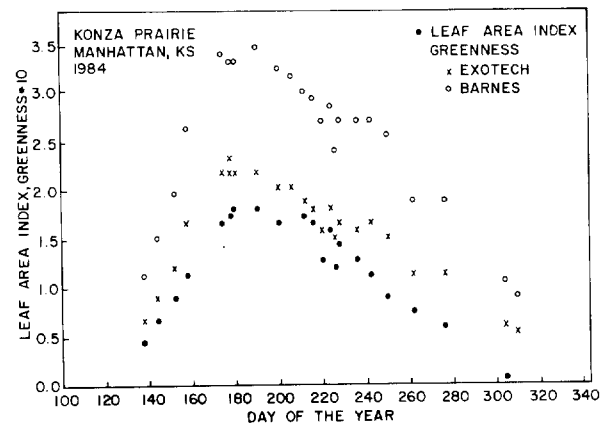


Fig. 3. Seasonal trends in leaf area index and G_n values obtained from spectral measurements on a tallgrass prairie in 1984.

geometry, G_n was selected as an index for estimating p from measurements of canopy reflectance because of their linear relationship to one another.

The measured p values were linearly regressed against the mean daily G_n values that were computed from (3) and (4) based on the canopy reflectance measurements. This subset of data then was eliminated from further analysis to reduce the dependency of the empirical relationships on the data set. The intercepts and slopes of linear regression equations that were established between measured and simulated p versus G_n values for a wide range of η were found to be in good agreement (Table II). Lower R^2 values for the measured data were due to the smaller number of observations and inherent variability in the field measurements, as indicated by larger root mean square error (RMSE) values. A simulated relationship between p and G_n for the Barnes MMR was not obtained due to unavailability of grass leaf spectral properties for the Barnes middle infrared wavelength bands. It was concluded that G_n transformation of spectral reflectance measurements can be used to estimate the fraction of intercepted PAR by grass canopies.

B. Leaf Area Index

Temporal profiles of G_n computed from (3) and (4) paralleled the growth of green leaves in grassland, Fig. 3. The

curves illustrate that G_n peaks at the same time that maximum green LAI occurs and then G_n declines due to decrease in canopy reflectance, as a result of changes in leaf color and structure. These data suggested that G_n indices are correlated with photosynthetically active green vegetation; therefore, G_n could be used to estimate green LAI. We used two different approaches to test this hypothesis.

In method 1 (RGR), empirical linear regression relationships were established between measured green LAI smoothed by a cubic spline procedure [18] and G_n values based on the 1983 data set

$$LAI = -0.369 + 6.585 G_{n_e} \tag{8}$$

and

$$LAI = -0.502 + 4.541 G_{n_b} \tag{9}$$

where G_{n_e} and G_{n_b} are the greenness values computed from (3) and (4), respectively. These relationships were then used to estimate the green LAI from G_n data of the 1984 season. The results are presented in Fig. 4. The LAI estimates based on both empirical equations underestimate the measured ones, in spite of relatively high R^2 values. This is illustrated by the slopes of the linear regression lines between the estimated and measured LAIs that were significantly ($\alpha = 0.0001$) smaller than one. This is probably due to the limitation of empirical relationships

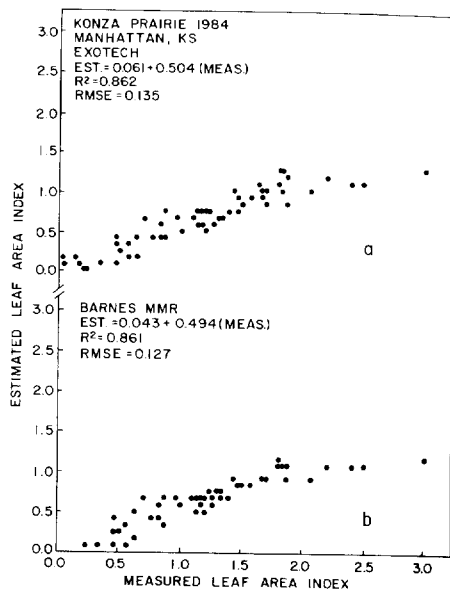


Fig. 4. Relationship between measured and estimated leaf area index based on the RGR method using measured canopy reflectance by (a) the Exotech and (b) Barnes MMR.

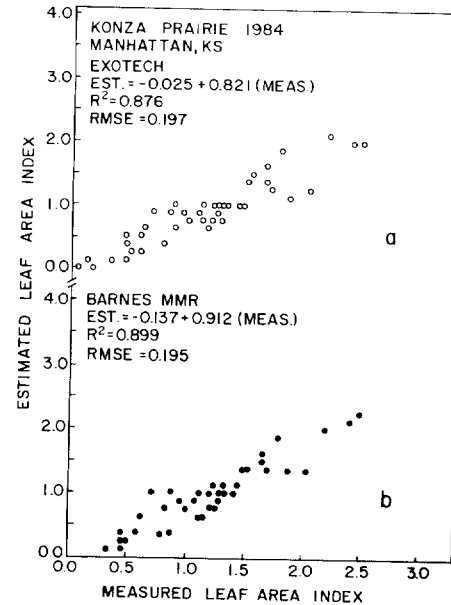


Fig. 6. Relationship between measured and estimated leaf area index based on the IND procedure and the measured relationship between p and G_n for the (a) Exotech and (b) Barnes MMR.

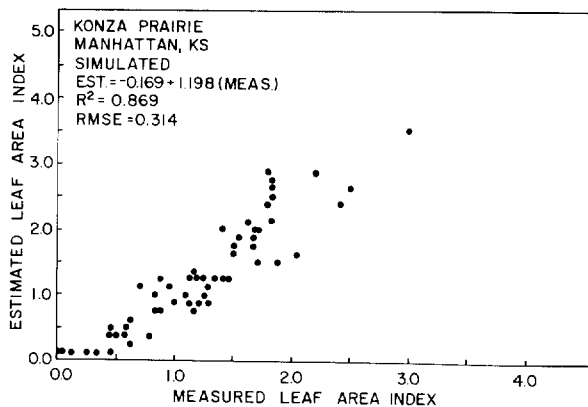


Fig. 5. Relationship between measured and estimated leaf area index based on the IND procedure and the simulated relationship between p and G_n .

that are usually data-set specific. Therefore, the effects of atmosphere, canopy architecture, soil background, and sun angle are not taken into account.

In method 2 (IND), the estimated p values from G_n were used in an indirect approach to compute green LAI as

$$\text{LAI} = -\ln \overline{(1-p)/K'} \quad (10)$$

where $\ln \overline{(1-p)}$ is the natural logarithm of the arithmetic mean of PAR interception estimated from grass canopy reflectance measurements, and $\overline{K'}$ is a mean leaf angle shape coefficient. In homogeneous canopies with spherical leaf angle distribution, K' is defined as

$$K' = 0.5/\cos \eta \quad (11)$$

and for canopies with fixed leaf angle, K' can be computed from the equations given in [11].

Fig. 5 shows the estimated and measured LAI's for the p versus G_n relationship, which was derived from simulated data (2). Good agreements ($R^2 = 0.869$) were obtained between the estimated and measured LAI values;

however, the estimated LAI values were slightly larger than the measured ones for $\text{LAI} > 2.0$. This is illustrated by the slope of the linear regression relationship between the estimated and measured LAI values, which was significantly ($\alpha = 0.0001$) greater than one. This was probably due to the wide range of canopy conditions that were assumed in deriving the p versus G_n equation (Table II). However, the magnitude of RMSE of estimated LAI's (0.314) was comparable with the standard error of mean measured values. A similar procedure was used to compute LAI indirectly from G_n values using the measured p versus G_n relationships (Table II). The results are presented in Fig. 6. The estimated LAI values based on canopy reflectance measurements with the two different sensor systems (Exotech and Barnes MMR), were in close agreement with the measured ones as indicated by the R^2 and RMSE presented in Fig. 6. The intercepts for the linear regression relationships between the estimated and measured LAI's were not different from zero, but the slopes were significantly ($\alpha = 0.0001$) different from one. The magnitude of the RMSE values were smaller than the one for LAI estimates presented in Fig. 5. In general, the IND method resulted in a better overall agreement between estimated and measured LAI values than the RGR method. This suggests that G_n transformation of canopy spectral reflectance measurements is closely related to the fraction of intercepted PAR by green foliage rather than the quantity of green LAI. Although green LAI and PAR interception are strongly correlated, the PAR interception also depends on the canopy geometry and the solar angle. These factors also affect the quality and quantity of the radiation that is reflected from the plant canopy. Therefore, the IND procedure accounted for some of these factors, as demonstrated in (2), and resulted in a more reliable estimate of green LAI in grass canopies.

VI. SUMMARY AND CONCLUSIONS

This study was conducted to assess the feasibility of estimating intercepted PAR and green LAI from measurements of grass canopy multispectral reflectance.

PAR interception was found to be more linearly related to G_n index than to RO or ND indices. The p versus G_n relationship, however, was found to depend on canopy geometry and solar angle due to variation of both canopy reflectance and p . Empirical linear regression equations were derived, based on a simple radiative transfer model and direct field measurements, that can be used to estimate p from measurements of canopy reflectance by the radiometers that mimic the MSS and TM sensor systems on board Landsat satellites.

An RGR was used to estimate the green LAI from the G_n index. The estimated LAI values by the RGR method were consistently smaller than the measured ones. In an IND, p values estimated from G_n index were used to estimate LAI from an exponential relationship between LAI and p , by assuming a spherical leaf angle distribution. The estimated LAI values based on the IND method were in good agreement with the measured ones. These results suggested that the G_n index is more closely related to the quantity of intercepted PAR by green foliage than green LAI. Although green LAI and PAR interception are strongly correlated, the interception of PAR also depends on the canopy geometry and solar angle. These factors affect the quantity and quality of radiation that is reflected from the plant canopy. The IND procedure accounted for some of these factors and, hence, resulted in a more reliable estimate of green LAI in grass canopies.

ACKNOWLEDGMENT

We thank D. W. Reed, P. Chapman, and J. M. Kileen for their technical assistance.

REFERENCES

- [1] G. L. Ajtay, P. Ketner, and P. Durigneaud, "Terrestrial primary production and phytomass," in *The Global Carbon Cycle*, B. Bolin, E. T. Degens, S. Kempe, and P. Ketner Eds. New York: Wiley, 1977, pp. 129-181.
- [2] R. G. Bailey, "Description of the ecoregions of the United States," U. S. Dep. of Agriculture, Intermt. Forest Service, Ogden, UT, 1978.
- [3] C. J. Tucker, "A critical review of remote sensing and other methods for non-destructive estimation of standing crop biomass," *Grass Forage Sci.*, vol. 35, pp. 177-182, 1980.
- [4] C. J. Tucker, C. L. Vanpraet, M. J. Sharman, and G. Vanlittersum, "Satellite remote sensing of total herbaceous biomass production in the Senegalese Sahel: 1980-1984," *Remote Sensing Environ.*, 1985.
- [5] J. L. Monteith, "Solar radiation and productivity in tropical ecosystems," *J. Appl. Ecol.*, vol. 9, pp. 747-766, 1970.
- [6] G. Asrar, E. T. Kanemasu, R. D. Jackson, and P. J. Pinter, Jr., "Estimation of total above-ground phytomass production using remotely sensed data," *Remote Sensing Environ.*, vol. 17, pp. 211-220, 1985.
- [7] J. E. Sanger, "Quantitative investigations of leaf pigments from their inception in buds through autumn coloration to decomposition in falling leaves," *Ecology*, vol. 52, pp. 1075-1089, 1971.
- [8] C. J. Tucker, "Post senescent grass canopy remote sensing," *Remote Sensing Environ.*, vol. 7, pp. 203-210, 1978.
- [9] C. S. T. Daughtry, K. P. Gallo, and M. E. Bauer, "Spectral estimates of solar radiation intercepted by corn canopies," *Agron. J.*, vol. 75, pp. 527-731 May-June 1983.
- [10] J. L. Hatfield, G. Asrar, and E. T. Kanemasu, "Intercepted photo-

synthetically active radiation estimated by spectral reflectance," *Remote Sensing Environ.*, vol. 14, pp. 65-75, Jan. 1984.

- [11] G. Asrar, M. Fuchs, E. T. Kanemasu, and J. L. Hatfield, "Estimating absorbed photosynthetic radiation and leaf area index from spectral reflectance measurements in wheat," *Agron. J.*, vol. 76, pp. 300-306, Mar.-Apr. 1984.
- [12] G. Asrar, E. T. Kanemasu, and M. Yoshida, "Estimates of leaf area index from spectral reflectance of wheat under different cultural practices and solar angle," *Remote Sensing Environ.*, vol. 17, pp. 1-11, Jan. 1985.
- [13] R. L. Weiser, G. Asrar, G. P. Miller, and E. T. Kanemasu, "Assessing biophysical characteristics of grassland from spectral measurements," in *Proc. 10th Int. Symp. Mach. Process. Remot. Sens. Data* (Purdue Univ., West Lafayette, IN), pp. 357-361, June 1984.
- [14] M. Monsi and T. Sacki, "Veber dem lichtfaktor in den pflanzengesellschaften und seine bedeutung fuer die stoffproduktion," *Japan. J. Bot.*, vol. 52, pp. 22-52, 1952.
- [15] G. P. Miller, M. Fuchs, M. J. Hall, G. Asrar, E. T. Kanemasu, and D. E. Johnson, "Analysis of seasonal multispectral reflectances of small grains," *Remote Sensing Environ.*, vol. 14, pp. 153-167, Jan. 1984.
- [16] J. D. Kollenkark, C. S. T. Daughtry, M. E. Bauer, and T. L. Housely, "Influence of cultural practices on the reflectance characteristics of soybean canopies," *Agron. J.*, vol. 74, pp. 751-758, July-Aug. 1982.
- [17] J. C. Kollenkark, V. C. Vanderbilt, C. S. T. Daughtry, and M. E. Bauer, "Influence of solar illumination angle on soybean canopy reflection," *Appl. Opt.*, vol. 21, pp. 1179-1184, 1982.
- [18] B. A. Kimball, "Smoothing data with cubic splines," *Agron. J.*, vol. 63, pp. 126-129, Jan.-Feb. 1976.

*



Ghassem Asrar received the M.S. degree in soil and fluid mechanics and the Ph.D. degree in microclimatology from Michigan State University.

He is currently an Assistant Professor of Agricultural Physics at the Evapotranspiration Laboratory, Kansas State University. His primary research interests have been in radiative transfer in plant canopies, fluid flow through porous media, microclimatology, remote sensing, and modeling of soil-plant-atmosphere continuum.

Dr. Asrar is a member and referee for several national and international professional societies.

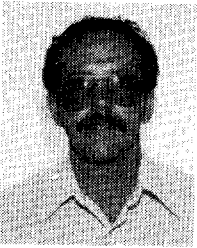
*



Edward T. Kanemasu received degrees from Montana State University and the University of Wisconsin.

He joined Kansas State University in 1969 where he is currently a Professor of Agronomy and leader of the Evapotranspiration Laboratory. His primary research interests have been in plant-water relations, evapotranspiration, crop-yield modeling, and remote sensing. He has been an invited lecturer at numerous conferences and symposiums in the U.S. and abroad, and has served on national committees for the USDA, NASA, and several other agencies.

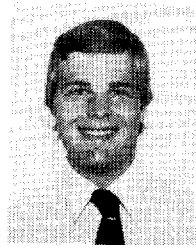
Dr. Kanemasu is a fellow of the American Society of Agronomy and has served as an Associate Editor and Technical Editor, *Agroclimatology and Crop Modeling*, of the *Agronomy Journal*.



George P. Miller received the B.S. degree from Colorado State University in 1973 and the M.S. degree in soil science from Washington State University in 1981.

He is currently a Research Assistant with the Evapotranspiration Laboratory at Kansas State University.

Mr. Miller is a member of the American Society of Agronomy.



R. L. Weiser received the B.S. degree in crop science from Oregon State University in 1983. He is working toward the M.S. degree in agronomy at Kansas State University where he is a Graduate Research Assistant studying under Prof. E. T. Kamenasu in the Evapotranspiration Laboratory.

Spectral Components Analysis: A Bridge Between Spectral Observations and Agrometeorological Crop Models

CRAIG L. WIEGAND, ARTHUR J. RICHARDSON, AND PAUL R. NIXON

Abstract—Spectral observations have been acknowledged to indicate general plant conditions over large areas but have yet to be exploited in connection with agrometeorological crop models. One reason is that it is not yet appreciated how periodic spectral observations of row-cropped and natural plant canopies, as expressed by vegetation indices (VI), can provide information on important crop model parameters, such as leaf area index (LAI) and absorbed photosynthetically active radiation (APAR).

Two experiments were conducted under AgRISTARS sponsorship, one with cotton and one with spring wheat, specifically to determine the relationships for each term in the "spectral components analysis" identity

$$\text{LAI/VI} \times \text{APAR/LAI} = \text{APAR/VI}$$

LAI and APAR could, indeed, be well estimated from vegetation indices such as normalized difference (ND) and perpendicular vegetation index (PVI)—apparently because of the close relation between the VI and amount of photosynthetically active tissue in the canopy. APAR and VI measurements are similarly affected by solar zenith angle (SZA), and LAI can be divided by \cos SZA at the time of the VI and APAR measurements to achieve correspondence. APAR, ND, and PVI plotted against LAI all asymptote to limiting values in the same way yield does as LAI exceeds 5, further linking canopy development to yield capability. In summary, the spectral components analysis results presented add credence to the information conveyed by spectral canopy observations about plant development and yield, and establish a bridge between remote observations and agrometeorological crop modeling through the variables of mutual concern, LAI, biomass, and yield.

I. INTRODUCTION

AGRICULTURAL scientists and engineers have developed crop growth, development, and yield models that use weather and soils data as inputs [3], [10]. But the plant canopies that develop will integrate the soil and aerial environments and also express development, stress response, and yield capabilities [22], [24]. Thus, there is opportunity to use direct canopy observations obtained remotely in conjunction with the agrometeorological models to either provide selected model inputs or as feedback to the agrometeorological models to keep them tracking actual crop performance [19], [23], and [25].

Spectral components analysis [24] is a bridge between the spectral observations and crop modeling. In its present

form, it uses the identities

$$\text{LAI/VI} \times \text{APAR/LAI} = \text{APAR/VI} \quad (1)$$

and

$$\text{LAI/VI} \times \text{YIELD/LAI} = \text{YIELD/VI} \quad (2)$$

where VI denotes any one of several spectral vegetation indices computed from remote spectral observations; LAI is leaf area index, APAR is absorbed photosynthetically active radiation, and YIELD is the salable plant part, e.g., grain of cereals, lint of cotton, root of beet, harvested phytomass of grasses or legumes for hay or silage, to interpret the information conveyed by canopies.

One objective of this paper is to report the results of experiments conducted under the AgRISTARS program that were specifically designed to obtain the relationships for each of the terms of (1). One experiment was conducted in the spring and summer of 1983 on cotton (*Gossypium hirsutum*, L.) and the other was conducted in the fall and winter, 1983–1984, on spring wheat (*Triticum aestivum*, L.). The only previous experiments in which all the necessary measurements had been made were conducted at Purdue University using corn (*Zea mays*, L.) and soybeans (*Glycine max*, L.) as the test crops [6], [5], and Kansas State University using winter wheat [9], also under AgRISTARS sponsorship. Hatfield *et al.* [8], used the APAR versus LAI relation from the Hipps *et al.* [9] study in connection with LAI and VI data from the U.S. Water Conservation Laboratory's serial cereal experiment to estimate APAR from VI. Similarly, Wiegand and Richardson [19] used the intercepted PAR (IPAR) versus LAI relation for sorghum (*Sorghum bicolor*, L. Moench) from Maas and Arkin [13] to complete the spectral components analysis identity expressed by (1).

The second objective of this paper is to document and briefly discuss how the information conveyed by canopy observations helps form a bridge between spectral observations and agrometeorological crop development and yield models, especially in connection with large-area crop condition and yield estimates.

II. METHODS

The cotton cultivar, McNair 220, was planted March 10, 1983, in north-south oriented rows spaced 1.02 m apart.

Manuscript received May 10, 1985; revised August 20, 1985.

The authors are with the Agricultural Research Service, U.S. Department of Agriculture, Weslaco, TX 78596.

IEEE Log Number 8406223.

Three treatments were thinned to 99 000 plants/ha, while a fourth was thinned to 52 000 plants/ha. One of the densely planted treatments (MC1) received an application of the growth regulator mepiquat chloride at the rate of 74 g/ha active ingredient applied at pinhead-size square (April 21). Another of the densely planted treatments (MC2) received a split application of the growth regulator (49 g/ha on April 21, and 25 g/ha at first bloom on May 19). The remaining densely planted treatment (NT) and the treatment thinned to 52 000 plants/ha (< NT) did not receive the growth regulator and were maintained as controls. The treatments were each replicated three times in a randomized block design. Individual treatment plots were 10 m \times 15 m in size.

The spring wheat cultivars Aim, Nadadores, and Yavaros were seeded on November 17, 1983, at the rate of 80 kg/ha with a commercial drill in rows spaced 0.2 m apart. Individual plots were 12 m \times 18 m in size. In half of each plot, 100 kg \cdot N/ha, 33 kg \cdot P/ha, and 33 kg \cdot K/ha had been applied prior to planting while the other half received no fertilizer. Populations achieved as counted two weeks after emergence were 302, 313, and 197 plants/m² for Aim, Nadadores, and Yavaros, respectively. The Aim and Nadadores cultivars were planted in randomized complete blocks with three replicates for each of two row directions, north-south and east-west. The Yavaros was a single unreplicated planting in east-west rows adjacent to the other plots. For both cotton and wheat the cultural practices were typical for the area.

The measurements needed to determine each term in (1) and (2) were made. Leaf area index was obtained periodically by harvesting 1-m row segments of cotton and 0.24 m² (0.4 m \times 0.6 m) areas of wheat. Leaf blades were detached at the petiole (cotton) and at the ligule (wheat) after Feekes growth stage 5 [12]. The leaves from two cotton plants within the 1-m row segment samples were optically planimetered. Then the leaves from the two plants and the leaves from the rest of the plants were oven dried. The relation between leaf dry weight and leaf area for the two plants was used for the whole samples. The equation for the nontreated (NT) controls was $LA = -389.9 + 324.3(LW) - 3.376(LW)^2$ and for the mepiquat chloride treated (MC) cotton plants and $LA = -260.2 + 279.1(LW) - 3.135(LW)^2$ where LA is leaf area in square centimeters per plant and LW is leaf dry weight in grams. The coefficient of determination (R^2) in both cases exceeded 0.99. LAI was determined on eight dates during the season.

For wheat, the equations published by Aase [1], were used to estimate leaf area in square centimeters from leaf dry weight after Feekes [12] stage 5 and from above ground plant weight up to stage 5. Nongreen leaf and plant material was removed from the samples so that our LAI are effectively green leaf area indices (GLAI). LAI was then calculated for the known sample area. LAI of wheat was determined on six dates.

The vegetation indices used were calculated from reflectance factor observations made approximately weekly

using a Mark-II radiometer [21] which has a visible (VIS) band in the 0.63-0.69- μ m-wavelength interval, and a reflective infrared (RIR) band in the 0.76-0.90- μ m interval. The spectral band responses plus incident solar radiation and time of observations were electronically logged concurrently for each of four observations per replicate and reduced by the procedures described by Richardson [16]. The vegetation indices employed were the normalized difference (ND) and perpendicular vegetation index (PVI) [17] for which the equations are

$$ND = (RIR - VIS)/(RIR + VIS) \quad (3)$$

and

$$PVI = 0.580(RIR) - 0.815(VIS) - 0.410. \quad (4)$$

The PVI equation is specific for the soil, a Raymondville clay loam (Vertic Calciustolls), of this study and is based on the soil line

$$VIS = -1.92 + 0.789(RIR) \quad (5)$$

as determined from bare soil reflectance factor observations taken in the uncropped, interplot alleys each time the cotton and wheat canopy observations were taken.

Photosynthetically active radiation (PAR) incident (I) on, transmitted (T) through, and reflected (R) from the cotton and wheat canopies, as measured with LI-COR[®] line quantum and irradiance sensors, provided the data for absorbed PAR, $(I-T-R)/I$, termed APAR. For the field measurements, an upward looking line quantum sensor was inserted perpendicular to the rows below the canopies to measure T , and a line quantum sensor was inverted 30 cm above the canopies and perpendicular to the rows to measure R from the canopy plus soil. The irradiance sensor was moved from plot to plot on a 2-m-tall stand that could be leveled. All three sensors were calibrated to yield the same value of irradiance when simultaneously exposed to the sun.

At the time of each sampling, up to two days were required to determine LAI, one day to make the PAR sensor observations, and about 1 h to make the reflectance factor measurements. Thus it was impossible to make all the necessary observations on the same day. Table I summarizes the dates on which the various measurements were made for each experiment. When data from various sources were merged, the sample date was considered to be that of the PAR or light absorption data and it was used as measured. The PAR data were paired with the reflectance factor data taken the same work week, except in January 1984, when a siege of extremely cloudy weather prevented our acquiring the reflectance factor data within three days of the PAR measurements. For that date we plotted the VI versus time and interpolated. LAI data for the eight measurement dates for cotton and six for wheat were plotted versus time and the LAI was interpolated to the dates of the PAR measurements.

¹Product names are mentioned for the convenience of the reader and do not infer preferential treatment or endorsement by the U.S. Department of Agriculture over other products that may be available.

TABLE I
DATES IN 1983 AND 1984 ON WHICH MEASUREMENTS FOR VARIABLES IN (1)
AND (2) WERE TAKEN
(Days of year, in parentheses, follow calendar date.)

| Crop | Reflectance Factor | Measurements | | |
|----------------------|--------------------|--------------|-----------------------------|-------|
| | | PAR | LAI | YIELD |
| Cotton (1983) | 11 Apr (101) | | | |
| | 18 Apr (108) | | | |
| | 25 Apr (115) | | 28 Apr (118) | |
| | 2 May (122) | | | |
| | 4 May (124) | 4 May (124) | 6 May (126) | |
| | 16 May (136) | | 16, 17 May (136, 137) | |
| | 23 May (143) | 23 May (143) | 23 May (143) | |
| | 1 Jun (152) | 2 Jun (153) | 1 Jun (152) | |
| | 9 Jun (160) | | 8 Jun (159) | |
| | 15 Jun (166) | 14 Jun (165) | | |
| | 20 Jun (171) | | 20 Jun (171) | |
| | 27 Jun (178) | 27 Jun (178) | | |
| | 6 Jul (187) | | 5 Jul (186) | |
| | 14 Jul (195) | | | |
| | 22 Jul (203) | | | |
| 28 Jul (209) | | | | |
| 3 Aug (215) | | | 3 Aug (215) 17 Aug (229) | |
| Wheat (1983-1984) | 5 Dec (329) | | 6 Dec (340) | |
| | 12 Dec (346) | 15 Dec (349) | 13 Dec (347) | |
| | 29 Dec (363) | | | |
| | 6 Jan (006) | 11 Jan (011) | 11, 12 Jan (011, 012) | |
| | 3 Feb (034) | | | |
| | 16 Feb (047) | 13 Feb (044) | 13, 14, Feb (044, 045) | |
| | 24 Feb (055) | | | |
| | 29 Feb (060) | 28 Feb (059) | | |
| | 8 Mar (068) | | 8 Mar (068) | |
| | 16 Mar (076) | | | |
| | 22 Mar (082) | | | |
| | 28 Mar (088) | 29 Mar (089) | 28 Mar (088) | |
| | 3 Apr (094) | | | |
| | 9 Apr (100) | | | |
| | 16 Apr (107) | | | |
| 24 Apr (115) | | | 27 Apr (118) | |

TABLE II
EQUATIONS FOR EACH TERM OF THE SPECTRAL COMPONENTS ANALYSIS
IDENTITY OF (1) FOR BOTH COTTON AND WHEAT

| | Crop | Equation | Coeff. of Deter., r ² | Eq. No. |
|------------------------------|---------|---|----------------------------------|---------|
| LAI vs VI (1st term) | Cotton: | LAI = .006e ^{6.54(ND)} | .979 | (3) |
| | " | LAI = .043e ^{-.134(PVI)} | .954 | (4) |
| | Wheat: | LAI = ND / (3.26 - 2.94(ND)) | .945 | (3a) |
| | " | LAI = .131e ^{-.108(PVI)} | .964 | (4a) |
| APAR vs LAI (2nd term) | Cotton: | APAR = .45R(LAI ^{-.555}) | .984 | (5) |
| | | APAR = (1 - .048LAI ^{-.786}) / (1 - 1.07e ^{-.794(LAI)}) | | (5') |
| | Wheat: | APAR = 1.02 - .296/LAI | .943 | (5a) |
| APAR vs VI (right hand side) | Cotton: | APAR = 1.07ND ^(3.85) | .979 | (6) |
| | " | APAR = .010 PVI ^(1.25) | .973 | (7) |
| | Wheat: | APAR = .032e ^{3.64(ND)} | .789 | (6a) |
| | | APAR = 1.18 - 8.11/PVI | .875 | (7a) |

Yield of seed plus lint (cotton) and grain (wheat) were obtained from 5-m row segments per replication and three 0.24-m² samples per replication for cotton and wheat, respectively.

The data for each of the terms of (1) were submitted to a program called W1105, from the statistical package provided by International Business Machines for the predecessor local IBM 1800 computer as adapted to the current in-house Hewlett-Packard Model 1000 mini-computer.

The program is a least squares procedure that fits the data to each of the following equation forms: $Y = A + (B * X)$, $Y = A * \text{EXP}(B * X)$, $Y = A * (X ** B)$, $Y = A + (B / X)$, $Y = 1 / (A + B * X)$, and $Y = X / (A + B * X)$. Applied to data herein, Y is the numerator variable and X the denominator variable of the terms in (1) and A and B are arbitrary coefficients. When more than one equation yielded almost the same coefficient of determination, we plotted the data and the curve for the contending equations and selected the equation form that fit the data best, as judged visually, over its entire range.

III. RESULTS

A. Data Presentation

The equations that expressed the relations obtained for each of the terms in (1) for the two crops are summarized in Table II. Equation (5') (given in the Table) represents the product $(I - R) / I$ times $(I - T) / I$ in which R and T are nonlinearly regressed onto LAI. Therein, $(I - R) / I$ is interpreted as the net downward flux of PAR and $(I - T) / I$ as that fraction of the downward flux that is intercepted by (not transmitted through) the canopy.

There is a close relation between leaf area index and the spectral vegetation indices (see (3), (3a), (4), and (4a) in Table II). Thus the vegetation indices are a good measure of the size of the photosynthetic apparatus of the crop canopies. As generally accepted in the literature, (5) and (5a) demonstrate that APAR can be estimated very well from LAI. The relation between APAR and the vegetation indices is closer for cotton than for the pooled wheat cultivars (see (6) and (7) versus (6a) and (7a) and Fig. 1). The data indicate that APAR can be satisfactorily estimated from vegetation indices as has been demonstrated also by [6] and [8].

Because the vegetation indices can respond to nonleaf photosynthetically active tissues such as heads and leaf sheaths of cereals, they may be more accurate monitors of the photosynthetic capacity of standing canopies than is green leaf area index (GLAI), *per se*. This distinction may permit the vegetation indices to characterize canopies more accurately for light interception or absorption than does GLAI during crop senescence, when leaves must be portioned into living and nonliving tissue parts and non-leafy photosynthetic tissue is excluded.

The RIR reflectance factors respond to the solar zenith angle due to the increasing optical path length through the canopy as solar zenith angle (SZA) deviates from nadir [11]. Thus, the vegetation indices, which are dominated by the RIR reflectance factors, also respond to solar zenith angle [20]. This response agrees with the expected increase in APAR as expressed in light interception equations by dividing LAI by cos SZA [14]. This means that for measurements of APAR and VI made at the same time, the cos SZA effect cancels out since it occurs in both the numerator and denominator of the right-hand side of (1). For APAR inferred from VI, the SZA effect is included in VI.

Cotton canopies are planophile (horizontal leaf dis-

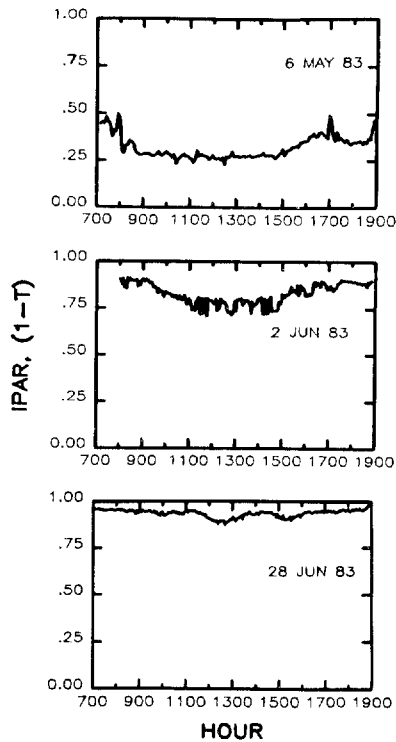


Fig. 1. Diurnal (solar zenith angle) effect on light interception for non-thinned NT treatment cotton on three dates corresponding to plant ground cover percentages of 23, 72, and 86 percent.

play), especially during midday since they are heliotropic. Wheat canopies generally are more erectophile (vertical elements including leaves). Diurnal light interception measurements were made on three dates in the NT treatment cotton canopy of this study, and on seven dates in the Yavaros cultivar of spring wheat of this study as reported by Richardson and Wiegand [18]. Light interception was very weakly affected by time of day for cotton (Fig. 1) especially for the lowest (23 percent) and highest (86 percent) plant cover on May 6 and June 28, respectively. Plants covered 72 percent of the ground area on June 2. For the wheat, both the RIR reflectance factor and light transmittance through the canopy (interception = $1 - T$) were linear versus $1/\cos$ SZA over a twofold range in $1/\cos$ SZA [18], that is for a SZA within 60° of nadir ($\cos 60^\circ = 0.50$).

Based on these results, we now recommend that LAI in (1) be normalized by \cos SZA at the time of the VI and APAR measurements. Measured values of VI and APAR already contain the effects of SZA. Thus, (1) becomes

$$\frac{\text{LAI}/\cos \text{SZA}}{\text{VI}} \times \frac{\text{APAR}}{\text{LAI}/\cos \text{SZA}} = \frac{\text{APAR}}{\text{VI}} \quad (1')$$

There are both seasonal (time of year) and diurnal (time of day) SZA effects on APAR and VI measurements. If APAR and VI measurements are taken within 2 or 3 h of solar noon in summer the effect is quite small because the sun is closest to nadir and $1/\cos$ SZA changes slowly around solar noon ($\cos 10^\circ$, 26° , and 41° are 0.98, 0.90, and 0.75, respectively). In winter the sun is quite low in the sky so that the SZA is larger and the diurnal effect on

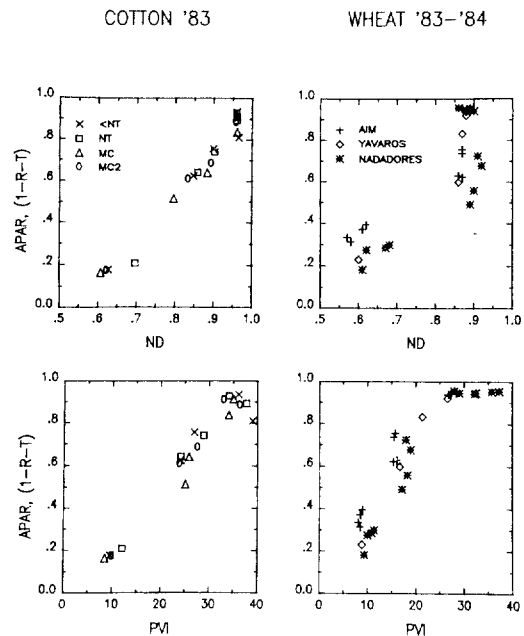


Fig. 2. APAR versus ND and PVI, respectively, for both cotton and wheat (right side of (1)).

APAR and VI measurements is more serious. Our wheat measurements were made from December through March and our cotton measurements from April through July. It took us about 5 h, beginning usually at 10:30 local clock time (local standard time except daylight savings time after the last Sunday in April) to make the light transmission measurements in both the wheat and the cotton experiments on clear days and longer if we had to wait for clouds to pass. In contrast, the reflectance factor measurements to calculate ND and PVI could be made in at most 45 min, beginning usually at 1300 h. Both the seasonal and diurnal effects of SZA on APAR and VI were greater for the wheat than for the cotton data and probably resulted in less of the variation being accounted for in Table II in (6a) and (7a) for wheat than by (6) and (7) for cotton.

In Fig. 2, where all treatment mean data points not obscured by others are shown, the scatter in the observations of APAR over the season is greater for the three wheat cultivars than for the one cotton cultivar treated with growth regulator. For the wheats of Fig. 2, it is evident that APAR was greater for Aim for a given value of the vegetation index than for the other two cultivars. Statistical analysis [15] has shown that Aim was more efficient in intercepting light than was Nadadores, i.e., that equation coefficients differed statistically significantly.

The other characteristic of the wheat data apparent in Fig. 1 is that ND reaches a maximum value of approximately 0.9 while APAR is still increasing, whereas APAR becomes asymptotic to a limit of 0.95 while PVI is still increasing. The saturation of ND at relatively low vegetation greenness is one of its disadvantages [20].

In summary of the above discussion, seasonal effects on solar zenith angle, time of day differences in determining APAR and the vegetation indices, and cultivar differences all contribute to scatter in the APAR versus VI data of

Fig. 2 for the wheat cultivars, yet the relationships are satisfactory. For cotton, the APAR versus VI relations are impeccable.

As we anticipated (2) did not apply well in either of our experiments because a limited range in LAI was achieved among treatments (and consequently in APAR and VI), the Nadadores wheat cultivar is adapted for forage production but not grain production (its harvest index, the ratio of grain to above ground phytomass, was 0.22 compared with 0.34 for Aim and 0.47 for Yavaros), and the mepiquat chloride treated cotton yielded somewhat better than the control cotton even though it had slightly lower LAI. (Mepiquat chloride shortens both main stem and branch internodes and thickens leaves slightly [7], but yield responses have been mixed [26]). Nonetheless, we believe, (1) and (2) are applicable to commercial fields that vary in soil, tillage and tillage, natural stresses, and quality of agronomic management, and that the periodic remote observations of crop canopies can provide valuable input and feedback to agrometeorological models.

B. Implications of Findings

The findings have important implications for applying agrometeorological crop models to many fields (large areas) since the spectral observations can be made from aircraft and satellite platforms with sensors that view large areas. Such observations can adequately estimate APAR and can closely follow canopy LAI development. Thus they can be responsive to soil conditions, disease, water, and other stresses that affect development of the photosynthetically active tissue area of the canopies. The findings are particularly useful in integrating the general understanding among plant productivity, plant canopy development, and light absorption. Fig. 3 presents the relation between LAI and the variables ND, PVI, and APAR for the cotton as expressed by (3), (4), and (5'), respectively. Likewise, Fig. 4 presents the same relations for wheat as expressed by (3a), (4a), and (5a). The similarity in shape of the APAR and vegetation index graphs is apparent; expressions such as (6), (6a), (7), and (7a) illustrate that APAR may be generally estimable from vegetation indices.

Wiegand and Richardson [17] discussed how APAR (or IPAR) and various vegetation indices become asymptotic to a limiting value as LAI increases. Fig. 5 developed from their data illustrates that YIELD and the VI during the reproductive stage of crop development (early grain filling of cereals, boll growth of cotton) versus LAI have the same shape. Thus light absorption, vegetation index, and yield behavior of crops versus LAI are mutually consistent and in agreement with field observations. This internal consistency strengthens the probability that correct inferences about present crop condition and yield capability can be reached from periodic canopy spectral characterization as expressed by vegetation indices. This contention is strengthened for large area application since it was the Landsat spectral data for sorghum obtained for commercial fields in south Texas over multiple years that sug-

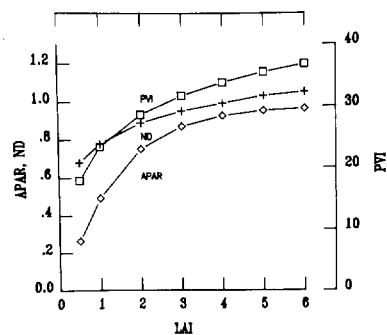


Fig. 3. Relation between leaf area index (LAI) and each of the variables, absorbed photosynthetically active radiation (APAR), and two vegetation indices, normalized difference (ND), and perpendicular vegetation index (PVI) for cotton.

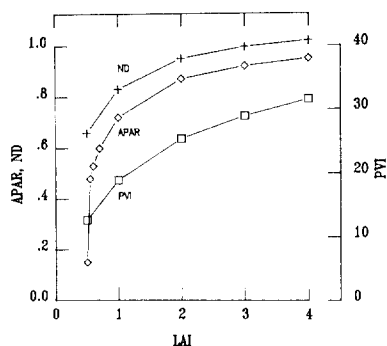


Fig. 4. The same relations as in Fig. 3, but for wheat.

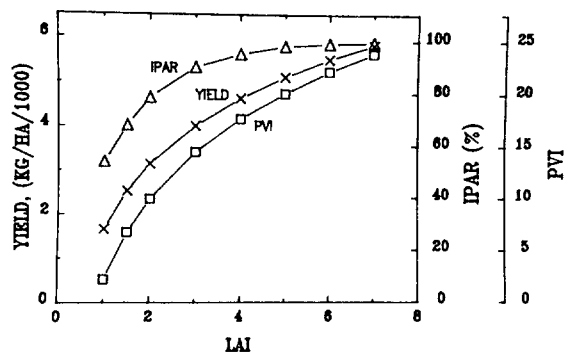


Fig. 5. Relation between leaf area index (LAI) and each of the variables, grain yield (YIELD), intercepted photosynthetically active radiation (IPAR), and perpendicular vegetation index (PVI) for sorghum. (see [23] for data.)

gested the spectral components analysis approach in the first place.

The right-hand sides of (1) and (2) indicate that cumulative APAR during the reproductive part of a crop's life cycle should relate to yield providing yield is limited by the size of the plant canopies achieved. For cultivars of adapted crops grown commercially in subhumid and drier climates, water availability often limits the LAI achieved by the canopies and yields are reduced proportionately. Even if high LAI's are achieved, low yields can occur due to catastrophic events, such as episodic weather, e.g., frost during anthesis, or outbreaks of insects that consume or cause abscission of fruiting forms. Thus an adequate canopy for effective light interception is a necessary, but not a sufficient, condition for high yields. The weather data

inputs to the agrometeorological models themselves can alert or warn that an episodic weather event may have occurred and branching within the model can change model computations to address the particular situation. Likewise, the plant phenological stages predicted by the agrometeorological model's plant development subroutine indicate whether or not the crop is at a susceptible stage for a given stress. The symptoms of stresses as diverse as drought, nematodes, and restricted rooting by tight soils will be revealed by the spectral data through effects on canopy size achieved. In short, agronomic and physiological information aid in determining, for a given situation, whether reproductive performance was consistent with vegetative development. However, the work of Aase and Siddoway [2] and Barnett and Thompson [4] indicate that, in commercial fields over large areas, yields are closely associated with the LAI of the canopies achieved.

IV. SUMMARY

In summary, the spectral indicators of crop development and canopy size available through vegetation indices help determine how the crops are actually doing compared with how weather- and soil-property-driven agrometeorological models predict they are doing. The individual spectral components terms provide information on leaf area index, biomass, and light absorption that can be used either as input or as feedback to the models. Finally, the relations expressed by (1) and (2) agree, in general, with canopy characteristics as they relate to yield. Thus, they add credence to the information conveyed by plant canopy observations and form a bridge between spectral observations and agrometeorological models. The joint use of spectral observations and agrometeorological models should improve crop condition and yield estimation efforts.

ACKNOWLEDGMENT

The authors thank J. Cuellar, W. Swanson, and M. Shibayama for assistance in making measurements, data reduction, and figure preparation.

REFERENCES

- [1] J. K. Aase, "Relationship between leaf area and dry matter in winter wheat," *Agron. J.*, vol. 70, pp. 563-565, 1978.
- [2] J. K. Aase, and F. H. Siddoway, "Spring wheat yield estimates from spectral reflectance measurements," *IEEE Trans. Geosci. Remote Sensing*, vol. GE-19, no. 2, pp. 77-84, 1982.
- [3] J. F. Arkin, C. L. Wiegand, and H. Huddleston, "The future role of a crop model in large area yield estimating," in *Proc. Crop Weather Modeling Workshop*, pp. 88-103, 1979.
- [4] T. L. Barnett and D. R. Thompson, "Large area relation of satellite spectral data to wheat yields," in *Proc. Symp. Machine Proc. of Remotely Sensed Data* (West Lafayette, IN), pp. 213-219, 1982.
- [5] C. S. T. Daughtry, K. P. Gallo, and M. E. Bauer, "Spectral estimates of solar radiation intercepted by corn canopies," *Agron. J.*, vol. 75, pp. 527-531, 1983.
- [6] K. P. Gallo, C. C. Brooks, C. S. T. Daughtry, M. E. Bauer, and V. C. Vanderbilt, "Spectral estimates of intercepted solar radiation by corn and soybean canopies," in *Proc. Symp. Machine Proc. of Remotely Sensed Data* (West Lafayette, IN), pp. 190-198, 1982.
- [7] H. W. Gausman, L. N. Namken, M. D. Heilman, H. Walker, and F. R. Rittig, in *Proc. Beltwide Cotton Prod. Res. Conf.* (Phoenix, AZ), pp. 51-52, 1979.

- [8] J. L. Hatfield, G. Asrar, and E. T. Kanemasu, "Intercepted photosynthetically active radiation in wheat canopies estimated by spectral reflectance," *Remote Sens. of Environ.*, vol. 14, pp. 65-75, 1984.
- [9] L. E. Hipps, G. Asrar, and E. T. Kanemasu, "Assessing the interception of photosynthetically active radiation in winter wheat," *Agric. Meteorol.*, vol. 28, pp. 253-259, 1983.
- [10] T. Hodges, "Second generation crop yield models review," NASA Johnson Space Center, Houston, TX, AgRISTARS Rep. YM-12-04306, JSC-18245, 1982.
- [11] D. S. Kimes, "Modeling the directional reflectance from complete homogeneous vegetation canopies with various leaf-orientation distributions," *J. Opt. Soc. Amer. A*, vol. 1, pp. 725-738, 1984.
- [12] E. C. Large, "Growth stages in cereals—Illustrations of the Feekes scale," *Plant Pathol.*, vol. 3, pp. 128-129, 1954.
- [13] S. J. Maas and G. F. Arkin, "User's guide to SORGF: A dynamic grain sorghum growth model with feedback capacity," Research Center Program and Model Documentation no. 78-1 (Blackland Res. Center at Temple), TAES, College Station, TX, 1978.
- [14] J. M. Norman and J. J. Welles, "Radiative transfer in an array of canopies," *Agron. J.*, vol. 75, pp. 481-488, 1983.
- [15] C. R. Perry Jr. and C. L. Wiegand, "Modeling photosynthetically active radiation intercepted or absorbed by crops," *Remote Sensing Environ.*, submitted for publication.
- [16] A. J. Richardson, "Measurement of reflectance factors under daily and intermittent irradiance variations," *Appl. Opt.*, vol. 20, pp. 3336-3340, 1981.
- [17] A. J. Richardson and C. L. Wiegand, "Distinguishing vegetation from soil background information," *Photogramm. Eng.*, vol. 43, pp. 1541-1552, 1977.
- [18] A. J. Richardson and C. L. Wiegand, "Diurnal-seasonal light interception, leaf area index, and vegetation index interrelations in a wheat canopy," *Photogramm. Eng.*, submitted for publication.
- [19] A. J. Richardson, C. L. Wiegand, G. F. Arkin, P. R. Nixon, and A. H. Gerbermann, "Remotely-sensed spectral indicators of sorghum development and their use in growth modeling," *Agric. Meteorol.*, vol. 26, pp. 11-23, 1982.
- [20] M. Shibayama, C. L. Wiegand, and A. J. Richardson, "Diurnal patterns of bidirectional vegetation indices," *Int. J. Remote Sensing*, to be published.
- [21] C. J. Tucker, W. H. Jones, W. A. Kley, and G. J. Sundstorm, "A three-band hand-held radiometer for field use," *Science*, vol. 211, pp. 281-283, 1981.
- [22] C. L. Wiegand, "Candidate spectral inputs to agrometeorological crop growth/yield models," in *Proc. 2nd Int. Colloq. Spectral Signatures of Objects in Remote Sensing* (Monfavet, France), pub. 23, pp. 865-872, 1983.
- [23] C. L. Wiegand, A. J. Richardson, and E. T. Kanemasu, "Leaf area index estimates for wheat from Landsat and their implications for evapotranspiration and crop modeling," *Agron. J.*, no. 71, pp. 336-342, 1979.
- [24] C. L. Wiegand and A. J. Richardson, "Leaf area, light interception, and yield estimates from spectral components analysis," *Agron. J.*, 76, pp. 543-548, 1984.
- [25] C. L. Wiegand, "The value of direct observations of crop canopies for indicating growth conditions and yield," in *Proc. 18th Int. Symp. Remote Sensing Environ.* (Paris, France, Oct. 1-5, 1984), vol. 2, pp. 1551-1560.
- [26] A. C. York, "Response of cotton to mepiquat chloride with varying N rates and plant populations," *Agron. J.*, 75, pp. 667-672, 1983.

*



Craig L. Wiegand received the B.S. and M.S. degrees in agronomy from Texas A&M University and the Ph.D degree in soil physics from Utah State University.

He is a Research Scientist in the Remote Sensing Research Unit, Agricultural Research Service, U.S. Department of Agriculture, Weslaco, TX. He has been involved in agricultural applications of remote-sensing research since the mid-1960's and is currently emphasizing spectral inputs to crop models and large-area crop condition assessments.



Arthur J. Richardson received the B.S. degree in secondary education from Texas A&I University, Kingsville, TX, in 1965.

He is currently a Research Physicist in the Remote Sensing Research Unit, Agricultural Research Service, U.S. Department of Agriculture, Weslaco, TX, where he has been involved in remote-sensing research for 18 years. He has tested agricultural applications of Landsat, Skylab, HCMM, and NOAA data under NASA and AgRISTARS programs.



Paul R. Nixon received the B.S. and M.S. degrees in agricultural engineering from Iowa State University and the M.S. degree in hydrology, Stanford University.

For seventeen years he worked in California in soil and water engineering and research of natural ground water recharge processes and use of water by vegetation. Since 1971, his research in Texas has involved thermal data obtained by aircraft and satellite. His current work includes use of multi-spectral video imaging for assessment and management of natural resources.

agement of natural resources.

Development of Agrometeorological Crop Model Inputs from Remotely Sensed Information

CRAIG L. WIEGAND, ARTHUR J. RICHARDSON, RAY D. JACKSON, PAUL J. PINTER, JR., J. KRIS AASE, DARRYL E. SMIKA, LYLE F. LAUTENSCHLAGER, AND J. E. McMURTREY, III

Abstract—The goal of developing agrometeorological crop model inputs from remotely sensed information (AgRISTARS Early Warning/Crop Condition Assessment Project Subtask 5 within the U.S. Department of Agriculture (USDA)) provided a focus and a mission for crop spectral investigations that would have been lacking otherwise. Because the task had never been attempted before, much effort has gone into developing measurement and interpretation skill, convincing the scientific community of the validity and information content of the spectral measurements, and providing new understanding of the crop scenes viewed as affected by bidirectional, atmospheric, and soil background variations. Nonetheless, experiments conducted demonstrate that spectral vegetation indices (VI) a) are an excellent measure of the amount of green photosynthetically active tissue present in plant stands at any time during the season, and b) can reliably estimate leaf area index (LAI) and intercepted photosynthetically active radiation (IPAR)—two of the inputs needed in agrometeorological models. Progress was also made on using VI to quantify the effects of yield-detracting stresses on crop canopy development. In a historical perspective, these are significant accomplishments in a short time span.

Spectral observations of fields from aircraft and satellite make direct checks on LAI and IPAR predicted by the agrometeorological models feasible and help extend the models to large areas. However, newness of the spectral interpretations, plus continual revisions in agrometeorological models and lack of feedback capability in them, have prevented the benefits of spectral inputs to agrometeorological models from being fully realized.

I. BACKGROUND

IN 1976, a decision was made in the Agricultural Research Service (ARS) of the U.S. Department of Agriculture (USDA) to launch an effort to develop an agrometeorological model for forecasting wheat (*Triticum aestivum* L.) yields. At the first meetings of the scientists and administrators to define and plan the project, there was limited awareness and even skepticism about the possibilities of using remote spectral observations in crop models,

Manuscript received April 26, 1985; revised June 27, 1985. This work was supported by the Agricultural Research Service and the Statistical Reporting Service, U.S. Department of Agriculture.

C. L. Wiegand and A. J. Richardson are with the Agricultural Research Service, U.S. Department of Agriculture, Weslaco, TX 78596.

R. D. Jackson and P. J. Pinter, Jr., are with the Agricultural Research Services, U.S. Department of Agriculture, Phoenix, AZ 85040.

J. K. Aase is with the Agricultural Research Service, U.S. Department of Agriculture, Sidney, MT 59270.

D. E. Smika is with the Agricultural Research Service, U.S. Department of Agriculture, Akron, CO 80720.

L. F. Lautenschlager is with the Statistical Reporting Service, U.S. Department of Agriculture, Washington, DC 20250.

J. E. McMurtrey, III, is with the Agricultural Research Service, U.S. Department of Agriculture, Beltsville, MD 20705.

IEEE Log Number 8406219.

except for one or two individuals who had been exposed to the Large Area Crop Inventory Experiment (LACIE) [34]. However, information such as the flow chart of Fig. 1 illustrated and interrelated spectral data and model inputs [53], [54] and provided evidence of technical feasibility.

Once remote observations were accepted as a legitimate part of the effort, the Wheat Yield Project gave a sense of mission and direction to the utilization of spectral measurements. The project also exposed additional scientists to spectral observations. The early decision of the project's leadership to acquire and disperse handheld radiometers [51] and data loggers (Polycorders®)¹ to the project's participants, and the workshop held on their use [15] were important contributors to the experiments that have been conducted under the impetus of and with at least partial funding from the ARS Wheat Yield Project.

When the multi-agency AgRISTARS effort began in 1979, the wheat modeling effort became part of the ARS's contribution to it. A subtask with the title of this paper was established within the Early Warning/Crop Condition Assessment Project managed by Glenn Boatwright of the ARS at Houston. The spectral research was concentrated at Weslaco, Texas; Phoenix, Arizona; and Beltsville, Maryland. Related additional experiments were conducted at Sidney, Montana; Mandan, North Dakota; Akron and Ft. Collins, Colorado; and Bushland and Lubbock, Texas. Personnel of the Statistical Reporting Service (SRS) of the USDA at Fort Collins, Houston, and Washington participated in various studies [28], [29], [35]. The crop modeling effort was centered at Fort Collins, Colorado, and Temple, Texas. The scope of the effort was to develop and test spectral data products for crop response to management variables, early warning and crop condition alarms and assessments, and crop growth and yield model inputs.

The purpose of this paper is to overview the research conducted within the USDA relevant to developing spectral inputs to agrometeorological crop models and to highlight some of the progress. Similar work conducted at Purdue University, Kansas State University, University of Nebraska, and at the Johnson and Goddard Space Flight Centers under NASA sponsorship will generally not be covered.

¹Product names are given for information purposes and do not imply consent or endorsement by the USDA.

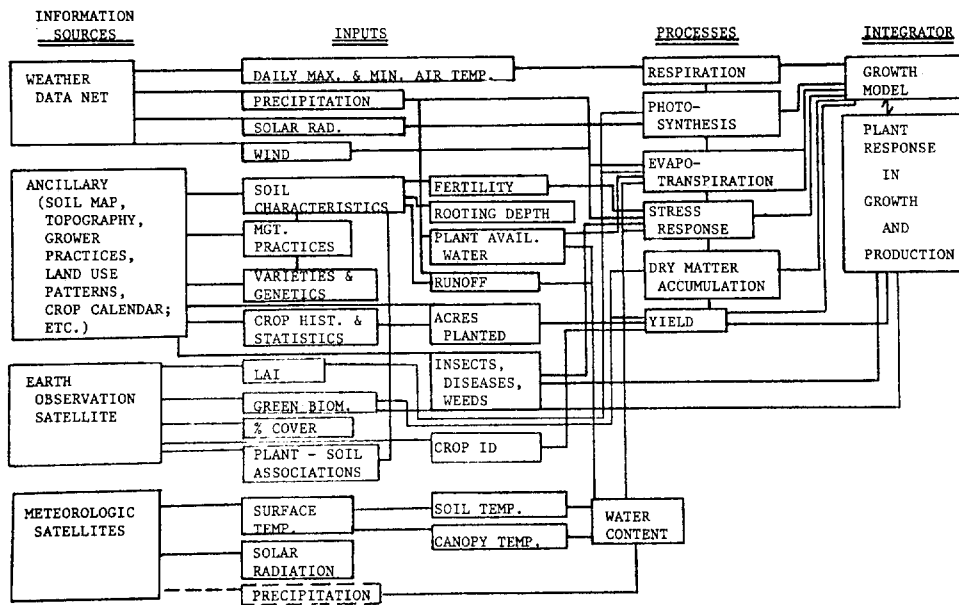


Fig. 1. Information sources, inputs, and plant processes for agrometeorological plant growth and yield models (after [59], [61]).

II. INTRODUCTION

The use of remotely sensed information in agrometeorological models depends on its availability compared with traditional data sources, and on the expertise and biases of the individual or group applying the model(s). Herein, we define remotely sensed information as noncontact observations in one or more wavelengths in the range $0.35 \mu\text{m}$ (lower limit of visible light) through $14 \mu\text{m}$ (thermally emitted electromagnetic radiation). Microwave (1–30 cm wavelength observations would be useful but are not generally available. The agrometeorological crop models in mind are those that: a) use soil properties (rooting depth and plant available water) and daily increments of weather data (temperature, precipitation, and insolation) as inputs to subroutines that simulate various plant processes (phenological or ontogenetic development, photosynthesis, respiration, evapotranspiration, dry matter accumulation); b) are designed to describe crop behavior on a field scale; c) are capable of simulating the crop from planting to maturity; and, d) estimate yield of the salable plant parts. Models in this category include TAMW [33], CERES [46], and SORGF [32].

Remotely sensed information can be used in two principal ways in conjunction with an agrometeorological model. One way is to provide surrogate estimates of one or more specific inputs that “drive” the model, e.g., leaf area index (LAI)² or intercepted³ photosynthetically ac-

tive ($0.4\text{--}0.7 \mu\text{m}$) radiation (IPAR). The other way is to provide independent feedback to override and reset the model simulated canopy development or yield estimates [43], [55], [59], [60], [61]. In the first approach the spectral data provide an alternative way of acquiring the necessary inputs for the model. In the second approach, for example, the LAI simulated by the model could be replaced with LAI estimated by handheld, aircraft- or spacecraft-mounted sensors viewing the same field(s). Since such feedback capability is lacking in most agrometeorological models at present, there is interest in a third way of using spectral data—as an independent direct assessment of crop condition and probable yield.

The information needed for any of the above spectral approaches is acquired by directly observing the plant canopies. Thus, the spectral or remote sensing approach takes advantage of the fact that the plants integrate their soil and aerial environments and express their development; stress response, and yield capabilities through the canopies achieved [60], [61]. Vegetation indices [15], [17], [19], [24], [29], [35], [39], [43], [49], [57] calculated from the spectral observations capture information on canopy development and condition; respond to past and current management (residual fertility, tillage, crop residue management, and cultural practices) and soil profile differences within and among fields that are not easily included in agrometeorological models; and provide a means of quantifying canopy development in response to stresses (current nutritional level, nematodes, diseases, herbicide residue, atmospheric pollutants, drought) [59], [61]. Thus, the use of spectral observations in conjunction with an agrometeorological model increases confidence that the model is tracking the actual behavior of plants in individual fields [62]. This confidence factor is extremely important. Crop models will not be applied for real world decisions unless consistently reasonable outputs can be expected.

²The ratio of the area of green leaves to the ground area occupied on the whole field basis.

³Typically, sensors sensitive to the PAR wavelength interval are used to measure the light incident (I) on the canopy, the light transmitted (T) through the canopy to the ground, the light reflected (R) from the plants and soil, and the soil (R_s). Intercepted PAR is defined as $(I-T)/I$ and absorbed PAR (APAR) as $(I-T-R + TR_s)/I$. Sometimes investigators report IPAR and sometimes APAR, but they differ by only a few percent for a canopy that fully covers the ground. They can differ more at low vegetative cover where surface wetness and organic matter and mineral content of the soil affect albedo in the PAR wavelengths.

III. PROGRESS UNDER THE ARS WHEAT AND AgRISTARS PROJECTS

The experiments have dealt with a large set of issues that contribute directly or indirectly to use of spectral data in models by documenting relationships that exist, providing new understanding of scene and atmospheric behavior, acquiring data sets for testing hypotheses and relationships, convincing the scientific community of the validity and information content of the spectral measurements, developing interpretation skill and meaning, and providing insights to support integration of spectral observations into crop models. This whole spectrum of activities was necessary to a) establish the scientific validity of new measurements and concepts, b) acquire the necessary expertise and equipment to use the technology, and c) change traditional or institutionalized procedures.

By 1981 the AgRISTARS effort was well underway. In October of that year the senior author suggested the following as viable research objectives in a memo to colleagues.

- 1) "Calibration of LAI, percent cover, and other agronomic characteristics versus vegetation indices; checking their geographic generality; and, determining the 'best' equation forms.
- 2) "Testing the above relations within and among crop species to determine, for example, whether the 'calibrations' are the same for the temperate cereals, soybeans and cotton, sorghum and corn... and pinpointing canopy 'architecture' and other reasons for differences.
- 3) "Understanding the properties of vegetation 'greenness' as expressed by the vegetation indices.
- 4) "Testing whether LAI is a necessary characterizer of canopies for light interception, or whether percent cover (PC) is adequate.
- 5) "Developing spectral measures of stress and comparing them with traditional ones, or defining and explaining new spectral ones.
- 6) "Developing spectral surrogates of LAI, biomass, or genetic canopy coefficients for use in growth and yield models, or to reinstate or override these models.
- 7) "Compiling data sets to test whether we can go directly from spectral measurements to intercepted light.
- 8) "Testing spectral models of yield versus those from agrometeorological and ecological-physiological models.
- 9) "Determining the effect of atmospheric corrections (sun angle, path radiance, haze) on the vegetation indices.
- 10) "Developing procedures to achieve agreement between space and ground-observed vegetation and soil indices."

Again, the list illustrates the diversity of activities that needed to proceed simultaneously to develop, understand, and use vegetation indices, the main vehicle for providing

spectral inputs to models. Despite this great diversity, and lack of a coordinated plan for research on such objectives significant progress was made.

Subject matter areas that were researched and documented included:

- 1) Spectral-agronomic relations [1], [4], [5], [10], [20], [43], [49], [52], [55].
- 2) Spectral-temporal and spectral-phenological relations [2], [30], [37], [45], [48], [49].
- 3) Spectral transforms, vegetation and soil indices, their relation with canopy characteristics (LAI, green biomass, percent cover, chlorophyll content, phytomass), and interpretation techniques [11], [15], [19], [35], [37], [39], [49], [52], [57], [59], [60]-[62].
- 4) Wavelengths in addition to the Landsat wavelength intervals (0.5-0.6, 0.6-0.7, 0.7-0.8, and 0.8-1.1 μm) and their utility and information content [15], [17], [30].
- 5) Procedures to achieve agreement between space (top of atmosphere) and ground-observed reflectance factors [17], [18], [40]-[42], [44].
- 6) Scene spectral modeling including effects of atmosphere, sun and view angles, and planting configurations on observations [14], [23], [26], [27], [37], [38], [47], [48].
- 7) Spectral measures of stress [16], [17], [21], [22], [36], [58].
- 8) Spectral estimates of yield [3], [5], [12], [13], [36], [50], [52], [60].
- 9) Spectral inputs or surrogates for agrometeorological models [9], [10], [43], [45], [55], [59], [60]-[62].
- 10) Plant development scale comparison [6].

In addition, USDA researchers made their field plots available to other scientists for experimental measurements [25]-[27], [31], [49].

Selected exemplary figures, tables, and equations from these publications illustrate the progress that has been made. Fig. 2 (after [43]) relates the LAI of grain sorghum on five dates to above-ground phytomass. Since the spectral observations are responding to the chlorophyll containing parts of the crop canopy [60], there is a close relation between LAI and above ground phytomass as long as the "stems" consist of leaf sheaths. But, when a true stem and then a head and grain develop, the latter contain most of the phytomass, and the relation between LAI and phytomass deteriorates. Whereas spectral vegetation indices relate less and less well to wet and dry phytomass as crops approach maturity, the VI relate well to LAI throughout the life cycle of the crop. In the agrometeorological models, LAI is used to characterize crops for penetration and interception of photosynthetically active radiation in the photosynthesis and growth subroutines, and to partition insolation between evaporation of water from the soil and transpiration from the plants [55]. Thus, remote estimates of LAI can be direct inputs to the models.

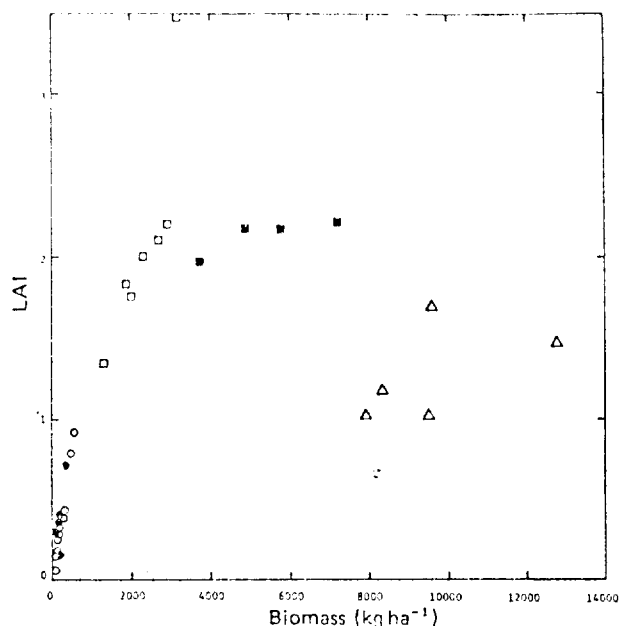


Fig. 2. Plot of sorghum leaf area index measurements versus above ground biomass measurements for five Landsat overpass dates during 1976 growing season in Bell County, TX. The correlation coefficients by date were: 0, May 3, 1976, 0.996**; ●, May 21, 1976, 0.990**; □, June 8, 1976, 0.946**; ■, June 26, 1976, -0.247; △, August 1, 1976, 0.459 (**, statistically significant at the 0.01 probability level) (after [43]).

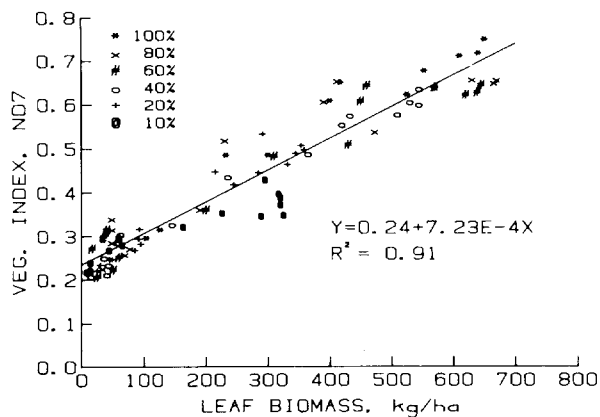


Fig. 3. Normalized difference vegetation index (ND7) versus leaf biomass for six spring wheat stand densities, expressed as a percentage of normal seeding rates (after [4]).

Many researchers have verified that vegetation indices—differences, ratios, and linear transformations of spectral reflectance or radiance observations [24], [39], [49], [15], [17], [19], [35], [48]—relate to crop canopy “greenness” [1], [4], [10], [17], [30], [37], [39], [43], [49], [52], [55], [60]. As an example of one vegetation index, Fig. 3 (after [3]) shows that leaf biomass is related to the normalized difference (ND) defined by $(MSS7 - MSS5)/(MSS7 + MSS5)$ where MSS5 and MSS7 denote the reflectance in visible red (0.6–0.7 μm) and reflective infrared (0.8–1.1 μm) wavelengths. These two wavelengths correspond to Landsat multispectral scanner (MSS) bands 5 and 7, respectively. Data such as those in Fig. 3 have been influential in convincing the scientific and user communities that spectral observations can be used to estimate important agronomic characteristics of crops. This

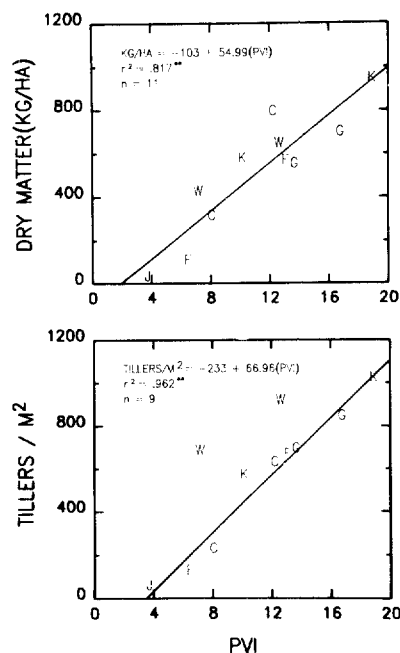


Fig. 4. Relation between perpendicular vegetation index (PVI) and two plant characteristics (tillers per square meter and dry matter, kilograms per hectare) during the fall growth period of the ARS Wheat Yield Project fields in the 1977–1978 season. Fields are located in Keith (K) Co., NB; Grant (G) Co., OK; Washington (W) Co., CO; Finney (F) Co., KS; Greeley (E) Co., KS; and Jewel (J) Co., KS.

accomplishment of the AgRISTARS effort should not be underrated. It was a necessary step in getting a new technology accepted; without the acceptance there would be no use. It is an accomplishment shared jointly by the NASA-funded and the USDA-funded research highlighted herein.

The value of the vegetation indices is that they condense observations in two or more wavelengths to a single number that relates well to the amount of photosynthetically active tissue [60], [62]. Thus the VI relate well to LAI, percent cover by green vegetation, leaf weight, plant population, green or dry biomass of nonstemmy vegetation, chlorophyll content per unit area, and consequently, to the crop's light interception capacity. Lautenschlager and Perry [29] and Perry and Lautenschlager [35] showed that a number of the vegetation indices are mathematically equivalent. Jackson *et al.* [17] described their sensitivity to atmospheric effects.

The relation between the perpendicular vegetation index (PVI) derived from Landsat-2 observations adjusted for solar zenith angle and atmospheric haze and two ground-truthed plant parameters, tillers per square meter and dry matter (kilograms per hectare) collected in fields of the ARS Wheat Project is shown in Fig. 4. The data are for the fall growth period preceding winter dormancy. There are two observation dates for five of the fields and one observation date for the Jewel Co., Kansas, field.

The coefficient of determination between PVI and tillers per square meter for the sites except Washington Co., Colorado, is 0.96 whereas it is 0.82 between PVI and dry matter including the Washington Co., Colorado, field. The slopes of the regression equations indicate there are 67

TABLE I
COEFFICIENTS OF DETERMINATION BETWEEN 9 SPECTRAL MEASURES AND \ln LAI, GRAIN YIELD, AND IPAR (PART A) AND AMONG THE 3 DEPENDENT VARIABLES (PART B)
(After Wiegand and Richardson [60].)

| (A) Veg. index or MSS band | \ln LAI | Yield kg ha^{-1} | IPAR % |
|----------------------------------|--------------------------|------------------------------|-----------|
| ----- r^2 ----- | | | |
| PVI | .601** | .676** | .526** |
| GR | .570** | .665** | .524** |
| GRw | .551** | .661** | .487** |
| RVI | .573** | .617** | .504** |
| ND | .619** | .670** | .565** |
| MSS4 | (-) ^{a/} .446** | (-).447** | (-).479** |
| MSS5 | (-).543** | (-).521** | (-).548** |
| MSS6 | .000 | .018 | .005 |
| MSS7 | .284** | .387** | .203* |
| (B) | | | |
| \ln LAI | 1.000 | | |
| Yield | .827** | 1.000 | |
| IPAR | .962** | .773** | 1.000 |

** Significant at $P=0.01$.
* Significant at $P=0.05$.

^{a/} Negative signs designate variable pairs that were inversely related.

tillers/m² per unit PVI and 55 kg/ha dry matter per unit PVI. Such relations between spectral and agronomic data may prove useful for monitoring crop growth. The fact that the relation between tillers per square meter and dry matter, $r^2 = 0.83$ (not shown) was no better than between the top of the atmosphere Landsat observations and these parameters individually indicates that the spectral samples represented these fields as well as the plant samples did.

Ability to estimate tiller population spectrally is useful for establishing the plant population needed as initial input to the models. (For a short time after emergence only primary tillers exist, so the tiller population is the plant population.) Also, the number of tillers estimated soon after spring greenup compared with the number prior to winter dormancy indicates the number that survived the winter. The tiller estimates may also be of value in checking on the number estimated by the agrometeorological model used; number of tillers has not been easy to mimic accurately in agrometeorological models.

Wiegand and Richardson [60] summarized the coefficients of determination among nine spectral measures (five VI and the four MSS bands) and LAI, grain yield, and intercepted photosynthetically active radiation (IPAR) for grain sorghum during the grain filling stage (Table I, part A). The coefficients of determination among the dependent variables LAI, YIELD, and IPAR are also presented (part B). The vegetation indices as they appear in the table, are the perpendicular vegetation index (PVI), the greenness (GR) using universal coefficients, a greenness derived using local (Weslaco) scenes (GRw), the ratio vegetation index (RVI), and the normalized difference (ND). The vegetation indices are superior to the individual Land-

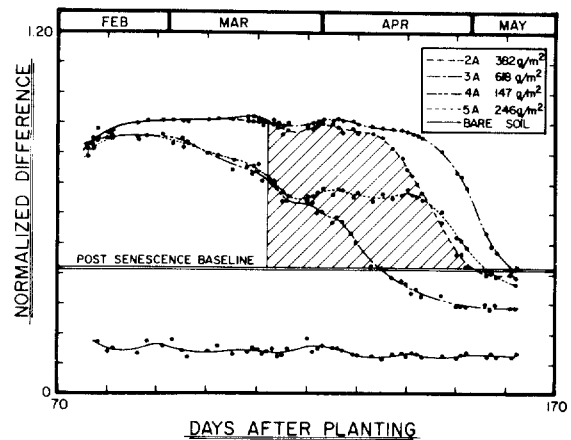


Fig. 5. The normalized difference (ND) versus time after planting for four Produra wheat fields with widely varying yields and a bare soil plot. The shaded portion under the curve for plot 2A is a graphic representation of the integration technique described in the text (after [36]).

sat MSS bands, and for the data set presented, ND and PVI related more closely to LAI and grain yield than did the other vegetation indices. Coefficients of determination between yield and LAI (0.827) and between yield and IPAR (0.773) illustrate the predictability of yield through spectral observations of crop canopies.

On most of the Great Plains, water deficits and other constraints usually prevent rainfed wheat from achieving a canopy dense enough to fully intercept the light. But since seeding rates and management practices are tuned to location specific climate and soil constraints, the harvest index of wheat is remarkably constant even on the western Great Plains [3]. Because high yields cannot be achieved unless the crop canopy development is sufficient to intercept most of the incident insolation during the reproductive phase, the spectral measurements frequently correlate well with yield [60]–[62]. For example, Tucker *et al.* [50] reported that there was a five-week period, from stem elongation through anthesis, over which the ND explained approximately 64 percent of the grain yield variation of wheat. Aase and Siddoway [3] reported that the highest correlations between spectral indices and yield for wheat were obtained from stem elongation through watery ripeness of the grain. The reason the relations are best through early grain filling is that the [green] leaf area index reaches a maximum at about boot stage and declines throughout grain filling. Consequently, the later in grain filling the spectral observations are made, the more the photosynthetically inactive tissue dominates the observations and the relationship degrades.

Pinter *et al.* [36] used a somewhat different approach (see Fig. 5). They summed the normalized differences daily for the period from heading to full senescence for all ND above the base value for harvest-ready (fully senescent) crops of wheat and barley. Thus, they took into account not only the greenness of the canopy but also its persistence. For Produra wheat whose canopy development had been affected by timing and amount of irrigation water applied, the summed ND accounted for 88 percent of the yield variation. However, because the duration of

grain filling in temperate cereals, including wheat, is temperature dependent [56], any method analogous to leaf area duration cannot hold across environments. [8].

Temporal spectral measurements, such as those shown in Fig. 5, are valuable for following the pattern of canopy development. For example, a leveling off in vegetation index during the period of normal, rapid development of the canopy may well correspond to a gradual depletion of soil water, especially if a rapid rise in the VI is observed following a known rainfall event. The vegetation index behavior would correspond to a decrease in growth (production of leaf and canopy) during a water stress period and "boom" growth upon relief by the rain. For wheat and other temperate cereals, the decline in VI following anthesis can be quantified into a senescence rate ($VI \text{ day}^{-1}$) that can be related to agronomic and environmental conditions. Idso *et al.* [13] have even proposed that yields be estimated from senescence rates.

Wiegand and Richardson [60], [62] have proposed equations that interrelate the information conveyed by plant canopies about their development (or restraint from development by stresses), light interception capability, and yield performance. The equations are

$$\frac{\ln LAI}{VI} \times \frac{IPAR}{\ln LAI} = \frac{IPAR}{VI} \quad (1)$$

$$\frac{\ln LAI}{VI} \times \frac{Yield}{\ln LAI} = \frac{Yield}{VI} \quad (2)$$

where VI denotes any one of several spectral vegetation indices available, IPAR is intercepted photosynthetically active radiation, and yield is grain yield.

Essentially, the integral VI are estimates of integral intercepted solar radiation which Daughtry *et al.* [7] and Hatfield *et al.* [9] have shown can be estimated spectrally. Since the IPAR versus $\ln LAI$ relations, available in the literature and already in use in the agrometeorological models, can be transferred directly to (1) it becomes possible to estimate IPAR remotely. This means in effect that IPAR generated by the models can be checked by direct spectral observations. Where the relation between LAI and VI is known from previous studies, such as it is for wheat, the VI's can also serve to check on the model's estimates of LAI.

From historical Landsat or the currently available NOAA meteorological satellite data, the relation between yield and VI can be established on field (Landsat) or county or crop reporting district synoptic scales (NOAA) from the VI observations those sensors provide and the yield data reported annually by the Statistical Reporting Service. Wiegand *et al.* [58] and Wiegand [59] reported such a relation for grain sorghum (*Sorghum bicolor* L., Moench) in South Texas, established during grain filling of the crop. By definition the difference between the spectral estimate for the current year and the long term average is the production deviation from the average. Such information when available in advance is useful in preparing to harvest, transport, store, and market the crop.

TABLE II
REMOТЕLY SENSED INPUTS OR FEEDBACK TO AGROMETEOROLOGICAL MODELS
GROUPED BY MODEL SUBROUTINES
(After Wiegand [59], [61].)

| Model Subroutines | Remotely Sensed Input or Check |
|-----------------------------------|---|
| Growth or dry matter accumulation | VI ^{a/} --spectral surrogate of green biomass --spectral profile ^{b/} --growth rate |
| Photosynthesis | VI--spectral surrogate of LAI for light absorption estimate Spectral estimates of IPAR |
| Evapotranspiration | BR or SLI ^{c/} --albedo, surface wetness --ground cover for partitioning evaporation and transpiration Tc-Ta ^{d/} --as related to ratio of actual to potential evapotranspiration, E/Ep |
| Phenology | Spectral profile--emergence or green-up date, maximum greenness date Tc--in lieu of air temperature to pace ontogenetic events |
| Stress | VI--Canopy "greenness" and magnitude vs. normal; senescence rate Tc-Ta--stress severity diagnostic, or in crop water stress index, (1-E/Ep) |
| Yield | VI--near maximum canopy development or early in grain filling; spectral profile integrals |

a/ VI = spectral vegetation indices GR, PVI, ND, etc. (see text)

b/ Spectral profile = vegetation index vs. time (see fig. 5, e.g.)

c/ BR, SLI = brightness and the soil line index, spectral indices dominated by soil background. (see Kauth and Thomas [24]; Wiegand and Richardson, [57]).

d/ Tc is canopy temperature; Ta is air temperature

The possibility of quantifying stress effects on yields through the canopy manifestations is an exciting one. Although the literature on crop stresses is voluminous, ways to relate stresses meaningfully to yields have been lacking [58]. Spectral observations to quantify stresses and relate them to yield merit further emphasis.

Table II summarizes additional opportunities to augment agrometeorological models with remote spectral observations. The table is organized by the subroutines (photosynthesis, growth or dry matter accumulation, evapotranspiration, phenology, stress, and yield) usually found in the growth/yield models. A number of the possibilities are hypothetical in that there is no known test in the literature, although tests are technically feasible. Others depend, for acceptance, on the outcome of tests of the relations expressed by (1) and (2). Still others depend on the availability of suitable data sets.

A point worth making is that there is no past experience on using and incorporating remotely sensed observations into crop growth/yield models because such observations have not been previously available, their usefulness had not been demonstrated, or operational products were not produced. For example, NOAA can provide surface temperature (canopy temperature when the canopies are well developed) and is developing precipitation estimates from the Advanced Very High Resolution Radiometer (AVHRR) aboard the operational meteorological satellites [63]. Thus the models and operational products will evolve gradually with experience.

An important aspect of any successful effort will be data bank and data base management. Current research on geographic information systems will be vital to successful operational application of crop models. As shown in Fig. 1 there are myriad sources of relevant information that could be acquired, archived, merged and processed to extract that needed to execute models. With current pressures on food, fuel, fiber, and forage vegetation resources, the scientists involved are working on projects with global consequences. In general, we feel that many of the candidate spectral inputs for Table II are now ready for testing and adaptation for incorporation into crop growth/yield models.

High priority needs to be placed on producing algorithms for resetting and continuing the execution of agrometeorological models when remotely sensed canopy observations are used as feedback to the models and on development of workable geographic information systems.

IV. SUMMARY

The progress made in developing and using spectral information promises to augment and enhance agrometeorological models by providing direct evidence of canopy condition that can be interpreted in terms of plant population, LAI, or IPAR for direct use in the models, or as feedback to them. Thus, use of spectral observations in conjunction with agrometeorological models increases confidence that the correct deductions are being made. In several instances the spectral data appear to be a meaningful way to quantify stresses—through their effects on the canopies the crops achieve. As a consequence of the constancy of the harvest index of wheat and environmental constraints on the canopies achieved over most of the Wheat Belt, grain yield of wheat relates well to spectral vegetation indices during the period late stem extension to early grain filling. Collectively these findings help determine whether or not agrometeorological model estimates of plant canopy characteristics, that in turn, affect the model's photosynthesis, evapotranspiration, stress response, and yield subroutines, are being correctly predicted for particular production areas. The understanding of plant canopies represented by these advances have been incorporated into the subjective operational yield predictions of the Foreign Agricultural Service (FAS) of the USDA, while agrometeorological models that would use spectral inputs are still being revised.

REFERENCES

- [1] J. K. Aase, "Relationship between leaf area and dry matter in winter wheat," *Argon. J.*, vol. 70, pp. 563-565, 1978.
- [2] J. K. Aase and F. H. Siddoway, "Determining winter wheat stand densities using spectral reflectance measurements," *Argon. J.*, vol. 72, pp. 149-152, 1980.
- [3] J. K. Aase and F. H. Siddoway, "Spring wheat yield estimates from spectral reflectance measurements," *IEEE Trans. Geosci. and Remote Sensing.*, vol. GE-19, pp. 78-84, 1981.
- [4] J. K. Aase and F. H. Siddoway, "Assessing winter wheat dry matter production via spectral reflectance measurements," *Remote Sensing Environ.*, vol. 11, pp. 267-277, 1981.
- [5] J. K. Aase, F. H. Siddoway, and J. P. Millard, "Spring wheat-leaf phytomass and yield estimates from airborne scanners and hand-held radiometer measurements," *Int. J. Remote Sensing*, vol. 5, pp. 771-781, 1984.
- [6] A. Bauer, D. Smika, and A. Black, "Correlation of five wheat growth stage scales used in the Great Plains," Pub. AAT-NC-7, ARS-USDA, Peoria, IL, 1983.
- [7] C. S. T. Daughtry, K. P. Gallo, and M. E. Bauer, "Spectral estimates of solar radiation intercepted by corn canopies," *Agron. J.*, vol. 75, pp. 527-531, 1983.
- [8] L. C. Evans and I. F. Wardlaw, "Aspects of the comparative physiology of grain yield in cereals," *Adv. Agron.*, vol. 28, pp. 301-350, 1976.
- [9] J. L. Hatfield, G. Asrar, and E. T. Kanemasu, "Intercepted photosynthetically active radiation in wheat canopies estimated by spectral reflectance," *Remote Sensing Environ.*, vol. 14, pp. 65-75, 1984.
- [10] J. L. Hatfield, E. T. Kanemasu, G. Asrar, R. D. Jackson, P. J. Pinter, Jr., R. G. Reginato, and S. B. Idso, "Leaf area estimates from spectral measurements over various planting dates of wheat," *Int. J. Remote Sensing*, vol. 6, pp. 167-175, 1985.
- [11] A. R. Huete, D. F. Post, and R. D. Jackson, "Soil spectral effects on 4-space vegetation discrimination," *Remote Sensing Environ.*, vol. 15, pp. 155-165, 1983.
- [12] S. B. Idso, P. J. Pinter, Jr., J. L. Hatfield, R. D. Jackson, and R. J. Reginato, "A remote sensing model for the prediction of wheat yield prior to harvest," *J. Theor. Biol.*, vol. 77, pp. 217-228, 1979.
- [13] S. B. Idso, P. J. Pinter, Jr., R. D. Jackson, and R. J. Reginato, "Estimation of grain yields by remote sensing of senescence rates," *Remote Sensing Environ.*, vol. 9, pp. 87-91, 1980.
- [14] R. D. Jackson, R. J. Reginato, P. J. Pinter, Jr., and S. B. Idso, "Plant canopy information extraction from composite scene reflectance of row crops," *Appl. Opt.*, vol. 18, pp. 3775-3782, 1979.
- [15] R. D. Jackson, P. J. Pinter, Jr., J. R. Reginato, and S. B. Idso, "Hand-held Radiometry," USDA-SEA, Agricultural Reviews and Manuals, ARM-W-19, 1980.
- [16] R. D. Jackson, "Canopy temperature and water stress," in *Advances in Irrigation*, D. Hillel, Ed. New York: Academic, 1982, pp. 43-85.
- [17] R. D. Jackson, P. N. Slater, and P. J. Pinter, Jr., "Discrimination of growth and water stress in wheat by various vegetation indices through a clear and a turbid atmosphere," *Remote Sensing Environ.*, vol. 13, pp. 187-208, 1983.
- [18] R. D. Jackson, P. N. Slater, and P. J. Pinter, Jr., "Adjusting the tasseled-cap brightness and greenness factors for atmospheric path radiance and absorption on a pixel by pixel basis," *Int. J. Remote Sensing*, vol. 4, pp. 313-323, 1983.
- [19] R. D. Jackson, "Spectral indices in N-Space," *Remote Sensing Environ.*, vol. 13, pp. 409-421, 1983.
- [20] R. D. Jackson, "Remote sensing of vegetation characteristics for farm management," in *Proc. Soc. Photo-Opt. Instru. Eng.*, vol. 475, pp. 81-96, 1984.
- [21] R. D. Jackson and B. F. Robinson, "Field evaluation of the temperature stability of a multispectral radiometer," *Remote Sensing Environ.*, vol. 17, pp. 103-108, 1985.
- [22] R. D. Jackson and C. E. Ezra, "Spectral response of cotton to suddenly induce water stress," *Int. J. Remote Sensing*, vol. 6, pp. 177-185, 1985.
- [23] R. D. Jackson, P. J. Pinter, Jr., and R. J. Reginato, "Net Radiation calculated from remote multispectral and ground station meteorological data," *Agricul. and Forest Meteor.*, vol. 35, pp. 153-164, 1985.
- [24] R. J. Kauth, G. S. Thomas, "The tasseled cap—A graphic description of the spectral temporal development of agricultural crops as seen by LANDSAT," in *Proc. Symp. Machine Proc. Remotely Sensed Data*, pp. 41-49, 1976.
- [25] D. S. Kimes and J. A. Kirchner, "Diurnal variations of vegetation canopy structure," *Int. J. Remote Sensing*, vol. 4, pp. 257-271, 1983.
- [26] D. S. Kimes, W. W. Newcomb, J. B. Schutt, P. J. Pinter, Jr., and R. D. Jackson, "Directional reflectance factor distributions for a cotton row crop," *Int. J. Remote Sensing*, vol. 5, pp. 263-277, 1984.
- [27] J. A. Kirchner, D. S. Kimes, and J. E. McMurtrey, III, "Variation of directional reflectance factors with structural changes of a developing alfalfa canopy," *Appl. Opt.*, vol. 21, pp. 3766-3771, 1982.
- [28] G. A. Larsen, "Progress report on the evaluation of plant growth models," Staff Rep. AGESS810716, Statistical Rep. Ser., USDA, Washington, DC, 1981.
- [29] L. F. Lautenschlager and C. R. Perry, Jr., "An empirical, graphical, and analytic study of the relationship between vegetation indices," AgRISTARS Rep. EW-JI-04150, JSC-17424, NASA Johnson Space Center, Houston, TX.
- [30] R. W. Leamer, J. R. Noriega, and C. L. Wiegand, "Seasonal changes

- in reflectance of two wheat cultivars," *Agron. J.*, vol. 70, pp. 113-118, 1978.
- [31] E. W. LeMaster, J. E. Chance and C. L. Wiegand, "A seasonal verification of the Suits spectral reflectance model for wheat," *Photogrammetr. Eng.*, vol. 46, pp. 107-114, 1984.
- [32] S. J. Maas and G. F. Arkin, "User's Guide to SORFG: A dynamic grain sorghum growth model with feedback capacity," Research Center Program and Documentation No. 78-1 (Blackland Res. Center at Temple), TAES, College Station, TX, 1978.
- [33] S. J. Maas and G. F. Arkin, "TAMW: A wheat growth and development simulation model," Res. Center Program and Documentation No. 80-3 (Blackland Res. Center at Temple), TAEX, College Station, TX, 1980.
- [34] R. B. MacDonald and F. G. Hall, "Global crop forecasting," *Science*, vol. 208, pp. 670-679, 1980.
- [35] C. R. Perry and L. F. Lautenschlager, "Functional equivalence of spectral vegetation indices," *Remote Sensing Environ.*, vol. 14, pp. 169-182, 1984.
- [36] P. J. Pinter, Jr., R. D. Jackson, S. B. Idso, and R. J. Reginato, "Multitdate spectral reflectance as predictors of yield in water stressed wheat and barley," *Int. J. Remote Sensing*, vol. 2, pp. 43-48, 1981.
- [37] P. J. Pinter, Jr., R. D. Jackson, S. B. Idso, and R. J. Reginato, "Diurnal patterns of wheat spectral reflectances," *IEEE Trans. Geosci. Remote Sensing*, vol. GE-21, pp. 156-163, 1983.
- [38] P. J. Pinter, Jr., R. D. Jackson, C. E. Ezra, and H. W. Gausman, "Sun angle and canopy architecture effects on the spectral reflectance of six wheat cultivars," *Int. J. Remote Sensing*, to be published.
- [39] A. J. Richardson and C. L. Wiegand, "Distinguishing vegetation from soil background information," *Photogrammetr. Eng.*, vol. 43, pp. 1541-1552, 1977.
- [40] A. J. Richardson, D. E. Escobar, H. W. Gausman, and J. H. Everitt, "Comparison of Landsat-2 and field spectrometer reflectance signatures of South Texas rangeland plant communities," in *Machine Processing of Remotely Sensed Data*. New York: IEEE, 1980, pp. 88-96.
- [41] A. J. Richardson, "Measurement of reflectance factors under daily and intermittent irradiance variation," *Appl. Opt.*, vol. 20, pp. 3336-3340, 1981.
- [42] A. J. Richardson, "Relating Landsat digital count values to ground reflectance for optically thin atmospheric conditions," *Appl. Opt.*, vol. 21, pp. 1457-1464, 1982.
- [43] A. J. Richardson, C. L. Wiegand, G. F. Arkin, P. R. Nixon, and A. H. Gerbermann, "Remotely-sensed spectral indicators of sorghum development and their use in growth modeling," *Agric. Meteorol.*, vol. 26, pp. 11-23, 1982.
- [44] A. J. Richardson, "The equivalence of three techniques for estimating ground reflectance from Landsat digital count data," AgRISTARS Rep. EW-U3-04407, NASA Johnson Space Center, Houston, TX, 1983.
- [45] A. J. Richardson, C. L. Wiegand, "Diurnal-seasonal light interception, leaf area index, and vegetation index interrelations in a wheat canopy," unpublished.
- [46] J. T. Ritchie, 1983, "CERES Wheat," in *Wheat Model Workshop Notebook* (Temple, TX, Feb. 22-25, 1983).
- [47] M. Shibayama and C. L. Wiegand, "View azimuth and zenith, and solar zenith angle effects on wheat canopy reflectance," *Remote Sensing Environ.*, vol. 18, pp. 91-103, 1985.
- [48] M. Shibayama, C. L. Wiegand, and A. J. Richardson, "Diurnal pattern of bidirectional vegetation indices for wheat canopies," *Int. J. Remote Sensing*, to be published.
- [49] C. J. Tucker, J. H. Elgin, Jr., J. E. McMurtrey, III, and C. J. Fan, "Monitoring corn and soybean crop development with hand-held radiometer spectral data," *Remote Sensing Environ.*, vol. 8, pp. 237-248, 1979.
- [50] C. J. Tucker, B. N. Holben, J. H. Elgin, Jr., and J. E. McMurtrey, III, "Relationship of spectral data to grain yield variation," *Photogrammetr. Eng.*, vol. 46, pp. 657-666, 1980.
- [51] C. J. Tucker, W. W. Jones, W. A. Kley, and G. J. Sundstrom, "A three-band radiometer for field use," *Science*, vol. 221, pp. 281-283, 1981.
- [52] D. F. Wanjura and J. L. Hatfield, "Spectral procedures for estimating crop biomass," *Trans. Amer. Soc. Agric. Eng.*, vol. 28, pp. 922-928, 1985.
- [53] C. L. Wiegand, G. F. Arkin, A. H. Gerbermann, and A. J. Richardson, "Complementary nature of spectral and physiological models of plant growth," *Agron. Abstr.*, p. 14, 1977.
- [54] C. L. Wiegand, "Using LANDSAT LAI and biomass estimates in conjunction with plant growth models," in *Abstr. Crop Modeling Workshop* (Dept. Agric. Eng., Clemson University, Clemson, SC), p. 15, 1977.
- [55] C. L. Wiegand, A. J. Richardson, and E. T. Kanemasu, "Leaf area index estimates for wheat from LANDSAT and their implications for evapotranspiration and crop modeling," *Agron. J.*, vol. 71, pp. 336-342, 1979.
- [56] C. L. Wiegand and A. J. Cuellar, "Duration of grain filling and kernel weight of wheat as affected by temperature," *Crop Sci.*, vol. 21, pp. 95-101, 1981.
- [57] C. L. Wiegand and A. J. Richardson, "Comparisons among a new soil index and other two- and four-dimensional vegetation indices," in *Proc. Tech. Papers ACSM-ASP Convention* (Amer. Soc. Photogram., Falls Church, VA), pp. 210-227, 1982.
- [58] C. L. Wiegand, P. R. Nixon, and R. D. Jackson, "Drought detection and quantification by reflectance and thermal responses," *Agric. Water Mgt.*, vol. 7, pp. 303-321, 1983.
- [59] C. L. Wiegand, "Candidate spectral inputs to agrometeorological crop growth/yield models," in *Proc. 2nd Int. Colloq. Spectral Signatures of Objects in Remote Sens.* (Montfavet, France), INRA Pub. 23, pp. 865-872, 1983.
- [60] C. L. Wiegand and A. J. Richardson, "Leaf area, light interception, and yield estimates from spectral components analysis," *Agron. J.*, vol. 76, pp. 543-548, 1984.
- [61] C. L. Wiegand, "The value of direct observations of crop canopies for indicating growth conditions and yield," in *Proc. 18th Int. Symp. Remote Sensing Environ.* (Environ. Res. Inst. of Michigan, Ann Arbor, MI), pp. 1551-1560, 1984.
- [62] C. L. Wiegand, A. J. Richardson, and P. R. Nixon, "Spectral components analysis: A bridge between spectral observations and agrometeorological crop models," *IEEE Trans. Geosci., and Remote Sensing*, this issue, pp. 83-89.
- [63] H. W. Yates, J. D. Tarpley, S. R. Schneider, D. F. McGinnis, and R. A. Scofield, "The role of meteorological satellites in agricultural remote sensing," *Remote Sensing Environ.*, vol. 14, pp. 219-233, 1984.

*



Craig L. Wiegand received the B.S. and M.S. degrees in agronomy from Texas A&M University and the Ph.D. degree in soil physics from Utah State University.

He is a Research Scientist in the Remote Sensing Research Unit, Agricultural Research Service, U.S. Department of Agriculture, Weslaco, TX. He has been involved in agricultural applications of remote-sensing research since the mid-1960's and is currently emphasizing spectral inputs to crop models and large-area crop condition assessments.

*



Arthur J. Richardson received the B.S. degree in secondary education from Texas A&I University, Kingsville, TX, in 1965.

He is currently a Research Physicist in the Remote Sensing Research Unit, Agricultural Research Service, U.S. Department of Agriculture, Weslaco, TX, where he has been involved in remote-sensing research for 18 years. He has tested agricultural applications of Landsat, Skylab, HCMM, and NOAA data under NASA and AgRISTARS programs.

*

Ray D. Jackson is a Research Physicist in the Soil-Plant-Atmosphere Systems Research Unit, U.S. Water Conservation Laboratory, ARS-USDA, Phoenix, AZ. He has been involved in developing remote-sensing techniques to measure evapotranspiration and to quantify water and nutrient stresses in crops.

*

Paul J. Pinter, Jr. is a Biologist in the Soil-Plant-Atmosphere Systems Research Unit, U.S. Water Conservation Laboratory, ARS-USDA, Phoenix, AZ. He is currently studying the diurnal effects of water stress and canopy architecture on the reflectance factors of crops.

J. Kris Aase is a Soil Scientist and Research Leader for the Soil and Water Management Research Unit, the Northern Plains Soil And Water Research Center, ARS-USDA, Sidney, MT. He has been active in remote sensing since 1977. His work has been on assessing stand, winter kill, phytomass, and yield of small grains spectrally.

*

Darryl E. Smika is a Soil Scientist and Research Leader at the Central Great Plains Research Station, ARS-USDA, Akron, CO. He has studied the effects of hot dry winds on wheat production, has used spectral inputs to assess crop conditions and growth in relation to production, and obtained verification data for the ARS Wheat Modeling Project.

Lyle F. Lautenschlager is a Mathematical Statistician in the Remote Sensing Branch, Applications Section, Statistical Reporting Service (SRS), USDA, South Building, Washington, DC. He worked on the multiagency LACIE and AgRISTARS Projects at the NASA Johnson Space Center, Houston, TX, from 1977 to 1984. He has been stationed in Washington, DC, since May 1984.

*

J. E. McMurtrey, III, is a Research Agronomist in the Field Crops Laboratory, Beltsville Agricultural Research Center, ARS-USDA, Beltsville, MD. He has worked cooperatively with personnel of the NASA Goddard Space Flight Center on the seasonal agronomic and spectral characterization of corn, alfalfa, and soybeans.
